EXHIBIT A

THE JOURNAL OF BIOLOGICAL CHEMISTRY
Vol. 273, No. 10, Issue of March 6, pp. 5970–5978, 1998
Printed in U.S.A.

The Conserved Carboxyl Terminus and Zinc Finger-like Domain of the Co-chaperone Ydj1 Assist Hsp70 in Protein Folding*

(Received for publication, September 8, 1997, and in revised form, December 22, 1997)

Zhen Lu and Douglas M. Cyr‡

From the Department of Cell Biology, School of Medicine, University of Alabama Medical Center, Birmingham, Alabama 35294-0005

Ydj1 is a member of the Hsp40 (DnaJ-related) chaperone family that facilitates cellular protein folding by regulating Hsp70 ATPase activity and binding unfolded polypeptides. Ydj1 contains four conserved subdomains that appear to represent functional units. To define the action of these regions, protease-resistant Ydj1 fragments and Ydj1 mutants were analyzed for activities exhibited by the unmodified protein. The Ydj1 mutant proteins analyzed were unable to support growth of yeast at elevated temperatures and were found to have alterations in the J-domain (Ydj1 H34Q), zinc finger-like region (Ydj1 C159T), and conserved carboxyl terminus (Ydj1 G315D). Fragment Ydj1 (1–90) contains the J-domain and a small portion of the G/F-rich region and could regulate Hsp70 ATPase activity but could not suppress the aggregation of the model protein rhodanese. Ydj1 H34Q could not regulate the ATPase activity of Hsp70 but could bind unfolded polypeptides. The J-domain functions independently and was sufficient to regulate Hsp70 ATPase activity. Fragment Ydj1 (179–384) could suppress rhodanese aggregation but was unable to regulate Hsp70. Ydj1 (179–384) contains the conserved carboxyl terminus of DnaJ but is missing the J-domain, G/F-rich region, and a major portion of the zinc finger-like region. Ydj1 G315D exhibited severe defects in its ability to suppress rhodanese aggregation and form complexes with unfolded luciferase. The conserved carboxyl terminus of Ydj1 appeared to participate in the binding of unfolded polypeptides. Ydj1 C159T could form stable complexes with unfolded proteins and suppress protein aggregation but was inefficient at refolding denatured luciferase. The zinc finger-like region of Ydj1 appeared to function in conjunction with the conserved carboxyl terminus to fold proteins. However, Ydj1 does not require an intact zinc finger-like region to bind unfolded polypeptides. These data suggest that the combined functions of the J-domain, zinc finger-like region, and the conserved carboxyl terminus are required for Ydj1 to cooperate with Hsp70 and facilitate protein folding in the cell.

Hsp40 proteins make up an essential family of molecular chaperones that function to specify the cellular processes facilitated by Hsp70 (1–5). Prokaryotic and eukaryotic cells contain multiple Hsp40 proteins that act in specific pairs with Hsp70 at different cellular locations via conserved mechanisms (6–9). *Escherichia coli* DnaJ, the progenitor of the Hsp40 family, functions to promote protein folding, degradation of misfolded proteins, and bacteriophage DNA replication (3, 10, 11). The mammalian Hsp40 protein Auxillin directs Hsp70 to uncoat clathrin-coated vesicles (12, 13). The cysteine string protein of *Drosophilia* is palmitolyated and localized to neurosecretory vesicles, where it is proposed to direct Hsp70 to catalyze putative protein assembly/disassembly events required for neurotransmitter release (14, 15). The yeast protein Tim44 is a component of the import machinery that directs the mitochondrial cognate of Hsp70 to drive protein translocation into the matrix space (16–20). Ydj1 is a cytosolic yeast protein that functions to deliver preproteins to organelle membranes (21, 22), refold model protein substrates (23, 24), and facilitate the ubiquitin-dependent degradation of proteins (25).

Hsp70 proteins bind and release unfolded polypeptides in an ATP-dependent reaction cycle, with the ADP-form of Hsp70 exhibiting a higher affinity for substrates than the ATP-form (26). It is proposed that Hsp40 helps stabilize Hsp70-polypeptide complexes through promoting the conversion of Hsp70-ATP to Hsp70-ADP (26–29). However, in some instances, Hsp40 proteins can promote the release of proteins that are bound to Hsp70 (7). Ydj1 and a subset of Hsp40 family members also recognize aspects of non-native protein structure and bind protein folding intermediates in a manner that facilitates subsequent interactions between them and Hsp70 (28, 30–33). In the absence of Hsp40, complex formation between Hsp70 and protein folding intermediates can be inefficient, which leads to the aggregation of substrate proteins (28, 31, 34).

Sequence analysis suggests that the regulatory and chaperone actions of Hsp40 family members are catalyzed by four different conserved sequence motifs that originate from DnaJ (3). Hsp40 proteins contain regions termed the J-domain, G/F-rich region, zinc finger-like domain, and conserved carboxyl terminus (1, 9). The J-domain corresponds to the amino-terminal 70 amino acid residues of DnaJ and is found in all Hsp40 proteins. The J-domain is responsible for regulation of the ATP hydrolytic cycle of Hsp70. The NMR structure of J-domain demonstrates that it contains four regions of α-helical conformation, with helices I and II lying in an anti-parallel orientation to helices III and IV (35–37). The orientation of helices I and II to III and IV is dictated by a loop in the J-domain formed by an HPD tripeptide that is found in all Hsp40 family members. Mutations in the HPD motif and faces of helices II and III abrogate the ability of Hsp40 proteins to interact with Hsp70 and regulate its ATPase activity (38–41).

Functions of the G/F-rich region, the zinc finger-like region and the conserved carboxyl terminus of Hsp40 proteins are not clear. The G/F-rich region is thought to act as a flexible spacer

* This work was supported by the UAB Center for Aging, the Cystic Fibrosis Foundation, a Grant in Aid from the Alabama Affiliate of the American Heart Association (AHA), a Scientist Development Award from the AHA and NIH RO1GM56981. The costs of publication of this article were defrayed in part by the payment of page charges. This article must therefore be hereby marked "*advertisement*" in accordance with 18 U.S.C. Section 1734 solely to indicate this fact.

‡ To whom correspondence should be addressed: Department of Cell Biology, School of Medicine, University of Alabama Medical Center, 1918 University Blvd., Birmingham, AL 35294-0005. Fax: 205-934-0950; E-mail; dcyr@cellbio.bhs.uab.edu.

between the J-domain and other regions in Hsp40 proteins (4). In the case of DnaJ, the G/F-rich region is required in conjunction with the J-domain in order for productive interactions with *E. coli* Hsp70 to occur (42, 43). However, because several Hsp40 family members lack the G/F-rich region and still interact with Hsp70, this conserved motif is not required for the function of all Hsp40 proteins (13, 14). Cysteine-rich repeats that resemble C4 zinc binding domains comprise the zinc finger-like domain and play a role in polypeptide binding by Hsp40 family members (44, 45). Fragments of DnaJ that contain the zinc finger-like region are capable of suppressing protein aggregation (45). However, family members that lack the zinc finger-like region can form complexes with cellular proteins and appear to function as molecular chaperones (1–3). These data suggest that other regions of Hsp40 are also involved in interactions with non-native proteins. The conserved region in the carboxyl terminus of DnaJ lies adjacent to the zinc finger-like region and is typically present in Hsp40 proteins that bind polypeptides (1–5). However, a role for this domain in the function of Hsp40 family members has not been determined.

To further define the mechanism of action for Hsp40 proteins in cellular protein metabolism, we have carried out a structure-function analysis of Ydj1. The functional analysis of protease-resistant fragments and mutant proteins has identified subdomains in Ydj1 responsible for its regulatory and chaperone activities. The J-domain functions independent of domains responsible for chaperone functions and is sufficient for regulation of Hsp70 ATPase activity. The conserved carboxyl terminus was identified as a region in Ydj1 that plays a major role in binding unfolded polypeptides. The zinc finger-like region was found to function in protein folding, but was not observed to be essential for stable binding of denatured model substrates. These data demonstrate that Ydj1 contains independent functional units that act via a coordinated mechanism to assist Hsp70 in interactions with cellular proteins.

MATERIALS AND METHODS

Purification of Hsp70 and Ydj1—Hsp70 Ssa1 protein, termed Hsp70 for the remainder of the text, was overexpressed in yeast strain MW141 and purified by ATP-agarose, DEAE, and hydroxyapatite chromatography by established techniques (46). The open reading frames for Ydj1, Ydj1 H34Q (39), and Ydj1 G315D (24) were subcloned into pET9d, overexpressed in *E. coli*, and purified by ion-exchange and hydroxyapatite chromatography as described previously (46). Ydj1 C159T was tagged with six histidine residues at its amino terminus and purified by metal chelate chromatography (21). In experiments with Ydj1 C159T, a histidine-tagged version of Ydj1 was utilized as a control.

Ydj1 H34Q and Ydj1 G315D both behaved similarly to Ydj1 on ion-exchange columns, and these proteins all ran as dimers on gel filtration columns (data not shown). Therefore, it does not appear that the mutant forms of Ydj1 we have purified are grossly misfolded. Histidine-tagged Ydj1 was capable of suppressing the temperature sensitive growth phenotype of ΔYdj1 strains and appeared to function with the same efficiency as Ydj1 (data not shown). Additionally, purified His-Ydj1 behaved identically to the nontagged version in assays for regulatory and chaperone function described below (data not shown). Ydj1 C159T behaved similarly to His-tagged Ydj1 in all purification steps and ran as a dimer on gel filtration columns.

Limited Proteolysis of Ydj1—Ydj1 (0.5 mg/ml) was digested with trypsin or proteinase K (PK)[1] at the concentrations indicated in digestion buffer (150 mM KCl, 25 mM Hepes, pH 7.4, and 10 mM DTT) for 1 h at 25 °C. Digestions were terminated by the addition of phenylmethylsulfonyl fluoride to a final concentration of 1 mM. Protease-resistant fragments of Ydj1 liberated were then analyzed by SDS-PAGE on 12.5 or 16% acrylamide gels for the trypsin and PK digestions, respectively.

Amino-terminal Sequencing of Proteolytic Fragments from Ydj1—Digested Ydj1 (4.0 μg) was run out on SDS-PAGE gels to resolve the products of the proteolytic digestion from each other. Gels were then soaked for 20 min in transfer buffer (10 mM 3-cyclohexylamino-1-propanesulfonic acid made in 10% methanol). Fragments were then electrophoretically transferred to polyvinylidene fluoride membranes in a Bio-Rad Mini-Wet cell blotter for 60 min with the power supply set at 50 V constant voltage. Membranes were then soaked in water for 5 min to remove the transfer buffer and stained with Coomassie Blue R-250 to illuminate the positions of the transferred protein fragments. Fragments were excised from the membranes, and the identity of the first six amino acid residues in them were determined with a Perkin-Elmer Applied Biosystems Microsequencing Apparatus.

Molecular Weight Determination of Ydj1 Fragments by Mass Spectroscopy—The molecular weights of the products liberated from Ydj1 by limited proteolysis were determined on a Perseptive Biosystems (Framingham, MA) Voyager Elite MALDI-TOF mass spectrometer. Aliquots of digested material (5 μl) were mixed with a saturated solution of α-cyano-4-hydroxy-cinnamic acid in a water:acetonitrile (50:50) mixture acidified with 0.1% trifluoroacetic acid. A 1-μl aliquot of this mixture was spotted onto a gold plate target. Ionization of the sample was then carried out with a nitrogen laser operating at 337 nm. A delayed extraction method was used in the determination of molecular weight. Measurement of ion flight times through the drift region of the mass spectrometer were carried out with a Tektronix (Beaverton, OR) TDS784A oscilloscope. The instrument was calibrated with external molecular weight standards.

Preparation of Protease-resistant Fragments from Ydj1 for Functional Analysis—To analyze the function of Ydj1 (1–383), Ydj1 was digested with 2 μg/ml of trypsin for 30 min at 25 °C. The trypsin was then inactivated with 0.5 mM phenylmethylsulfonyl fluoride, and the activity of Ydj1 (1–383) was analyzed. At this trypsin concentration, Ydj1 is almost completely converted to Ydj1 (1–383) and contains less than 1% contamination with Ydj1 or other fragments (Fig. 1*B, lane 3*). The levels of contaminants in this preparation were calculated to be insufficient to account for the observed activity of Ydj1 (1–383).

To generate Ydj1 (102–394), Ydj1 (179–384), and Ydj1 (1–90) for functional analysis, digestions of Ydj1 with two different concentrations of PK were carried out. Then, the different Ydj1 fragments generated were separated from each other by high performance liquid chromatography gel filtration chromatography, concentrated, and immediately assayed for activity. To generate Ydj1 (102–394) virtually free of Ydj1 (179–384) and Ydj1 (1–90), 1 mg of Ydj1 (1 mg/ml) was digested with 1–2.0 μg/ml PK for 45 min at 25 °C. The concentration of PK utilized for this digestion was adjusted so that Ydj1 was efficiently converted to Ydj1 (102–394), but only minimal conversion to Ydj1 (179–384) could occur (see Fig. 1*C, lane 3*). To separate Ydj1 (102–394) from Ydj1 (1–90) generated in protease digestions, reaction mixtures loaded onto a Bio-Rad Bio-Select G-250 gel filtration column. The column was then developed with a mobile phase consisting of 150 mM KCl, 20 mM Hepes, pH 7.4, and 2 mM DTT that was pumped at 0.6 ml/min with a back pressure of 850 psi. Fractions (0.5 ml) were collected with a Bio-Rad Biologic medium pressure chromatography system and analyzed by SDS-PAGE to identify peaks. Ydj1 (102–394) and Ydj1 (179–384) eluted at 7.8 ml, and Ydj1 (1–90) eluted at 9.0 ml. The recovery of Ydj1 fragments in this step was typically 40% of the starting material. Gel filtration typically resolved the majority of Ydj1 (1–90) from Ydj1 (102–394), but a 3% contamination of this fragment remained, and Ydj1 (179–384) was present as a 5% contaminant. The quantity of Ydj1 (179–384) and Ydj1 (1–90) present in the Ydj1 (102–394) preparations were calculated to be insufficient to account for the activity of this fragments in functional assays.

To prepare Ydj1 (179–394) free of Ydj1 (102–394), Ydj1 was digested under the conditions listed above, with 7.5 μg/ml PK. Ydj1 fragments liberated in a representative digestion are exhibited in Fig. 1*C, lane 5*. To separate Ydj1 (179–384) from Ydj1 (1–90) and the unidentified lower molecular weight fragments generated, these samples were loaded onto on a Bio-Rad Bio-Select G-250 column and treated as described above. Ydj1 (179–384) eluted at 8.0 ml of mobile phase, and Ydj1 (1–90) eluted at 9.0 ml. The Ydj1 (179–384) fraction was routinely 93% pure with a 4% contamination of Ydj1 (1–90) and a 3% contamination of unidentified proteolytic products. The level of Ydj1 (1–90) and other contaminating bands present in this preparation were calculated to be insufficient to account for the activity attributed to Ydj1 (179–384).

To generate a preparation of Ydj1 (1–90) that was free of larger Ydj1 fragments, digestions were carried out with 2.0 μg/ml as described above. Ydj1 (1–90) was then resolved from the Ydj1 (102–394) and Ydj1 (179–384) generated by the PK digestion (Fig. 1*C, lane 3*) by gel filtration as described above. The Ydj1 (1–90) peak fraction was about 95% pure and contained a 5% contamination with Ydj1 (102–394) and Ydj1 (179–384). Ydj1 (1–90) ran as a broad band on SDS-PAGE gels, but

[1] The abbreviations used are: PK, proteinase K; DTT, dithiothreitol; PAGE, polyacrylamide gel electrophoresis.

microsequence analysis indicated that the majority of protein in this band had an amino terminus that corresponded to residues 1–6 of Ydj1 (Fig. 1*D*) and to the J-domain of Ydj1. Analysis of the peptides in the Ydj1 band by mass spectroscopy indicated that the major fragment of Ydj1 present in this band was 9596 Da in size and corresponded to Ydj1 (1–90). We have calculated that the levels of Ydj1 (102–394) and Ydj1 (179–384) that contaminate the Ydj1 (1–90) preparation are too low to account for the functional activity attributed to this fraction.

Assay for Hsp70 ATPase Activity—Purified Hsp70 was incubated in a reaction mixture containing 10 mM Hepes, pH 7.4, 80 mM KCl, 10 mM DTT, 1 mM $MgCl_2$, and 50 μM ATP ([α-^{32}P]ATP, 2.0–3.0 × 10^5 cpm/pmol) for 10 min at 30 °C. Reactions were then placed on ice, and duplicate 2-μl aliquots were assayed for ADP formation by thin layer chromatography on PEI cellulose plates (46). Spontaneous ADP formation was assayed and subtracted prior to calculations for rates of ATP hydrolysis. The kinetics of Hsp70 ATPase activity were linear for at least 20 min under these experimental conditions (46).

Rhodanese Aggregation Assay—Rates of rhodanese aggregation were determined by light scattering as described previously (31). Briefly, bovine rhodanese (50 μM; Sigma) was denatured for 1 h at 25 °C in 6 M guanidinium-HCl buffered with 20 mM Hepes, pH 7.4, and fresh 10 mM DTT. Denatured rhodanese was diluted 100-fold into 300 μl of reaction buffer composed of 20 mM Hepes, pH 7.4, 80 mM KCl, and 10 mM DTT. When present, respective chaperone proteins were added prior to rhodanese. Rates of rhodanese aggregation were determined by monitoring increases in light scattering over time with a spectrophotometer set at 320 nm at 25 °C.

Luciferase Folding Assays—Refolding of firefly luciferase (Promega) by Ydj1 and Hsp70 was carried out as described previously (47). Luciferase (13 mg/ml) was diluted 42-fold into denaturation buffer (25 mM Hepes, pH 7.4, 50 mM KCl, 5 mM $MgCl_2$, 6 M guanidinum-HCl, 5 mM DTT). The denaturation reaction was allowed to proceed for 40 min at 25 °C, and then a 1-μl aliquot was removed and mixed with 125 μl of refolding buffer (25 mM Hepes, pH 7.4, 50 mM KCl, 5 mM $MgCl_2$, 1 mM ATP) and incubated at 30 °C. Aliquots of 1 μl were removed from the refolding buffer at indicated times and mixed with 60 μl of luciferase assay reagent (Promega). Luciferase activity was then measured with a Turner TD-20/20 luminometer. Ydj1 (1.6 μM), the Ydj1 mutants (1.6 μM), and Hsp70 (0.8 μM) were added to reactions prior to luciferase. The level of luciferase activity observed when Ydj1 and Hsp70 were present in reaction mixture was 17-fold higher than that activity observed when these chaperone proteins were omitted, which is consistent with previous reports (47).

Measurement of Complex Formation between Ydj1 and Luciferase—Firefly luciferase (7.5 μl) in a 100 μM stock that was denatured in 6 M guanidinium-HCl, 10 mM Hepes, pH 7.4, and 10 mM DTT and was mixed with 292.5 μl of folding buffer (150 mM KCl, 10 mM Hepes, pH 7.4, 1 mM DTT) to give a final concentration of 2.5 μM. Where indicated, 5 μM Ydj1 or its mutant forms were added to folding buffer prior to the addition of luciferase. After a 20-min incubation period at 25 °C to allow complexes between Ydj1 and luciferase to form, reactions were loaded onto a Novarose SE-1000/17 column (Bio-Rad) equilibrated with folding buffer and eluted at a flow rate of 1 ml/min. To determine where Ydj1 and luciferase migrated, 0.5 ml fractions were collected, and the proteins present in 400 μl aliquots of each fraction were precipitated by the addition of 1.2 ml of acetone. Pelleted material was resuspended in 10 μl of sample buffer and analyzed on 10% SDS-PAGE gels. The concentration of Ydj1 and luciferase present in different fractions was quantitated by densitometry. In the absence of luciferase, Ydj1 eluted at 9.0 ml of mobile phase. In the absence of Ydj1, less than 1% of the unfolded luciferase eluted, whereas almost 50% of native luciferase was recovered in a peak at 10 ml. When Ydj1 (5 μM) and native luciferase (2.5 μM) were mixed and then injected onto the column, no alteration in the migration of either protein was observed. When Ydj1 and unfolded luciferase (2.5 μM) were mixed and then injected, approximately 10% of Ydj1 eluted in a peak at 5 ml, as did approximately 10% of the added luciferase. Shown in Fig. 6*D* is the quantitation of the luciferase that co-migrated with Ydj1 and its mutants under these assay conditions.

RESULTS

To determine its domain structure, Ydj1 was digested with limited concentrations of trypsin and PK, and the fragments that were liberated were analyzed by SDS-PAGE (Fig. 1). Amino-terminal amino acid sequencing and mass spectrometry was then utilized to determine the origin of the fragments liberated by these treatments. This analysis revealed that Ydj1 contains several protease-resistant subdomains that might correspond

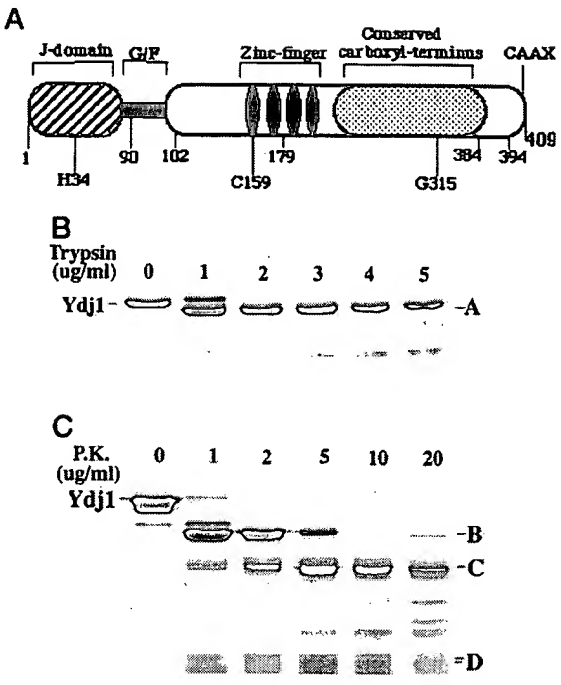

D

Protease Digestion of Ydj1	Proteolytic Fragment	Molecular Mass (Da)	Amino Terminal Sequence	Amino Acid Residues
Trypsin	A	41990	MVKETK	1-383
Proteinase K	B	32268	GGAQRP	102-394
Proteinase K	C	22800	QRFQTE	179-384
Proteinase K	D	9596	MVKETK	1-90

FIG. 1. **Limited proteolytic digestion of YDJ1 liberates several protease-resistant subdomains.** *A*, schematic diagram of YDJ1 showing the location of its conserved motifs. The *numbers* indicate residues where YDJ1 was cleaved by trypsin or PK. *H34*, *C159*, and *G315* denote the positions of residues in YDJ1 that are mutated in YDJ1 H34Q, YDJ1 C159T, and YDJ1 G315D, respectively (see below). *B*, digestion of YDJ1 (0.5 mg/ml) with indicated concentrations of trypsin at 25 °C for 1 h. *C*, digestion of YDJ1 with indicated concentrations of PK at 25 °C for 1 h. *D*, characterization of the protease-resistant fragments from YDJ1. In *panel D*, *A*, *B*, *C*, and *D* correspond to bands labeled as such on SDS-PAGE gels in *panels B* and *C*. Molecular mass of individual fragments was determined by mass spectroscopy. The amino-terminal sequence of the respective Ydj1 fragments was determined by microsequencing. The column titled *amino acid residues* denotes the position in YDJ1 to which the respective protease-resistant fragments correspond (see under "Materials and Methods" for details).

to independent functional units. Trypsin cleaved a 2602-Da peptide from the carboxyl terminus of Ydj1 to generate band A, which corresponded to amino acids 1–383 (Fig. 1, *B* and *D*). Digestion of Ydj1 with PK converted Ydj1 into bands B, C, and D, which were 32268, 22800, and 9596 Da in size and corresponded to Ydj1 (102–394), Ydj1 (179–384), and Ydj1 (1–90), respectively. Ydj1 (102–394) and Ydj1 (1–90) were prominent when digestions were carried out with 1 μg/ml PK, whereas Ydj1 (179–384) was observed at higher protease concentrations (Fig. 1*C*). Ydj1 (1–90) contains the complete J-domain of Ydj1 and a small portion of G/F region (Fig. 1*A*). Ydj1 (102–394) is missing the J-domain and G/F region, but contains the zinc finger-like region and the conserved carboxyl terminus of DnaJ. Ydj1 (179–384) contains two of the four cysteine-rich repeats that make up the zinc finger-like region and the entire conserved carboxyl terminus.

To determine the function of the different subdomains in Ydj1 that were defined by limited proteolysis, several unsuc-

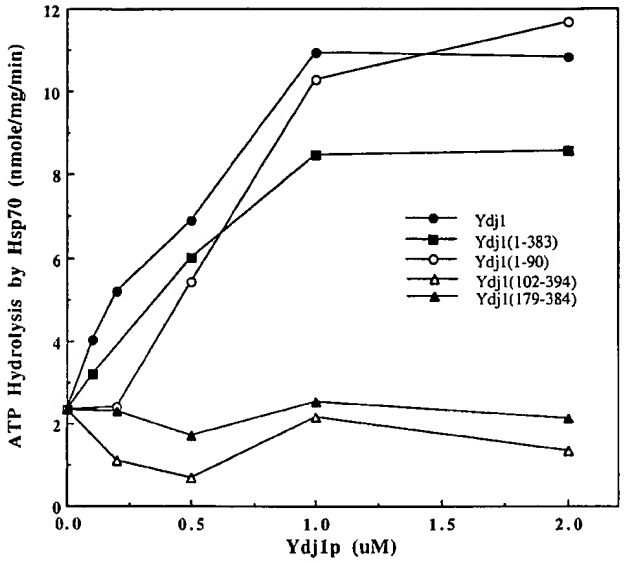

FIG. 2. **Stimulation of Hsp70 ATPase activity by different subdomains in YDJ1.** Hsp70 (0.5 μM) was incubated with [^{32}P]ATP for 10 min at 30 °C, and YDJ1 or its subdomains were added as indicated. YDJ1 and its fragments were not capable of hydrolyzing ATP independent of Hsp70 (see under "Materials and Methods" for details).

cessful attempts were made to express corresponding fragments of Ydj1 in *E. coli* (data not shown). Fragments of Ydj1 that contained just the J-domain appeared to be toxic to the cell and were expressed at levels too low to allow for purification to homogeneity. Ydj1 (102–394) and Ydj1 (179–384) were not toxic to cells but did not accumulate to high levels in *E. coli*. Histidine-tagged versions of the Ydj1 fragments could be purified, but these proteins appeared to be misfolded and were inactive. Therefore, we chose to purify the different protease-resistant Ydj1 fragments by gel filtration and analyze them for activity in reactions that are catalyzed by the full-length protein (see under "Materials and Methods" for details).

To identify regions in Ydj1 responsible for interaction with Hsp70, Ydj1 (1–90), Ydj1 (1–383), Ydj1 (102–394), and Ydj1 (179–384) were tested for their ability to stimulate Hsp70 ATPase activity (Fig. 2). Ydj1 (1–90) and Ydj1 (1–383) were able to stimulate the ATPase activity of Hsp70 to the same degree and in the same concentration range as Ydj1. Conversely, Ydj1 (102–394) and Ydj1 (179–384) appeared unable to interact with Hsp70. The J-domain of Ydj1 contains sufficient information for high affinity recognition by Hsp70.

To define regions in Ydj1 responsible for interactions with unfolded polypeptides (31), the aforementioned Ydj1 fragments were tested for their ability to suppress the aggregation of denatured rhodanese (Fig. 3). Ydj1 reduced rhodanese aggregation in a dose-dependent manner with maximal suppression occurring at a 10:1 molar ratio of chaperone to substrate (Fig. 3). Ydj1 (1–90) was completely inactive, whereas Ydj1 (1–383) suppressed rhodanese aggregation in a manner nearly identical to Ydj1. Ydj1 (102–394) and Ydj1 (179–384) were also capable of suppressing rhodanese aggregation, but a 2-fold higher concentration was required.

These data suggest that a region capable of binding unfolded proteins is present within Ydj1 (179–384). Ydj1 (179–384) is missing the J-domain, G/F region, and two of the four cysteine-rich repeats present in the zinc finger-like region (Fig. 1*A*) but contains the conserved carboxyl terminus of DnaJ. Ydj1 (102–394) contains the complete zinc finger-like region and the conserved carboxyl terminus of Ydj1 but is no more effective than Ydj1 (179–384) in suppressing rhodanese aggregation. Loss of half of the zinc finger-like region, therefore, does not alter the ability of Ydj1 to suppress protein aggregation. The portion of the zinc finger-like region that remains in Ydj1 (179–384) may contribute to the polypeptide binding activity of this fragment. Attempts to generate a fragment of Ydj1 that contained only the conserved carboxyl terminus were unsuccessful (data not shown). Nonetheless, these data support the conclusion that regions in the carboxyl terminus of Ydj1 participate in the binding of unfolded polypeptides.

Ydj1 and Hsp70 synergistically cooperate to suppress protein aggregation in a process that requires hydrolysis of ATP (31). To determine what regions of Ydj1 are required for this synergism to occur, the ability of the Ydj1 fragments to aid Hsp70 in the suppression of protein aggregation was measured (Fig. 4*A*). When added at concentrations where Hsp70 (0.5 μM) or Ydj1 (1.0 μM) alone had no influence on aggregation of 0.5 μM rhodanese, the combination of these two chaperone proteins suppressed this reaction by over 80%. When Ydj1 (1–90) was added at concentrations at which it saturates the ATP regulatory site on Hsp70, it could not enhance the action of Hsp70, whereas Ydj1 (1–383) suppressed protein aggregation by over 70%. Ydj1 (102–394) and Ydj1 (179–384) were also unable to assist Hsp70 in the suppression of protein aggregation. Similar results were observed when the combination of Ydj1 (1–90) and Ydj1 (102–394) was added to reaction mixtures with Hsp70. Thus, the regulatory or chaperone activity of Ydj1 alone is insufficient to assist Hsp70 in the suppression of protein aggregation. The coordinated action of the regulatory and chaperone domains on Ydj1 assist Hsp70 in facilitating cellular protein folding.

Regions within the J-domain that are recognized by Hsp70 are not clearly defined. Sequence analysis and structural data suggest that helix II and the HPD tripeptide may be specifically recognized by Hsp70 (35–37). Tsai and Douglas (39) have reported that a 20-residue peptide, Ydj1 (21–40), which corresponds to helix II and the HPD motif, blocks interactions between Ydj1 and Hsp70. However, whether Hsp70 recognizes other regions of the J-domain that contain the HPD tripeptide remains unclear. Therefore, we compared the ability of Ydj1 (1–90), Ydj1 (21–40), and YDJ1 (33–52) to interact with Hsp70. Ydj1 (33–52) contains the HPD motif, which is flanked by helix III instead of helix II. To assay for interactions between these peptides and Hsp70, their ability to block the cooperative suppression of protein aggregation by Ydj1 and Hsp70 was determined (Fig. 4*B*). Ydj1 (1–90), which contains the HPD tripeptide flanked by both helix II and helix III, blocked Ydj1-Hsp70 interactions at a 10:1 molar ratio of Ydj1 (1–90) to Ydj1. At concentrations up to 250 μM, a control peptide, Ydj1 (1–20), which contains helix I of the J-domain, had very little influence on Ydj1-Hsp70 interactions. Ydj1 (21–40) inhibited Ydj1-Hsp70 interactions, with maximal inhibition occurring at 100 μM peptide. Ydj1 (33–52) could also block Ydj1-Hsp70 interactions but was 2.5-fold less effective than Ydj1 (21–40) and 25-fold less effective than Ydj1 (1–90). When the ability of Ydj1 or Hsp70 to suppress protein aggregation was assayed independently, none of the aforementioned peptides were inhibitory (data not shown).

Helix II and the HPD motif appear to interact with Hsp70 with higher affinity than HPD-helix III. However, Ydj1 (21–40) and Ydj1 (33–53) were both an order of magnitude less effective than Ydj1 (1–90) at blocking interactions between Ydj1 and Hsp70. Therefore, Hsp70 can recognize HPD-helix II and HPD-helix III peptides, but with a much lower affinity than Ydj1 (1–90).

To further understand the role the J-domain, the zinc finger-like region, and the conserved carboxyl terminus play in Ydj1 function, Ydj1 H34Q, Ydj1 C159T, and Ydj1 G315D were puri-

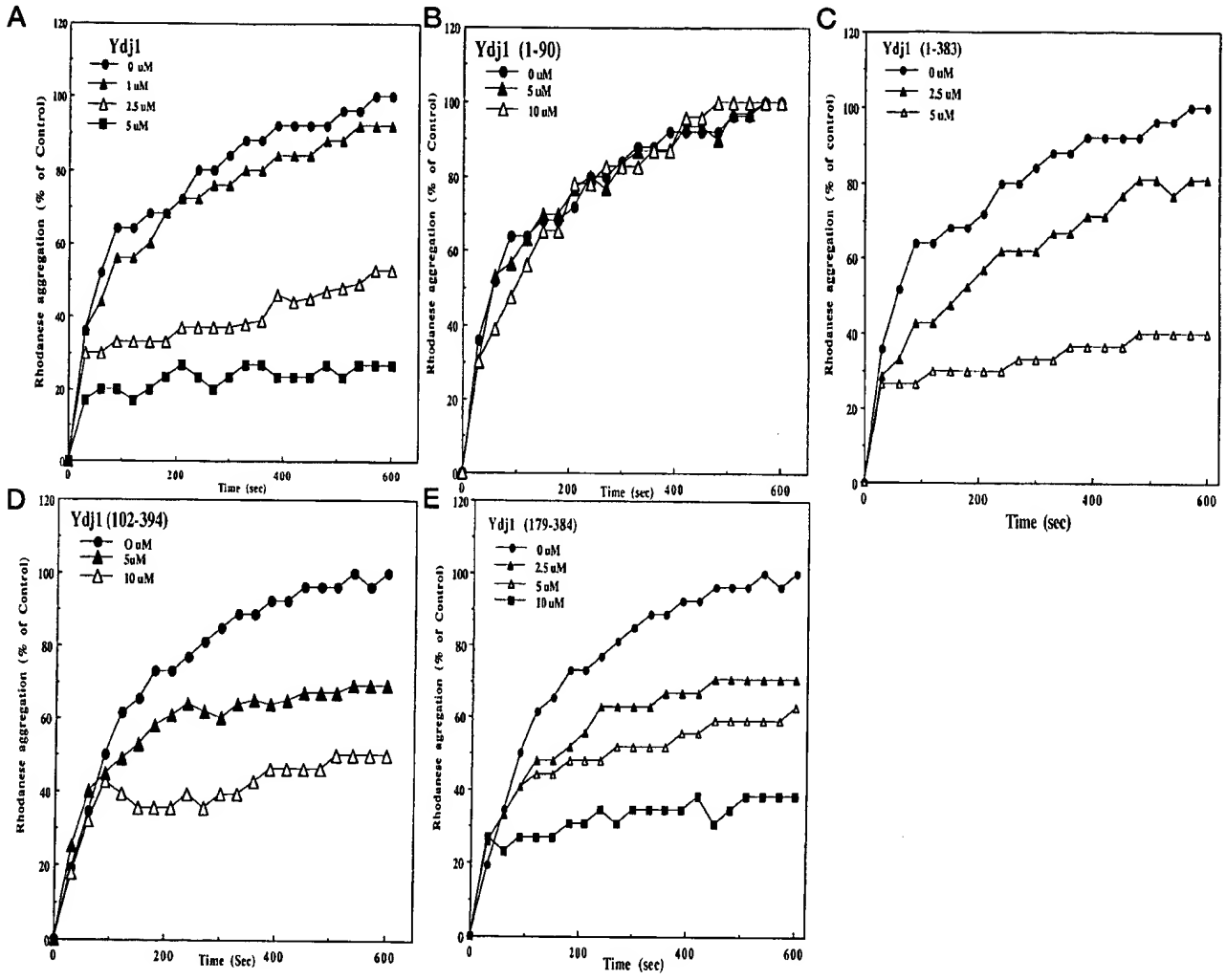

FIG. 3. **Suppression of protein aggregation by different subdomains of YDJ1.** Bovine rhodanese (50 μM) was denatured in 6 M guanidinum-HCl and was allowed to aggregate after a 100-fold dilution into buffer that contained no denaturant. When present, different forms of YDJ1 were added to reactions prior to unfolded rhodanese. Protein aggregation was monitored by light scattering at 320 nm at 25 °C for the indicated times. Protein aggregation is expressed as a percentage of the total amount of light scattering observed in the absence of chaperones after a 10-min incubation (see under "Materials and Methods" for details).

fied and tested for functions exhibited by Ydj1. Ydj1 H34Q has a point mutation in the HPD motif that hinders the ability of Ydj1 to interact with Hsp70 (39). Ydj1 C159T contains a mutation in a conserved cysteine found in the first of two putative zinc binding domains in Ydj1 (Fig. 1*A*) and is unable to support protein translocation into mitochondria (21). Ydj1 G315D has a mutation in a highly conserved glycine in the carboxyl terminus and is not capable of supporting Hsp90 mediated signal transduction to the nucleus (24). The respective Ydj1 mutants can support growth of yeast at 30 °C and therefore appear to fold properly *in vivo*, but strains become nonviable at 37 °C (21, 24, 39). All three mutant proteins were purified by standard techniques and ran as dimers on gel filtration columns, which suggested that they did not misfold during overexpression in *E. coli* or purification by column chromatography (data not shown).

Ydj1 C159T and Ydj1 G315D were both able to stimulate the ATPase activity of Hsp70 approximately 6–7-fold (Fig. 5*A*). The shapes of titration curves for stimulation of Hsp70 ATPase by Ydj1 C159T and Ydj1 G315D were identical to those of Ydj1 (data not shown; Fig. 2). As reported by Tsai and Douglas (39), Ydj1 H34Q was unable to regulate the ATP hydrolytic cycle of Hsp70 (Fig. 5*A*). These data demonstrate that mutations in the zinc finger-like region and the conserved carboxyl terminus do not hinder the ability of Ydj1 to regulate Hsp70 ATPase activity and that Ydj1 C159T and Ydj1 G315D are functional proteins.

Next, the ability of the different forms of Ydj1 to function as molecular chaperones and suppress protein aggregation was examined (Fig. 5*B*). Ydj1 H34Q and Ydj1 C159T behaved similarly to Ydj1 and were both able to suppress the aggregation of rhodanese in a dose-dependent manner. Maximal suppression of protein aggregation by Ydj1, Ydj1 H34Q, and Ydj1 C159T was observed at a 10:1 molar ratio of chaperone to substrate. These data suggest that the J-domain and residue Cys-159 in the zinc finger-like region are not essential for interactions between Ydj1 and unfolded polypeptides to occur. On the other hand, mutation of the conserved carboxyl terminus caused severe defects in Ydj1 chaperone function. Ydj1 G315D at 10:1 and 20:1 molar ratios to rhodanese was inefficient at suppressing protein aggregation (Fig. 5*C*). In three independent experiments, 5 μM Ydj1 suppressed the aggregation of 0.5 μM rhodanese and average ($\pm$ S.D.) of 77 $\pm$ 3.2%, whereas 5 μM Ydj1 G315D reduced aggregation by 7.5 $\pm$ 7.0%. It therefore appears that Gly-315 is required for efficient interactions between Ydj1 and unfolded proteins. These data support the previous inter-

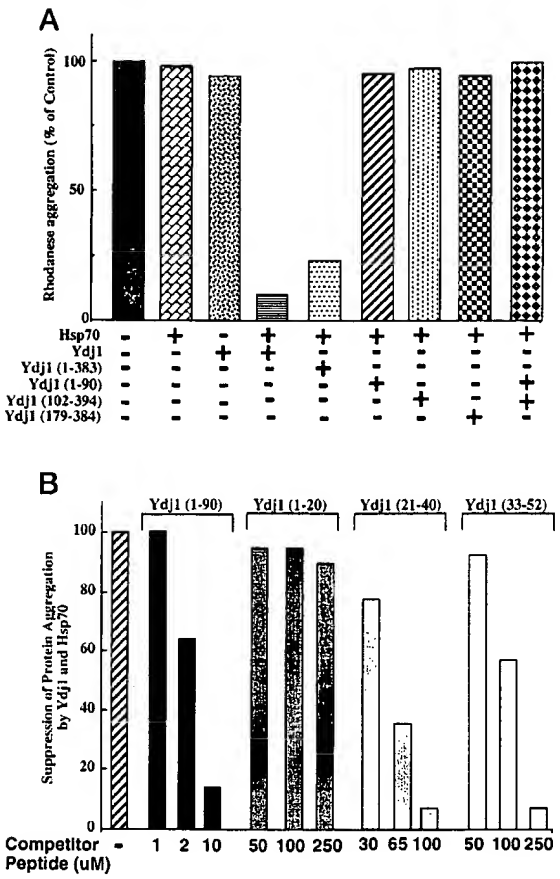

FIG. 4. **Suppression of protein aggregation by Ydj1 and Hsp70.** Rates of rhodanese aggregation were measured as described in the legend to Fig. 3. Where indicated, Hsp70 (0.5 μM), YDJ1 (1.0 μM), and the respective protease-resistant fragments (1.0 μM) were added to reactions prior to rhodanese. All reactions contained 1 mM Mg-ATP. In the absence of ATP, no synergistic interactions between YDJ1 and Hsp70 were observed. Results are expressed as a percentage of the rhodanese aggregation that occurred during a 10-min incubation in the absence of chaperone proteins.

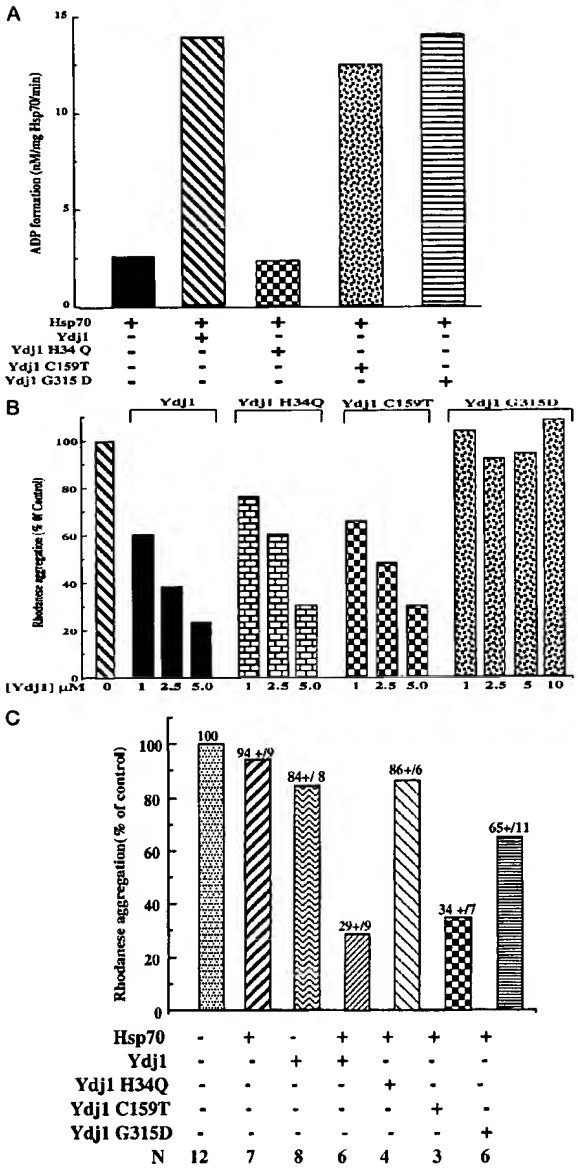

FIG. 5. **Biochemical characterization of YDJ1 mutants.** *A*, regulation of Hsp70 ATPase activity by YDJ1 H34Q, YDJ1 C159T, and YDJ1 G315D. Hsp70 (0.5 μM) was incubated with the different forms of YDJ1 in the presence of [α-^{32}P]ATP for 10 min at 30 °C. At the 2:1 YDJ1:Hsp70 molar ratio utilized in this assay, maximal stimulation of Hsp70 ATPase activity by YDJ1, YDJ1 C159T, and YDJ1 G315D was observed. *B*, suppression of rhodanese aggregation by mutant forms of YDJ1. Aggregation of denatured rhodanese (0.5 μM) was measured as described in the legend to Fig. 3. *C*, cooperation between Ydj1 and Hsp70 in the suppression of protein aggregation. When present, Hsp70 (0.5 μM) and the different forms of YDJ1 (1.0 μM) were added prior to unfolded rhodanese (0.5 μM). Results are expressed as a percentage of the total rhodanese aggregation that occurred in the absence of chaperone proteins during a 10-min incubation at 25 °C. *N* denotes the number experiments carried out to generate the averages (+/ indicates ± S.D.) of the results obtained and presented here.

pretation that the conserved carboxyl terminus of Ydj1 functions in polypeptide binding.

Tested next was the ability of the respective Ydj1 mutants to cooperate with Hsp70 in the suppression of rhodanese aggregation. Ydj1 H34Q was unable to cooperate with Hsp70, whereas Ydj1 C159T was almost as effective as Ydj1 in assisting Hsp70 in the suppression of protein aggregation (Fig. 5*C*). Interestingly, Ydj1 G315D was able to partially suppress protein aggregation when added in combination with Hsp70. In six separate trials, the combination of Ydj1 G315D and Hsp70 reduced rhodanese aggregation to 65 ± 11% of control levels as compared with 29 ± 9% for Ydj1. Analysis of these data by Student's *t* test indicates that the activity of the Hsp70/Ydj1 G315D co-chaperone pair is significantly different from the control and the Hsp70/Ydj1 pair to a confidence level of greater than 99%. Therefore, the data presented in Fig. 5 demonstrate that Ydj1 G315D exhibits a reduced level of polypeptide binding activity and is less efficient than Ydj1 at assisting Hsp70 in the suppression of protein aggregation.

If Ydj1 C159T can regulate the ATPase activity of Hsp70 and suppress the aggregation of protein folding intermediates, then what is the defect in its function? One possibility is that Ydj1 C159T can bind unfolded proteins efficiently but is inefficient at folding them. To address this issue, we examined the ability of Ydj1 C159T to refold the model protein luciferase, which had been denatured with guanidinium-HCl and allowed to refold at 25 °C (Fig. 6*A*). The molar ratios of Hsp70 and Ydj1 to luciferase in these reactions were optimized to allow efficient refolding of luciferase to occur (data not shown). The combination of Ydj1 and Hsp70 enhanced the folding of luciferase 17-fold over spontaneous rates and 8–9-fold over rates observed when these chaperone proteins were added independently. Substitution of Ydj1 H34Q for Ydj1 reduced folding rates to those observed

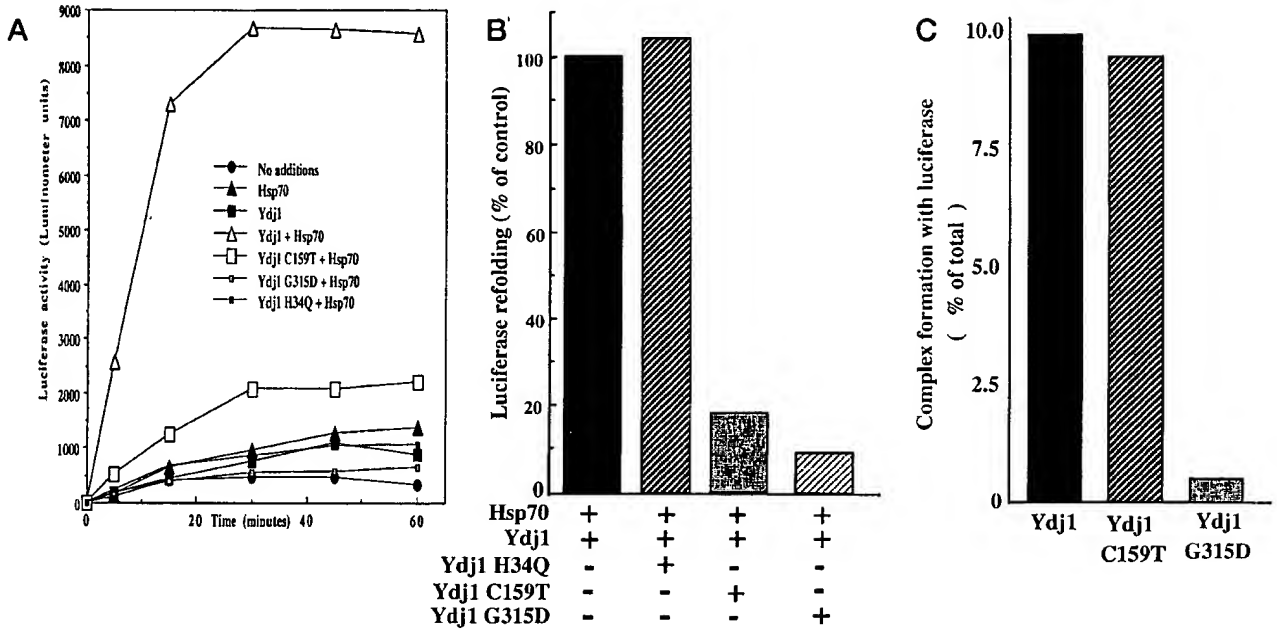

FIG. 6. **Analysis of Ydj1 mutants in luciferase refolding assays.** *A*, refolding of guanidinium-HCl denatured luciferase (0.04 μM) at 25 °C by Hsp70 (0.8 μM) and YDJ1 (1.6 μM) (see under "Materials and Methods" for details). When added, the mutant YDJ1 proteins were also present at 1.6 μM. Activity of refolded luciferase was quantitated in a Turner TD 20/20 luminometer and expressed in arbitrary units. *B*, inhibition of luciferase refolding by YDJ1 mutants. Reactions contained Hsp70 (0.8 μM), YDJ1 (1.0 μM), and the YDJ1 mutant (indicated at 10 μM). Luciferase activity after 20 min of incubation was measured with a luminometer. Values are expressed as the percentage of luciferase activity observed in the presence of YDJ1 and Hsp70, which was equivalent to 7200 units. *C*, complex formation between Ydj1 and denatured luciferase. Complex formation between YDJ1 and unfolded luciferase was measured by gel filtration chromatography as described under "Materials and Methods." Complex formation is expressed as a percentage of the total quantity of luciferase (2.5 μM) bound to the different forms of YDJ1 (5.0 μM). YDJ1 bound luciferase in a 1:1 molar ratio.

when just Hsp70 was present, which demonstrated that a functional J-domain is required for protein folding by Ydj1. The combination of Ydj1 G315D and Hsp70 was also inactive in refolding luciferase. Ydj1 C159T exhibited severe defects in its ability to cooperate with Hsp70 and refold luciferase but was partially active. Over the first 30 min of the folding reaction, Ydj1 C159T cooperated with Hsp70 to refold luciferase at rates that were 4–5-fold slower than with Ydj1.

Ydj1 C159T and Ydj1 G315D might refold luciferase inefficiently because their J-domains are not accessible to Hsp70 under these assay conditions. To exclude this possibility, the ability of Ydj1 C159T and Ydj1 G315D to block protein refolding by the Hsp70-Ydj1 co-chaperone pair was determined (Fig. 6*B*). Addition of Ydj1 C159T and Ydj1 G315D to incubations at 10:1 molar ratio over Ydj1 reduced the level of luciferase folding by greater than 80%. Addition of Ydj1 H34Q at similar concentrations had no influence on the ability of Ydj1 and Hsp70 to refold luciferase. Thus, it appears that defects in the chaperone functions of Ydj1 C159T and Ydj1 G315D are the reason for their inability to fold proteins.

Inability of Ydj1 to form complexes with unfolded luciferase might explain why Ydj1 C159T and Ydj1 G315D exhibit defects in protein folding. To test this possibility, complex formation between Ydj1 and luciferase was measured by monitoring the co-migration of these proteins on a gel filtration column (see under "Materials and Methods" for details). Shown in Fig. 6*D* is the quantitation of such a binding assay, which demonstrated that Ydj1 C159T is capable of forming tight complexes with protein folding intermediates. The level of complex formation between luciferase and Ydj1 C159T was routinely the same as that observed with Ydj1 and corresponded to approximately 10% of the total luciferase added to reactions. Ydj1 C159T was also able to form ternary complexes with unfolded luciferase and Hsp70 with an efficiency similar to that of Ydj1 (data not shown). Levels of complex formation between Ydj1 G315D and unfolded luciferase were approximately 90% lower than that observed for Ydj1, but they were detectable.

These data demonstrate that mutation of Cys-159 in the zinc finger-like region does not grossly alter the ability of Ydj1 to form stable complexes with unfolded luciferase, whereas mutation of the conserved carboxyl terminus severely reduces polypeptide binding activity. Defects in formation of stable complexes with unfolded polypeptides are likely to account for the inability of Ydj1 G315D to suppress the aggregation of rhodanese (Fig. 3) and refold luciferase (Fig. 6). Defects in the function of Ydj1 C159T appear more complex and are discussed below.

DISCUSSION

To fold polypeptides, Hsp70 and Hsp40 form complexes with folding intermediates to prevent them from entering nonproductive pathways that lead to aggregation (5). Polypeptides released from this ternary complex are often in non-native conformations and must be rebound by Hsp70 and Hsp40 several times before they fold properly. Data presented herein indicate that the combined action of the J-domain, the zinc finger-like region, and the conserved carboxyl terminus is required for Ydj1 and Hsp70 to efficiently bind polypeptides at different stages of folding and promote their passage to the native state.

Defective chaperone function of Ydj1 C159T and Ydj1 G315D appears to be the mechanism attributable to their inability to support growth of yeast at elevated temperatures (21, 24). Inability of Ydj1 C159T to interact productively with nascent polypeptides would explain why mitochondrial precursor proteins accumulate in import-incompetent conformations in strains that harbor this allele of Ydj1 (21). Reduced complex formation between Ydj1 G315D and hormone receptors has

been observed (24). Our data suggest that a defect in the polypeptide binding activity of Ydj1 is the cause of this result, and it leads to diminished signal transduction to the nucleus in strains that harbor Ydj1 G315D (24).

The J-domain of Ydj1 appears sufficient for regulation of Hsp70 ATPase activity, but the sequence within it that is recognized by Hsp70 is not defined. Based on the NMR structure, it has been suggested that helix II-HPD is the minimal unit of the J-domain that is recognized by Hsp70 (35–37). Consistent with this proposal, synthetic peptides that correspond to helix II and the HPD tripeptide are recognized by Hsp70. However, this J-domain peptide is one-tenth as efficient as fragment Ydj1 (1–90) at blocking interactions between Ydj1 and Hsp70. Perhaps the helix II-HPD sequence is the minimal sequence recognized by Hsp70, but the presence of adjacent regions in the J-domain, such as helix III, is required to stabilize it in a high affinity conformation. This might explain why Ydj1 (1–90) is 10–25-fold more effective than the helix II-HPD and helix III-HPD peptides as an inhibitor of interactions between Ydj1 and Hsp70.

Data from domain swap experiments carried out by the Silver group support the interpretation that the helix II-HPD-helix III region plays an important role in J-domain function (8). When the J-domain from a cytosolic Hsp40 protein was substituted for this same region in an endoplasmic reticulum-localized family member cells became inviable. Through conservatively mutating two amino acid residues in helix II and one residue in helix III in the J-domain of the cytosolic Hsp40 protein, these investigators were able to convert this inactive J-domain to one that was capable of interacting with endoplasmic reticulum Hsp70 and supporting cell growth. When made independently, the alterations in helix II and helix III were insufficient to generate a functional J-domain (8). Thus, information in helices II and III is required for the formation of a functional J-domain.

How Hsp40 proteins interact with non-native polypeptides and function as molecular chaperones is not understood at the mechanistic level. To address this issue, we have examined which region of Ydj1 is responsible for its polypeptide binding activity. We present data that strongly argue that the conserved carboxyl terminus of Ydj1 participates in the binding of unfolded polypeptides. This conclusion is based on two observations: 1) a 22-kDa internal fragment of Ydj1, Ydj1 (179–384), can suppress rhodanese aggregation with similar efficiency as the full-length protein. This fragment lacks the J-domain, the G/F region, and the first zinc binding cleft but contains the conserved carboxyl terminus of DnaJ. 2) Ydj1 G315D contains a mutation in the conserved carboxyl terminus and exhibits severe defects in polypeptide binding as evidenced by its inability to suppress rhodanese aggregation and to form complexes with denatured luciferase.

The portion of Ydj1 that is referred to as the conserved carboxyl terminus corresponds to amino acid residues 206–380. This region contains a series of seven highly conserved glycine residues that are present in Hsp40 family members demonstrated to function as polypeptide-binding proteins (1–5, 22). Substitution of Gly-315 with Asp in this region could diminish polypeptide binding activity by altering the conformation of the polypeptide binding fold of Ydj1. Such alterations in Ydj1 structure are predicted to result from restrictions in allowed backbone conformations caused by the G315D amino acid substitution. Glycine can adopt a ϕ/ψ angle about the α-carbon, and residues (such as aspartate) that contain a β-carbon cannot form this angle. Alternatively, chaperone function of Ydj1 G315D may be compromised because it has a charged hydrophilic side chain projecting into a region of the protein that is predicted to interact with hydrophobic portions of unfolded proteins.

The zinc finger-like region also appears to participate in interactions between Ydj1 and unfolded polypeptides, but the action of this domain does not appear essential for the binding of the model substrate proteins we examined in this study. Proteolytic removal of the first zinc binding domain from Ydj1 did not significantly diminish the ability of Ydj1 (179–384) to suppress rhodanese aggregation. The Ydj1 C159T mutant was able to bind proteins in a manner that was similar to the wild type protein. However, Ydj1 C159T exhibited severe defects in its ability to cooperate with Hsp70 and refold the denatured luciferase. These data suggest that the first zinc binding cleft and possibly the whole zinc finger-like domain of Ydj1 are dispensable for binding unfolded proteins. However, the zinc-finger region appears to play a critical role in the folding polypeptides once they are bound to Ydj1.

Consistent with our studies on Ydj1, the zinc finger-like region of DnaJ has been shown to participate in interactions with unfolded proteins (44, 45). However, the relative importance of the zinc finger-like region in polypeptide binding reactions carried out by different Hsp40 family members appears to require further clarification. Szabo *et al.* (45) reported that site-directed mutagenesis of conserved cysteines in the zinc finger-like domain of DnaJ caused severe defects in its ability to suppress rhodanese aggregation. This result suggested that the zinc finger-like domain is critical for polypeptide binding by DnaJ. Zylicz and colleagues (44) recently reported that deletion of the zinc finger-like region of DnaJ reduced the binding of some but not all substrates. Therefore, these investigators concluded that the zinc finger-like region helped determine the substrate specificity of DnaJ. Thus, although it is clear that the zinc finger-like region helps Hsp40 proteins interact with unfolded polypeptides, its exact role in the binding and folding of proteins requires further study.

How do the conserved carboxyl terminus and the zinc finger-like region cooperate to facilitate protein folding by Ydj1? In order for Hsp70 and Ydj1 to fold proteins, they must bind and release them in an efficient manner. The zinc finger-like region may act at either or both of these steps in the Hsp70 reaction cycle. At early stages of protein folding, the conserved carboxyl terminus of Ydj1 might be competent for binding unfolded polypeptides that are in unordered conformations. However, the conserved carboxyl terminus may require the assistance of the zinc finger-like region to bind late stage folding intermediates that have adopted secondary or tertiary structure. Inability of Ydj1 C159T to interact productively with molten globule intermediates of protein folding pathways could be why it is unable to efficiently refold denatured polypeptides.

Zylicz and colleagues (44) have suggested the zinc finger-like domain of DnaJ functions to alter the conformation of Hsp70 in a manner that alters its affinity for unfolded proteins. The zinc finger-like region of Ydj1 may have a similar function, and this may be abrogated in Ydj1 C159T, which causes a decrease in its efficiency in protein folding reactions. Ongoing studies are focused on investigating how the zinc finger-like region of Ydj1 functions to increase the efficiency of Hsp70 action in the cell.

Acknowledgments—The authors thank Drs. Susan Lindquist, Joyce Tsai, and Michael Yaffe for providing strains. Joyce Tsai and Michael Douglas provided the synthetic peptides utilized in this study. We thank Margaret Scully for comments on the manuscript. Sylvia McPherson of the University of Alabama at Birmingham AIDS Center core was responsible for generation of the Ydj1 expression plasmids. Kim Estel of the University of Alabama at Birmingham Protein Sequence core was responsible for microsequencing. Lori Coward was the operator of the MALDI-TOF mass spectrometer, which was located in the University of Alabama at Birmingham Comprehensive Cancer Center Mass Spectrometry Shared Facility.

REFERENCES

1. Cyr, D. M., Langer, T., and Douglas, M. G. (1994) *Trends Biochem. Sci.* **19,** 176–181
2. Caplan, A. J., Cyr, D. M., and Douglas, M. G. (1993) *Mol. Biol. Cell* **4,** 555–563
3. Georgopoulos, C. (1992) *Trends Biochem. Sci.* **17,** 295–299
4. Silver, P. A., and Way, J. C. (1993) *Cell* **74,** 5–6
5. Hartl, F. U. (1996) *Nature* **381,** 571–579
6. Brodsky, J. L., Hamamoto, S., Feldheim, D., and Schekman, R. (1993) *J. Cell Biol.* **120,** 95–102
7. Cyr, D. M., and Douglas, M. G. (1994) *J. Biol. Chem.* **269,** 9798–9804
8. Schlenstedt, G., Harris, S., Risse, B., Lill, R., and Silver, P. A. (1995) *J. Cell Biol.* **129(4),** 979–988
9. Cyr, D. M. (1997) in: *Guidebook to Molecular Chaperones and Protein Folding Factors* (Gething, M.-J., Ed.) pp. 89–95, Oxford University Press, Oxford, United Kingdom
10. Zylicz, M. (1993) *Philos. Trans. R. Soc. Lond. B Biol. Sci.* **339,** 271–278
11. Sherman, M., and Goldberg, A. L. (1992) *EMBO J.* **11,** 71–77
12. Barouch, W., Prasad, K., Greene, L., and Eisenberg, E. (1997) *Biochemistry* **36,** 4303–4308
13. Jiang, R.-F., Greener, T., Barouch, W., Greene, L., and Eisenberg, E. (1997) *J. Biol. Chem.* **272,** 6141–6145
14. Braun, J. E. A., Wilbanks, S. M., and Scheller, R. H. (1996) *J. Biol. Chem.* **271,** 25989–25993
15. Chamberlain, L. H., and Burgoyne, R. D. (1997) *Biochem. J.* **322,** 853–858
16. Ungermann, C., Neupert, W., and Cyr, D. M. (1994) *Science* **266,** 1250–1253
17. Ungermann, C., Guiard, B., Neupert, W., and Cyr, D. M. (1996) *EMBO J.* **15,** 735–744
18. Cyr, D. M. (1997) *J. Bioenerg. Biomembr.* **29,** 29–34
19. Lill, R., Nargang, F. E., and Neupert, W. (1996) *Curr. Opin. Cell Biol.* **8,** 505–512
20. Schatz, G. (1996) *J. Biol. Chem.* **271,** 31763–31766
21. Atencio, D. P., and Yaffe, M. P. (1992) *Mol. Cell. Biol.* **12,** 283–291
22. Caplan, A. J., Cyr, D. M., and Douglas, M. G. (1992) *Cell* **71,** 1143–1155
23. Caplan, A. J., Langley, E., Wilson, E. M., and Vidal, J. (1995) *J. Biol. Chem.* **270,** 5251–5257
24. Kimura, Y., Yahara, I., and Lindquist, S. (1995) *Science* **268,** 1362–1365
25. Lee, D. H., Sherman, M. Y., and Goldberg, A. L. (1996) *Mol. Cell. Biol.* **16,** 4773–4781
26. Palleros, D. R., Welch, W. J., and Fink, A. L. (1991) *Proc. Natl. Acad. Sci. U. S. A.* **88,** 5719–5723
27. Liberek, K., Marszalek, J., Ang, D., Georgopoulos, C., and Zylicz, M. (1991) *Proc. Natl. Acad. Sci. U. S. A.* **88,** 2874–2878
28. Langer, T., Lu, C., Echols, H., Flanagan, J., Hayer, M. K., and Hartl, F. U. (1992) *Nature* **356,** 683–689
29. McCarty, J. S., Buchberger, A., Reinstein, J., and Bukau, B. (1995) *J. Mol. Biol.* **249,** 126–137
30. Wickner, S., Hoskins, J., and McKenney, K. (1991) *Proc. Natl. Acad. Sci. U. S. A.* **88,** 7903–7907
31. Cyr, D. M. (1995) *FEBS Lett.* **359,** 129–132
32. Wawrzynow, A., and Zylicz, M. (1995) *J. Biol. Chem.* **270,** 19300–19306
33. Minami, Y., Hohfeld, J., Ohtsuka, K., and Hartl, F.-U. (1996) *J. Biol. Chem.* **271,** 19617–19624
34. Wagner, I., Arlt, H., van Dyck, L., Langer, T., and Neupert, W. (1994) *EMBO J.* **13,** 5135–5145
35. Hill, R. B., Flanagan, J. M., and Prestegard, J. H. (1995) *Biochemistry* **34,** 5587–5596
36. Qian, Y. Q., Patel, D., Hartl, F. U., and McColl, D. J. (1996) *J. Mol. Biol.* **260,** 224–235
37. Szyperski, T., Pellecchia, M., Wall, D., Georgopoulos, C., and Wuthrich, K. (1994) *Proc. Natl. Acad. Sci. U. S. A.* **91,** 11343–11347
38. Feldheim, D., Rothblatt, J., and Schekman, R. (1992) *Mol. Cell. Biol.* **12,** 3288–3296
39. Tsai, J., and Douglas, M. G. (1996) *J. Biol. Chem.* **271,** 9347–9354
40. Wall, D., Zylicz, M., and Georgopoulos, C. (1994) *J. Biol. Chem.* **269,** 5446–5451
41. Dey, B., Caplan, A. J., and Boschelli, F. (1996) *Mol. Biol. Cell* **7,** 91–100
42. Karzai, A. W., and McMacken, R. (1996) *J. Biol. Chem.* **271,** 11236–11246
43. Wall, D., Zylicz, M., and Georgopoulos, C. (1995) *J. Biol. Chem.* **270,** 2139–2144
44. Banecki, B., Liberek, K., Wall, D., Wawrzynow, A., Georgopoulos, C., Bertoli, E., Tanfani, F., and Zylicz, M. (1996) *J. Biol. Chem.* **271,** 14840–14848
45. Szabo, A., Korszun, R., Hartl, F. U., and Flanagan, J. (1996) *EMBO J.* **15,** 408–417
46. Cyr, D. M., Lu, X., and Douglas, M. G. (1992) *J. Biol. Chem.* **267,** 20927–20931
47. Levy, E. J., McCarty, J., Bukau, B., and Chirico, W. J. (1995) *FEBS Lett.* **368,** 435–440

REVIEW ARTICLE

Molecular chaperones in cellular protein folding

F. Ulrich Hartl

The folding of many newly synthesized proteins in the cell depends on a set of conserved proteins known as molecular chaperones. These prevent the formation of misfolded protein structures, both under normal conditions and when cells are exposed to stresses such as high temperature. Significant progress has been made in the understanding of the ATP-dependent mechanisms used by the Hsp70 and chaperonin families of molecular chaperones, which can cooperate to assist in folding new polypeptide chains.

PROTEIN folding is the process by which the linear information contained in the amino-acid sequence of a polypeptide gives rise to the well-defined three-dimensional conformation of the functional protein. How this is accomplished constitutes a central problem in biology. Because unfolded proteins can reach their native state spontaneously *in vitro*[1], it was assumed that the folding (acquisition of tertiary structure) and assembly (formation of protein oligomers) of newly synthesized polypeptides *in vivo* also occur essentially uncatalysed and without the input of metabolic energy. This long-held view has been revised in recent years owing to the discovery that in the cell the correct folding of many proteins depends on the function of a pre-existing protein machinery—the molecular chaperones[2–5]. Here I summarize our present understanding of the structure and function of these components. The main focus will be on the ATP-dependent mechanisms used by the heat-shock protein 70 (Hsp70) and the chaperonin families (Table 1), which fulfil distinct roles in protein folding: the Hsp70s and their partner proteins can stabilize translating and newly synthesized polypeptides until all segments of the chain necessary for folding are available; the chaperonins are large cylindrical complexes that promote protein folding in the sequestered environment of their central cavity.

Molecular chaperones were originally defined as a group of unrelated classes of proteins that mediate the correct assembly of other proteins, but are not themselves components of the final functional structures[2]. They occur ubiquitously and many of them are classified as stress proteins, although they have essential functions under normal growth conditions. More recently, chaperones have been defined as proteins that bind to and stabilize an otherwise unstable conformer of another protein– and by controlled binding and release, facilitate its correct fate *in vivo*, be it folding, oligomeric assembly, transport to a particular subcellular compartment, or disposal by degradation[5]. Molecular chaperones do not contain steric information specifying correct folding: instead, they prevent incorrect interactions within and between non-native polypeptides, thus typically increasing the yield but not the rate of folding reactions. This distinguishes them from the so-called folding catalysts, protein disulphide isomerases and peptidyl–prolyl isomerases. These enzymes accelerate intrinsically slow steps in the folding of some proteins, namely the rearrangement of disulphide bonds in secretory proteins and the *cis–trans* isomerization of peptide bonds preceding proline residues, respectively (reviewed in refs 6,7).

Origins of the chaperone concept

Although the term 'molecular chaperone' was coined to describe the specialized function of the nuclear protein nucleoplasmin in promoting chromatin assembly[8], our understanding of the general role of chaperones in protein folding emerged mainly from research on the Hsp70s and the chaperonins. Based on their striking heat inducibility, it was proposed that the Hsp70s aid the repair or degradation of polypeptides that denature under stress[9,10]. 'Guilt by association' indicated that Hsp70 has an equally important role under non-stress conditions in stabilizing the folding and assembly intermediates of newly synthesized polypeptides: the Hsp70 homologue in the lumen of the endoplasmic reticulum (ER), BiP, was found in a complex with unassembled immunoglobulin heavy chains[11] and other secretory proteins (reviewed in ref. 4). Similarly, cytosolic Hsp70 in yeast associates transiently with newly synthesized precursor polypeptides, stabilizing them for uptake into the mitochondrion and the ER[12–14]. Mammalian Hsp70 was shown to interact with a large fraction of nascent polypeptide chains in the cytosol[15], on the basis of its ability to bind hydrophobic peptide segments in an ATP-dependent manner[16].

The functional analysis of the chaperonins provided the most compelling evidence that protein folding *in vivo* requires molecular chaperones. *Escherichia coli* cells with mutations in the gene coding for the chaperonin, GroEL, were shown to be defective in assembling bacteriophage particles[17,18]. Curiously, it was the analysis of the assembly of ribulose bisphosphate carboxylase oxygenase (Rubisco) in chloroplasts that clarified the significance of this finding. Before assembly, the Rubisco subunits form a complex with a large binding protein from which they dissociate in an ATP-dependent reaction[19,20]. This binding protein was subsequently identified as the chloroplast homologue of GroEL and of the mitochondrial chaperonin, Hsp60 (refs 21,22). Indeed, purified GroEL allowed the reconstitution of correctly assembled bacterial Rubisco *in vitro*[23], and the analysis of a yeast mutant defective in Hsp60 revealed that the biogenesis of many proteins imported into mitochondria required the chaperonin[24]. Finally, the mitochondrial system provided evidence that the chaperonins mediate the folding of monomeric proteins, rather than actively promoting assembly[25].

A puzzling conclusion from these independent lines of research was that cells contain at least two different chaperone systems with apparently overlapping functions. A coherent view emerged from the demonstration that the Hsp70 and chaperonin families can cooperate functionally *in vitro*[26]. The Hsp70 homologue of *E. coli*, DnaK, and its partner chaperone DnaJ maintain an unfolded polypeptide in a soluble, folding-competent conformation, in which it can be transferred to GroEL for folding to the native state. There is increasing evidence that similar chaperone pathways operate in the cytosol and organelles of eukaryotic cells.

Folding *in vitro* versus folding *in vivo*

Significant progress has been made in recent years in understanding the kinetics and pathways of spontaneous refolding *in*

TABLE 1 Components of the Hsp70 and chaperonin systems in bacteria and eukaryotic cells

Bacteria	Eukaryotic homologues		
Hsp70 system	Compartment	Yeast	Higher eukaryotes
Hsp70			
~70K ATPases, bind extended peptides, interact with DnaJ homologues and GrpE	Cytosol	SSA1-4; heat-inducible and constitutive forms SSB1,2: bind to polysomes	Hsp72: stress-inducible Hsc73: constitutive; binds to nascent chains
	Mitochondria	SSC1: required for protein import and folding	mHsp70
DnaK	ER lumen	Kar2/BiP: required for post-translational protein import and folding	BiP: abundant, binds unfolded ER proteins
Hsp40			
~40K proteins, bind unfolded proteins, interact with matching Hsp70s and stimulate ATP hydrolysis	Cytosol	YDJ1: interacts with Hsp70 SSA1; involved in protein transport across membranes SIS1: similarity to mammalian Hsp40	Hsp40: binds nascent polypeptides Hdj1: human Hsp40 homologue
	Mitochondria	MDJ1: required for folding of newly imported proteins	
DnaJ	ER	SCJ1 (lumen), Sec63 (membrane)	
GrpE			
~20K nucleotide-exchange factor for Hsp70	Mitochondria	MGE1: interacts with Hsp70 SSC1	
GrpE			
Chaperonin system			
GroEL family (Cpn60)			
Two rings of 7 ~60K subunits; ATPase activity, bind protein-folding intermediates, promote folding together with Hsp10 (Cpn10) cofactor	Mitochondria	Hsp60/Hsp10: required for folding of imported proteins	Hsp60/Hsp10
	Chloroplasts		Cpn60*: two homologous subunits (α and β); cooperates with cpn20† in folding Rubisco subunits
GroEL/GroES			
TRiC‡ family			
Hetero-oligomeric, 2 rings of 8 ~55K subunits; ATPase activity, bind protein-folding intermediates, promote folding in eukaryotes and Archaea	Cytosol	Defects in genes encoding TRiC subunits result in cell-cycle mutants with defects in actin and tubulin assembly	TRiC particles purified, 8 related ~55K subunits with homology to TCP1

* Chloroplast Cpn60 is also known as Rubisco-subunit-binding protein.
† The subunits of Cpn60's cooperating factor Cpn20 consist of two fused Cpn10-homologous domains.
‡ TRiC is also known as CCT (chaperonin containing t-complex polypeptide).

vitro for small proteins (reviewed in refs 27,28) (Fig. 1*a*). Briefly: (1) upon removal from denaturant, the polypeptide chain collapses into a compact shape within milliseconds, driven by the tendency to bury hydrophobic residues. This coincides with the formation of secondary structure. (2) Native tertiary structure forms as these secondary elements interact with each other to assume defined positions in space. During this process, which usually takes seconds to minutes, the polypeptide may pass through a series of kinetically defined intermediates. (3) The major rate-limiting transition state in folding lies close to the fully native state. In the case of multidomain proteins, individual domains fold first, followed by their association to folded monomers. Monomers may then associate to form oligomers.

It seems highly unlikely that two fundamentally different mechanisms exist *in vitro* and *in vivo* to explain a reaction as complex as protein folding. Yet folding *in vivo* depends on a cellular machinery that prevents protein aggregation. To understand this requirement, we have to consider the conditions in which *de novo* folding differs from *in vitro* refolding: (1) the cell cytosol is a highly crowded macromolecular environment; and (2) folding in the cell must be accomplished in the context of the vectorial synthesis of polypeptide chains on ribosomes.

(1) **Molecular crowding and protein aggregation.** Unfolded polypeptides, including compact intermediates that contain various amounts of native-like secondary structure but lack a stable hydrophobic core ('molten globules'), expose hydrophobic amino-acid side chains and therefore tend to aggregate[5,27] (Fig. 1). More advanced intermediates on the folding pathway can also give rise to aggregation[29]. The extent of aggregation *in vitro* can often be controlled by lowering the protein concentration and temperature. In contrast, cellular conditions dictate that without the intervention of a specific machinery, aggregation would outcompete correct folding, at least for a significant fraction of newly synthesized polypeptides. The concentration of nascent (ribosome-bound) chains in the cytoplasm of *E. coli* is as high as ~35 μM, assuming a uniform distribution[30]. Their effective concentration will be significantly greater, however, because of molecular crowding and because translating ribosomes are organized in polysomes. Molecular crowding refers to the fact that a considerable fraction of the cellular volume is occupied by protein and other macromolecules at a total concentration of ~340 g per litre and is therefore not available to other macromolecules[31]. Crowding is predicted to cause an increase in macromolecular association constants over those in dilute solution by several orders of magnitude.

(2) **Folding and translation.** Stable folding requires the presence of at least a complete protein domain (usually ~100–200 amino-acid residues in length). As the C-terminal ~30 amino acids of a translating polypeptide are topologically restricted by the ribosome, nascent chains remain unfolded until an entire domain has emerged (Fig. 1*b*). Thus, actively growing cells must maintain a large population of aggregation-sensitive nascent chains in a folding-competent conformation. This is thought to be achieved by the co-translational binding of molecular chaperones,

including Hsp70 and DnaJ, to the nascent chain[15,32–35], but a protective function of the ribosome itself may also be important[36]. In any case, a single-domain protein will have to fold post-translationally, after its release from the ribosome (Fig. 1*b*).

In principle, polypeptides consisting of two or more consecutive domains may fold cotranslationally and thus avoid incorrect interactions between domains during folding (Fig. 1*c*). At present, however, only scant evidence for cotranslational folding is available[35,37,38], including the finding that secretory proteins can form disulphide bonds between cysteine residues distant in sequence as they are extruded into the ER lumen (for example, see ref. 39). Cotranslational folding in the eukaryotic cytosol may require the protective function of the Hsp70 system until a protein domain is completed, and for certain proteins may then involve the cooperation of a chaperonin[35] (Fig. 5). The following sections will consider the detailed mechanisms of these two major chaperone systems.

The Hsp70 chaperone system

The Hsp70s are a family of highly conserved ATPases of relative molecular mass about 70,000 (M_r 70K) found in prokaryotes and in most of the compartments of eukaryotic cells (Table 1). They have essential roles in protein metabolism under both stress- and non-stress conditions, including functions in *de novo* protein folding and membrane translocation, the degradation of misfolded proteins as well as regulatory processes. This versatility of the Hsp70s results from their basic function, which is to bind and release hydrophobic segments of an unfolded polypeptide chain in an ATP-hydrolytic reaction cycle. Whereas binding results in the stabilization of the unfolded state, controlled release may allow progression along the folding pathway.

Important insight came from the finding that this binding/release cycle is modulated by other proteins of the Hsp70 system, most notably the DnaJs or Hsp40s. The central feature of this protein class is a conserved J-domain (named for *E. coli* DnaJ) that has been implicated in the interaction of Hsp40s with their respective Hsp70 partners. In DnaJ, this interacting domain is coupled to a polypeptide-binding domain, so that recruitment of the Hsp70, DnaK, provides the combined functions of two chaperones and ATP-dependent cycling. By joining the J-domain with a variety of protein moieties, cells use the Hsp70/Hsp40 system not only to protect a range of transiently aggregation-prone substrates, but also for specialized cellular functions[40–42]. For example, the mammalian protein auxilin binds to the clathrin coats of endocytotic vesicles, and via its C-terminal J-domain recruits the constitutively expressed Hsp70 (Hsc70) for ATP-dependent clathrin uncoating[41].

Structure of Hsp70 and DnaJ. Three-dimensional structures of these proteins are only known in part. The Hsp70s are structurally subdivided into an N-terminal ATPase domain of ~45K, which is followed by an ~18K portion containing the peptide-binding site, and a more variable ~10K segment (Fig. 2*a*). The ATPase domain has a fold identical to the globular G-actin monomer[43] and transmits ATP-dependent conformational changes to the C-terminal peptide-binding domain[44]. The ATPase domain of *E. coli* DnaK interacts with GrpE (ref. 45), DnaK's 22K nucleotide-exchange factor[44]. DnaJ may also contact the ATPase domain. An analysis by multidimensional NMR[46] indicated that the peptide-binding domain of Hsc70 (ref. 47) consists of two four-stranded antiparallel β-sheets and a single α-helix. Thus it does not show the previously proposed structural similarity to the peptide-binding region of the human major histocompatibility complex (MHC) class I molecule.

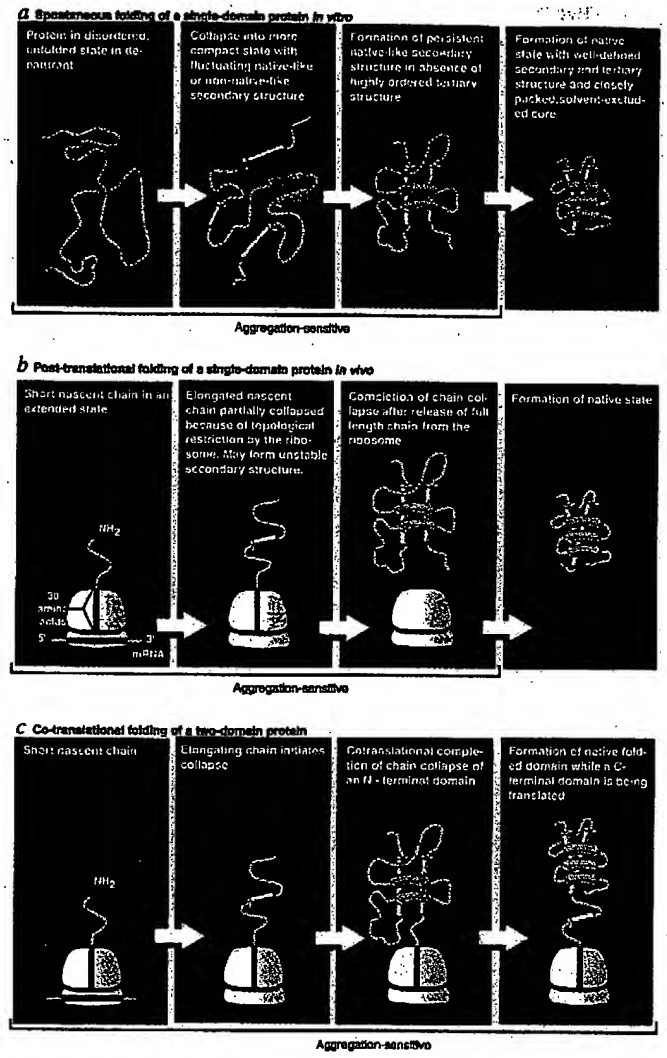

FIG. 1 Possible steps in protein folding shown for a hypothetical protein upon dilution from denaturant *in vitro* (*a*) and for translating polypeptides *in vivo* (*b*, *c*). Part *a* is adapted from ref. 153. Cylinders correspond to α-helices and arrows to β-sheets. Note that the synthesis of an average 40K polypeptide takes about 15 s in *E. coli* and 2–3 min in the eukaryotic cytosol.

Proteins of the Hsp40 family typically contain one or more blocks of sequence homology to *E. coli* DnaJ, a 41K protein with a clear domain structure (Fig. 2*a*). The N-terminal 70-amino-acid J-domain is present in all Hsp40s. The NMR-based structure of this domain describes a scaffolding of four α-helices, at the tip of which lies the conserved tripeptide His-Pro-Asp in a solvent-accessible loop region[48,49]. Substitutions within this tripeptide abrogate the interaction with DnaK[50]. Subtle structural differences between the J-domains of different Hsp40s seem to be critical in mediating their interaction with specific Hsp70 partners[42]. The J-domain is followed by a glycine-phenylalanine-rich region, a cysteine-rich central domain not present in all Hsp40s, and a C-terminal stretch found in most homologues (Fig. 2*a*). The central region contains two zinc atoms, each coordinated to four cysteines as in the zinc-fingers of DNA-binding proteins[51]. In DnaJ, this region and part of the C-terminal domain apparently participate in binding unfolded polypeptide.

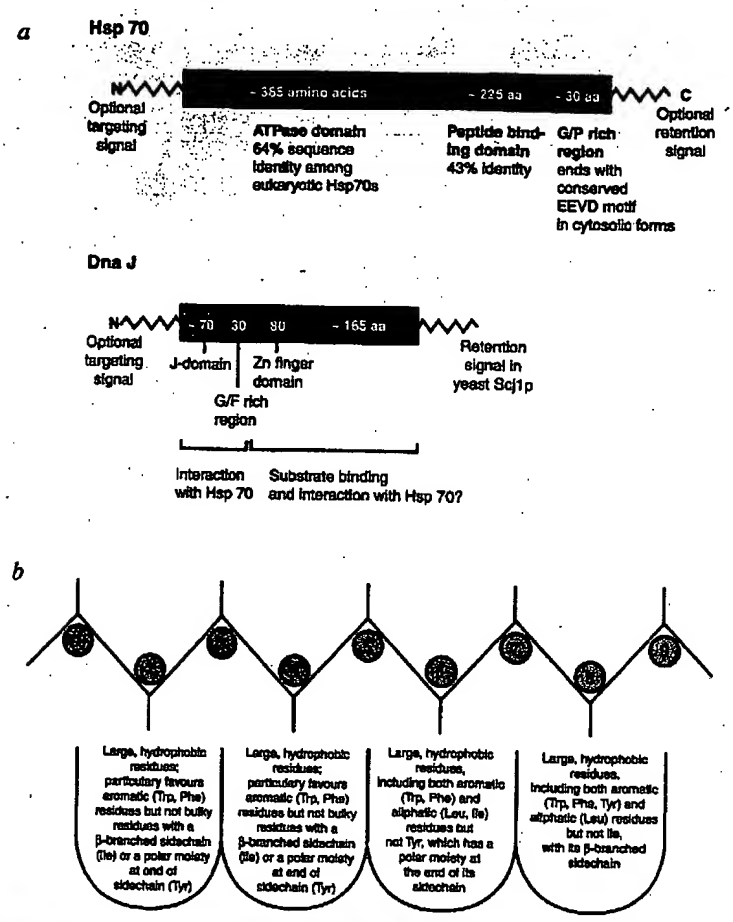

FIG. 2. Structure and function of the Hsp70 system. *a*, Consensus domain-structure of Hsp70 and DnaJ. N-terminal targeting signals for mitochondria and ER and a C-terminal ER retention signal (KDEL) occur in the eukaryotic forms localized in these organelles (Table 1). The C-terminal EEVD motif in mammalian cytosolic forms is involved in regulating interactions with the ATPase domain and with Hsp40 (ref. 151). *b*, Peptide-binding specificity of the ER homologue of Hsp70, BiP, according to ref. 52. The four putative binding pockets of Hsp70 for alternating amino-acid residues are shown. *c*, Model of the Hsp70 reaction cycle in polypeptide binding and release for bacterial DnaK, DnaJ and GrpE. U, unfolded polypeptide substrate; N, polypeptide substrate in its native state. *d*, ATP-dependent refolding of rhodanese by purified DnaJ, DnaK, GrpE, GroEL and GroES. Denatured rhodanese was first bound to DnaJ and DnaK in the presence of ATP, followed by the addition of GroEL/GroES. Folding was initiated by the GrpE-catalysed transfer of rhodanese to GroEL (from ref. 26).

Peptide binding. The various Hsp70s all have binding specificity for hydrophobic peptides, but their preference for certain amino-acid patterns may vary from compartment to compartment[16,52-54]. The ER homologue, BiP, binds with micromolar affinity to 7–8-residue peptides[16,52] corresponding to segments of a polypeptide chain that would be exposed in the unfolded state but are buried within the hydrophobic core of the folded protein. This explains the ability of Hsp70 to interact with a wide range of unfolded polypeptides while ignoring the native states of these proteins. More than one Hsp70 may interact with an unfolded polypeptide. The peptides are bound in an extended conformation[26,55,56] and a preferred pattern of certain aliphatic and aromatic residues at alternating positions in BiP-bound peptides has been described[52] (Fig. 2*b*).

The binding specificities of Hsp40 and Hsp70 differ considerably: only Hsp70 interacts efficiently with α-lactalbumin which is in an extended conformation[26]. On the other hand, *E. coli* DnaJ but not DnaK is efficient in preventing the aggregation of proteins

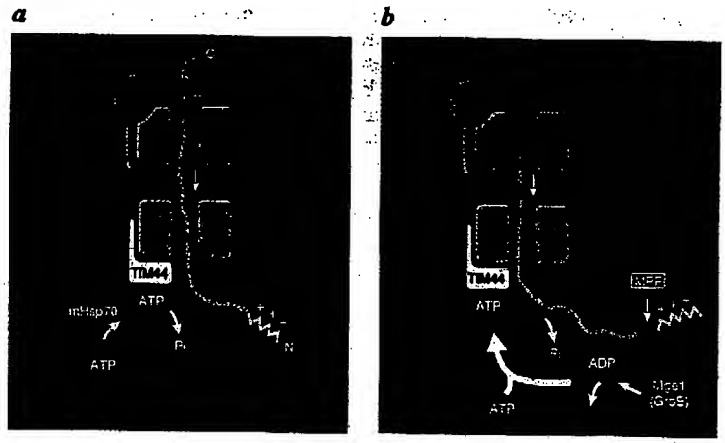

FIG. 3 Role of mitochondrial Hsp70 (mHsp70) and the GrpE homologue Mge1 in protein translocation. *a*, ATP-bound mHsp70 accepts a polypeptide segment from Tim44 (previously known as Mim44). *b*, mHsp70 binds polypeptide tightly as ATP is hydrolysed and translocation proceeds. The ADP form of mHsp70 is recycled by Mge1. R, receptor for precursor protein; OM, outer, and IM, inner mitochrondrial membrane; MPP, mitochondrial processing peptidase (adapted from ref. 73).

upon dilution from denaturant[26,57,58]. DnaJ can interact efficiently with the N-terminal segments of nascent polypeptides[33,34] and combining the binding properties of DnaJ with those of DnaK appears to be essential for the function of this chaperone system in protein folding.

The Hsp70 reaction cycle in protein folding. The ATP-dependent cycle of peptide binding and release is best understood for the bacterial Hsp70 homologue DnaK and its cofactors DnaJ and GrpE. The ATP-bound form of DnaK binds and releases peptide rapidly. In contrast, the ADP-bound form has both slow on- and off-rates for peptide[55,59]. DnaJ and GrpE, and peptide binding itself, accelerate the interconversion between these two states[58,60]. An ATP hydrolytic reaction cycle has been proposed that parallels the regulation of certain GTP-binding proteins (Fig. 2*c*). (1) The chaperone DnaJ interacts first with an unfolded polypeptide, such as a translating chain, and then targets it to DnaK. (2) DnaK binds to the polypeptide in its ATP-bound state. The interaction with DnaJ then stimulates the hydrolysis of ATP by DnaK and stabilizes its ADP-bound state. This results in the formation of a stable ternary complex of unfolded substrate polypeptide, DnaJ and DnaK. (3) The nucleotide-exchange factor GrpE promotes the release of ADP from DnaK, which is rate-limiting in the cycle. ADP dissociation may destabilize the ternary complex and may cause the release of DnaJ. (4) Substrate dissociates from DnaK upon subsequent ATP binding (not hydrolysis) to DnaK[59,61]. It then has the option of either folding, rebinding to DnaJ and DnaK, or being transferred to another chaperone system, such as the chaperonin GroEL, for final folding[26,58] (Fig. 2*c*).

In each release event from DnaJ/DnaK, a fraction of the bound polypeptide may fold, as shown for firefly luciferase *in vitro*[58]. The remainder, kinetically trapped as an unproductive intermediate, will rebind. The fraction of protein that folds upon release from DnaJ/DnaK is very small for mitochondrial rhodanese. Efficient folding of this protein depends on its GrpE-catalysed transfer from DnaJ/DnaK to GroEL[26] (Fig. 2*d*). Significantly, DnaJ/DnaK releases its substrate protein in an unfolded conformation[58,62], in contrast to the chaperonins (see below).

Although the prokaryotic and eukaryotic Hsp70 systems have similar functional properties, a GrpE-like nucleotide-exchange factor has not been found in the eukaryotic cytosol. It may be dispensable because the rate-limiting step in the ATPase cycle of eukaryotic Hsp70 is not the dissociation of ADP but rather the hydrolysis of ATP itself[63,64]. In this system ADP dissociation is even subject to negative regulation: the 41K protein Hip (also known as p48) binds specifically to the ATPase domain of mammalian Hsp70, slowing the dissociation of ADP[64,65], and may thus stabilize the interaction between Hsp70 and substrate proteins.

Function under stress conditions. Surprisingly little is known about the protective function of Hsp70s under stress conditions, such as the exposure of cells to high temperature. Although a capacity to solubilize the aggregates of certain heat-denatured proteins has been demonstrated for DnaK *in vitro*[66], a mechanism in which the chaperone binds to the substrate polypeptide during the stress-induced unfolding, thereby preventing aggregation, may predominate *in vivo*. For example, firefly luciferase expressed in *E. coli* is deactivated when the cells are shifted to 42 °C. Enzyme activity is subsequently regained at 30 °C, but only when functional DnaK, DnaJ and GrpE proteins were present during the inactivation period[57]. In eukaryotic cells, Hsp70 may cooperate with DnaJ homologues and the abundant stress-protein Hsp90 in preventing heat-induced protein denaturation[67]. The function of these components is probably complemented by a class of ATP-independent small heat-shock proteins of ~25K, which may act as a first line of defence against aggregation[68]. Notably, a capacity to solubilize pre-existent protein aggregates *in vivo* has been demonstrated for Hsp104 in yeast, a member of the Hsp100 (Clp) family of stress proteins which help organisms to survive extreme conditions[69]. There is increasing evidence that the function of chaperones in preventing or reversing protein aggregation is linked with their role in presenting misfolded polypeptides to the cellular machinery for proteolytic degradation (reviewed in ref. 70).

Protein translocation across membranes. The Hsp70s in mitochondria and the ER are not only required for the folding of newly translocated proteins, but also for the translocation process itself. The polypeptide chain traverses the mitochondrial membranes through a proteinaceous channel in an extended conformation (Fig. 3). Mitochondrial Hsp70 binds to suitable segments of the translocating chain as it emerges from the inner membrane[71], thus preventing it from sliding backwards[72] (Fig. 3*a*). Multiple events of Hsp70 binding and ATP-dependent release would then promote translocation[73] in a molecular ratchet-like mechanism[74]. Translocation requires the interaction between Hsp70 and Tim44, an inner mitochondrial membrane protein of the translocation machinery[73,75,76] which may have a limited homology to DnaJ[75]. Tim44 is thought to present segments of the incoming polypeptide to the ATP-bound form of Hsp70 (Fig. 3*a*). Recycling of Hsp70 requires the nucleotide-exchange factor Mge1 (ref. 77), the mitochondrial GrpE homologue (Fig. 3*b*). The post-translational uptake of proteins into the yeast ER seems to rely on a similar mechanism that involves the interaction of the Hsp70 in the ER lumen with the J-domain of Sec63, a membrane component of the translocation machinery[40].

In addition to its function in protein translocation, Hsp70 fulfills a regulatory role in diverse cellular processes because of its capacity to induce the disassembly of specific protein complexes. Examples include the initiation of DNA synthesis from various phage and plasmid origins of replication in *E. coli* and the uncoating of clathrin-coated endocytotic vesicles in mammalian cells (reviewed in refs 4, 66). In these cases, Hsp70 apparently interacts with proteins that expose chaperone recognition motifs in their folded states.

The chaperonin system

The chaperonins[21] have an essential function in promoting the ATP-dependent folding of proteins, both under normal growth conditions and under stress. There are two chaperonin subgroups: members of the GroEL (or Hsp60) family, and the chaperonins of the TRiC family (Table 1). (1) The GroEL-type chaperonins in eubacteria, mitochondria and chloroplasts are made of two stacked seven-membered rings of ~60K. They cooperate with a smaller protein cofactor, GroES in *E. coli*, which is a single heptameric ring of ~10K subunits. These proteins are stress-inducible, except for the chloroplast homologue. *E. coli* GroEL has an additional role in the regulation of messenger RNA turnover, which could reflect a link between chaperonins and an ancient RNA world[78]. (2) The TRiC (TCP-1 ring complex) chaperonins in archaebacteria and the eukaryotic cytosol are 8- or 9-membered double rings containing a family of ~55K subunits with homology to the TCP-1 tail complex protein from mouse. They are apparently independent of a GroES-like cofactor. Only the archaebacterial members of this family are stress-inducible. Mechanistic studies have concentrated on GroEL and GroES of *E. coli*, which together function as a protein-folding cage. Functional data for TRiC are sparse, but the conservation of the cylindrical structure suggests that it, too, provides a folding compartment. However, in contrast to the GroEL chaperonins, the eukaryotic cytosolic chaperonin appears to have a restricted range of substrates.

GroEL and GroES structure. GroEL has been widely studied by electron microscopy[79–82] and recently by X-ray crystallography[83,84]. GroEL is a cylindrical complex of ~150 Å height and ~140 Å width that encloses a central cavity ~50 Å wide, the site of polypeptide binding[79,80,81,85] (Fig. 4*a*, *b*). Each 57K subunit is composed of an apical, an intermediate and an equatorial domain. The equatorial domain contains the ATP-binding site[84] and provides most of the intersubunit interactions (Fig. 4*a*–*c*). The small intermediate domain has potential hinge regions at the domain junctions that allow for the movement of the two major domains relative to each other[82,86]. The apical domains form the flexible opening of the cylinder. Two crystal structures of GroES[87,88] revealed the dome-shaped structure of the GroES heptamer (Fig. 4*b*). Each GroES subunit contains a functionally critical loop region that protrudes from the base of the dome and becomes structured upon docking of GroES onto GroEL[89].

Polypeptide binding. In the absence of GroES, GroEL can typically bind up to two molecules of polypeptide, one in the centre of each of the two rings at the level of the apical domains[79,80,82,85]. Stable complex formation probably requires that the polypeptide makes contact with several GroEL subunits. Bound protein is in a collapsed, molten globule-like conformation containing unstable secondary structure[56,90–93]. GroEL recognizes with decreasing affinity a series of equilibrium intermediates of α-lactalbumin, ranging from extended to native-like molten globule species, and may thus assist a protein along most of its folding pathway[94]. The interaction with the substrate seems to be primarily hydrophobic in nature[94–96]. Indeed, in the crystal structure the apical domains of GroEL expose a number of hydrophobic amino-acid residues towards the cavity, mutation of which abolishes polypeptide binding[85] (Fig. 4*c*). The apical domains can undergo an *en bloc* movement relative to the intermediate domains[86], probably necessary for GroEL to accommodate its large variety of different substrates that range form ~15K to 60K in size[97–99].

The chaperonin cycle in folding. Three functional elements contribute to the high efficiency of chaperonin-assisted polypeptide folding: (1) prevention of aggregation by binding unfolded or partially folded polypeptides; (2) release of unfolded polypeptides into an enclosed folding compartment; and (3) rebinding and structural rearrangement of polypeptides that fail to fold. Although the binding of unfolded protein is independent of cofactors, the role of GroEL in providing a folding compartment critically depends on conformational changes that are induced by GroES. The exit of folded protein into free solution and the rebinding of incompletely folded substrate require the timed cycling of GroES between GroEL-bound and free states, which is controlled by the ATP-hydrolytic activity of GroEL. These aspects will be considered first, followed by a discussion of the distinct steps of the folding cycle.

As revealed by electron microscopy, the asymmetrical binding of GroES to one end-surface of GroEL induces dramatic conformational changes in the interacting GroEL ring[79,82]. The apical domains in this ring move upwards and outwards relative to the intermediate hinge domains, generating a large enclosed chamber of ~65 Å by 80 Å (ref. 82) (Fig. 4*d*). Because the hydrophobic binding regions of GroEL for polypeptide overlap with those for GoES[85], GroES binding leads to the displacement

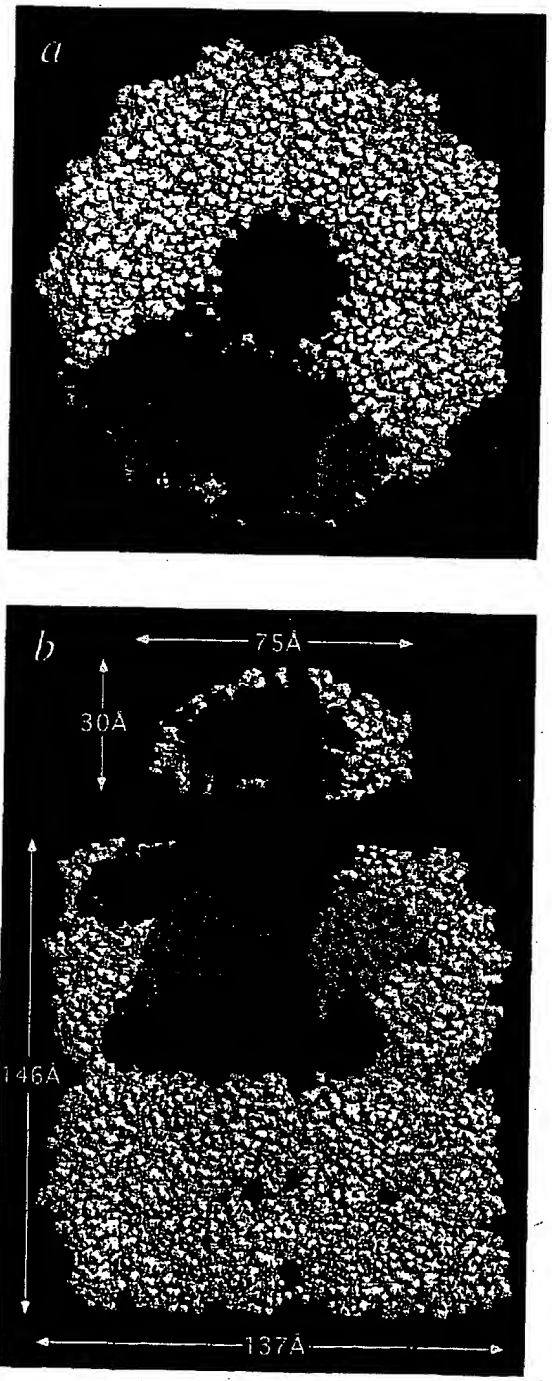

of the bound protein from its attachment sites on GroEL, forcing it into a more hydrophilic cage which is permissive for folding[100–103]. The association of GroES is sufficient to prevent the protein from diffusing out of the cage, because there is no free passage for polypeptide between GroEL rings[81,83].

The binding and unbinding of GroES relies on an interesting network of allosteric interactions, characterized by a positive cooperativity of nucleotide binding and hydrolysis at the level of the individual GroEL rings and a negative cooperativity for ligand binding between rings[100,104–110]. Initially one ring of GroEL will bind ATP and GroES, thereby directing the formation of asymmetrical GroEL:GroES particles[79,81] (Fig. 4*d*). ATP hydrolysis in the GroEL subunits that interact with GroES then gives rise to a tight GroEL–7ADP–GroES complex[100]. ATP hydrolysis in the opposite ring causes dissociation of the ADP and GroES[100,107], hence the requirement for two rings in the functional cycle.

Sufficient information is now available to describe a basic reaction scheme for GroEL–GroES function, although some details of this model may change in the future (Fig. 4*e*). (1) The acceptor state for unfolded polypeptide is the asymmetrical GroEL–GroES complex which binds substrate in the GroEL ring that is not occupied by GroES[82,100,111]. (2–3) ATP binding and hydrolysis in this ring (as well as polypeptide binding itself) cause the dissociation of ADP and GroES from the opposite ring[100,108]. (4) GroES will then rebind, together with ATP, to either GroEL ring, enclosing ~50 per cent of the bound polypeptide in the cavity[100,102,112]. The enclosed polypeptide initiates folding, whereas binding of substrate and GroES to opposite GroEL rings may result in the release of non-native polypeptide (not shown in the model; see below). (4–5) ATP hydrolysis in the GroES-bound ring tightens the interaction with GroES. (6) ATP binding and hydrolysis in the opposite ring then triggers the opening of the GroEL–GroES cage[102]. At this point, the folded polypeptide leaves, whereas incompletely folded polypeptide

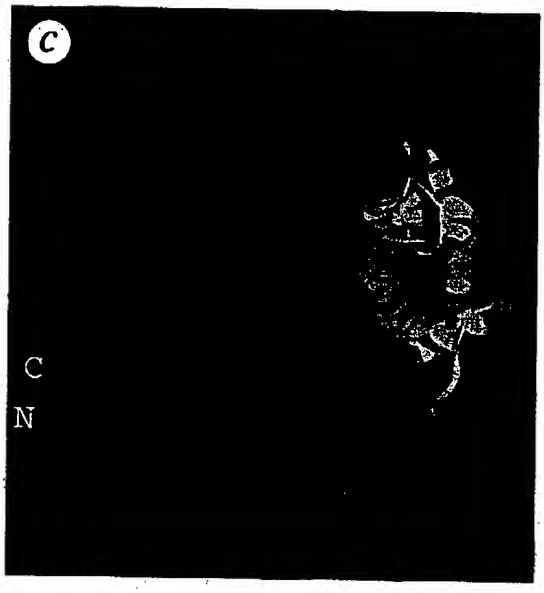

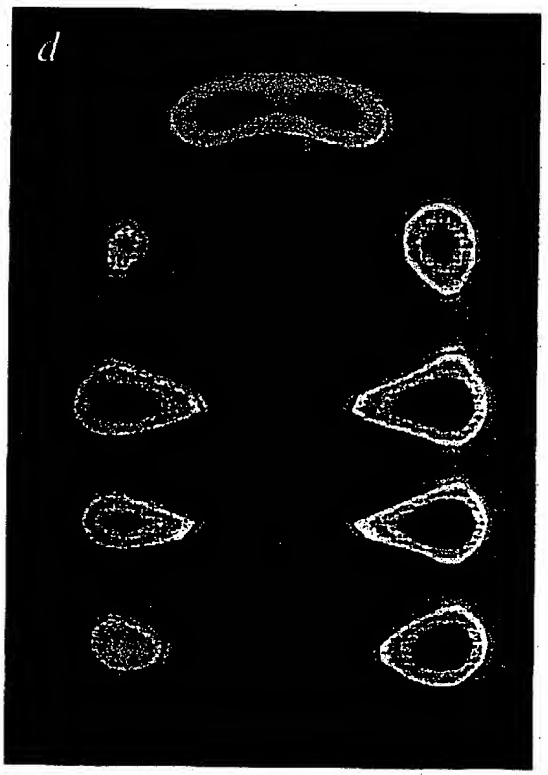

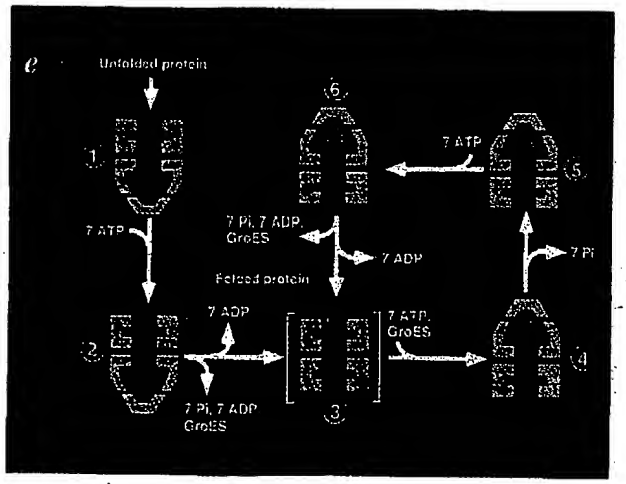

FIG. 4 Structure and function of the chaperonin system. *a*, *b*, Space-filling representations showing a top and side view, respectively, of the crystal structure of GroEL[83]. Two adjacent subunits are coloured with the apical domains in red and purple, the intermediate domains in orange and yellow, and the equatorial domains in blue and green, respectively. Free passage between GroEL rings is obstructed by N- and C-terminal residues not resolved in the crystal structure. Side view of the crystal structure of GroES[87] (shown in *b*). Two adjacent domains and the single mobile loop that is structured in the crystal owing to crystal packing are coloured. The loop regions normally protrude from the base of GroES downwards. *c*, Ribbon diagram of a GroEL subunit showing in red the location of hydrophobic residues (Tyr 199, Ser 201, Tyr 203, Phe 204, Leu 234, 237, 259, Val 263, 264) involved in polypeptide binding on the cavity-facing surface of the apical domain[85,88]. Apical, intermediate and equatorial domains in purple, yellow and green, respectively. *d*, The asymmetrical GroEL–GroES complex as revealed by cryoelectronmicroscopy (from ref. 154). Note the upward and outward movement of the apical GroEL domains interacting with GroES. *e*, Model of the GroEL–GroES reaction cycle in folding (from refs 101,102). Nucleotide-free GroEL in step (3) is thought to occur only transiently and is shown for simplicity. In step (4), GroES may either associate with the polypeptide-containing ring of GroEL or with the free ring (not shown). Light and dark pink spheres represent unfolded and folded substrate protein, respectively, and the hatched sphere indicates the presence of a mixture of folded and unfolded substrate in the population of GroEL molecules. Unfolded protein can be retained in steps (6) to (3).

rebinds[100]. The energy of rebinding may be used for (partial) unfolding[5,90,93,102] in preparation for another folding trial. Thus, folding occurs in an iterative series of reactions with first-order kinetics[102], corresponding to multiple ATPase cycles[90]. The fraction of enclosed protein that folds in a single cycle varies, dependent on the folding propensity of the specific protein and the time available between GroES binding and release[102], approximately 20 seconds at 25 °C (refs 107,108).

The release of GroES in steps (2) and (6) of the cycle can occur independently of the binding of a second GroES[108,109,112] (Fig. 4*e*). However, the transient formation of a symmetrical chaperonin particle with GroES bound to both ends of GroEL may enhance the efficiency of this reaction. Such complexes can be populated *in vitro* under a specific set of conditions[111,113–115]. Their functional significance remains to be established.

Folding in the GroEL cage. Folding in the GroEL cavity would be comparable, to a first approximation, to the folding of a single protein molecule in a test tube[5,116–118]. The basic features of this so-called Anfinsen-cage model[119,120] have been experimentally established[100,102,103]. However, placing the folding protein into the confined space of the GroEL cage may have additional physical consequences. Changing the wall of the cylinder from hydrophobic to hydrophilic may drive the burial of hydrophobic residues by the enclosed polypeptide more effectively than in free solution. The rearrangement of not-yet folded protein is a further significant improvement over spontaneous folding *in vitro*[5,93,102]. It would be equivalent to a proofreading mechanism and may result in catalysis of folding by returning incorrectly folded or kinetically trapped intermediates to a faster-folding track[121] (S. Radford, unpublished).

Strong evidence is now existing in favour of the cage model. Early experiments with purified chaperonin led to the proposal that GroES allows a protein to fold in association with GroEL to a state that is no longer aggregation-prone and is committed to complete folding successfully[90]. Indeed, several monomeric proteins reach their native, enzymatically active conformation in the GroEL cavity[102,103,122]. Assembly in the case of oligomeric proteins, however, occurs in free solution after the subunits have folded in the chaperonin cage. An alternative view held that GroEL functions by unfolding misfolded polypeptides and ejecting them in a non-native form. Folding would then occur in the bulk solution[107,112,123]. This was based on the observation that in the presence of ATP and GroES a significant fraction of bound protein can be rapidly released from GroEL in an unfolded state[107,112,123]. However, it has become clear that this reaction is not productive for folding[102,103] and rather represents a premature loss of protein that may occur when GroES and substrate protein are bound to opposite GroEL rings (see above) or when GroES unbinds. Although the magnitude of this effect in the intact *E. coli* cell is unknown, the possibility of releasing non-native protein from GroEL is probably relevant for providing an exit route for aberrant polypeptides that must be degraded[102] or in allowing the transient interaction with polypeptides that are too large to be enclosed by GroES.

Chaperonin specificity: GroEL versus TRiC. A functional comparison of GroEL with TRiC, the chaperonin of the eukaryotic cytosol (also known as CCT[124]), has shown that the chaperonin mechanism is more specific than previously assumed. TRiC is required *in vivo* for the folding of a subset of polypeptides, including actin and tubulin[125,126], and folds firefly luciferase *in vitro*[35,127]. Interestingly, both unfolded actin and luciferase form a complex with GroEL, but will not fold in the presence of ATP and GroES[127,128]. Only TRiC has the capacity of generating a set of folding intermediates that allow these proteins to proceed to the native state. TRiC differs from GroEL in that it contains up to eight distinct subunits[124]. Although the general architecture and the overall domain structure of the subunits is conserved between both chaperonins[125,127,129–132], little sequence conservation is detected between the apical polypeptide-binding domains[131,132]. This is also the region where the individual TRiC subunits deviate most from one another. Thus, TRiC may have coevolved to stabilize the productive folding intermediates of certain eukaryotic proteins. As folding apparently occurs in association with TRiC[128,133], the absence of a GroES raises the question of how the substrate is prevented from leaving the chaperonin cavity prematurely. Perhaps release from TRiC involves a stepwise dissociation of the polypeptide by domains or subdomains.

Cellular protein folding pathways

An important question concerns the extent to which molecular chaperones are actually involved in *de novo* protein folding and how different chaperones cooperate *in vivo*. A small number of recent studies, carried out in whole cells or in translation extracts, provide some information about the folding pathways of specific newly synthesized polypeptides and about the mechanisms that ensure their orderly interaction with defined sets of chaperones. A brief description of protein folding in the cytosol and in mitochondria may serve to illustrate this. A discussion of protein folding in the ER is beyond the scope of this article (reviewed in refs 4, 134).

Bacterial cytosol and mitochondrial matrix: homologous folding compartments. Both DnaK/DnaJ/GrpE and GroEL/GroES must be expressed in the *E. coli* cytosol to prevent the aggregation of a large fraction of newly synthesized polypeptides, even under non-stress conditions[135]. These components constitute a minimal set of chaperones which are typically conserved, even in small bacterial genomes[136]. Both systems interact with similar subsets of proteins, consistent with their proposed functional cooperation[26]. DnaJ and DnaK, but not GroEL, have been found in association with nascent chains and ribosomes *in vivo* and *in vitro*[33,34,137,138]. Efficient folding of rhodanese upon cell-free translation can be dependent on all five chaperone components, whereby DnaJ and DnaK must bind the polypeptide before its release from the ribosome to allow efficient transfer to GroEL[139] (J. Hendrick and F.U.H., unpublished) (Fig. 5). The interaction with DnaJ/DnaK may be preceded by the binding of trigger factor (TF) to the nascent chain[140,141], a 48K protein with ribosome affinity that was initially described as a putative chaperone for secretory proteins[142]. TF has prolyl isomerase activity *in vitro* and may act as both chaperone and folding catalyst *in vivo*[143]. An interaction between TF and GroEL has also been reported[144].

It is still unclear what fraction of cytosolic polypeptides have to interact with chaperones during translation, and the protective function of the ribosome itself needs to be fully investigated. The concentration of potential nascent chain-binding proteins is at least equivalent to that of ribosomes, but the basal level of GroEL is much lower (~4 μM, compared to ~35 μM ribosomes)[30]. Thus, the post-translational interaction with GroEL may be restricted to those proteins, which are highly aggregation-sensitive. Consistent with this, under normal growth conditions, the folding of ~30% of all cytosolic protein species was affected in a GroEL mutant strain[99]. Understanding the common structural properties of the *in vivo* substrates of GroEL and the mechanisms by which they are delivered to the chaperonin will be of considerable interest. Other questions concern the directionality of polypeptide transfer between different chaperones during folding and assembly. For example, the subunits of oligomeric proteins may engage in a renewed interaction with DnaK/DnaJ after their folding on GroEL. A retrograde transfer from the chaperonin to the Hsp70 system may also be involved in the targeting of polypeptides for degradation[70] (Fig. 5). Finally, how do large cytosolic proteins fold, such as β-galactosidase, which do not fit into the central cavity of GroEL?

Some of these questions have been addressed for the folding of proteins in the mitochondrial matrix, the evolutionary equivalent of the bacterial cytosol. Upon import into the organelles, all proteins interact first with mitochondrial Hsp70 (Fig. 3), a reaction that may be analogous to the binding of cytosolic Hsp70 to nascent chains[32]. In a process dependent on mitochondrial DnaJ and GrpE[77,145], aggregation-sensitive proteins must subsequently be transferred to the chaperonin Hsp60 for folding to the native

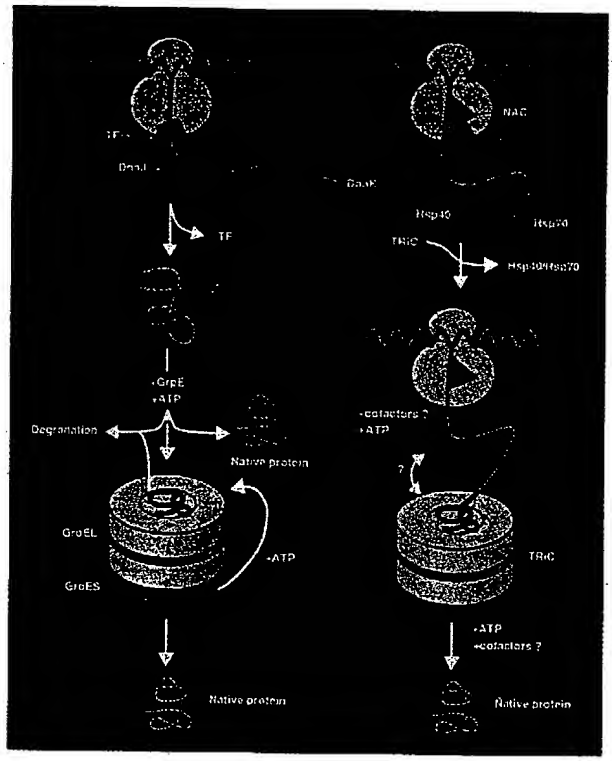

FIG. 5 Possible chaperone pathways for the folding of cytosolic proteins in bacteria (left) and in mammalian cells (right). Although alternative routes for folding are likely to exist, these pathways are thought to be involved in the folding of a subset of aggregation-sensitive polypeptides (see text). The possibility of folding without participation of chaperones in a scheme as shown in Fig. 1*b* and c is not excluded. Left, DnaJ and DnaK may also interact at a late stage of translation or post-translationally (only co-translational interaction is shown). Aberrant proteins that are unable to fold may be presented to the proteolytic degradation machinery either from DnaK/DnaJ or from GroEL (shown as release from the GroEL ring opposite GroES). Folded monomeric proteins or the folded subunits of oligomeric protein complexes are released from underneath GroES. TF, trigger factor. Right, proposed pathway for the folding of actin and firefly luciferase, based on studies in cell-free extracts[35,133]. The action of Hsp70/Hsp40 and TRiC may be functionally coupled. A polypeptide consisting of more than one domain may initiate folding cotranslationally.

state[5]. The directionality of this pathway, established in reconstitution experiments with mitochondrial rhodanese *in vitro*[26] (Fig. 2*d*), has been confirmed for rhodanese in intact organelles[146]. In contrast, proteins that refold spontaneously *in vitro* with high efficiency, such as the normally cytosolic protein dihydrofolate reductase (DHFR) from mouse, can fold independently of Hsp60, at least in mitochondria of the yeast *Saccharomyces cerevisiae* at 25 °C (refs 146, 147). Folding of these proteins may however become Hsp60-dependent at higher temperature[98]. Interestingly, in the mitochondria of another fungus, *Neurospora crassa*, DHFR interacts efficiently with Hsp60 during folding even at 25 °C (refs 25, 148), and this interaction is prolonged in organelles defective in a prolyl isomerase that accelerates DHFR folding[148]. Thus, not only the intrinsic folding propensity of a given protein and the protein environment, but also the binding properties of the chaperones it encounters may determine the extent to which the chaperone machinery participates in folding *in vivo*.

Folding in the eukaryotic cytosol. A number of components have been found to associate with nascent chains in the mammalian cytosol and are thought to be involved in their folding, including the nascent-chain-associated complex (NAC), the signal-recognition particle (SRP), Hsp70/Hsc70, the DnaJ homologue Hsp40, and the chaperonin TRiC. Although most chains seem to interact cotranslationally with Hsp70/DnaJ[15,32,35], the chaperonin TRiC apparently mediates only the folding of a limited set of proteins, as suggested by its low abundance in many cell types[5]. Thus, how the majority of cytosolic proteins in eukaryotes fold at the chaperonin step remains to be established. There is no evidence that other abundant chaperones, such as Hsp90, have a general role in *de novo* folding[68], and it is possible that only a small fraction of eukaryotic proteins need a chaperonin.

A cooperative chaperone pathway involving NAC, Hsc70/Hsp40 and TRiC has been proposed for the folding of firefly luciferase and actin based on experiments in a mammalian translation extract[35,133,149]. This pathway may be important *in vivo* for substrates such as actin and tubulin, whose folding is TRiC dependent. A model proposed to describe the sequence of steps in this reaction is shown in Fig. 5. (1) The first cytosolic factor thought to be encountered by many nascent chains is NAC, a heterodimer of 33K and 21K subunits with an affinity for ribosomes[149,150]. NAC shields the ~33 residues of a nascent polypeptide adjacent to the peptidyl transferase site and prevents the association of translating ribosomes with the ER membrane, except when a secretory protein destined for translocation into the ER is synthesized that is recognized by SRP. (2) NAC binding may signal that a nascent polypeptide is about to emerge from the ribosome and could be involved in recruiting the chaperone components required for further protection of the growing polypeptide. In any case, Hsc70 and Hsp40 can associate with nascent chains that expose less than 50 amino acid residues beyond the NAC binding site[35]. Hsp40 activates the Hsc70 ATPase[64,151] and has a catalytic function in loading Hsc70 onto the nascent chain[35] (Fig. 2*c*). (3) Unlike GroEL, TRiC has the capacity to bind to nascent polypeptides[35,133] (H. Sternlicht, unpublished), at least in an *in vitro* translation extract. TRiC can be recruited to the elongating chain when ~150–200 amino-acid residues have emerged from the ribosome, consistent with a role of TRiC in mediating the cotranslational folding of certain polypeptide domains[35] (Fig. 5). However, completion of folding is only observed after the release of the full-length polypeptide from the ribosome[35,37,133] (Fig. 1). At this point, the polypeptide–TRiC complex dissociates in an ATP-dependent reaction, resulting in the rapid formation of the native protein. Future research will have to reveal the mechanisms by which the different chaperones are specifically recruited to the translating polypeptide and the degree of their functional coupling in this pathway.

Perspectives

The principles of protein refolding established *in vitro* also govern the *de novo* folding of proteins *in vivo*. This has become clear in particular from recent studies of the chaperonin mechanism. However, the requirement of a highly coordinated protein machinery to assist a polypeptide along most of its cellular folding pathway provides a fascinating additional layer of complexity that warrants detailed analysis. It must be emphasized that proteins and the cellular folding machinery have coevolved. Thus, using chaperone components as tools, much may be learned about the properties of critical folding intermediates and the rules of the folding process.

Another focus of future research is likely to concern the possible role of molecular chaperones in various pathological states. The basic defect in a number of human genetic diseases is known to affect the folding and intracellular trafficking of key proteins[152], cystic fibrosis being perhaps the most prominent example. Molecular chaperones may also be involved in the pathogenesis of other protein-folding defects, including certain prion diseases and perhaps amyloidosis. □

F. Ulrich Hartl is in the Howard Hughes Medical Institute and Cellular Biochemistry and Biophysics Program, Memorial Sloan-Kettering Cancer Center, 1275 York Avenue, New York, New York 10021, USA

1. Anfinsen, C. B. *Science* **181,** 223–230 (1973).
2. Ellis, R. J. *Nature* **328,** 378–379 (1987).
3. Rothman, J. E. *Cell* **59,** 591–601 (1989).
4. Gething, M.-J. & Sambrook, J. *Nature* **355,** 33–45 (1992).
5. Hendrick, J. P. & Hartl, F. U. *A. Rev. Biochem.* **62,** 349–384 (1993).
6. Freedman, R. B., Hirst, T. R. & Tuite, M. F. *Trends biochem. Sci.* **19,** 331–336 (1994).
7. Schmid, F. X. *A. Rev. Biophys. biomol. Struct.* **22,** 123–143 (1993).
8. Laskey, R. A., Honda, B. M. & Finch, J. T. *Nature* **275,** 416–420 (1978).
9. Hightower, L. E. *J. Cell Physiol.* **102,** 407–427 (1980).
10. Pelham, H. R. B. *Cell* **46,** 959–961 (1986).
11. Haas, I. G. & Wabl, M. *Nature* **306,** 387–389 (1983).
12. Deshaies, R. J., Koch, B. D., Werner-Washburne, M., Craig, E. A. & Schekman, R. *Nature* **332,** 800–805 (1988).
13. Chirico, W. J., Waters, M. G. & Blobel, G. *Nature* **332,** 805–810 (1988).
14. Zimmermann, R., Sagstetter, M., Lewis, M. J. & Pelham, H. R. B. *EMBO J.* **7,** 2875–2880 (1988).
15. Beckmann, R. P., Mizzen, L. A. & Welch, W. J. *Science* **248,** 850–854 (1990).
16. Flynn, G. C., Pohl, J., Flocco, M. T. & Rothman, J. E. *Nature* **353,** 726–730 (1991).
17. Georgopoulos, C., Hendrix, R. W., Casjens, S. R. & Kaiser, A. D. *J. molec. Biol.* **76,** 45–60 (1973).
18. Coppo, A., Manzi, A., Pulitzer, J. F. & Takahashi, H. *J. molec. Biol.* **76,** 61–87 (1973).
19. Barraclough, R. & Ellis, R. J. *Biochim. biophys. Acta* **608,** 18–31 (1980).
20. Cannon, S., Wang, P. & Roy, H. *J. Cell Biol.* **103,** 1327–1335 (1986).
21. Hemmingsen, S. M. *et al. Nature* **333,** 330–334 (1988).
22. McMullin, T. W. & Hallberg, R. L. *Molec. cell. Biol.* **8,** 371–380 (1988).
23. Goloubinoff, P., Christeller, J. T., Gatenby, A. A. & Lorimer, G. H. *Nature* **342,** 884–889 (1989).
24. Cheng, M. Y. *et al. Nature* **337,** 620–625 (1989).
25. Ostermann, J., Horwich, A. L., Neupert, W. & Hartl, F.-U. *Nature* **341,** 125–130 (1989).
26. Langer, T. *et al. Nature* **356,** 683–689 (1992).
27. Creighton, T. E. *Proteins: Structures and Molecular Properties* (Freeman, New York, 1993).
28. Dobson, C. M., Radford, S. E. & Evans, P. A. *Trends biochem. Sci.* **19,** 31–37 (1994).
29. Mitraki, A., Fane, B., Haase-Pettingell, C., Sturtevant, J. & King, J. *Science* **253,** 54–58 (1991).
30. Ellis, R. J. & Hartl, F. U. *FASEB J.* **10,** 20–26 (1996).
31. Zimmerman, S. B. & Trach, S. O. *J. molec. Biol.* **222,** 599–620 (1991).
32. Nelson, R. J., Ziegelhoffer, T., Nicolet, C., Werner-Washburne, M. & Craig, E. A. *Cell* **71,** 97–105 (1993).
33. Kudlicki, W. *et al. J. biol. Chem.* **270,** 10650–10657 (1995).
34. Hendrick, J. P., Langer, T., Davis, T. A., Hartl, F. U. & Wiedmann, M. *Proc. natn. Acad. Sci. U.S.A.* **90,** 10216–10220 (1993).
35. Frydman, J., Nimmesgern, E., Ohtsuka, K. & Hartl, F. U. *Nature* **370,** 111–117 (1994).
36. Chattopadhyay, S., Das, B., Bera, A. K., Dasgupta, D. & Dasgupta, C. *Biochem. J.* **300,** 717–721 (1994).
37. Kolb, V. A., Makeyev, E. V. & Spirin, A. S. *EMBO J.* **13,** 3631–3637 (1994).
38. Fedorov, A. N. & Baldwin, T. O. *Proc. natn. Acad. Sci. U.S.A.* **92,** 1227–1231 (1995).
39. Chen, W., Helenius, J., Braakman, I. & Helenius, A. *Proc. natn. Acad. Sci. U.S.A.* **92,** 6229–6233 (1995).
40. Sanders, S. L., Whitfield, K. M., Vogel, J. P., Rose, M. D. & Schekman, R. W. *Cell* **69,** 353–365 (1992).
41. Ungewickell, E. *et al. Nature* **378,** 632–635 (1995).
42. Schlenstedt, G., Harris, S., Risse, B., Lill, R. & Silver, P. A. *J. Cell Biol.* **129,** 979–988 (1995).
43. Flaherty, K. M., DeLuca-Flaherty, C. & McKay, D. B. *Nature* **346,** 623–628 (1990).
44. Liberek, K., Skowyra, D., Zylicz, M., Johnson, C. & Georgopoulos, C. *J. biol. Chem.* **266,** 14491–14496 (1991).
45. Buchberger, A., Schröder, H., Buttner, M., Valencia, A. & Bukau, B. *Nature struct. Biol.* **1,** 95–101 (1994).
46. Morshauser, R. C., Wang, H., Flynn, G. C. & Zuiderweg, E. R. P. *Biochemistry* **34,** 6261–6266 (1995).
47. Wang, T.-F., Chang, J.-H. & Wang, C. *J. biol. Chem.* **268,** 26049–26051 (1993).
48. Szyperski, T., Pellecchia, M., Wall, D., Georgopoulos, C. & Wuthrich, K. *Proc. natn. Acad. Sci. U.S.A.* **91,** 11343–11347 (1994).
49. Hill, R. B., Flanagan, J. M. & Prestegard, J. H. *Biochemistry* **34,** 5587–5596 (1995).
50. Wall, D., Zylicz, M. & Georgopoulos, C. *J. biol. Chem.* **269,** 5446–5451 (1994).
51. Szabo, A., Korszun, R., Hartl, F. U. & Flanagan, J. *EMBO J.* **15,** 408–417 (1996).
52. Blond-Elguindi, S. *et al. Cell* **75,** 717–728 (1993).
53. Gragerov, A. & Gottesman, M. E. *J. molec. Biol.* **241,** 133–135 (1994).
54. Takenaka, I. M., Leung, S. M., Mcandrew, S. J., Brown, J. P. & Hightower, L. E. *J. biol. Chem.* **270,** 19839–19844 (1995).
55. Palleros, D. R., Welch, W. J. & Fink, A. L. *Proc. natn. Acad. Sci. U.S.A.* **88,** 5719–5723 (1991).
56. Landry, S. J., Jordan, R., McMacken, R. & Gierasch, L. M. *Nature* **355,** 455–457 (1992).
57. Schröder, H., Langer, T., Hartl, F. U. & Bukau, B. *EMBO J.* **12,** 4137–4144 (1993).
58. Xtabo, A. *et al. Proc. natn. Acad. Sci. U.S.A.* **91,** 10345–10349 (1994).
59. Schmid, D., Baici, A., Gehring, H. & Christen, P. *Science* **263,** 971–973 (1994).
60. Liberek, K., Marszalek, J., Ang, D., Georgopoulos, D. & Zylicz, M. *Proc. natn. Acad. Sci. U.S.A.* **88,** 2874–2878 (1991).
61. Palleros, D. R., Reid, K. L., Shi, L., Welch, W. J. & Fink, A. L. *Nature* **365,** 664–666 (1993).
62. Palleros, D. R., Shi, L., Reid, K. L. & Fink, A. L. *J. biol. Chem.* **269,** 13107–13114 (1994).
63. Ziegelhoffer, T., Lopezbuesa, P. & Craig, E. A. *J. biol. Chem.* **270,** 10412–10419 (1995).
64. Höhfeld, J., Minami, Y. & Hartl, F. U. *Cell* **83,** 589–598 (1995).
65. Prapapanich, V., Chen, S., Nair, S., Rimerman, R. A. & Smith, D. F. *Molec. Endocr.* **11,** 420–428 (1996).
66. Georgopoulos, C., Liberek, K., Zylicz, M. & Ang, D. *Heat-shock Proteins in Biology and Medicine* 209–249 (Cold Spring Harbor Laboratory Press, Cold Spring Harbor, New York, 1994).
67. Freeman, B. C. & Morimoto, R. I. *EMBO J.* **12,** 2969–2979 (1996).
68. Jakob, U. & Buchner, J. *Trends biochem. Sci.* **19,** 205–211 (1994).
69. Parsell, D. A., Kowal, A. S., Singer, M. A. & Lindquist, S. *Nature* **372,** 475–478 (1994).
70. Hayes, S. A. & Dice, F. J. *Cell Biol.* **132,** 255–258 (1996).
71. Kang, P. J. *et al. Nature* **348,** 137–143 (1990).
72. Ungermann, C., Neupert, W. & Cyr, D. M. *Science* **266,** 1250–1253 (1994).
73. Schneider, H. C. *et al. Nature* **371,** 768–774 (1994).
74. Simon, S. M., Peskin, C. S. & Oster, G. F. *Proc. natn. Acad. Sci. U.S.A.* **89,** 3770–3774 (1992).
75. Rassow, J. *et al. J. Cell Biol.* **127,** 1547–1556 (1994).
76. Kronidou, N. G. *et al. Proc. natn. Acad. Sci. U.S.A.* **91,** 12818–12822 (1994).
77. Westermann, B., Pripbuus, C., Neupert, W. & Schwarz, E. *EMBO J.* **14,** 3452–3460 (1995).
78. Georgellis, D., Schiberg, B., Hartl, F. U. & von Gabain, A. *Molec. Microbiol.* **16,** 1259–1268 (1995).
79. Langer, T., Pfeifer, G., Martin, J., Baumeister, W. & Hartl, F. U. *EMBO J.* **11,** 4757–4765 (1992).
80. Braig, K., Simon, M., Furuya, F., Hainfeld, J. F. & Horwich, A. L. *Proc. natn. Acad. Sci. U.S.A.* **90,** 3978–3982 (1993).
81. Saibil, H. R. *et al. Curr. Biol.* **3,** 265–273 (1993).
82. Chen, S. *et al. Nature* **371,** 261–264 (1994).
83. Braig, K. *et al. Nature* **371,** 578–586 (1994).
84. Bolsvert, D. C., Wang, J., Otwinowski, Z., Horwich, A. L. & Sigler, P. B. *Nature struct. Biol* **3,** 170–177 (1996).
85. Fenton, W. A., Kashi, Y., Furtak, K. & Horwich, A. L. *Nature* **371,** 614–619 (1994).
86. Braig, K., Adams, P. D. & Brünger, A. T. *Nature struct. Biol.* **2,** 1083–1084 (1995).
87. Hunt, J. F., Weaver, A. J., Landry, S. J., Gierasch, L. & Deisenhofer, J. *Nature* **379,** 37–42 (1996).
88. Mande, S. C., Mehra, V., Bloom, B. & Hol, W. G. J. *Science* **271,** 203–207 (1996).
89. Landry, S. J., Zeilstra, R. J., Fayet, O., Georgopoulos, C. & Gierasch, L. M. *Nature* **364,** 255–258 (1993).
90. Martin, J. *et al. Nature* **352,** 36–42 (1991).
91. Robinson, C. V. *et al. Nature* **372,** 646–651 (1994).
92. Zahn, R., Spitzfaden, C., Ottiger, M., Wuthrich, K. & Pluckthun, A. *Nature* **368,** 261–265 (1994).
93. Zahn, R., Perret, S., Stenberg, G. & Fersht, A. R. *Science* **271,** 642–645 (1996).
94. Hayer-Hartl, M. K., Ewbank, J. J., Creighton, T. E. & Hartl, F. U. *EMBO J.* **13,** 3192–3202 (1994).
95. Lin, Z., Schwarz, F. P. & Eisenstein, E. *J. biol. Chem.* **270,** 1011–1014 (1995).
96. Hlodan, R., Tempst, P. & Hartl, F. U. *Nature struct. Biol.* **2,** 587–595 (1995).
97. Viitanen, P. V., Gatenby, A. A. & Lorimer, G. H. *Protein Sci.* **1,** 363–369 (1992).
98. Martin, J., Horwich, A. L. & Hartl, F. U. *Science* **258,** 995–998 (1992).
99. Horwich, A. L., Low, K. B., Fenton, W. A., Hirshfield, I. N. & Furtak, K. *Cell* **74,** 909–917 (1993).
100. Martin, J., Mayhew, M., Langer, T. & Hartl, F. U. *Nature* **366,** 228–233 (1993).
101. Hartl, F. U. *Nature* **371,** 557–559 (1994).
102. Mayhew, M. *et al. Nature* **379,** 420–426 (1996).
103. Weissman, J. S., Rye, H. S., Fenton, W. A., Beechem, J. M. & Horwich, A. L. *Cell* **84,** 481–490 (1996).
104. Gray, T. E. & Fersht, A. R. *FEBS Lett.* **292,** 254–258 (1991).
105. Todd, M. J., Viitanen, P. V. & Lorimer, G. H. *Biochemistry* **32,** 8560–8567 (1993).
106. Jackson, G. S. *et al. Biochemistry* **32,** 2554–2563 (1993).
107. Todd, M. J., Viitanen, P. V. & Lorimer, G. H. *Science* **265,** 659–666 (1994).
108. Hayer-Hartl, M. K., Martin, J. & Hartl, F. U. *Science* **269,** 836–841 (1995).
109. Burston, S. G., Ranson, N. A. & Clarke, A. R. *J. molec. Biol.* **249,** 138–152 (1995).
110. Yifrach, O. & Horovitz, A. *Biochemistry* **34,** 5303–5308 (1995).
111. Engel, A. *et al. Science* **279,** 832–836 (1995).
112. Weissman, J. S. *et al. Cell* **83,** 577–587 (1995).
113. Llorca, O., Marco, S., Carrascosa, J. L. & Valpuesta, J. M. *FEBS Lett.* **345,** 181–186 (1994).
114. Schmidt, M. *et al. Science* **265,** 656–659 (1994).
115. Azem, A., Kessel, M. & Goloubinoff, P. *Science* **265,** 653–656 (1994).
116. Nilsson, B. & Anderson, S. *A. Rev. Microbiol.* **45,** 607–635 (1991).
117. Creighton, T. E. *Nature* **352,** 17–18 (1991).
118. Agard, D. A. *Science* **260,** 1903–1904 (1993).
119. Ellis, R. J. *Curr. Biol.* **4,** 633–635 (1994).
120. Ellis, R. J. *Fold. Des.* **1,** R9–R15 (1996).
121. Ranson, N. A., Dunster, N. J., Burston, S. G. & Clarke, A. R. *J. molec. Biol.* **250,** 581–586 (1995).
122. Gray, T. E. & Fersht, A. R. *J. molec. Biol.* **232,** 1197–1207 (1993).
123. Weissman, J. S., Kashi, Y., Fenton, W. A. & Horwich, A. L. *Cell* **78,** 693–702 (1994).
124. Kubota, H., Hynes, G., Carne, A., Ashworth, A. & Willison, K. *Curr. Biol.* **4,** 89–99 (1994).
125. Gao, Y., Thomas, J. O., Chow, R. L., Lee, G. H. & Cowan, N. J. *Cell* **69,** 1043–1050 (1992).
126. Yaffe, M. B. *et al. Nature* **358,** 245–248 (1992).
127. Frydman, J. *et al. EMBO J.* **11,** 4767–4778 (1992).
128. Tian, G. L., Vainberg, I. E., Tap, W. D., Lewis, S. A. & Cowan, N. J. *Nature* **375,** 250–253 (1995).
129. Trent, J. D., Nimmesgern, E., Wall, J. S., Hartl, F. U. & Horwich, A. L. *Nature* **354,** 490–493 (1991).
130. Phipps, B. M. *et al. Nature* **361,** 475–477 (1993).
131. Kim, S., Willison, K. R. & Horwich, A. L. *Trends biochem. Sci.* **19,** 543–548 (1994).
132. Waldmann, T., Lupas, A., Kellermann, J., Peters, J. & Baumeister, W. *Biol. Chem. Hoppe Seyler* **376,** 119–126 (1995).
133. Frydman, J. & Hartl, F. U. *Science* **272,** 1497–1502 (1996).
134. Bergeron, J. J., Brenner, M. B., Thomas, D. Y. & Williams, D. B. *Trends biochem. Sci.* **19,** 124–128 (1994).
135. Gragerov, A. *et al. Proc. natn. Acad. Sci. U.S.A.* **89,** 10341–10344 (1992).
136. Koonin, E. V., Mushegian, A. R. & Rudd, K. E. *Curr. Biol.* **6,** 404–416 (1966).
137. Gaitanaris, G. A., Vysokanov, A., Hung, S.-Z., Gottesman, M. & Gragerov, A. *Molec. Microbiol.* **14,** 861–869 (1994).
138. Vysokanov, A. V. *FEBS Lett.* **378,** 211–214 (1995).
139. Kudlicki, W., Odom, O. W., Kramer, G. & Hardesty, B. *J. molec. Biol.* **244,** 319–331 (1994).
140. Valent, Q. A. *et al. EMBO J.* **14,** 5494–5505 (1995).
141. Hesterkamp, T., Hauser, S., Lütcke, H. & Bukau, B. *Proc. natn. Acad. Sci. U.S.A.* **93,** 4437–4441 (1996).
142. Crooke, E. & Wickner, W. *Proc. natn. Acad. Sci. U.S.A.* **84,** 5216–5220 (1987).
143. Stoller, G. *et al. EMBO J.* **14,** 4939–4948 (1995).
144. Kandror, O., Sherman, M., Rhode, M. & Goldberg, A. L. *EMBO J.* **14,** 6021–6027 (1995).
145. Rowley, N. *et al. Cell* **77,** 249–259 (1994).
146. Rospert, S. *et al. EMBO J.* **15,** 764–774 (1996).
147. Höhfeld, J. & Hartl, F. U. *J. Cell Biol.* **126,** 305–315 (1994).
148. Rassow, J. *et al. Molec. cell. Biol.* **15,** 2654–2662 (1995).
149. Wiedmann, B., Sakai, H., Davis, T. A. & Wiedmann, M. *Nature* **370,** 434–440 (1994).
150. Wang, S., Sakai, H. & Wiedmann, M. *J. Cell Biol.* **130,** 519–527 (1995).
151. Freeman, B. C., Myers, M. P., Schumacher, R. & Morimoto, R. I. *EMBO J.* **14,** 2281–2292 (1995).
152. Amara, J. F., Cheng, S. H. & Smith, A. E. *Trends Cell Biol.* **2,** 145–149 (1992).
153. Dobson, C. M. *Curr. Biol.* **2,** 343–345 (1992).
154. Saibil, H. R. *Nature struct. Biol.* **1,** 838–842 (1994).

ACKNOWLEDGEMENTS. Limited space has meant that it has not been possible to cite all relevant references. I thank F. Ichert and M. Mayhew for preparing the figures; B. Netzer, J. Hendrick, J. Frydman and M. Hartl for critically reading the manuscript; T. Creighton, J. Ellis, C. Dobson, J. Hunt and S. Radford for discussion; H. Deisenhofer and J. Hunt for the crystallographic coordinates of GroES; and R. Morimoto, W. Neupert, H. Sternlicht and S. Radford for sharing unpublished data.

Wilson, K. L. 1992. *J. Cell Biol.* 116:281–94
184. Serafini, T., Orci, L., Amherdt, M., Brunner, M., Kuhn, R. A., et al. 1991. *Cell* 18:239–53
185. Donaldson, J. G., Cassel, D., Kuhn, R. A., Klausner, R. D. 1992. *Proc. Natl. Acad. Sci. USA* 89:6408–12
186. Tartakoff, A. M. 1986. *EMBO J.* 5: 1477–82
187. Bergmann, J. E., Singer, S. J. 1983. *J. Cell Biol.* 97:1777–87
188. Burke, B. 1990. *Exp. Cell Res.* 186: 169–76
189. Glass, J. R., Gerace, L. 1990. *J. Cell Biol.* 111:1047–57
190. Doering, V., Stick, R. 1990. *EMBO J.* 9:4073–81
191. Wilson, K. L., Newport, J. 1988. *J. Cell Biol.* 107:57–68
192. Palement, J. 1981. *Exp. Cell Res.* 134:93–102
193. Wilson, D. W., Wilcox, C. A., Flynn, G. C., Chen, E., Kuang, W.-J., et al. 1989. *Nature* 339:355–60
194. Beckers, C. J. M., Block, M. R., Glick, B. S., Rothman, J. E., Balch, W. E. 1989. *Nature* 339:397–98
195. Diaz, R., Mayorga, L. S., Weidman, P. J., Rothman, J. E., Stahl, P. D. 1989. *Nature* 339:398–400
196. Stick, R., Angres, B., Lehner, C. F., Nigg, E. A. 1988. *J. Cell Biol.* 107: 397–406
197. Alcade, J., Bonay, P., Roa, A., Vilaro, S., Sandoval, I. V. 1992. *J. Cell Biol.* 116:69–83
198. Schroer, T. A., Sheetz, M. P. 1991. *Annu. Rev. Physiol.* 53:629–52
199. Allan, V. J., Vale, R. D. 1991. *J. Cell Biol.* 113:347–59
200. Ho, W. C., Allan, V. J., van Meer, G., Berger, E. G., Kreis, T. E. 1989. *Eur. J. Cell. Biol.* 48:250–63
201. Corthésy-Theulaz, I., Pauloin, A., Pfeffer, S. R. 1992. *J. Cell Biol.* 118:1333–45
202. Moskalewski, S., Thyberg, J. 1992. *J. Submicrosc. Cytol. Pathol.* 24:In press
203. Wilson, E. B. 1931. *J. Morphol. Physiol.* 52:429–83
204. Stachelin, L. A., Giddings, T. H., Kiss, J. Z., Sack, F. D. 1990. *Protoplasma* 157:75–91
205. Rappaport, R. 1986. *Int. Rev. Cytol.* 105:245–81
206. Johnson, B. F., Calleja, G. B., Boisclair, L., Yoo, B. Y. 1979. *Exp. Cell Res.* 123:253–59
207. Preuss, D., Mulholland, J., Kaiser, C. A., Orlean, P., Albright, C., et al. 1992. *Yeast* 7:891–911
208. Weisman, L. S., Wickner, W. 1988. *Science* 241:589–91
209. Yaffe, M. P. 1991. *Trends Cell Biol.* 1:160–64
210. McConnell, S. J., Yaffe, M. P. 1992. *J. Cell Biol.* 118:385–95
211. Stewart, L. C., Yaffe, M. P. 1991. *J. Cell Biol.* 115:1249–57
212. Raymond, C. K., O'Hara, P. J., Eichinger, G., Rothman, J. H., Stevens, T. H. 1990. *J. Cell Biol.* 111:877–92
213. Weisman, L. S., Bacallao, R., Wickner, W. 1987. *J. Cell Biol.* 105:1539–47
214. Weisman, L. S., Emr, S. D., Wickner, W. T. 1990. *Proc. Natl. Acad. Sci. USA* 87:1076–80
215. Shaw, J. M., Wickner, W. T. 1991. *EMBO J.* 10:1741–48
216. Zorn, G. A., Lucas, J. J., Kates, J. R. 1979. *Cell* 18:659–72
217. Maniatis, A., Schliwa, M. 1991. *Cell* 67:495–504
218. Quintart, J., Baudhuin, P. 1976. *Arch. Int. Physiol. Biochim.* 84:409–10
219. Quintart, J., Leroy-Houyet, M. A., Trouet, A., Baudhuin, P. 1979. *J. Cell Biol.* 82:644–53
220. Rothberg, K. G., Heuser, J. E., Donzell, W. C., Ying, Y.-S., Glenney, J. R., et al. 1992. *Cell* 68:673–82

Annu. Rev. Biochem. 1993. 62:349–84

MOLECULAR CHAPERONE FUNCTIONS OF HEAT-SHOCK PROTEINS

Joseph P. Hendrick and Franz-Ulrich Hartl
Program of Cellular Biochemistry and Biophysics, Rockefeller Research Laboratories, Sloan-Kettering Institute, 1275 York Avenue, New York, New York 10021

KEY WORDS: protein folding in the cell, Hsp60, Hsp70, Hsp90, TCP1

CONTENTS

0066-4154/93/0701-0349$02.00

1. PERSPECTIVES AND OVERVIEW

Molecular chaperones, many of them so-called heat-shock or stress proteins (hsps), have emerged over recent years as an important topic in cell biology. The functions of these proteins under normal cellular conditions as well as under conditions of stress are the focus of intensive research activity of cell biologists, biochemists, and, more recently, biophysicists. From the wealth of studies available to date, it appears that the major importance of molecular chaperones lies in the area of protein folding. The long-held view that newly synthesized proteins in the cell fold in a largely spontaneous process has been called into question. Although the basic principle that the primary sequence of a protein is sufficient to specify its three-dimensional structure remains unchallenged, protein folding in cells, as opposed to the test tube, depends on helper proteins (Table 1). In this review we focus on the function of the major hsp70, hsp60, and hsp90 classes of molecular chaperones, emphasizing the functional cooperation between different chaperones and their interactions with specific regulatory proteins. We summarize the major lines of evidence (1–59) that molecular chaperones are involved in a multitude of processes, in different cellular compartments, wherever the folded state of proteins has to be achieved de novo, stabilized under stress conditions, or modulated to regulate their activity state. Our discussion also includes the recently discovered chaperones of the TCP1 family, which may have hsp60-like functions in the eukaryotic cytosol. For an overview of the functions of other non-heat-shock chaperone systems, the reader may be referred to recent articles by Gething & Sambrook (60) and Freedman (61).

The Molecular Chaperone Concept

A biochemist of our acquaintance, probably echoing the thoughts of others, has declared that a molecular chaperone is "any protein that binds another protein and has no function of its own." According to a more traditional definition, chaperones are "a family of unrelated classes of protein that mediate the correct assembly of other polypeptides, but are not themselves components of the final functional structure" (62). A survey of the literature suggests that "molecular chaperone" has a broad range of meanings. Clearly, one defining characteristic is the role of chaperones in modulating protein conformation.

The term "molecular chaperone" was coined to describe the function of nucleoplasmin, an abundant protein found in *Xenopus* oocytes that binds tightly to purified histones and promotes nucleosome assembly by donating the bound histone to assembling chromatin (1). The term was subsequently applied to a larger family of proteins, whose function is to ensure that the assembly of certain other polypeptide chains occurs correctly (63). Identification of molecular chaperones has profited from the fact that many of them are among the set of heat-shock proteins (hsps) selectively expressed in cells

Table 1 Molecular chaperone functions of heat shock proteins hsp70, hsp60, and hsp90

Subcellular localization	Organism	Chaperone	Cooperating factors	Activity
Hsp70 family				
Prokaryotes				
Cytosol	*E. coli*	DnaK	DnaJ, GrpE	Stabilizes newly made proteins in vivo (28); preserves folding competence of proteins in vitro (29); stimulates protein export (30); promotes assembly/disassembly of replication complexes (24, 150–152); reactivates heat-inactivated RNA polymerase (15); facilitates degradation of abnormal proteins (20); controls heat-shock response (167).
Eukaryotes				
Cytosol	*S. cerevisiae*	Ssa1-4p	NEM-sensitive factor, YDJ1p	Stimulates protein transport into ER (7, 8), mitochondria (8, 9, 132), chloroplasts (244), and nucleus (106); binds to nascent polypeptides (12), and to polypeptides containing abnormal amino acids (133); dissociates clathrin from clathrin coats (6); promotes lysosomal degradation of cytosolic proteins (21); interacts with HSF transcription factor (167).
	Rabbit	Hsc73	NEM-sensitive factor	
	Human	Hsc73	None identified	
Endoplasmic reticulum	*S. cerevisiae*	Kar2p	Sec63p	Promotes protein translocation into ER (16, 19, 158); binds unassembled or misfolded subunits of multisubunit ER proteins (2, 4, 5, 159–162).
	Mammals	BiP/Grp78	None identified	
Mitochondria	*S. cerevisiae*	Ssc1p		Promotes protein translocation into mitochondria and subsequent folding (13, 14, 93).
Chloroplasts	*P. sativum*	cHsp70	None identified	Promotes insertion of light-harvesting complex protein into thylakoid membrane (245, 246).
	E. gracilis			

Table 1 (*continued*)

Subcellular localization	Organism	Chaperone	Cooperating factors	Activity
Hsp60 family				
Prokaryotes				
Cytosol	*E. coli*	GroEL	GroES	Promotes folding in vivo of overproduced proteins and refolding of many proteins in vitro (34, 35, 37, 38, 40–44, 189–195); required for phage assembly in vivo (31); facilitates export of β-lactamase (247); stabilizes proteins during heat stress (208–210).
Eukaryotes				
Mitochondria	*S. cerevisiae* *N. crassa*	Hsp60	Hsp10	Promotes folding and assembly of newly imported proteins (36, 39); stabilizes proteins destined for re-export to intermembrane space (240); binds heat-denatured mitochondrial proteins and prevents aggregation (208).
	Mammals	Hsp58	Hsp10	Binds newly imported proteins (248); promotes in vitro assembly of trimeric ornithine carbamoyltransferase (183).
Chloroplasts	Plants	Cpn60, rubisco binding protein	Cpn10	Required for assembly of ribulose bisphosphate carboxylase (32, 33, 85), and probably other chloroplast proteins.
TRiC family				
Archaebacteria				
Cytosol	*Sulfolobus*	TF55	None identified	Binds thermally denatured proteins, hydrolyzes ATP (45).
	Pyrodictium			Has ATPase activity (211).
Eukaryotes				
Cytosol	Mammals	TRiC (TCP1-containing ring complex)	None identified	Binds newly synthesized tubulin in reticulocyte extracts (49); promotes folding of actin, tubulin, and firefly luciferase (46–48).
Hsp90 family				
Prokaryotes				
Cytosol	*E. coli*	HtpG	None identified	Function unknown (220).
Eukaryotes				
Cytosol	Mammals	Hsp90 (Hsp83, 89)	p59 immunophilin (p50, hsp56); hsp70	Binds to steroid receptors (217) and dioxin receptor (219) and stabilizes the high-affinity ligand-binding form; binds $pp60^{v\text{-}src}$ and inhibits its tyrosine kinase activity (223); binds ATP and autophosphorylates (56); binds casein kinase II and prevents its aggregation (227); chaperones in vitro folding of citrate synthase (237).
	S. cerevisiae			Promotes hormone response by introduced glucocorticoid receptor (54).
	T. cruzii, C. fasciculata trypanosome	Hsp83	None identified	Has high peptide-stimulated ATPase activity (249).
Endoplasmic reticulum	Mammals	Grp94 (ERp99)	None identified	Function unknown (221, 222).
	Chicken	(Hsp100)		Binds actin and Ca/calmodulin (223). Function unknown (224).

exposed to metabolic stress. Pelham, speculating on possible roles of the abundant hsp70 family of heat-shock proteins, proposed that they might function via binding and release of solvent-exposed hydrophobic regions of unfolded proteins that would normally be buried in the native state (64). Rothman, comparing the features of protein folding deduced from in vitro refolding studies with the features of protein synthesis in the cell, concluded that protein folding in the cell must involve stabilization of nascent polypeptides and folding chains (65). The polypeptide-binding properties of hsp70s and hsp60s make them likely candidates as protein-folding proteins. Indeed, the concept of molecular chaperones has evolved from their original definition as temporary partners of unassembled subunits of oligomeric enzymes to the current idea that they are components that function during the folding of monomeric polypeptide chains (66, 67).

The relatively long-lived stabilization of protein subunits of oligomeric assemblies by molecular chaperones can now be seen as one extreme of their normally transient interaction with newly made proteins. Unstable or aggregation-prone conformations of proteins occur unavoidably as intermediates in the synthesis, transport, assembly, and perhaps even during the normal functioning of many cellular proteins. *Presently, we define a molecular chaperone as a protein that binds to and stabilizes an otherwise unstable conformer of another protein—and by controlled binding and release of the substrate protein, facilitates its correct fate in vivo: be it folding, oligomeric assembly, transport to a particular subcellular compartment, or controlled switching between active/inactive conformations.* To fulfill these functions, chaperones must recognize structural elements generally exposed by proteins in non-native conformations.

Common features but also distinct differences between the families of molecular chaperones have recently emerged. The basic paradigm of ATP-independent binding and ATP-hydrolysis-dependent release of substrate proteins links the members of the hsp70 and hsp60 families. Yet it is their structural and functional differences that are most interesting. While the hsp70s are functional as monomers or dimers, the hsp60 proteins (chaperonins) are large oligomers, usually a 14-subunit double toroid of stacked heptamers. DnaK protein from *Escherichia coli* (an hsp70) and GroEL (an hsp60) have distinct binding specificities towards proteins and peptides, which may reflect a sequential pathway of interactions with folding proteins. The emerging paradigm is that the binding and release of unfolded proteins is controlled through (*a*) the regulation of chaperones by specific protein modulators of their binding (and ATP hydrolyzing) activities and (*b*) through the functional cooperation of different chaperones with each other. As a result, newly made, unfolded, or partly folded proteins could be transferred in an orderly manner to the various polypeptide-handling systems of the cell.

2. MOLECULAR CHAPERONE FUNCTION DURING PROTEIN FOLDING

Anfinsen's pioneering work on the refolding of ribonuclease established that, in principle, all the information needed to specify the three-dimensional fold of a protein is contained in its amino acid sequence (68). Yet it has been calculated that the time required for a large polypeptide to sample all possible conformations on its way to the native state would be on the order of the age of the universe (69). In light of this, the study of protein folding has centered on the description of folding intermediates and the characterization of pathways during the refolding of denatured proteins (68, 70–73). Most proteins can be refolded if conditions (for example, low protein concentration and low temperature) are chosen such that folding is favored over the major competing reaction, aggregation of early folding intermediates (74). A number of intermediate steps in protein folding, occurring on distinct time scales, have been described (75). Only in recent years, however, have cell biologists and physical biochemists turned their attention to the problem of how the details of protein refolding from the denatured state relate to the process of folding as it occurs in the cell (60, 61, 65, 76–78).

Differences Between In Vitro and In Vivo Folding

Early intermediates in refolding form on a millisecond time scale, while extrusion of a protein from the ribosome or across a membrane takes seconds to minutes. In principle, N-terminal peptides could adopt a native-like structure during translation (79–82). However, the consensus from refolding experiments is that early elements of folded structure, although they might be native-like, are in rapid equilibrium with the unfolded state (71, 72, 83). The formation of stable structure requires the presence of a complete protein domain. For example, C-terminally truncated versions of ribonuclease A and staphylococcal nuclease, which can be regarded as in vitro mimics of a ribosome-associated chain, assume compact conformations but do not fold to an enzymatically active state (84, 84a).

Although a nascent polypeptide would not be expected to adopt a stable structure, neither could such a polypeptide chain retain an extended conformation. In an aqueous milieu, hydrophobic forces drive the rapid collapse of a polypeptide chain into a compact state (75); reviewed in (71–73, 85). The kinetic intermediates arising from hydrophobic collapse are thought to have properties similar to the equilibrium "molten globule" state of some proteins: they are compact in size, being slightly larger than the native state, possess significant secondary structure, but have few persistent tertiary interactions and a conformational flexibility more like the unfolded than the native state (73, 86–88). In such molecules, hydrophobic residues normally buried in the

interior of the native protein are transiently exposed on the surface, giving rise to a tendency to aggregate that is an important characteristic of both equilibrium molten globule forms and early folding intermediates (74, 86). An actively growing cell, then, must maintain a population of aggregation-prone nascent and newly synthesized polypeptides in a folding-competent state. Synthesis and folding must proceed in an orderly manner at a wide range of temperatures, and within the dense protein solution of the cell, which has an estimated concentration of nascent polypeptides as high as 50 μM (the concentration of ribosomes in a bacterial cell) (89).

Chaperones Allow Proteins To Pursue Their Folding Potential

As a direct consequence of the cellular conditions for protein folding, an important aspect of molecular chaperone function is to prevent the aggregation of partially folded nascent and newly completed polypeptides and to ensure their proper folding. Thus, the modulation of protein folding by chaperones reaches beyond the stabilization of nascent chains. This becomes apparent with proteins that fold following posttranslational transfer from the cytosol into organelles such as mitochondria. For these proteins the formation of stable tertiary structure prior to membrane transfer must be prevented (90, 91). During translocation across the mitochondrial membranes proteins apparently adopt an extended structure (92). Their folding within the organelles occurs in a process dependent on ATP hydrolysis and molecular chaperones of the hsp70 and hsp60 classes (13, 39, 93). As is discussed in subsequent sections, similar mechanisms of sequential chaperone action may apply to the folding of newly translated polypeptides in the cytosol. Protein folding in the endoplasmic reticulum (ER) also can occur long after translation, in a process that requires ATP and the hsp70 BiP in the ER lumen (60, 94).

The native form of many proteins is a covalently modified version of the initial translation product. As a result, the form of a protein that undergoes the early stages of de novo folding may be distinct from the stably folded mature form. For example, newly synthesized proteins can be modified by specific proteolysis, as in the removal of amino-terminal presequences containing the targeting information for protein export. These additional peptides function in part by modifying the folding kinetics of the attached mature sequences, which in turn increases their ability to interact with molecular chaperones (25, 95, 96). In addition, N-terminal propeptides exist on certain secreted proteins in both eukaryotes and prokaryotes, which act in a manner distinct from presequences. In a reaction that has been called "intramolecular chaperoning," the propeptides of subtilisin (97), α-lytic protease (98), activin A, and TGF-β1 (99) promote the formation of biologically active forms of these polypeptides prior to their removal by

cellular proteases or by autocatalyzed cleavage. In the endoplasmic reticulum, many proteins undergo covalent modifications such as the attachment of carbohydrate moieties, the formation of disulfide bonds, and the hydroxylation of prolines (60, 61). The possible interaction of the enzymes responsible for these modifications with the molecular chaperones during folding will be a subject of future research.

3. HSP70 PROTEINS: CHAPERONES WITH DIVERSE ROLES IN PROTEIN METABOLISM

Members of the hsp70 protein family were first noted as a family of stress-inducible proteins of approximately 70 kDa found in many different organisms [for reviews, see (100, 101)]. Homologs of these proteins occur throughout eukaryotic cells, in the cytoplasm, nucleus, endoplasmic reticulum, mitochondria, and chloroplasts (see Table 1). Most cells carry both heat-inducible and constitutive (hsc70) forms of hsp70. *E. coli* has a single hsp70, DnaK, that is present constitutively at high levels and is inducible upon heat treatment or other metabolic stresses (102). The heat-inducible hsp70 proteins of mammalian and *Drosophila* cells are the major translation products of heat-shocked cells. Upon heat shock, hsp70 accumulates in the nucleolus of these cells, bound to nucleolar structures; release of bound hsp70 occurs upon addition of ATP, but not with nonhydrolyzable ATP analogues (103). From this observation, Pelham inferred a general mechanism of action for hsp70 proteins, in which the binding of hydrophobic regions exposed on an unfolded protein such as the pro-ribosomal fragments abundant in the nucleolus would serve to solubilize and thus protect such proteins. ATP-dependent release of the chaperone would then allow the substrate protein to refold (64). This simple scheme has a myriad of uses within the cell, and roles for hsp70 proteins have been described in protein metabolism from synthesis to degradation (6, 60, 65, 101, 104–106). The versatility of the hsp70 proteins is in part the result of combining their basic function, namely the reversible binding of portions of a polypeptide chain that resemble the interior of a folded protein, with a variety of protein modulators of that function that respond to other signals in the cell.

Structure and Function of Hsp70 Chaperones

The high degree of sequence conservation in the hsp70 family has spawned a consensus model for hsp70 structure. All members of the family carry a highly conserved amino-terminal ATPase domain followed by a less conserved carboxy-terminal portion thought to contain the peptide-binding site. Some members of the family also have compartment-specific amino-terminal

targeting signals and carboxy-terminal retention signals (e.g. the KDEL peptide on the endoplasmic reticulum protein BiP). A 44-kDa amino-terminal proteolytic fragment of bovine cytosolic hsc70 hydrolyzes ATP, but this ATP hydrolysis is no longer responsive to peptide substrates and runs continuously (107). The crystal structure of this ATPase fragment has been determined to 2.2 Å, and reveals an identical fold to the globular G-actin monomer and hexokinase (108, 109). Binding of nucleotide by hexokinase fosters global changes in the tertiary structure of the protein (110, 111). ATP binding changes the conformation of actin and allows its polymerization into a filament (112). By analogy, it has been proposed that ATP hydrolysis by hsp70 effects a conformational change that is transmitted to the carboxy-terminal domain. Indeed, the DnaK protein has been shown to undergo a conformational alteration upon binding ATP as revealed by a change in the pattern of tryptic fragments (113). The change in conformation correlates with reduced binding of an unfolded polypeptide (113). Mammalian hsp70 binds unfolded proteins less tightly in the presence of hydrolyzable ATP, but addition of ADP inhibits the ATP-dependent release of hsp70 from an unfolded protein (114). This is most easily explained by the exchange of bound ADP for ATP being a critical slow step in the release of substrate. Under normal circumstances complexes of hsp70 alone with substrate protein would be only transiently stable at the ATP concentration present in the cytosol.

A three-dimensional structure of the carboxy-terminus of hsp70 has been proposed based on a consensus secondary structure deduced from the amino acid sequences of 33 hsp70 proteins (115). This consensus secondary structure can be modelled onto the crystallographic structure of the soluble domain of HLA-A2 protein of the human MHC. The peptide-binding groove of the MHC protein (which binds an extended nine-amino-acid residue peptide) in the hsp70 model is lined with hydrophobic residues. Flynn et al tested the activity of various peptide substrates in stimulation of ATP hydrolysis by the ER hsp70 BiP. Optimal stimulation was achieved with a minimal peptide length of seven residues. By selecting a collection of hsp70 (BiP)-binding peptides from a set of synthetic heptapeptides of random sequence, the preference of BiP for particular amino acid residues was ascertained (17). Hydrophobic residues were enriched at every position of the seven-mer peptides, in an abundance very similar to that found in the interior regions of proteins. Such hsp70-binding segments would occur statistically every 16 residues in a globular protein (17). Nuclear magnetic resonance (NMR) of peptides interacting with the *E. coli* hsp70 DnaK indicates that the bound peptide is in an extended structure (18, 116). Furthermore, DnaK (29) and mammalian hsp70 (114) form stable complexes with reduced, carboxymethylated α-lactalbumin, a modified protein that has little secondary structure as shown by far-UV circular dichroism measurements.

Maintenance of the Translocation-Competent State of Precursor Proteins

Formation of stable folded structure inhibits translocation of proteins across the *E. coli* inner membrane (90, 117), into mitochondria (91, 118), and into isolated microsomes (119, 120). If purified precursor proteins are denatured, they can be translocated across these membranes after dilution from denaturant. However, once transferred into physiological buffer solution, these unfolded or partially folded proteins rapidly become incompetent for translocation, probably due to formation of insoluble aggregates (7, 120–125). The question arises how misfolding and aggregation of newly synthesized precursor proteins is prevented within the cell.

The antifolding role of chaperones during protein sorting is perhaps best understood for the case of the *E. coli* SecB protein, which is not structurally related to the hsp70s. SecB is a tetramer of 16.5-kDa subunits that binds to and promotes the export of periplasmic and outer membrane proteins (126–128). SecB binding stabilizes a loosely folded precursor conformation, thus preventing aggregation or premature folding of precursors (22, 23, 128–131). The membrane protein precursor proOmpA, when bound to SecB, contains detectable secondary structure and long-range interactions between widely separated backbone residues (23). Thus "translocation-competent" conformations may resemble the "molten globule" or collapsed intermediate forms observed in the refolding of proteins in vitro, providing a protein with the conformational flexibility necessary to adopt an extended structure transiently during membrane transit.

Precursor proteins destined to mitochondria and endoplasmic reticulum are maintained competent for posttranslational membrane translocation by the action of hsp70s, additional components, and cytosolic ATP (7–9, 125, 132). Genetic depletion of hsp70 proteins was used to demonstrate a role for these proteins in secretion and mitochondrial import in yeast (8). Strains were constructed carrying a single constitutive *SSA* (cytosolic hsp70) gene, expressed from a GAL1 promoter that would not be transcribed in the presence of glucose in the growth medium. Upon shift of the culture to glucose, resulting in the depletion of SSA protein, a newly made mitochondrial protein, F1-ATPase β, accumulated in precursor form, as did the secreted protein prepro-α-factor. The effect of hsp70 on translocation was also tested in a cell-free system (7). Import into microsomes of prepro-α-factor synthesized in a wheat germ extract was markedly stimulated by addition of yeast cytosol. Depletion of cytosol of hsp70 homologs abolished the stimulatory activity. In order to stimulate translocation, hsp70 had to be added along with at least one additional as-yet-unidentified factor of the cytosol, which was sensitive to inactivation by the thiol-modifying reagent N-ethylmaleimide (NEM) (7).

The nature of hsp70 action in maintaining precursor competence is not fully understood. While cytosolic hsp70s can be co-immune-precipitated with nascent chains, stable binary complexes between hsp70s and completely synthesized precursor proteins have not been isolated (12, 132, 133). Sheffield et al demonstrated that mammalian hsp70 prevented aggregation of a mitochondrial precursor protein and slowed its folding (132). However, competence for translocation was conferred only by a combination of hsp70 and other cytosolic factors, again including an NEM-sensitive component. The translocation-competent precursor was in a large complex of 200–250 kDa containing hsp70.

The Hsp70 DnaK and DnaJ are a Chaperone Team

Maintenance of precursor conformation might generally involve complex formation with both hsp70 and other cytosolic factors, or might require specific regulation of hsp70. In support of this, Wild et al have recently demonstrated that the bacterial hsp70 DnaK and its partner DnaJ together, but neither chaperone alone, can promote in vivo translocation of the alkaline phosphatase precursor across the *E. coli* plasma membrane, and that overproduction of both DnaK and DnaJ can compensate for deletion of the secretory pathway chaperone SecB (30).

Many functions of DnaK are indeed potentiated by cooperation with the *E. coli* heat-shock proteins DnaJ and GrpE, and the interactions between these proteins may provide a model for the functioning of other hsp70 chaperones. DnaJ is encoded by the same operon as DnaK. The protein is active as a homodimer of 41-kDa subunits and stimulates ATP hydrolysis by DnaK (26, 134–137). This would effectively increase the concentration of ADP-DnaK, which by analogy to mammalian hsp70 is expected to bind substrate with higher affinity (114). Consistent with this assumption, in a model reaction in vitro DnaJ potentiates the stabilizing effect of DnaK on unfolded rhodanese (29), a mitochondrial protein that aggregates rapidly upon dilution out of denaturant (138). This effect is only in part explained by the affinity of DnaJ for the unfolded polypeptide itself, which characterizes DnaJ as a molecular chaperone on its own (29). The *E. coli grpE* gene codes for a heat-shock protein of 22 kDa that is essential for both λ DNA replication and host growth at all temperatures (139). GrpE has been shown to stimulate ADP-ATP exchange by DnaK (26). The combined effect of DnaJ and GrpE is an up-to-50-fold increase of ATP hydrolysis by DnaK. The effect of GrpE on DnaK-DnaJ-rhodanese complexes is in good agreement with an exchange of ADP-DnaK for ATP-DnaK; the rhodanese-chaperone interaction can come apart under these conditions, allowing the transfer of a rhodanese folding intermediate to the *E. coli* hsp60 GroEL (29) (see Section 7).

In analogy, maintenance of translocation competence in the cytosol of

eukaryotes might involve ternary complexes similar to those observed in vitro with unfolded proteins and *E. coli* chaperones. There are several DnaJ-like proteins in yeast that might be found in such complexes (140). The *MAS5/YDJ1* gene encodes a yeast cytosolic protein and was independently identified as a DnaJ homolog and as a gene involved in import of proteins into mitochondria (27, 141). *SIS1* is another DnaJ homolog from yeast, isolated as a suppressor of a mutation in the *SIT4* gene, which encodes a serine/threonine protein kinase (142). Scj1p, a DnaJ homolog possibly localized within mitochondria, was identified by a genetic screen for mutants that failed to sort proteins between the nucleus and other compartments (143, 144). Sec63p is a membrane protein of the endoplasmic reticulum, with a large domain in the ER lumen homologous to DnaJ that might interact with the luminal hsp70 protein, BiP, during translocation (145). All DnaJ homologs contain in their sequences a conserved cysteine-rich motif (140), but it is still unclear whether the NEM-sensitive factor(s) involved in maintenance of translocation competence (7, 132) belong to this class of components.

While the more general functions of DnaK, DnaJ, and GrpE may be in stabilizing polypeptide chains during de novo folding (28, 29, 146) and under stress conditions (see below), these three proteins have been known for some time to cooperate in specific processes such as the initiation of λ DNA replication. The critical step in this process is the dissociation of the λP protein from the replication initiation complex [reviewed in (105, 147)]. First DnaJ binds to the initiation complex targeting DnaK to λP, which can then be released by DnaK in the presence of hydrolyzable ATP (148–150). GrpE reduces the amount of DnaK needed for this reaction by tenfold (148, 150). A similar cooperation between DnaK and DnaJ is seen in the activation of the RepA replication protein of phage P1 (24, 151, 152) [reviewed in (147)]. In this case, the inactive RepA exists as a tetramer of two RepA molecules and two DnaJ molecules. Activation by DnaK and ATP hydrolysis releases RepA monomers, which are the competent origin-binding species (152). The kinetics of this reaction are revealing; active RepA accumulates slowly during incubation at 24C with ATP. This suggests that activation involves a conformational change that requires work by DnaK. Notably, in this type of reaction, the chaperones interact with native folded proteins, which perhaps expose some structural element typical of an unfolded protein. The uncoating of clathrin-coated vesicles by eukaryotic hsc70 (6, 153) provides another example for how the general abilities of the hsp70s can be utilized for specific purposes.

Organellar Hsp70s in Membrane Translocation and Folding

The hsp70 in the matrix of mitochondria is required for protein import into this organelle (13). Partly translocated precursor proteins, spanning both outer

and inner membranes, bind to the hsp70 in the mitochondrial matrix, suggesting that the chaperone interacts with the extended polypeptide chain as it exits the inner membrane (13, 14, 92, 154). Accumulation of incompletely translocated protein is observed in a yeast mutant temperature-sensitive defective for the mitochondrial hsp70 Ssc1p (13). Based on these findings, it has been proposed that the energy of binding by matrix-localized hsp70 may lead to unfolding of precursor parts still outside the outer membrane and may thus provide all or part of the driving force for translocation (155). Following their interaction with hsp70, newly imported proteins are transferred to mitochondrial hsp60, where they fold in a reaction dependent on ATP hydrolysis (39, 93). Mitochondrial hsp70 thus has a dual role in membrane translocation and subsequent folding of proteins.

BiP (for binding protein), the single member of the hsp70 family in the endoplasmic reticulum (ER), was first identified by its association with not-yet-assembled immunoglobulin heavy chains in pre-B cells (2). Based on this finding, BiP was the first protein recognized as a "polypeptide chain binding protein." The yeast homolog of BiP is termed Kar2p (5, 11, 156) [reviewed in (157)]. This protein appears to play a similar role in protein import to that of mitochondrial hsp70. A temperature-sensitive mutant in KAR2 shows a defect in translocation (16). Depletion of yeast cells for Kar2p leads to the accumulation of partially translocated secreted proteins (158), and a protein spanning the ER membrane in the act of translocation is found to be bound to the DnaJ-homologous membrane protein Sec63p and to Kar2p (19). Following translocation, assembly-defective mutant proteins, unassembled protein subunits, and misfolded proteins can form stable complexes with BiP (2, 4, 5, 159), which is induced by the accumulation of abnormal protein (160). The persistent interaction of BiP with unassembled protein appears to involve hydrophobic surfaces on the bound subunit, which are normally buried by association with other subunits in the assembled protein (157). On the other hand, several normal proteins on the native folding pathway appear to interact only transiently (5, 160–162). These findings are consistent with a general role of BiP in the folding and oligomeric assembly of proteins imported into the ER.

Hsp70 in Cells Under Metabolic Stress

Recent experiments have probed the function of *E. coli* DnaK under conditions of stress, using both in vivo and in vitro approaches. An excess of DnaK protein present during heat treatment can protect *E. coli* RNA polymerase from thermal inactivation in vitro (15). The thermally inactivated enzyme can be reactivated to 60% by a high molar excess of DnaK in a process dependent on hydrolyzable ATP. Recent studies suggest that this apparently inefficient

protection may be potentiated by addition of the DnaK partner proteins DnaJ and GrpE. For example, the activity of the thermolabile firefly luciferase, expressed in *E. coli*, depends on DnaK, DnaJ, and GrpE (H. Schröder, T. Langer, F.-U. Hartl, B. Bukau, submitted). At 42C, pre-existent, active luciferase loses its activity. Recovery to 50% of the original enzyme activity is observed upon temperature downshift to 30C in wild-type cells but not in DnaK or DnaJ mutant strains. The interaction of luciferase with DnaK and DnaJ has been reproduced in vitro. At 42C luciferase unfolds and forms a ternary complex with DnaK and DnaJ, which is stable in the presence of Mg-ATP and GrpE. Under these conditions luciferase may cycle between free and DnaK/DnaJ-bound forms, while it aggregates in the absence of chaperones. At 30C the enzyme regains its activity in a reaction dependent on ATP and all three heat-shock proteins. The interaction of luciferase with hsp70 of mammalian cells shows similar properties, although in this case the participation of DnaJ or GrpE homologs has not yet been demonstrated (163–165). More generally, many cellular proteins can be co-immune-precipitated with a monoclonal antibody to mammalian hsp72 from cells exposed to heat shock or treatment with the proline analog azetidine (133). Upon recovery from heat shock, the complexes between normal proteins and hsp72 are resolved while proteins containing azetidine remain bound, probably because they cannot fold properly.

Hsp70 may be the central regulator of its own stress-induced synthesis. In cultured mammalian cells, conditions such as puromycin or heat-shock treatment, which increase the level of unfolded polypeptides and thus decrease the content of free hsp70, lead ultimately to induction of heat-shock gene transcription (133, 166). If heat shock is performed in the presence of translation inhibitors, thus reducing the concentration of nascent chains and increasing free hsp70 levels, the transcriptional response is diminished. For reviews of the interaction of hsp70 proteins with heat-shock transcription factor (HSF) and bacterial σ32, see (101, 167).

Hsp70 and Protein Degradation

Withdrawal of serum from mammalian cells in culture initiates the degradation of a specific subset of cellular proteins by lysosomal proteases (104, 168). A consensus peptide sequence motif (K-F-E-R-Q) common to these proteins has been identified. A proteolytic fragment of ribonuclease without the KFERQ motif is no longer degraded in response to serum starvation (169). A 70-kDa cytosolic protein called prp73 has been identified as a crucial component in the targeting for degradation of KFERQ-proteins (170). Interestingly, prp73 is biochemically indistinguishable from the constitutive mammalian hsp70 homolog, hsc73, but the relationship between KFERQ binding and other

functions of hsc73 is not known. If hsc73 targets these proteins for degradation, how does it interact with the machinery that transports them to and into the lysosome?

In *E. coli*, abnormal proteins that are rapidly degraded by the ATP-dependent La protease bind DnaK and GrpE proteins (171). Intracellular proteolysis of puromycin-released peptides is reduced somewhat in DnaK mutants but is dramatically reduced in DnaJ mutants (172). It has been suggested that cooperation between the in vivo folding pathway and the protein degradation system would provide effective control over the level of abnormal proteins in the cell.

4. HSP60 PROTEINS: CHAPERONES THAT HELP PROTEINS TO FOLD

This family of highly conserved proteins of approximately 60 kDa was first distinguished by the unusual structure of its members, usually a 14-subunit oligomer with a characteristic double toroid appearance in the electron microscope (35, 36, 173–175). The hsp60s were dubbed "chaperonins" or "chaperonin 60s" (cpn60s), to define a subclass of sequence-related molecular chaperones including stress-inducible and non-inducible members found in the bacterial cytosol, and in the inner space of mitochondria and chloroplasts (35) (see Table 1). The bacterial hsp60 is GroEL, named according to its activity as a host protein required for bacteriophage assembly (31, 173, 176–179). Mitochondrial hsp60 was first identified in *Tetrahymena*, where it is one of the few proteins made during the dramatic response of this organism to stress (174). The chloroplast chaperonin is required for the assembly of ribulose-bisphosphate carboxylase/oxygenase (rubisco), hence the name rubisco binding-protein (33, 180). Highly related hsp60 homologs have not been detected in the cytosol of eukaryotic cells or in the endoplasmic reticulum. Recently, however, weak homology has been found between the hsp60s and the TCP1 proteins of the eukaryotic cytosol, which seem to fulfill chaperonin-like functions (181, 182) (see Section 5).

The hsp60s in bacteria, mitochondria, and chloroplasts functionally cooperate with a smaller co-chaperonin protein of 10 kDa subunit size (termed chaperonin 10) (see below). In *E. coli* and in mitochondria these proteins are stress-inducible and are called GroES and hsp10, respectively (183, 184). They are single seven-subunit rings that form a complex with the GroEL and hsp60 double-rings. GroES is encoded in the GroE operon together with GroEL. The definition of GroES and hsp10 as chaperonins relies on a limited sequence homology between GroES and GroEL (35).

Chaperonins Promote Protein Folding and Assembly

GroEL mutants of *E. coli* fail to assemble head structures of phage λ and tail assemblies of phage T5 (31, 176–178). A complex found in the chloroplast stromal compartment between the cytoplasmically synthesized large subunit of chloroplast rubisco and a nuclear-encoded 60-kDa binding protein was shown to be an intermediate in the assembly of this enzyme from its eight large and eight small subunits; chase of complexed subunit to assembled enzyme could be demonstrated upon addition of ATP (33, 180, 185–187). The idea that there may be a conserved function for chaperonins was strengthened by the successful assembly of a dimeric prokaryotic form of rubisco by co-overproduction of this protein in *E. coli* together with GroEL and GroES (38). The first evidence that protein assembly in general (as opposed to specialized overproduction) might require cellular factors came from the study of *mif4* mutant yeast, which harbor a temperature-sensitive mitochondrial hsp60. Although in these yeast import of proteins into the organelle occurs normally, newly imported proteins, including hsp60 itself, fail to assemble (36, 188). The kinetic and spatial separation of synthesis and folding/assembly in this experimental system has been further utilized in analyzing the function of mitochondrial hsp60. A fusion protein containing a cleavable targeting signal joined to the enzyme dihydrofolate reductase (DHFR) was found associated with hsp60 in a protease-sensitive, unfolded state upon import into ATP-depleted mitochondria. The hsp60-bound DHFR could be chased to a folded, protease-resistant form upon incubation with Mg-ATP (39). The surprising observation that the chaperonins also function in the folding of monomeric polypeptide chains such as DHFR (39, 41, 189), which can fold spontaneously in vitro, was important in developing our present view of protein folding in vivo (65). It is possible that the role of the chaperonins in oligomeric assembly is a mere consequence of their capacity to fold subunits into the form required for productive association. On the other hand, a specific chaperonin function in the association reaction itself cannot be excluded at present.

Mechanism of GroEL/ES-Mediated Protein Folding

Chaperonins do not only promote the folding of proteins that have first crossed a membrane. Evidence for this comes from the study of bacterial GroEL/ES. GroEL is able to interact with a wide range of bacterial proteins; overproduction of the GroE operon suppresses a number of temperature-sensitive protein mutants, presumably by stabilizing their less stable native states (190).

GROEL BINDS TO LOOSELY FOLDED PROTEINS A large fraction of denatured *E. coli* proteins form complexes with purified GroEL that can be dissolved

upon addition of hydrolyzable ATP, leading to the suggestion that folding of proteins in general may occur in association with the chaperonin (44). Indeed, ^{35}S-labeled pre-β-lactamase and chloramphenicol acetyl transferase are found in a complex with GroEL immediately following synthesis in a bacterial translation system (34). Heat-denatured myoglobin, but not the native protein, could displace the labeled proteins, indicating the specificity of GroEL for unfolded forms. Unfolded proteins are prone to aggregation upon dilution from denaturant, but in numerous examples GroEL was able to prevent this by binding one to two molecules of protein-folding intermediate to each GroEL tetradecamer (40, 41, 191, 192).

Denatured rhodanese and DHFR, proteins with different in vitro folding properties, were bound to GroEL (41). Rhodanese usually aggregates upon dilution from denaturant (138). However, if GroEL is present in the renaturation buffer in a molar excess over added rhodanese, the unfolded protein binds to the chaperonin (41, 191). DHFR, on the other hand, can rapidly refold upon difution of denaturant (193); yet it too binds GroEL if it is present, and is prevented from folding as long as Mg-ATP is absent (41, 189). Rhodanese and DHFR bound to GroEL are sensitive to protease, bind 1,8-anilino-naphthalene sulfonate (ANS, a fluorophore with high affinity for hydrophobic protein surfaces) and have intrinsic fluorescence properties intermediate between the unfolded and native state (41). These properties are all consistent with those of the collapsed intermediate formed rapidly upon dilution from denaturant. Indeed, GroEL is able to bind the collapsed intermediate form of rhodanese (stabilized by detergent) (42) and of ribulose bisphosphate carboxylase (prepared by acid denaturation) (194). One critical property of such folding intermediates is the presence of secondary structure elements, and GroEL is apparently unable to recognize an extended polypeptide chain (29). Based on NMR measurements with a 13-residue peptide derived from the amino-terminal of rhodanese, Landry & Gierasch have proposed that GroEL can stabilize certain peptides in α-helical conformation, perhaps by interacting with the hydrophobic face of an amphiphilic α-helix (18). Interaction with GroEL has also been detected with an all-β-protein, however (195). This suggests that the critical factors for binding may be the features of early folding intermediates, such as exposure of hydrophobic residues, rather than a defined secondary structure motif.

Where at the chaperonin does the substrate protein bind? The stoichiometry of binding of only 1–2 substrate molecules may suggest that binding occurs to the central region of the 840-kDa particle. The chaperonin cylinder is 14.5 × 16 nm, with an internal cavity of about 6 nm in diameter. This space could in principle accommodate a compact folding intermediate, for a protein of up to about 60 kDa. A recent electron microscopic image analysis of GroEL with bound rhodanese (35 kDa) or alcohol oxidase (75 kDa) suggests that this may

indeed be the case: binding of unfolded protein leads to the accumulation of a stain-excluding mass within the central cavity of GroEL, which is visible on negatively stained images of the complex (43). In an independent approach, Horwich and colleagues have detected gold-labeled, unfolded DHFR in the central space of GroEL (K. Braig, M. Simon, F. Furuya, J. F. Hainfeld, A. L. Horwich, submitted). The topology of the substrate protein along the long axis of the GroEL cylinder is not yet clear. The observation that a single ring of the chaperonin has the basic capability to bind a molecule of substrate protein becomes important in this context. Viitanen et al have isolated from mammalian mitochondria a form of hsp60 that appears to be active as a single-ring chaperonin (196).

GROEL-BOUND PROTEINS FOLD UPON ADDITION OF ATP AND GROES GroEL has a weak K^+-dependent ATPase and contains probably 14 binding sites for ATP, i.e. one per monomer (41, 42, 197). Addition of Mg-ATP to GroEL-DHFR complexes leads to the release of the folded protein (41). Refolding of many other proteins from the GroEL-bound state requires in addition to Mg-ATP the "co-chaperonin" GroES (37, 40, 41, 191, 192, 197–199). Likewise, hsp10, the mammalian mitochondrial homolog of GroES, has been shown to be required for the folding and assembly of ornithine carbamoyltransferase by mitochondrial hsp60 (183).

The role of GroES in modulating the function of GroEL is only partially understood. Binding of GroES strongly reduces the uncoupled ATPase activity of GroEL measurable in the absence of substrate protein (41, 197, 200). ATP binding and hydrolysis by GroEL are cooperative processes, and GroES increases this cooperativity (42, 201). In the absence of GroES, slow folding proteins cannot be released from GroEL in folded form. Rhodanese, for example, remains largely associated with GroEL in the presence of Mg-ATP, perhaps because the partially folded protein rapidly rebinds to the chaperonin upon ATP-dependent release (41). Transient release of partially folded rhodanese from the chaperonin is revealed by the addition of casein, a protein with properties of a compact folding intermediate in aqueous solution. In the presence of Mg-ATP, addition of casein to rhodanese-GroEL complexes leads to the displacement of rhodanese, which then aggregates. Interestingly, when GroES is added, the ability of casein to displace the substrate protein from GroEL, thereby interrupting productive folding, is strongly reduced, despite the presence of Mg-ATP. A protein such as rhodanese is apparently sequestered from the bulk solution during GroEL/ES-mediated folding. In experiments in which progression of rhodanese folding was halted after a brief pulse of ATP hydrolysis (stopped by removal of magnesium with chelator), GroEL/ES-bound rhodanese was converted to a somewhat more protease-resistant form that was still associated with GroEL. In the case of GroEL/ES-

bound DHFR, the tryptophan fluorescence properties of the bound form of the protein changed part way towards those of the native state under these conditions (41). These results suggest that at least partial folding of a protein may occur in close association with the chaperonin. The energy requirement of chaperonin-dependent folding can be relatively high, at least in vitro: about 100 ATP were hydrolyzed per molecule of rhodanese folded, indicating that the reaction requires several cycles of ATP hydrolysis per GroEL tetradecamer (41).

Electron microscopic studies of the GroEL-GroES complex have provided a glimpse into the workings of this folding machine. The GroES heptamer forms a one-to-one complex with a GroEL tetradecamer, which is stabilized by Mg-ATP or Mg-ADP (43, 202, 203). GroES binds asymmetrically to the GroEL cylinder, sitting like a cap on one end-surface (43, 202, 203). Upon binding of GroES, conformational changes can be observed in both the GroES-adjacent and the distal ring of GroEL, which are probably of functional importance for the folding reaction (43).

A Model for GroEL/ES Action

The following experimental observations, summarized above, form the basis of a proposed model for the mechanism of chaperonin-mediated protein folding:

1. Substrate protein binds in the conformation of a compact folding intermediate within the central cavity of the GroEL double-ring.
2. A single heptameric ring can bind unfolded protein.
3. The GroES seven-mer ring binds asymmetrically to one end surface of the GroEL cylinder, modulating the conformation of both the GroES-adjacent and opposite rings of GroEL.
4. At least partial, ATP-dependent folding is possible in close association with GroEL.
5. This process depends on the regulation of the GroEL ATPase by GroES.
6. This process can require several cycles of ATP-hydrolysis by the GroEL tetradecamer.

How can GroEL allow folding to proceed while at the same time maintaining close association with the folding polypeptide? The subunits of the GroEL cylinder may interact with several segments of the protein substrate and release them upon ATP hydrolysis in a step-wise manner, rather than all at once. This may allow a domain or subdomain of a polypeptide such as rhodanese to engage in folding while another portion of the polypeptide maintains the association with GroEL. In principle, a folding reaction of this type has been described with unfolded protein bound to ion exchange resin

(204). The situation would be different, however, when folding of a small, one-domain protein is considered. While an ion exchange resin is expected to interact preferentially with regions of a protein that remain exposed in the final folded structure, the chaperonin, by definition, has to recognize structural elements that are only accessible in the unfolded state. Thus, at least for a single-domain protein, concomitant release of all GroEL-bound elements would have to occur in order to allow folding. Such a release event could be followed by rapid re-binding of elements that failed to be buried within the folded structure.

Is such a mechanism consistent with the experimental observations? A compact folding intermediate could attach to multiple GroEL subunits within the cavity of the cylinder (Figure 1*A*). The initial interaction with the substrate protein would be restricted to one of the seven-subunit rings, say the one distal to GroES (I). Cooperative ATP hydrolysis (enhanced by GroES) would then be accompanied by concerted release of the bound protein, making a number of folding elements available simultaneously (II). As a result, folding could proceed, while immediate exit of the released protein from the chaperonin cavity may be retarded by GroES-induced conformational changes in GroEL. A substrate protein that upon ATP-dependent release has folded only partially may re-bind to the GroEL ring it initially interacted with (III) and undergo another cycle of release (IV). In this model, only one of the two chaperonin rings would be involved in the interaction with substrate (Figure 1*A*). The role of GroES would mainly consist in coordinating the release and re-binding activity of the substrate-interacting ring so that all seven subunits are either in a high-affinity or low-affinity state for substrate binding. Interaction of a single GroEL ring with subunits of a multimeric protein may be an important part of its function in protein assembly reactions (205). On the other hand, taking the asymmetrical properties of the GroEL-GroES complex into account, we also consider the scheme shown in Figure 1*B*: Based on the "half-the-sites reactivity" model for GroEL action proposed by Creighton (206), the opposing rings of GroEL may exist in opposite binding states. If via ATP hydrolysis one ring has converted to a state with low affinity for substrate, the other will preferentially adopt a high-affinity conformation (dark shading in figure). An unfolded protein could shuttle between the two rings of the chaperonin, thereby advancing along the folding pathway [see (41)], until the protein has folded to bury a sufficient amount of its interior residues. The option of shuttling may depend on the properties of a specific substrate protein such as size. For certain proteins, one round of interaction might be sufficient for completion of folding. This is supported by the finding that the single-ring hsp60 of mammalian mitochondria can promote the folding/assembly of rubisco.

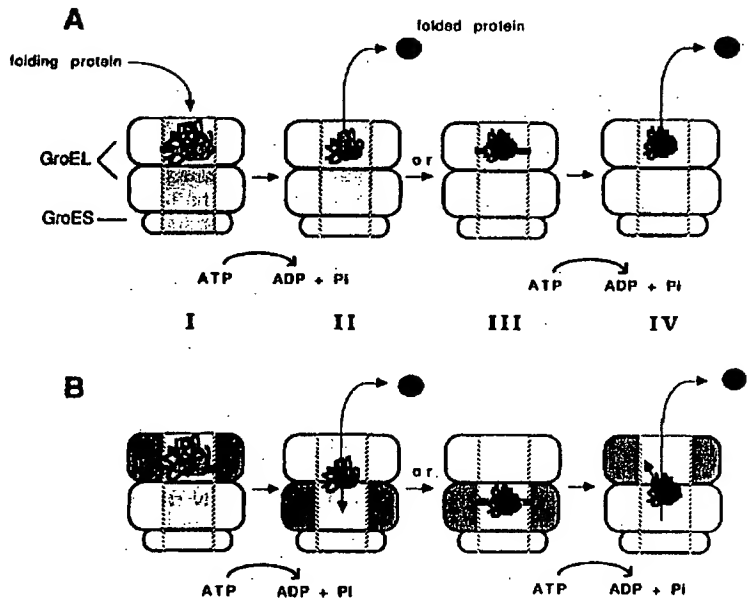

Figure 1 Hypothetical model for the function of GroEL/ES in protein folding. Steps are as described in text.

In our model the substrate protein within the GroEL cylinder may be compared with a single protein molecule refolding in the test tube, thus excluding the possibility of unfavorable intermolecular interactions. Unlike the test-tube situation, however, the energy of rebinding to GroEL could be utilized to reverse unproductive interactions within the folding chain. One important aspect of the model concerns the number of protein molecules that can bind to the GroEL cylinder. Bochkareva et al find up to two molecules of rhodanese associated with GroEL in the presence of the nonhydrolyzable analog ATPγS. However, in the presence of GroES only a single rhodanese binds to GroEL and no more than one molecule can interact in a manner productive for folding (42). In vitro binding of unfolded protein to GroEL alone ignores the likelihood that the predominant state in the cell is a GroEL/GroES complex (207). Presumably, the GroES-adjacent ring of GroEL/ES is in the ADP-bound form, and the opposite ring, which in the

model would accept the substrate protein, is bound to ATP; we imagine that this difference may govern the binding of one substrate molecule at a time. There is as yet insufficient data to support this contention, but it is clear that binding of GroES alters the structure of both rings of GroEL (43). Another important question concerns the fate of substrate proteins that are too large to be accommodated within the central binding region of GroEL. Proteins larger than 60 kDa usually consist of two or more domains that may be able to fold independently. Possibly the chaperonin deals with one domain at a time while the remainder of the polypeptide is stabilized by cooperating chaperones such as DnaK/DnaJ (see Section 7).

Hsp60 as a Stress Protein

Overproduction of GroEL and GroES in bacterial cells lacking a normal heat-shock response protects intracellular proteins from aggregation into insoluble complexes (28). GroEL alone is not sufficient. Similarly, mitochondrial hsp60 forms complexes with a number of organellar proteins under conditions of heat stress and prevents the in vivo thermal inactivation of dihydrofolate reductase (DHFR) imported into the mitochondrial matrix (208). This interaction was modelled in vitro using GroEL and GroES to maintain DHFR activity at elevated temperature in the presence of Mg-ATP. GroEL lowered the thermal inactivation curve of DHFR by 15C (208), consistent with its net unfolding activity observed with DHFR and pre-β-lactamase in the absence of enzyme substrate (189, 192, 198). DHFR that was bound to GroEL by thermal unfolding had the spectral characteristics of protein bound after dilution from denaturant. At an intermediate temperature of 40C, GroEL/ES and Mg-ATP can maintain DHFR in an active state, whereas in the absence of chaperonin the protein becomes inactive (208). Mitochondrial rhodanese in a binary complex with GroEL is protected from thermal inactivation at 48C (209), and can be released in active form upon addition of GroES and ATP at 25C. GroEL (in the absence of ATP) can also protect yeast α-glucosidase from thermal aggregation in vitro by forming a one-to-one complex with this protein (210). Here GroEL does not influence the kinetics or the temperature dependence of inactivation, probably because thermally unfolded α-glucosidase rapidly aggregates and is thereby withdrawn from equilibrium. The division of labor between GroEL/ES and DnaK/DnaJ in protecting pre-existent proteins during heat shock in intact bacteria is not known. The prevention of irreversible denaturation of firefly luciferase expressed in *E. coli* may depend exclusively on DnaK, DnaJ, and GrpE as it is not affected in a GroEL mutant strain (H. Schröder, T. Langer, F.-U. Hartl, B. Bukau, submitted).

5. CHAPERONIN-LIKE PROTEINS IN THE EUKARYOTIC CYTOSOL

No hsp60/GroEL immuno-cross-reactive proteins have been identified in the eukaryotic cytosol. However, chaperonin-related protein complexes in the cytosol with double toroid appearance in the electron microscope have been observed by several investigators. Their discovery followed the identification of a family of evolutionarily related components in archaebacteria: A large cylindrical protein complex with a very thermostable ATPase activity is an abundant component of the cytoplasm of the extreme thermophile *Pyrodictium occultum* (211). The related component TF-55 (for thermophilic factor of 55-kDa subunits) is the major protein synthesized in *Sulfolobus shibatae* following heat shock (which for this organism is 88C); it is made up of two rings of probably eight TF-55 monomers each. TF-55 binds unfolded proteins but not their native counterparts, and has a weak ATPase activity (45). Interestingly, TF-55 is homologous to a ubiquitous eukaryotic protein, TCP1 (for "T-complex polypeptide 1). TCP1 was originally identified as a gene product of the mouse T locus expressed at high levels in developing spermatids and has been implicated in the phenomenon of male-specific transmission ratio distortion (212, 213). However, the ubiquitous expression of TCP1 indicates the possibility of a more general function for the protein (214). TCP1 is an essential gene in the yeast *Saccharomyces cerevisiae*. A yeast cold-sensitive *tcp1* mutant fails to assemble a normal mitotic spindle at the nonpermissive temperature and is hypersensitive to microtubule-disrupting drugs at all temperatures (215).

TRiC, a Hetero-oligomeric Ring Complex

TCP1 has been purified from mouse and bovine testis (46, 48) and from rabbit reticulocyte lysate (47, 49). The protein exists in a 970-kDa hetero-oligomeric complex termed TRiC (for TCP1 ring complex) that contains the 60-kDa TCP1 along with five to seven proteins of 50 to 68 kDa (46–49). Variable amounts of hsp70 have also been observed in the complex (48). These additional polypeptides, which are not found in archaebacterial TF55, do not cross-react with a monoclonal anti-TCP1 antibody; but at least three of them are related to TCP1 (46). This is consistent with the identification of several TCP1-related genes in humans and mice (K. Willison, personal communication). TRiC appears in the electron microscope as a cylindrical particle consisting of two stacked rings with eightfold symmetry, 17 nm in diameter. Despite its hetero-oligomeric composition, the complex closely resembles its homo-oligomeric archaebacterial homologs. The internal cavity of these particles appears considerably larger than that of GroEL (46, 215a).

TRiC has been shown to have chaperonin activity (46, 47, 49). Gao et al used unfolded actin obtained from inclusion bodies formed in an *E. coli* overproducing strain to assay for actin-folding factors in reticulocyte lysate (47). They identified a high-molecular-weight folding activity that corresponded to TRiC. In the absence of added ATP, actin could be isolated in association with the chaperonin. Upon incubation of TRiC-bound actin with hydrolyzable ATP, monomeric native actin was released that was competent to assemble with native actin into filaments. Frydman et al have purified the TRiC double toroid from bovine testis and reconstituted chaperonin-dependent protein folding using all purified components (46). TRiC-mediated folding of guadinidium-Cl unfolded α and β tubulin, and firefly luciferase was compared to the folding of the same proteins by GroEL/ES. Interestingly, isolated TRiC could refold tubulin efficiently upon addition of ATP and GTP (the latter may stabilize folded tubulin, which is a GTP-binding protein), without the apparent need for any additional small co-chaperonin such as a GroES analog. The ATP-dependent release of folded tubulin from GroEL was dependent on GroES. Luciferase could not be released from GroEL even in the presence of co-chaperonin and ATP, while it could be refolded by isolated TRiC. The importance of the differences between the two chaperonin families should become apparent with further research. The detection of hsp70 in TRiC-containing fractions raises the possibility that this chaperone cooperates in TRiC-mediated folding (48) (E. Ninnnesgern, unpublished results).

Yaffe et al discovered TRiC in reticulocyte cytosol by monitoring the time course of tubulin folding during in vitro translation (49). Several different fractions containing newly synthesized tubulin were identified, one 900 kDa in size. The 900-kDa fraction, corresponding to TRiC-bound tubulin, could be stabilized by addition of EDTA to inhibit nucleotide hydrolysis. Upon addition of Mg-ATP the protein was released in a conformation more resistant to protease than the initially bound form, consistent with a folding function for TRiC.

Identification of a protein-folding machine in the eukaryotic cytosol has been greeted with great enthusiasm (216). Much needs to be learned, however, about the TCP1-containing complex. The in vivo effects of the yeast TCP1 mutation are as yet only an indirect indication of its protein folding role. Notably, two of the three identified substrates of TRiC are cytoskeletal proteins, which may suggest a specialized function. It is also striking that TCP1 is not a heat-shock protein, when so many of the molecular chaperones are. Probably the search for other chaperonin homologs in the eukaryotic cytosol will have to continue.

6. HSP90: A CHAPERONE THAT REGULATES PROTEIN FUNCTION

When glucocorticoid receptors are synthesized in vitro in a reticulocyte lysate, they are found shortly after synthesis in a large complex containing an abundant heat-shock protein, hsp90 (51, 53) (Table 1). Binding of hsp90 to the receptor is competed by synthetic peptides whose sequence matches that of the hormone-binding site (217). The chaperone-bound receptor is stabilized in a state that has a high affinity for hormone, but that cannot bind DNA (218). Activation of hsp90-bound receptors by addition of ligand is an ATP-requiring reaction that involves binding of ligand, release from hsp90, and a change in receptor conformation to a form that has high affinity for DNA (218, 219). Expression of glucocorticoid receptors in a yeast strain depleted for hsp90 leads to the synthesis of receptors that do not stimulate transcription of an introduced receptor-responsive gene (54). Addition of hormone activates the receptors, but with a reduced efficiency relative to the hsp90-bound form. From these experiments, it was concluded that the chaperone does not just sterically hinder binding of receptor to DNA, but indeed facilitates the receptor response to hormone.

Hsp90 proteins are a highly conserved family of heat-shock proteins, found in many kinds of cells and in many organisms, including *Escherichia coli* (220). Homologous proteins have been identified in the endoplasmic reticulum, with the bulk of the protein thought to face the cytoplasm (221–224). The progesterone (225) and dioxin (226) receptors, as well as the cytosolic signal transduction proteins casein kinase II (227) and the oncogene product $pp60^{v\text{-}src}$ (50, 228), bind hsp90. This broad substrate specificity characterizes hsp90 as a molecular chaperone. The tyrosine kinase activity of $pp60^{v\text{-}src}$ bound to hsp90 is inhibited; it is hypothesized that the chaperone serves both to inactivate and to foster transport of the oncogene product (228) [see (229) for review]. Casein kinase II, on the other hand, is kept from aggregating by binding to hsp90, and its activity is stimulated (227). Assembly of the hsp90-substrate protein complexes is not a simple bimolecular reaction (55), but in the case of the progesterone receptors and $pp60^{v\text{-}src}$ requires ATP hydrolysis (58, 230). The hsp90-containing receptor complex isolated from cells is a 9S particle that includes hsp90, variable amounts of hsp70, and in addition a 59-kDa immunophilin that binds hsp90 (57, 59, 231–233).

As these different components of the complex are characterized, a novel principle of biological control may be revealed. Hsp90 in mammalian cells is a highly phosphorylated protein. It has an ATP-binding site and autophosphorylating activity (56, 234). The immunophilins are thought to interact with protein phosphatases of the signal-transducing pathways of the cell, although this interaction has only been detected in the presence of the

immunosuppressant drugs whose tight binding gives these proteins their name (235). All the immunophilins identified so far are capable of catalyzing the *cis-trans* isomerization of peptidyl-prolyl bonds in polypeptide chains [reviewed in (236)]. Although this activity, which is inhibited by immunosuppressants such as cyclosporin or FK506, is not the biological target in immunosuppression, it may play an important role by activating the drug through conformational modulation. In the context with hsp90, the immunophilins may trigger a conformational switch in the chaperone-bound receptor.

The nature of the hsp90 interaction with a target protein is still not understood; the chaperone may interact with transiently exposed hydrophobic surfaces, as suggested by the observation that hsp90 can prevent aggregation and promote refolding of citrate synthase in vitro (237). However, in the absence of evidence of controlled binding and release, it is difficult to evaluate the significance of this observation for processes of in vivo folding (238).

7. COOPERATION BETWEEN CHAPERONES IN PROTEIN FOLDING

The traditional form of discussing each class of molecular chaperones separately might create the impression that these components act on their own in independent cellular functions. Quite to the contrary, chaperone cooperation in various reactions has emerged as a novel theme. The division of labor in de novo protein folding between members of the hsp70 and hsp60/GroEL families of molecular chaperones may serve as an example of central biological importance.

During protein import into mitochondria, a polypeptide chain that has partially traversed the outer and inner membranes of the organelle interacts with the hsp70 in the mitochondrial matrix. Subsequent folding depends, at least in a number of cases, on the transfer of the newly imported protein to hsp60, the mitochondrial GroEL homolog (13, 39, 93, 239, 240). The sequential action of hsp70 and hsp60 may apply more generally to the folding of newly synthesized polypeptides, not only in mitochondria but also in the cytosol. Based on the reconstitution of the pathway in vitro using the homologous chaperones of *E. coli*, the following steps of the reaction can be defined: (*a*) prevention of aggregation of nascent or membrane-translocating polypeptide chains by hsp70, probably in cooperation with DnaJ homologs, (*b*) ATP-dependent transfer of partially folded chains to hsp60/GroEL or a functional chaperonin equivalent, and finally (*c*) ATP-dependent folding at the chaperonin.

Two Chaperone Teams Cooperate in Protein Folding

The basis for the sequential action of hsp70 and hsp60 appears to be the differential specificity of these chaperones for structural features of a polypeptide chain that are exposed sequentially during translation/translocation and folding. Several lines of evidence indicate that hsp70s recognize extended peptide segments enriched in hydrophobic residues (17, 18, 29, 114). Studies with GroEL, on the other hand, suggest that the chaperonin recognizes and stabilizes proteins in a conformation that resembles the compact intermediate or "molten globule"-state (18, 41, 42, 116). After ATP-depletion, nascent polypeptide chains in mammalian cells can be co-immune-precipitated with antibodies specific for mammalian hsp70 (12). On the other hand, only newly synthesized full-length proteins but not nascent polypeptides have been cross-linked to GroEL (34).

A role in protein folding for the differential specificity of hsp70s and hsp60s has been directly tested. Working with the mitochondrial model protein rhodanese, the sequential binding of a folding polypeptide seen during mitochondrial import has been reconstituted (29). DnaK in high stoichiometric excess prevented the aggregation of refolding rhodanese, but this stabilization was lost upon addition of Mg-ATP. In an effort to modify the activity of DnaK, the DnaJ protein, which is known to interact with DnaK in other contexts, was introduced (see Section 3). The DnaJ protein had a chaperone activity of its own; added in equimolar ratio with rhodanese, it prevented aggregation. More importantly, in combination with DnaK, submolar amounts of DnaJ versus substrate protein potentiated the stabilizing activity of DnaK and reversed the effect of ATP, such that rhodanese stabilization by the DnaK/DnaJ combination was maximal in the presence of hydrolyzable ATP (see Section 3). In fact, refolding of DnaK/DnaJ-bound rhodanese in vitro was prohibited in the presence of hydrolyzable ATP, even if a folding-competent chaperonin (GroEL/ES) was available. Transfer to GroEL and folding only occurred if a third protein, GrpE, was added together with Mg-ATP. The DnaK/DnaJ-complexed folding intermediates then supplied the substrate for multiple rounds of GroEL/ES-catalyzed folding. This differs markedly from most experiments in chaperonin refolding, in which the experimental design limits GroEL turnover to single folding reactions.

These observations led to the formulation of the hypothesis that DnaK/DnaJ/GrpE and GroEL/ES could cooperate in the folding of newly synthesized proteins in *E. coli* (Figure 2): During early stages of translation DnaK (and/or DnaJ) would recognize extended segments of nascent polypeptide chains, preventing their aggregation (I). Some of the bound DnaK molecules become stabilized by the interaction of DnaK with DnaJ, which is present at a 1:2 ratio with DnaK in *E. coli* (J. Hendrick, T. Langer,

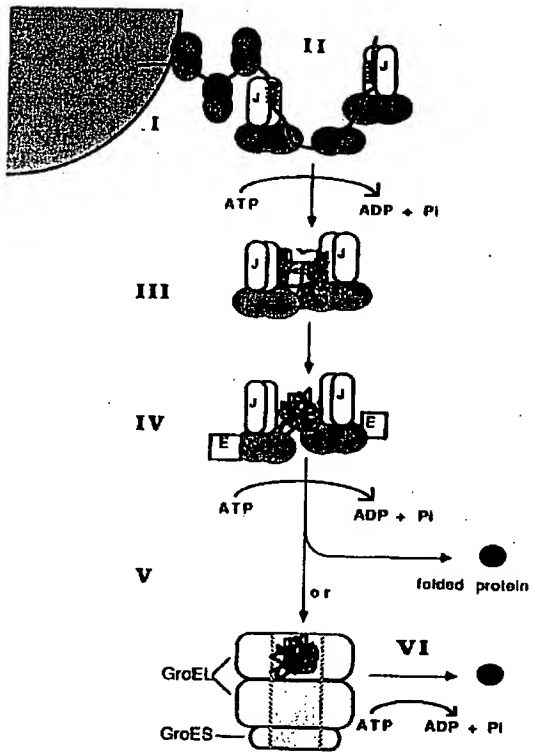

Figure 2 Model for cooperation between DnaK, DnaJ, GrpE, and GroEL/ES during de novo protein folding. Steps are as described in text.

unpublished observations) (II). As the polypeptide grows this would allow its collapse to a more compact state now stabilized by fewer molecules of DnaK (II–III). DnaJ interacts more efficiently with a collapsed folding intermediate than does DnaK (29), but it is still unclear what structural elements of the polypeptide chain DnaJ recognizes. The role of DnaK/DnaJ could merely consist of stabilizing newly made proteins in a "folding-competent state" for transfer to the chaperonin GroEL (III). Release of the protein from DnaK/DnaJ requires GrpE (IV), which can function as a coupling factor between the DnaK/DnaJ and chaperonin systems (V). While in the case of rhodanese,

release from DnaK/DnaJ and folding, even in the presence of GrpE and Mg-ATP, only occurs when GroEL is present (VI), this may be different with other proteins (V). For example, unfolded firefly luciferase, added from denaturant into a solution containing DnaK, DnaJ, and Mg-ATP, can fold successfully to the native state upon addition of GrpE (T. Langer, unpublished). A number of proteins may fold without subsequent interaction with the chaperonin.

Clearly, the sequence of interactions proposed by this model needs to be confirmed in vivo and in cell-free translation systems in vitro. We have to understand why DnaK and DnaJ deletion strains of *E. coli* can grow, albeit slowly, within a narrow temperature window around 30C (241, 242). Are there other chaperone proteins that can function generally but with lower efficiency? Recent in vivo evidence obtained with a RpoH mutant strain of *E. coli* lacking most heat-shock proteins (or containing them at very low levels) suggests that DnaK/DnaJ and GroEL/ES have overlapping substrate specificity: Overexpression of DnaK/DnaJ in this strain prevents the aggregation of most newly synthesized proteins and so does overexpression of GroEL/ES (28). However, both chaperone systems, expressed at normal level, are most efficient in protecting newly made polypeptides, suggesting their functional cooperation. Given these observations, how similar then is the pathway of chaperoned protein folding in the eukaryotic cytosol? The yeast DnaJ homolog Ydj1p is able to modulate the interaction of the hsp70 Ssa1p with an extended polypeptide chain in vitro (243), but a GrpE homolog has not yet been discovered in eukaryotes. The TCP1 ring complex has chaperonin-like function in the eukaryotic cytosol, but any possible cooperation with other chaperones remains to be established.

8. FUTURE ASPECTS

Since the appearance of the last reviews on this topic in Annual Reviews series (62, 78), considerable progress has been made in understanding the functional interaction of molecular chaperones in different cellular pathways. By an interdisciplinary approach involving cell biologists, biochemists, and biophysicists we may now gain detailed insight into how proteins fold in vivo, one of the single most important processes in biology. The process of translation itself will have to be included in this analysis. At the same time the molecular dissection of the mechanism of chaperone action has to be driven forward using in vitro systems based on pure proteins. Uncovering the mechanism by which the double-toroid chaperonins mediate ATP-dependent folding may well reveal novel principles of enzyme action. Progress is still limited by the lack of three-dimensional structural information, although several crystallography laboratories are attempting to grow chaperone protein crystals. In the meantime, the potential of alternative methodologies to analyze protein structure, such as the modern techniques of structural electron microscopy, will have to be exploited. Given the considerable interest in molecular chaperones, any effort seems justified to finally provide the answers to the most burning questions.

ACKNOWLEDGMENTS

We are grateful to many of our colleagues for sharing unpublished information and for stimulating discussion. Specifically we thank Drs. W. Baumeister, B. Bukau, E. Craig, T. Creighton, M. Douglas, H. Echols, J. Ellis, J. Flanagan, C. Georgopoulos, A. Goldberg, A. Grigorov, C. Gross, R. Hlodan, A. Horwich, T. Langer, E. Nimmesgern, W. Neupert, J. Rothman, M. Wiedmann, and K. Willison. J.P.H. is supported by a postdoctoral training grant from the American Cancer Society.

Literature Cited

1. Laskey, R. A., Honda, B. M., Finch, J. T. 1978. *Nature* 275:416–20
2. Haas, I. G., Wabl, M. 1983. *Nature* 306:387–89
3. Bole, D. G., Hendershot, L. M., Kearney, J. F. 1986. *J. Cell Biol.* 102:1558–66
4. Copeland, C. S., Doms, R. W., Bolzau, E. M., Webster, R. G., Helenius, A. 1986. *J. Cell Biol.* 103:1179–91
5. Gething, M.-J., McCammon, K., Sambrook, J. 1986. *Cell* 46:939–50
6. Rothman, J. E., Schmid, S. L. 1986. *Cell* 46:5–9
7. Chirico, W. J., Waters, M. G., Blobel, G. 1988. *Nature* 332:805–10
8. Deshaies, R. J., Koch, B. D., Werner-Washburne, M., Craig, E. A., Schekman, R. 1988. *Nature* 332:800–5
9. Murakami, H., Pain, D., Blobel, G. 1988. *J. Cell Biol.* 107:2051–57
10. Normington, K., Kohno, K., Kozutsumi, Y., Gething, M.-J., Sambrook, J. 1989. *Cell* 57:1223–36
11. Rose, M. D., Misra, L. M., Vogel, J. P. 1989. *Cell* 57:1211–21
12. Beckmann, R. P., Mizzen, L. A., Welch, W. J. 1990. *Science* 248:850–54
13. Kang, P.-J., Ostermann, J., Shilling, J., Neupert, W., Craig, E. A., et al. 1990. *Nature* 348:137–43
14. Scherer, P. E., Krieg, U. C., Hwang, S. T., Vestweber, D., Schatz, G. 1990. *EMBO J.* 9:4315–22
15. Skowyra, D., Georgopoulos, C., Zylicz, M. 1990. *Cell* 62:939–44
16. Vogel, J. P., Misra, L. M., Rose, M. D. 1990. *J. Cell Biol.* 110:1885–95
17. Flynn, G. C., Rohl, J., Flocco, M. T., Rothman, J. E. 1991. *Nature* 353:726–30
18. Landry, S., Jordan, R., McMacken, R., Gierasch, L. 1992. *Nature* 355:455–57
19. Sanders, S. L., Whitfield, K. M., Vogel, J. P., Rose, M. D., Schekman, R. W. 1992. *Cell* 69:353–65
20. Sherman, M. Y., Goldberg, A. L. 1992. *EMBO J.* 11:71–77
21. Terlecky, S. R., Chiang, H.-L., Olson, T. S., Dice, J. F. 1992. *J. Biol. Chem.* 267:9202–9
22. Collier, D. N., Bankaitis, V. A., Weiss, J. B. Jr., Bassford, P. J. 1988. *Cell* 53:273–83
23. Lecker, S. H., Driessen, A. J. M., Wickner, W. 1990. *EMBO J.* 9:2309–14
24. Wickner, S. H. 1990. *Proc. Natl. Acad. Sci. USA* 87:2690–94
25. Hardy, S. J. S., Randall, L. L. 1991. *Science* 251:439–43
26. Liberek, K., Marszalek, J., Ang, D., Georgopoulos, C., Zylicz, M. 1991. *Proc. Natl. Acad. Sci. USA* 88:2874–78
27. Atencio, D. P., Yaffe, M. P. 1992. *Mol. Cell. Biol.* 12:283–91
28. Grigorov, A., Nudler, E., Komissarova, N., Goltsaris, G. A.,

Gottesman, M. E., et al. 1992. *Proc. Natl. Acad. Sci. USA*. 89:10341–44
29. Langer, T., Lu, C., Echols, H., Flanagan, J., Hayer, M. K., et al. 1992. *Nature* 356:683–89
30. Wild, J., Altman, E., Yura, T., Gross, C. A. 1992. *Genes Dev.* 6:1165–72
31. Georgopoulos, C., Hendrix, R. W., Casjens, S. R., Kaiser, A. D. 1973. *J. Mol. Biol.* 76:45–60
32. Barraclough, R., Ellis, R. J. 1980. *Biochim. Biophys. Acta* 608:18–31
33. Cannon, S., Wang, P., Roy, H. 1986. *J. Cell Biol.* 103:1327–35
34. Bochkareva, E. S., Lissin, N. M., Girshovich, A. S. 1988. *Nature* 336: 254–57
35. Hemmingsen, S. M., Woolford, C., van der Vies, S. M., Tilly, K., Dennis, D. T., et al. 1988. *Nature* 333:330–34
36. Cheng, M. Y., Hartl, F.-U., Martin, J., Pollock, R. A., Kalousek, F., et al. 1989. *Nature* 337:620–25
37. Goloubinoff, P., Christeller, J. T., Gatenby, A. A., Lorimer, G. H. 1989. *Nature* 342:884–89
38. Goloubinoff, P., Gatenby, A. A., Lorimer, G. H. 1989. *Nature* 337:44–47
39. Ostermann, J., Horwich, A. L., Neupert, W., Hartl, F.-U. 1989. *Nature* 341:125–30
40. Buchner, J., Schmidt, M., Fuchs, M., Jaenicke, R., Rudolph, R., et al. 1991. *Biochemistry* 30:1586–91
41. Martin, J., Langer, T., Boteva, R., Schramel, A., Horwich, A. L., et al. 1991. *Nature* 352:36–42
42. Bochkareva, E. S., Lissin, N. M., Flynn, G. C., Rothman, J. E., Girshovich, A. S. 1992. *J. Biol. Chem.* 267:6796–800
43. Langer, T., Pfeifer, G., Martin, J., Baumeister, W., Hartl, F.-U. 1992. *EMBO J.* In press
44. Viitanen, P., Gatenby, A. A., Lorimer, G. H. 1992. *Protein Sci.* 1:363–69
45. Trent, J. D., Nimmesgern, E., Wall, J. S., Hartl, F.-U., Horwich, A. L. 1991. *Nature* 354:490–93
46. Frydman, J., Nimmesgern, E., Erdjument-Bromage, H., Wall, J. S., Tempst, P., et al. 1992. *EMBO J.* In press
47. Gao, Y., Thomas, O., Chow, R. L., Lee, G.-H., Cowan, N. J. 1992. *Cell* 69:1043–50
48. Lewis, V. A., Hynes, G. M., Zheng, D., Saibil, H., Willison, K. 1992. *Nature* 358:249–52
49. Yaffe, M. B., Farr, G. W., Miklos, D., Horwich, A. L., Sternlicht, M. L., et al. 1992. *Nature* 358:245–48
50. Sefton, B. M., Beemon, K., Hunter, T. 1978. *J. Virol.* 28:957–71
51. Catelli, M. G., Binart, N., Jung-Testa, I., Renoir, J. M., Baulieu, E. E., et al. 1985. *EMBO J.* 4:3131–37
52. Sanchez, E. R., Toft, D. O., Schlesinger, M. J., Pratt, W. B. 1985. *J. Biol. Chem.* 260:12398–401
53. Dalman, F. C., Bresnick, E. H., Patel, P. D., Perdew, G. H., Watson, S. J., et al. 1989. *J. Biol. Chem.* 264:19815–21
54. Picard, D., Khursheed, B., Garabedian, B., Fortin, M. G., Lindquist, S., et al. 1990. *Nature* 348:166–68
55. Scherrer, L. C., Dalman, F. C., Massa, E., Meshinchi, S., Pratt, W. B. 1990. *J. Biol. Chem.* 265:21397–400
56. Czermely, P., Kahn, R. C. 1991. *J. Biol. Chem.* 266:4943–50
57. Callebaut, I., Renoir, J.-M., Lebeau, M.-C., Massol, N., Burny, A., et al. 1992. *Proc. Natl. Acad. Sci. USA* 89:6270–74
58. Smith, D. F., Stensgard, B. A., Welch, W. J., Toft, D. O. 1992. *J. Biol. Chem.* 267:1350–56
59. Tai, P.-K. K., Albers, M. W., Chang, H., Faber, L. E., Schreiber, S. L. 1992. *Science* 256:1315–18
60. Gething, M.-J., Sambrook, J. 1992. *Nature* 355:33–45
61. Freedman, R. B. 1992. *Protein Folding*, ed. T. E. Creighton. New York: Freeman
62. Ellis, R. J., van der Vies, S. M. 1991. *Annu. Rev. Biochem.* 60:321–47
63. Ellis, R. J. 1987. *Nature* 328:378–79
64. Pelham, H. R. B. 1986. *Cell* 46:959–61
65. Rothman, J. E. 1989. *Cell* 59:591–601
66. Horwich, A. L., Neupert, W., Hartl, F.-U. 1990. *Trends Biotechnol.* 8:126–31
67. Hartl, F.-U., Neupert, W. 1990. *Science* 247:930–38
68. Anfinsen, C. B. 1973. *Science* 181: 223–30
69. Levinthal, C. 1968. *J. Chem. Phys.* 65:44–45
70. Anfinsen, C. B., Haber, E., Sela, M., White, F. H. 1961. *Proc. Natl. Acad. Sci. USA* 47:1309–14
71. Creighton, T. E. 1990. *Biochem. J.* 270:1–16
72. Dobson, C. M. 1992. *Curr. Opin. Struct. Biol.* 2:343–45
73. Christensen, H., Pain, R. H. 1991. *Eur. Biophys. J.* 19:221–29
74. Jaenicke, R. 1987. *Prog. Biophys. Mol. Biol.* 49:117–237
75. Radford, S. E., Dobson, C. M., Evans, P. A. 1992. *Nature* 358:302–7
76. Fischer, G., Schmid, F. X. 1990. *Biochemistry* 29:2205–12

77. Nilsson, B., Anderson, S. 1991. *Annu. Rev. Microbiol.* 45:607–35
78. Hartl, F.-U., Martin, J., Neupert, W. 1992. *Annu. Rev. Biophys. Biomol. Struct.* 21:293–322
79. Kim, P. S., Baldwin, R. L. 1984. *Nature* 307:329–34
80. Wright, P. E., Dyson, H. J., Lerner, R. A. 1988. *Biochemistry* 27:7167–75
81. Oas, T. G., Kim, P. S. 1988. *Nature* 336:42–48
82. Blond, S., Goldberg, M. 1987. *Proc. Natl. Acad. Sci. USA* 84:1147–51
83. Kim, P. S., Baldwin, R. L. 1990. *Annu. Rev. Biochem.* 59:631–60
84. Andrin, G., Taniuchi, H. 1978. *J. Biol. Chem.* 253:2262–70
84a. Flanagan, J. M., Kataoka, M., Sortie, D., Engelman, D. M. 1991. *Proc. Natl. Acad. Sci. USA* 89:748–52
85. Dill, K. A. 1990. *Biochemistry* 29: 7133–55
86. Kuwajima, K. 1989. *Proteins* 6:87–103
87. Miranker, A., Radford, S. E., Karplus, M., Dobson, C. M. 1991. *Nature* 349:633–36
88. Ptitsyn, O. B. 1991. *J. Protein Chem.* 6:272–93
89. Darnell, J., Lodish, H., Baltimore, D. 1986. *Molecular Cell Biology*. New York: Freeman
90. Randall, L. L., Hardy, S. J. S. 1986. *Cell* 46:921–28
91. Eilers, M., Schatz, G. 1986. *Nature* 322:228–32
92. Rassow, J., Hartl, F.-U., Guiard, B., Pfanner, N., Neupert, W. 1990. *FEBS Lett.* 275:190–94
93. Manning-Krieg, U. C., Scherer, P. E., Schatz, G. 1991. *EMBO J.* 10:3273–80
94. Braakman, I., Helenius, J., Helenius, A. 1992. *Nature* 356:260–62
95. Park, S., Liu, G., Topping, T. B., Cover, W. H., Randall, L. L. 1988. *Science* 239:1033–35
96. Laminet, A. A., Pluckthun, A. 1989. *EMBO J.* 8:1469–77
97. Zhu, X., Ohta, Y., Jordan, F., Inouye, M. 1989. *Nature* 339:483–85
98. Silen, J. L., Agard, D. A. 1989. *Nature* 341:462–64
99. Gray, A. M., Mason, A. J. 1990. *Science* 247:1328–30
100. Lindquist, S., Craig, E. A. 1988. *Annu. Rev. Genet.* 22:631–77
101. Craig, E. A., Gross, C. A. 1991. *Trends Biochem. Sci.* 16:135–40
102. Georgopoulos, C., Ang, D., Liberek, K., Zylicz, M. 1990. *Stress Proteins in Biology and Medicine*, ed. R. I. Morimoto, A. Tissieres, C. Georgopoulos, pp. 191–222. Cold Spring Harbor, NY: Cold Spring Harbor Press
103. Lewis, M. J., Pelham, H. R. B. 1985. *EMBO J.* 4:3137–42
104. Dice, J. F. 1990. *Trends Biochem. Sci.* 376:305–9
105. Echols, H. 1990. *J. Biol. Chem.* 265: 14697–700
106. Shi, Y., Thomas, J. O. 1992. *Mol. Cell. Biol.* 12:2186–92
107. Chappell, T. G., Konforti, B. B., Schmid, S. L., Rothman, J. E. 1987. *J. Biol. Chem.* 262:746–51
108. Flaherty, K. M., DeLuca-Flaherty, C., McKay, D. B. 1990. *Nature* 346:623–28
109. Flaherty, K. M., McKay, D. B., Kabsch, W., Holmes, K. C. 1991. *Proc. Natl. Acad. Sci. USA* 88:5041–45
110. Steitz, T. A., Shoham, M., Bennett, W. S. 1981. *Philos. Trans. R. Soc. London Ser. B* 293:43–52
111. Bennett, W. S., Steitz, T. A. 1978. *Proc. Natl. Acad. Sci. USA* 75:4848–52
112. Korn, B. D., Carlier, M.-F., Pantaloni, D. 1987. *Science* 238:638–44
113. Liberek, K., Skowyra, D., Zylicz, M., Johnson, C., Georgopoulos, C. 1991. *J. Biol. Chem.* 266:14491–96
114. Palleros, D. R., Welch, W. J., Fink, A. 1991. *Proc. Natl. Acad. Sci. USA* 88:5719–23
115. Rippmann, F., Taylor, W. R., Rothbard, J. B., Green, N. M. 1991. *EMBO J.* 10:1053–59
116. Landry, S. J., Gierasch, L. M. 1991. *Biochemistry* 30:7359–62
117. Schiebel, E., Driessen, A. J., Hartl, F.-U., Wickner, W. 1991. *Cell* 64:927–39
118. Rassow, J., Guiard, B., Wienhues, U., Herzog, V., Hartl, F.-U., et al. 1989. *J. Cell. Biol.* 109:1421–28
119. Schlenstedt, G., Hudmundsson, G. H., Boman, H. G., Zimmermann, R. 1990. *J. Biol. Chem.* 265:13960–68
120. Zimmermann, R., Zimmermann, J., Wiech, H., Schlenstedt, G., Muller, G., et al. 1990. *J. Bioeng. Biomem.* 22:711–23
121. Eilers, M., Schatz, G. 1988. *Cell* 52: 481–83
122. Eilers, M., Hwang, S., Schatz, G. 1988. *EMBO J.* 7:1139–45
123. Crooke, E., Guthrie, B., Lecker, S., Lill, R., Wickner, W. 1988. *Cell* 54: 1003–11
124. Sanz, P., Meyer, D. I. 1988. *EMBO J.* 7:3553–57
125. Zimmermann, R., Sagstetter, M., Lewis, M. J., Pelham, H. R. B. 1988. *EMBO J.* 7:2875–80
126. Kumamoto, C. A., Beckwith, J. 1985. *J. Bacteriol.* 163:267–74

127. Kumamoto, C. A. 1989. *Proc. Natl. Acad. Sci. USA* 86:5320–24
128. Weiss, J. B., Ray, P. H. Jr., Bassford, P. J. 1988. *Proc. Natl. Acad. Sci. USA* 85:8978–82
129. Crooke, E., Wickner, W. 1987. *Proc. Natl. Acad. Sci. USA* 84:5216–20
130. Lecker, S., Lill, R., Ziegelhoffer, T., Georgopoulos, C., Bassford, P. J., et al. 1989. *EMBO J.* 8:2703–9
131. Liu, G., Topping, T. B., Randall, L. L. 1989. *Proc. Natl. Acad. Sci. USA* 86:9213–17
132. Sheffield, W. P., Shore, G. C., Randall, S. K. 1990. *J. Biol. Chem.* 265:11069–76
133. Beckmann, R. P., Lovett, M., Welch, W. J. 1992. *J. Cell Biol.* 117:1137–50
134. Saito, H., Uchida, H. 1978. *Mol. Gen. Genet.* 164:1–8
135. Yochem, J., Uchida, H., Sunshine, M., Saito, H., Georgopoulos, C. P., et al. 1978. *Mol. Gen. Genet.* 164:9–14
136. Zylicz, M., Yamamoto, T., McKittrick, N., Sell, S., Georgopoulos, C. 1985. *J. Biol. Chem.* 260:7591–98
137. Ohki, M., Tamura, F., Nishimura, S., Uchida, H. 1986. *J. Biol. Chem.* 261: 1778–81
138. Tandon, S., Horowitz, P. M. 1990. *J. Biol. Chem.* 265:5967–70
139. Ang, D., Chandrasekhar, G. N., Zylicz, M., Georgopoulos, C. 1986. *J. Bacteriol.* 167:25–29
140. Kurihara, T., Silver, P. A. 1992. *Membrane Biogenesis and Protein Targeting*, ed. W. Neupert, R. Lill, pp. 305–27. Amsterdam: Elsevier Sci.
141. Caplan, A. J., Douglas, M. G. 1991. *J. Cell Biol.* 114:609–21
142. Luke, M. M., Sutton, A., Arndt, K. T. 1991. *J. Cell Biol.* 114:623–38
143. Sadler, I., Chiang, A., Kurihara, T., Rothblatt, J., Way, J., et al. 1989. *J. Cell. Biol.* 109:2665–75
144. Blumberg, H., Silver, P. 1991. *Nature* 349:627–30
145. Feldheim, D., Rothblatt, J., Schekman, R. 1992. *Mol. Cell. Biol.* 12:3288–96
146. Wild, J., Kamath-Loeb, A., Ziegelhoffer, E., Lonetto, M., Kawasaki, Y., et al. 1992. *Proc. Natl. Acad. Sci. USA* 89:7139–43
147. Lindquist, S. 1992. *Curr. Biol.* 2:119–21
148. Alfano, C., McMacken, R. 1989. *J. Biol. Chem.* 264:10699–708
149. Dodson, M., McMacken, R., Echols, H. 1989. *J. Biol. Chem.* 264:10719–25
150. Zylicz, M., Ang, D., Liberek, K., Georgopoulos, C. 1989. *EMBO J.* 8: 1601–8
151. Wickner, S., Hoskins, J., McKenney, K. 1991. *Nature* 350:165–67
152. Wickner, S., Hoskins, J., McKenney, K. 1991. *Proc. Natl. Acad. Sci. USA* 88:7903–7
153. Ungewickell, E. 1985. *EMBO J.* 4: 3385–91
154. Ostermann, J., Voos, W., Kang, P. J., Craig, E. A., Neupert, W., et al. 1990. *FEBS Lett.* 277:281–84
155. Neupert, W., Hartl, F.-U., Craig, E. A., Pfanner, N. 1990. *Cell* 63:447–50
156. Munro, S., Pelham, H. 1986. *Cell* 46:291–300
157. Gething, M. J., Sambrook, J. 1990. *Semin. Cell Biol.* 1:65–72
158. Nguyen, T. H., Law, D. T. S., Williams, D. B. 1991. *Proc. Natl. Acad. Sci. USA* 88:1565–69
159. Lippincott-Schwartz, J., Bonifacino, J., Yuan, L., Klausner, R. 1988. *Cell* 54:209–20
160. Kozutsumi, Y., Segal, M., Normington, K., Gething, M.-J., Sambrook, J. 1988. *Nature* 332:462–64
161. Kassenbrock, C. K., Garcia, P. D., Walter, P., Kelly, R. B. 1988. *Nature* 333:90–93
162. Hurtley, S. M., Helenius, A. 1989. *Annu. Rev. Cell Biol.* 5:227–307
163. Nguyen, V. T., Morange, M., Bensaude, O. 1989. *J. Biol. Chem.* 264:10487–92
164. Pinto, M., Morange, M., Bensaude, O. 1991. *J. Biol. Chem.* 266:13941–46
165. Li, G. C., Li, L., Liu, R. Y., Rehman, M., Lee, W. M. F. 1992. *Proc. Natl. Acad. Sci. USA* 89:2036–40
166. Baler, R., Welch, W. J., Voellmy, R. 1992. *J. Cell Biol.* 117:1151–59
167. Gamer, J., Bujard, H., Bukau, B. 1992. *Cell* 69:833–42
168. Chiang, H.-L., Dice, J. F. 1988. *J. Biol. Chem.* 263:6797–805
169. Dice, J. F., Chiang, H.-L., Spenser, E. P., Backer, J. M. 1986. *J. Biol. Chem.* 262:6853–59
170. Chiang, H.-L., Terlecky, S. R., Plant, C. P., Dice, J. F. 1989. *Science* 246: 382–85
171. Sherman, M. Y., Goldberg, A. L. 1991. *J. Bacteriol.* 173:7249–56
172. Straus, D. B., Walter, W. A., Gross, C. A. 1988. *Genes Dev.* 2:1851–58
173. Hendrix, R. W. 1979. *J. Mol. Biol.* 129:375–92
174. McMullin, T. W., Hallberg, R. L. 1987. *Mol. Cell. Biol.* 7:4414–23
175. Hutchison, E. G., Tichelaar, W., Hofhaus, G., Weiss, H., Leonard, K. R. 1989. *EMBO J.* 8:1485–90
176. Takano, T., Kakefuda, T. 1972. *Nature New Biol.* 239:34–37

177. Coppo, A., Manzi, A., Pulitzer, J. F., Takahashi, H. 1973. *J. Mol. Biol.* 76:61–87
178. Zweig, M., Cummings, D. 1973. *J. Mol. Biol.* 80:505–18
179. Hohn, T., Hohn, B., Engel, A., Wortz, M., Smith, P. R. 1979. *J. Mol. Biol.* 129:359–73
180. Hemmingsen, S. M., Ellis, R. J. 1986. *Plant Physiol.* 80:269–76
181. Gupta, R. S. 1990. *Biochem. Int.* 4: 833–39
182. Ellis, R. J. 1990. *Science* 250:954–59
183. Hartman, D. J., Hoogenraad, N. J., Condron, R., Hoj, P. B. 1992. *Proc. Natl. Acad. Sci. USA* 89:3394–98
184. Lubben, T. H., Gatenby, A. A., Donaldson, G. K., Lorimer, G. H., Viitanen, P. V. 1990. *Proc. Natl. Acad. Sci. USA* 87:7683–87
185. Milos, P., Roy, H. 1984. *J. Cell Biochem.* 24:153–62
186. Musgrove, J. E., Johnson, R. A., Ellis, R. J. 1987. *Eur. J. Biochem.* 163:529–34
187. Roy, H., Hubbs, A., Cannon, S. 1988. *Plant Physiol.* 86:50–53
188. Cheng, M. Y., Hartl, F.-U., Horwich, A. L. 1990. *Nature* 348:455–58
189. Viitanen, P. V., Donaldson, G. K., Lorimer, G. H., Lubben, T. H., Gatenby, A. A. 1991. *Biochemistry* 30:9716–23
190. VanDyk, T., Gatenby, A., LaRossa, R. 1989. *Nature* 342:451–53
191. Mendoza, J. A., Rogers, E., Lorimer, G. H., Horowitz, P. M. 1991. *J. Biol. Chem.* 266:13044–49
192. Zahn, R., Pluckthun, A. 1992. *Biochemistry* 31:3249–55
193. Touchette, N., Perry, K., Matthews, C. R. 1986. *Biochemistry* 25:5445–52
194. van der Vies, S. M., Viitanen, P. V., Gatenby, A. A., Lorimer, G. H., Jaenicke, R. 1992. *Biochemistry* 31: 3635–44
195. Schmidt, M., Buchner, J. 1992. *J. Biol. Chem.* 267:16829–33
196. Viitanen, P. V., Lorimer, G. H., Seetharam, R., Gupta, R. S., Oppenheim, J., et al. 1992. *J. Biol. Chem.* 267:695–68
197. Viitanen, P. V., Lubben, T. H., Reed, J., Goloubinoff, P., O'Keefe, D. P., et al. 1990. *Biochemistry* 29: 5665–71
198. Laminet, A. A., Ziegelhoffer, T., Georgopoulos, C., Pluckthun, A. 1990. *EMBO J.* 9:2315–19
199. Badcoe, I. G., Smith, C. J., Wood, S., Halsall, D. J., Holbrook, J., et al. 1991. *Biochemistry* 30:9195–200
200. Chadrasekhar, G. N., Tilly, K., Woolford, C., Hendrix, R., Georgopoulos, C. 1986. *J. Biol. Chem.* 261:12414–19
201. Gray, T. E., Fersht, A. R. 1992. *FEBS Lett.* 292:254–58
202. Saibil, H., Dong, Z., Wood, S., AutoDerMauer, A. 1991. *Nature* 353:25[illegible]
203. Ishii, N., Taguchi, H., Sumi, M., Yoshida, M. 1992. *FEBS Lett.* 299: 169–74
204. Creighton, T. E. 1986. *Protein Structure, Folding, and Design*, ed. D. [illegible] Oxender, pp. 249–57 New York: [illegible]
205. Mizobata, T., Akiyama, Y., Ito, Yumoto, N., Kawata, Y. 1992. *Biol. Chem.* 267:17773–79
206. Creighton, T. E. 1991. *Nature* 352:17–18
207. Taguchi, H., Konishi, J., Ishii, N., Yoshida, M. 1991. *J. Biol. Chem.* 266:22411–18
208. Martin, J., Horwich, A. L., Hartl, F.-U. 1992. *Science.* 258:995–98
209. Mendoza, J. A., Lorimer, G. H., Horowitz, P. M. 1992. *J. Biol. Chem.* 267:17631–34
210. Holl-Neugebauer, B., Rudolph, [illegible] Schmidt, M., Buchner, J. 1991. [illegible] *chemistry* 30:11609–14
211. Phipps, B. M., Hoffmann, A., Stetter, K. O., Baumeister, W. 1991. *EMBO J.* 10:1711–22
212. Silver, L. M., Artzt, K., Bennett, [illegible] 1979. *Cell* 17:275–84
213. Silver, L. M., Remis, D. 1987. *Genet. Res.* 49:51–56
214. Willison, K., Lewis, V., Zuckerman, K. S., Cordell, J., Dean, C., et al. 1989. *Cell* 57:621–32
215. Ursic, D., Culbertson, M. R. 1991. *Mol. Cell. Biol.* 11:2629–40
215a. Phipps, B. M., Typke, D., Hegerl, R., Volker, S., Hoffman, A., et al. 1993. *Nature.* In press
216. Ellis, R. J. 1992. *Nature* 358:191–92
217. Dalman, F. C., Scherrer, L. C., Taylor, L. P., Akil, H., Pratt, W. B. 1991. *J. Biol. Chem.* 266:3482–90
218. Pratt, W. B. 1990. *Mol. Cell Endocrinol.* 74:C69-C76
219. Pongratz, I., Mason, G. G., Poellinger, L. 1992. *J. Biol. Chem.* 267:13728–34
220. Spence, J., Georgopoulos, C. 1989. *J. Biol. Chem.* 264:4398–403
221. Sorger, P. K., Pelham, H. R. 1987. *J. Mol. Biol.* 194:341–44
222. Mazzarella, R. A., Green, M. 1987. *J. Biol. Chem.* 262:8875–83
223. Koyasu, S., Nishida, E., Miyata, Y., Sakai, H., Yahara, I. 1989. *J. Biol. Chem.* 264:15083–87
224. Sargan, D. R., Tsai, M. J., O'Malley, B. W. 1986. *Biochemistry* 25:6252–58
225. Denis, M., Cuthill, S., Wikström, A.

C., Gustafsson, J.-Å. 1998. *Biochem. Biophys. Res. Commun.* 155:801–7
226. Perdew, G. H. 1988. *J. Biol. Chem.* 263:1841–52
227. Miyata, Y., Yahara, I. 1992. *J. Biol. Chem.* 267:7042–47
228. Oppermann, H., Levinson, W., Bishop, J. M. 1981. *Proc. Natl. Acad. Sci. USA* 78:1067–71
229. Brugge, J. S. 1986. *Curr. Top. Microbiol. Immunol.* 123:1–23
230. Hutchison, K. A., Stancato, L. F., Jove, R., Pratt, W. B. 1992. *J. Biol. Chem.* 267:13952–57
231. Sanchez, E. R. 1990. *J. Biol. Chem.* 265:22067–70
232. Perdew, G. H., Whitelaw, M. L. 1991. *J. Biol. Chem.* 266:6708–13
233. Yem, A. W., Tomasselli, A. G., Heinrikson, R. L., Zurcher, N. H., Ruff, V. A., et al. 1992. *J. Biol. Chem.* 267:2868–71
234. Lees, M. S., Anderson, C. W. 1989. *J. Biol. Chem.* 264:17275–80
235. Liu, J., Farmer, J. D., Lane, W. S., Friedman, J., Weissman, I., et al. 1991. *Cell* 66:807–15
236. Walsh, C. T., Zydowsky, L. D., McKeon, F. D. 1992. *J. Biol. Chem.* 267:13115–18
237. Wiech, H., Buchner, J., Zimmermann, R., Jacob, U. 1992. *Nature* 358:169–70
238. Zhi, W., Landry, S. J., Gierasch, L. M., Srere, P. A. 1992. *Protein Sci.* 1:522–29
239. Mizzen, L. A., Kabiling, A. N., Welch, W. J. 1991. *Cell Regul.* 2:165–79
240. Koll, H., Guiard, B., Rassow, J., Ostermann, J., Horwich, A. L., et al. 1992. *Cell* 68:1163–75
241. Puck, K.-H., Walker, G. C. 1987. *J. Bacteriol.* 169:283–90
242. Bukau, B., Walker, G. C. 1989. *J. Bacteriol.* 171:2337–46
243. Cyr, D. M., Lu, X., Douglas, M. G. 1992. *J. Biol. Chem.* 267:20927–31
244. Waegemann, K., Paulsen, H., Soll, J. 1990. *FEBS Lett.* 261:89–92
245. Amir-Shapira, D., Leustek, T., Dalie, B., Weisshach, H., Brot, N. 1990. *Proc. Natl. Acad. Sci. USA* 87:1749–52
246. Yalovsky, S., Paulsen, H., Michaeli, D., Chitnis, P. R., Nechushtai, R. 1992. *Proc. Natl. Acad. Sci. USA* 89:5616–19
247. Laminet, A. A., Kumamoto, C. A., Pluckthun, A. 1991. *Mol. Microbiol.* 5:117–22
248. Mizzen, L. A., Kabiling, A. N., Welch, W. J. 1991. *Cell Regul.* 2:165–79
249. Nadeau, K., Sullivan, M. A., Bradley, M., Engman, D. M., Walsh, C. T. 1992. *Protein Sci.* 1:970–79

Annu. Rev. Biochem. 1993. 62:385–427

BIOCHEMISTRY OF MULTIDRUG RESISTANCE MEDIATED BY THE MULTIDRUG TRANSPORTER[1]

Michael M. Gottesman[*] *and Ira Pastan*[**]
Laboratory of Cell Biology[*] and Laboratory of Molecular Biology,[**] National Cancer Institute, National Institutes of Health, Bethesda, Maryland 20892

KEY WORDS: chemotherapy, cancer, ATPase, gene therapy

CONTENTS

Human Molecular Genetics, 2001, Vol. 10, No. 14 1511–1518

Over-expression of inducible HSP70 chaperone suppresses neuropathology and improves motor function in *SCA1* mice

Christopher J. Cummings[1], Yaling Sun[1], Puneet Opal[2], Barbara Antalffy[3], Ruben Mestril[6], Harry T. Orr[7], Wolfgang H. Dillmann[8] and Huda Y. Zoghbi[1,2,4,5,*]

[1]Department of Pediatrics, [2]Department of Neurology, [3]Department of Pathology, [4]Department of Molecular and Human Genetics, [5]Howard Hughes Medical Institute, Baylor College of Medicine, Houston, TX 77030, USA, [6]Department of Physiology, Loyola University, Maywood, IL 60153, USA, [7]Departments of Laboratory Medicine and Pathology and Institute of Human Genetics, University of Minnesota, Minneapolis, MN 55455, USA and [8]Department of Medicine, Division of Endocrinology and Metabolism, University of California at San Diego, San Diego, CA 92103, USA

Received April 18, 2001; Revised and Accepted May 14, 2001

Many neurodegenerative diseases are caused by gain-of-function mechanisms in which the disease-causing protein is altered, becomes toxic to the cell, and aggregates. Among these 'proteinopathies' are Alzheimer's and Parkinson's disease, prion disorders and polyglutamine diseases. Members of this latter group, also known as triplet repeat diseases, are caused by the expansion of unstable CAG repeats coding for glutamine within the respective proteins. Spinocerebellar ataxia type 1 (SCA1) is one such disease, characterized by loss of motor coordination due to the degeneration of cerebellar Purkinje cells and brain stem neurons. In SCA1 and several other polyglutamine diseases, the expanded protein aggregates into nuclear inclusions (NIs). Because these NIs accumulate molecular chaperones, ubiquitin and proteasomal subunits—all components of the cellular protein re-folding and degradation machinery—we hypothesized that protein misfolding and impaired protein clearance might underlie the pathogenesis of polyglutamine diseases. Over-expressing specific chaperones reduces protein aggregation in transfected cells and suppresses neurodegeneration in invertebrate animal models of polyglutamine disorders. To determine whether enhancing chaperone activity could mitigate the phenotype in a mammalian model, we crossbred SCA1 mice with mice over-expressing a molecular chaperone (inducible HSP70 or iHSP70). We found that high levels of HSP70 did indeed afford protection against neurodegeneration.

INTRODUCTION

Spinocerebellar ataxia type 1 (SCA1) is an autosomal dominant neurodegenerative disorder characterized by progressive ataxia and degeneration of cerebellar Purkinje cells, inferior olivary neurons, and neurons within the brain stem. Symptons typically strike in midlife and worsen over the next 10–15 years; there is no established therapy to delay the onset or slow the progression of the disease (1). SCA1 is caused by the abnormal expansion of polyglutamine within the SCA1 gene product ataxin-1; normal alleles have between six and 44 glutamines, whereas disease alleles may bear as many as 82 units (2). At least seven other human neurodegenerative diseases are caused by a polyglutamine repeat expansion, including Huntington's disease, dentatorubro-pallidoluysian atrophy, spinocerebellar ataxia types 2, 3, 6, 7 and 12, and spinobulbar muscular atrophy (3). The mechanism by which expanded proteins lead to long-term neurodegeneration remains elusive, but it is clear from numerous studies that the expanded polyglutamine tract confers a toxic property or 'gain of function' on the otherwise unrelated disease proteins.

One hallmark of these diseases—and many other neurodegenerative disorders, including Alzheimer' disease, Parkinson' disease, amyotrophic lateral sclerosis and the prion disorders—is the formation of insoluble protein aggregates or inclusion bodies. These aggregates are immunoreactive for ubiquitin, and most have been reported to contain molecular chaperones and components of the proteasome (4). In previous work we put forward the hypothesis that the expanded polyglutamine tract alters the conformation of the ataxin-1, and that the misfolded protein is targeted for re-folding and proteolysis by the ubiquitin-proteasome pathway. The earliest suggestion that this might be the case came from a study showing that nuclear inclusions (NIs) in both SCA1 patient tissue and transgenic mice stain positively for the molecular chaperones Hsp70 and Hsp40, ubiquitin and proteasomal subunits (5). In

*To whom correspondence should be addressed at: Department of Pediatrics, Baylor College of Medicine, 1 Baylor Plaza, Houston, TX 77030, USA; Tel: +1 713 798 6558; Fax: +1 713 798 8728; Email: hzoghbi@bcm.tmc.edu
Present address: Christopher J. Cummings, AGY Therapeutics, 290 Utah Avenue, South San Francisco, CA 94080, USA

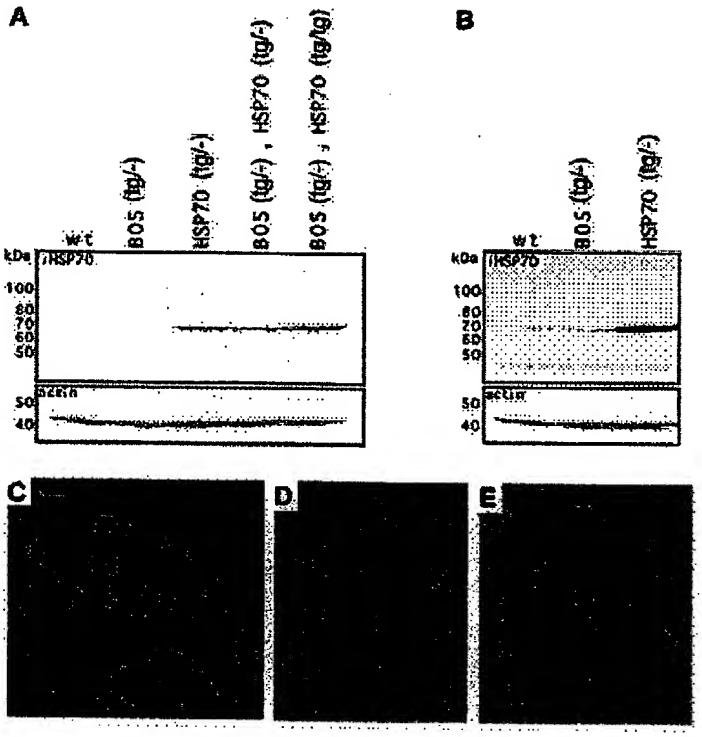

Figure 1. Transgenic mice ($HSP70^{tg/-}$; $B05^{tg/-}$, $HSP70^{tg/-}$; and $B05^{tg/-}$, $HSP70^{tg/tg}$) express high levels of rat iHSP70 in cerebellar Purkinje cells. Note that the SCA1 transgene in the double transgenic does not alter HSP70 levels. (**A**) Western blot analysis of total cerebellar protein lysate with antibodies specific for the inducible form of HSP70 shows a single band migrating at ~70 kDa in HSP70 transgenic mice but not in wild-type or B05 mice. (**B**) Maximum exposure of a similar western blot to reveal the low levels of endogenous iHSP70 demonstrates that rat iHSP70 expression is ~10-fold greater than endogenous iHSP70. (**C–E**) *In situ* RNA analysis demonstrates that the transgene is predominantly expressed in the Purkinje cell layer. Higher magnification in (**E**) reveals that the iHSP70 transcript in wild-type control animals is only slightly above the background. Therefore, unstressed transgene-positive mice express high levels of iHSP70 in cerebellar Purkinje cells. This high level of expression appears to occur without any apparent detrimental effect on gross cerebellar morphology.

support of a role for chaperones, we found that over-expression of an HSP40 chaperone, HDJ-2, reduces aggregation in tissue culture (5). To investigate the role of the ubiquitin-proteasome pathway in SCA1 pathogenesis, we crossed SCA1 transgenic mice (the B05 line) with mice lacking the ubiquitin E3 ligase, Ube3a. Neuronal degeneration was accelerated in these double mutants, and these results provided the first *in vivo* (albeit indirect) support for our hypothesis (6,7).

A genetic screen in an SCA1 fly model provided the most recent evidence that protein clearance pathways are involved in SCA1 pathology. Significantly, some of the more prominent exacerbations of the SCA1 phenotype occurred in the context of deficiency of chaperone proteins, including HSP70 (8). Other *Drosophila* models have also been used to demonstrate that overproduction of the Hsp70 and Hsp40 molecular chaperones suppresses polyglutamine-induced neurotoxicity (8–11). Chan *et al.* (11) further demonstrated that over-expression of the HSP40 chaperone dHdj-1 can suppress polyglutamine toxicity only in the presence of functional HSP70. Since HSP40 chaperones present substrates to HSP70 and stimulate its activity, it is not surprising that dHdj-1 would require functional HSP70 in order to modify the phenotype in flies.

RESULTS

Crossbreeding and iHSP70 expression analysis of HSP70/SCA1 mice

To determine whether over-expression of HSP70 could ameliorate the disease phenotype in an animal model which closely approximates the human disease, we crossed the well characterized B05 line (12) with mice that over-express the inducible form of rat HSP70, under the control of the human cytomegalovirus enhancer and chicken β-actin promoter (13). To evaluate their suitability for studies of the role of HSP70 on SCA1-induced neurodegeneration, we first sought to determine whether they express high levels of the transgene in cerebellar Purkinje cells. We used western blot analysis to compare the expression of endogenous HSP70 with that of iHSP70 in whole cerebellar extracts from Hsp70 transgenic and wild-type mice, B05 and B05/HSP70 double transgenics. Levels of endogenous iHSP70 in non-stressed wild-type mice are extremely low; HSP70 transgene expression is ~10-fold higher in $HSP70^{(tg/-)}$ mice (Fig. 1A and B). It is interesting that there is no difference between wild-type and B05 animals in HSP70 expression, which suggests that mutant ataxin-1

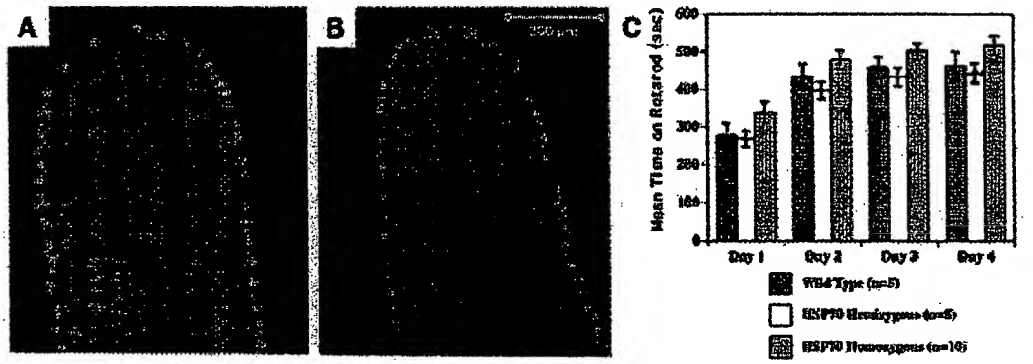

Figure 2. Cerebellar morphology and function in transgenic mice expressing rat iHSP70. Calbindin staining of cerebellar sections from 12.5-week-old wild-type (A) and HSP70$^{(tg/-)}$ mice (B) show similar morphology, indicating that HSP70 over-expression has no detectable effect on cerebellar and Purkinje cell morphology. (C) Expression of HSP70 alone has no significant effect on Rotarod performance.

expression alone does not elicit a notable HSP70 stress response. HSP70$^{(tg/-)}$ and B05$^{(tg/-)}$/HSP70$^{(tg/-)}$ mice demonstrate equal HSP70 levels (Fig. 1B). As homozygotes, HSP70$^{(tg/tg)}$ (data not shown) or B05$^{(tg/-)}$/HSP70$^{(tg/tg)}$ mice exhibit twice the HSP70 levels of HSP70 hemizygotes. Since it is conceivable that the abundant expression might be contributed by non-Purkinje cells—either neuronal or glial populations—we performed RNA *in situ* analysis to examine HSP70 expression within the cerebellum. We found that the strongest *in situ* signal localizes to the Purkinje cell layer (Fig. 1C and D). Immunohistochemical studies of the same HSP70 transgenic line confirmed that Purkinje cells contain high levels of the transgene product (14) and that the protein is predominantly cytoplasmic.

Chaperone over-expression alone is not deleterious to morphology or function

Because molecular chaperones have such a wide variety of functions, we first sought to determine whether over-expression of HSP70 might have deleterious effects on neuronal architecture or function. Because our subsequent analysis would be restricted to the cerebellum, we focused on cerebellar cyto-architecture and Purkinje cell dendritic morphology using the Purkinje cell-specific marker, calbindin. The fissura prima, which defines the anterior boundary of the central lobe, shows a similar degree of neuronal degeneration from one B05 animal to another, so we examined it at high magnification for comparison. Examination of wild-type and HSP70$^{(tg/-)}$ sections at 12.5 weeks (Fig. 2A and B, respectively) reveals that over-expression of rat iHSP70 alone does not have any detectable effect on normal cerebellar development or Purkinje cell morphology. Cerebellar function in HSP70 mice also seems unaffected; accelerating Rotarod analysis of 9.5-week-old mice revealed no difference between non-transgenic and transgenic mice over-expressing HSP70 at either hemizygous or homozygous levels (Fig. 2C; statistical analysis of variance revealed no differences in performance). These studies indicate that over-expression of the iHSP70 chaperone alone does not impair Purkinje cell development, survival or function.

High levels of chaperone expression mitigate the SCA1 behavioral phenotype

Having established that HSP70 over-expression does not itself cause a phenotype that would confound the results of our proposed study, we performed accelerating Rotarod tests at 9.5 and 12.5 weeks with B05 and B05/HSP70$^{(tg/-)}$ animals (Fig. 3A and B). B05 transgenic mice become ataxic by home cage behavior at 12 weeks of age and show motor incoordination by Rotarod testing as early as 5 weeks after birth (6,12). At 9.5 weeks of age, the B05 mice were significantly more impaired on the Rotarod than B05 littermates over-expressing HSP70$^{(tg/-)}$ (for the latter 3 of 4 days of trial) (Fig. 3A). Although both B05 and B05/HSP70$^{(tg/-)}$ mice performed worse at 12.5 weeks than at 9.5 weeks, the B05 littermates expressing HSP70$^{(tg/-)}$ (Fig. 3B) were notably better than the B05 mice. The 12.5-week-old B05/HSP70$^{(tg/-)}$ mice often lasted on the Rotarod until it reached maximum speed. In fact, two of the six B05/HSP70$^{(tg/-)}$ mice performed until the trial was complete (600 s). This level of coordination is very rare in B05 mice at 12.5 weeks (6,12).

To ensure that the improved motor coordination was due to the activity of HSP70 rather than genetic background effects, we next extended the Rotarod analysis to include B05/HSP70$^{(tg/tg)}$ mice at 9.5 weeks of age. The doubled HSP70 levels provided even greater improvement over the B05 animals (Fig. 3C). During all four days of the trial, the B05/HSP70$^{(tg/tg)}$ mice showed a statistically significant increase in mean performance time, suggesting that higher HSP70 levels offer protection against the polyglutamine-induced behavioral phenotype.

High HSP70 levels reduce SCA1 pathological changes

As reported previously, anti-calbindin immunofluorescence studies of B05 mice at 9.5 weeks revealed thinning of Purkinje cell dendritic arborization and slightly misaligned Purkinje cell layers with heterotopic Purkinje cells (Fig. 4A) (12). B05/HSP70$^{(tg/-)}$ mice at 9.5 weeks manifest a similar thinning of the Purkinje cell dendritic arborization but less spatial alteration in the Purkinje cell layer (Fig. 4B). In light of the dose-dependent protection seen by Rotarod analysis, we expected to find better

Purkinje cell morphology in B05 mice doubly transgenic for HSP70$^{(tg/tg)}$. Indeed, a 9.5-week-old B05/HSP70$^{(tg/tg)}$ cerebellum shows numerous Purkinje cells having thicker and more arborized dendritic branches than B05 neurons (Fig. 4C). The protective effect of HSP70 was still apparent at 12.5 weeks, as can be seen by comparing the B05 neuropathology with that of B05/HSP70$^{(tg/tg)}$ mice. The B05 cerebella contain numerous heterotopic Purkinje cells (arrowheads) with dramatically reduced dendritic arborization (Fig. 4D). Cerebella from B05/HSP70$^{(tg/tg)}$ mice, on the other hand, show markedly fewer heterotopic Purkinje cells and more robust dendritic arborization (Fig. 4E). Over-expression of iHPS70 thus suppresses the polyglutamine-induced neuropathology of SCA1 transgenic animals.

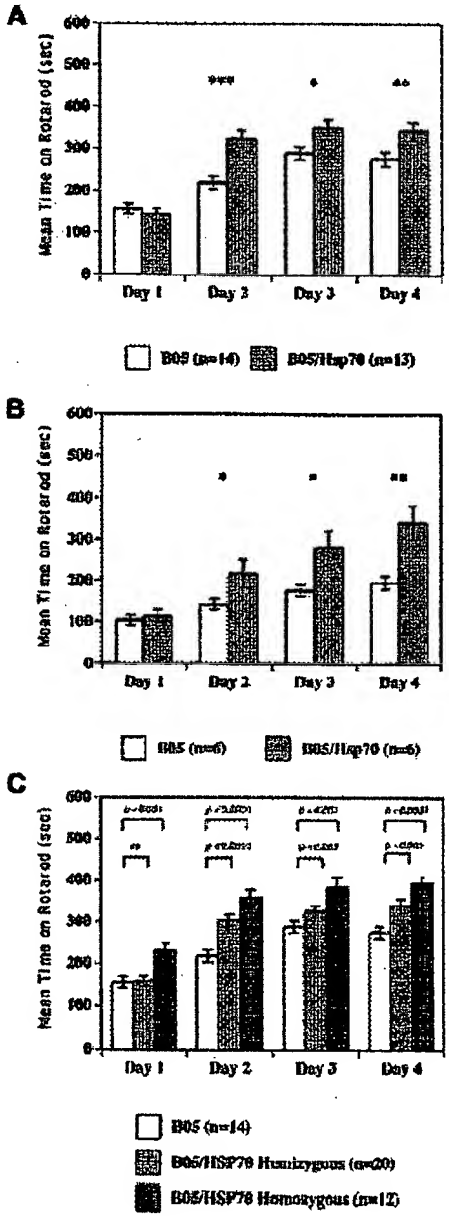

Figure 3. B05 transgenic mice expressing rat iHSP70 perform better on Rotarod than B05 littermates. For 3 of the 4 days of trial at both 9.5 (A) and 12.5 (B) weeks, the B05 transgenic mice expressing rat iHSP70$^{(tg/-)}$ last longer on the Rotarod than B05 littermates. Although both groups of animals show progressive loss of neurological function, the B05 animals expressing higher chaperone levels are able to maintain their balance on the rotating rod when it reaches the maximum speed (240 rotations/s). At 12.5 weeks, two of six double transgenic animals stayed on the Rotarod until the trial was complete at 600 s. This is rare with B05 animals at 12.5 weeks (none of six in this study). The performance levels with statistical difference between B05/HSP70$^{(tg/-)}$ and B05 littermates are noted with asterisks; *, $P < 0.05$; **, $P < 0.005$; ***, $P < 0.001$. (C) At 9.5 weeks of age, B05 mice expressing homozygous levels of HSP70$^{(tg/tg)}$ perform better on the Rotarod than B05/HSP70$^{(tg/-)}$ and B05 animals. In a larger set of animals the analysis was expanded to include B05 mice expressing homozygous levels of Hsp70$^{tg/tg}$. B05/HSP70$^{tg/tg}$ performed better than B05/HSP70$^{tg/-}$ animals, which in turn performed better than B05 mice.

Chaperone over-expression does not alter NI formation

In Purkinje cells from B05 mice, ataxin-1 is localized primarily to a single nuclear structure, with limited distribution throughout the nucleus (Fig. 5A) (5,7,15). Purkinje cells from age-matched (9.5 weeks) littermate B05 animals over-expressing inducible HSP70$^{(tg/tg)}$ had identical staining patterns (Fig. 5B). To quantify the occurrence of NI in the different lines, we divided the number of Purkinje cells with aggregates by the total number of Purkinje cells counted in 5 μm sections of the entire midsagittal cerebellar hemisphere. The percentage of B05 Purkinje cells bearing NI increases with age from ~27.5% at 6.5 weeks to ~55% at 9.5 weeks (Fig. 5C) (7,15). The double transgenic mice manifested similar rates of NI formation: ~25% at 6.5 weeks and ~50% at 9.5 weeks. Like the B05/HSP70$^{(tg/-)}$ at 9.5 weeks, B05/HSP70$^{(tg/tg)}$ mice had similar percentages of Purkinje cells with NI as the B05 line (~49%). These results are reminiscent of two studies in *Drosophila* which found that over-expression of HSP70 with or without dHdj-1 suppressed neuronal degeneration but did not noticeably affect NI formation (9,11).

DISCUSSION

This report is the first to demonstrate that high expression levels of iHSP70 afford protection against polyglutamine-induced neurodegeneration in a mammalian model of SCA1. By what mechanisms might the chaperones be conveying their ameliorative effect? One possibility is that they moderate the folding or ubiquitin-proteasomal clearance of mutant ataxin-1 (and other polyglutamine proteins). We previously showed that the NIs were smaller in the presence of higher-than-normal levels of DNAJ/HDJ-2, and Fernandez-Funez *et al.* (8) found that over-expression of dHdj-1 changed the pattern of NI formation in flies over-expressing mutant ataxin-1 (5). Others also found that hsp40 and hsp70 were able to inhibit polyglutamine fibril formation *in vitro* (16). Although Hsp70 and dHdj1 have not appreciably reduced the size of NI in a *Drosophila* model of SCA3, more of the mutant protein is extractable in these flies, since a greater proportion of the

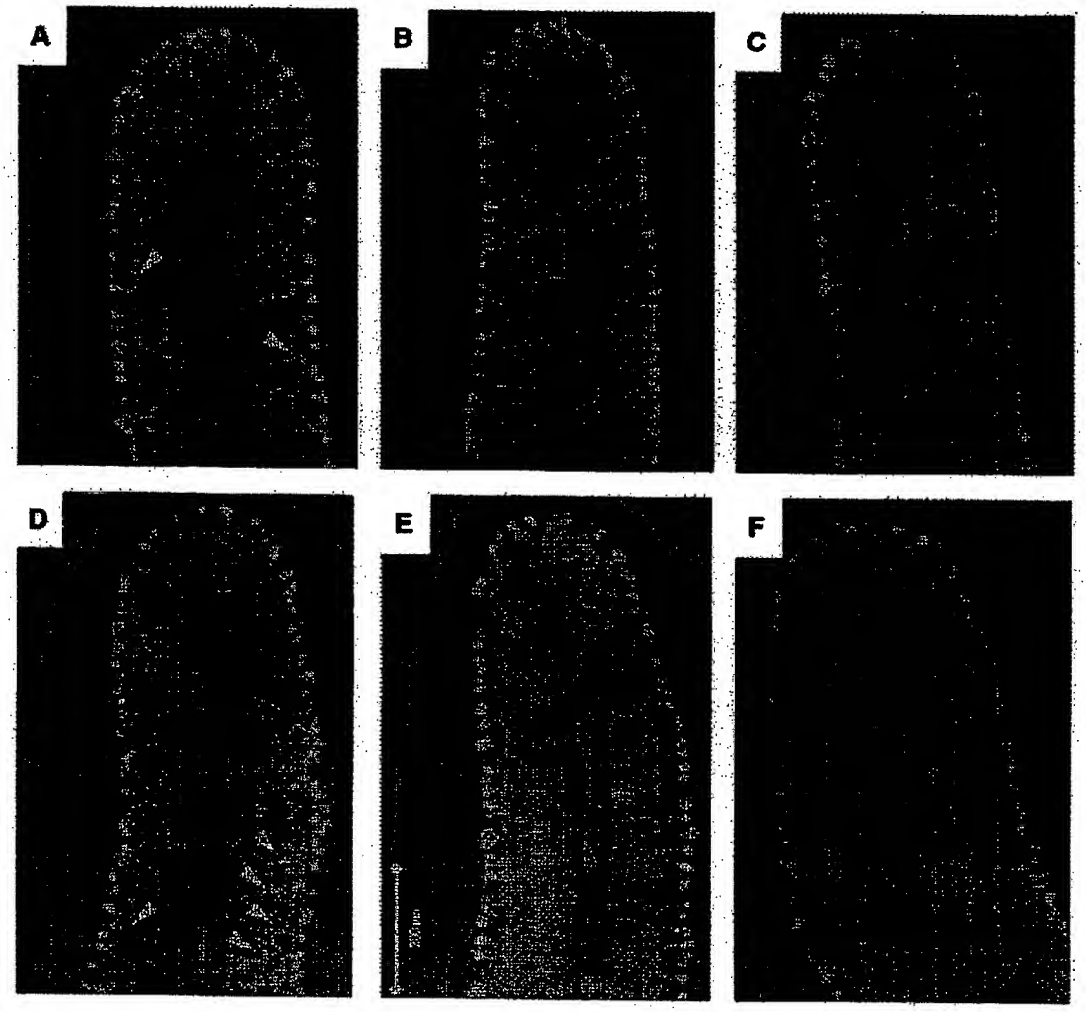

Figure 4. Cerebellar morphology in *SCA1* B05 transgenic mice expressing rat iHSP70. Calbindin staining of cerebellar sections at the level of the fissura prima between the anterodorsal and central lobes (A–F). Cerebellar section from (A) a 9.5-week-old B05 mouse demonstrating early alterations in Purkinje cells morphology, including thinning of the dendritic arborization and disruption of the Purkinje cell layer (arrowhead). (B) Sections from B05/HSP70$^{(+/-)}$ mice show similar Purkinje cell alterations. Transgenic mice hemizygous for B05 and homozygous for iHSP70 (C), however, have slightly thicker Purkinje cell dendritic arborization at 9.5 weeks than B05 and B05/HSP70$^{(+/-)}$ littermates. Progressive Purkinje cell pathology is seen in B05 mice at 12 weeks in (D), including loss of dendritic arborization and heterotopically localized Purkinje cells (arrowheads). (E) B05/HSP70$^{(+/+)}$ mice at 12 weeks have better dendritic arborization than B05 littermates, with marked reduction in Purkinje cell heterotopia [compare (D) and (E)]. (F) Wild-type at 12.5 weeks.

protein is visualized as a monomer on SDS gels when either or both of these chaperones are expressed (11).

Mutant ataxin-1 has proven to be difficult to extract or solubilize from cerebella of transgenic SCA1 mice (6). We did attempt to ascertain whether increased levels of Hsp70 in Purkinje cells could render expanded ataxin-1 more extractable or soluble. High salt and SDS extraction treatment of cerebella from B05 and B05/HSP70 mice, however, showed no appreciable effect; indeed, virtually none of the protein was soluble in SDS in either instance (data not shown). This lack of effect on protein solubilization might lie in the properties of complexed ataxin-1 in Purkinje cells (as opposed to complexes of other polyglutamine proteins such as ataxin-3 in *Drosophila*). Also, other factors such as the context of the polyglutamine tract, the stoichiometry of the chaperones, and cell-specific factors might contribute to differences in extractibility (17). It might be possible to solubilize ataxin-1 with more stringent extraction protocols; nonetheless, the disease phenotype is clearly mitigated with little apparent difference in the properties of the aggregating polyglutamine protein.

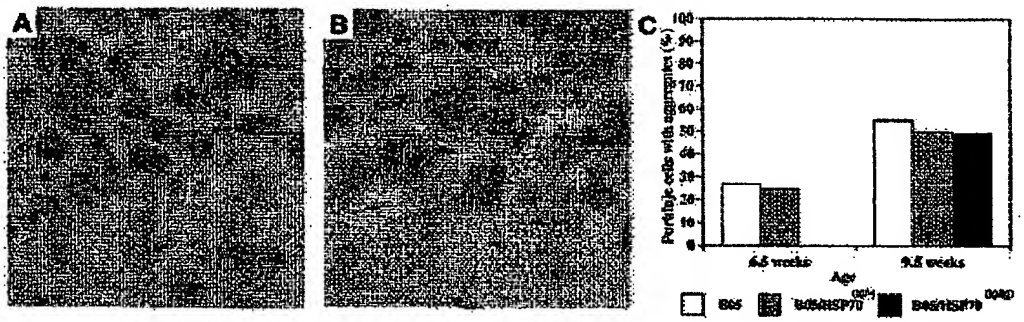

Figure 5. *SCA1* B05 transgenic mice expressing rat iHSP70 have NIs. Immunohistochemistry of cerebellar sections from 6.5-week-old B05$^{(tg/-)}$ (A) and B05/HSP70$^{(tg/tg)}$ littermate (B) stained with anti-ataxin-1 antibody. Both animals have Purkinje cells containing ataxin-1-positive nuclear aggregates. (C) B05 mice expressing HSP70 have approximately the same numbers of Purkinje cells with nuclear aggregates as age-matched B05 mice. The bars represent the percentage of Purkinje cells with nuclear aggregates at 6.5 and 9.5 weeks. The data were generated from two B05/HSP70$^{(tg/-)}$ animals at each age, one B05 at 6.5 weeks, and one B05/HSP70$^{(tg/tg)}$ at 9.5 weeks. The total number of Purkinje cells used to calculate the frequency of aggregates is: $n = 2046$ and 2027 for B05/HSP70$^{(tg/-)}$ at 6.5 and 9.5 weeks, respectively; $n = 1292$ for B05 6.5 weeks; and $n = 930$ for B05/HSP70$^{(tg/tg)}$.

There are other avenues by which chaperones may act to improve polyglutamine-induced phenotypes. HSP70 over-expression could act competitively to protect against toxic interactions between mutant ataxin-1 and its normal or acquired interacting partners. Alternatively, HSP70 could suppress apoptosis by acting downstream of cytochrome c release and upstream of caspase-3 activation (18,19). HSP70 is able to suppress the stress kinase c-Jun W-terminal kinase (JNK) (20); this activity is independent of HSP70's protein refolding function, as it can be mediated by a deletion mutant which lacks the ATP-binding domain (21). JNK activation has been observed in a hippocampal neuronal cell line which expresses expanded huntingtin (22,23), raising the possibility that activation of stress-signaling kinase and JNK might be one of the pathways involved in polyglutamine-induced neurodegeneration.

Notwithstanding our present uncertainty as to mechanism, there are three important outcomes of this study. First, chaperone over-expression in Purkinje cells does not appear to have untoward effects on the morphology of these neurons or their role in motor coordination. Second, because the same molecular changes (altered subcellular distribution of chaperones and components of the ubiquitin proteasome pathway, and downregulation of Purkinje cell-specific genes) (5,24) are seen in the SCA1 B05 mice and in human patients, the success of the double mutant mice gives hope that upregulating chaperone activity offers a possible therapeutic strategy to suppress polyglutamine-induced neurotoxicity in a mammalian central nervous system. This beneficial effect is assayable and responsive to chaperone dosage. Of course, the studies in mice do not parallel the human condition completely; the B05 line expresses ataxin-1 82Q at 50–100× endogenous levels. Either substantial over-expression or an extremely long polyglutamine tract is necessary to produce a disease phenotype in the mouse, presumably because the life-span of the mouse is too short for its neurons to accumulate damage from glutamine toxicity (a process which takes decades in humans). On the other hand, this may explain why the phenotype in the double mutant mice was still apparent, if diminished; the iHSP70 mice over-express the chaperone by only 10–20× endogenous levels. It is tempting to speculate that further benefit might be achieved by enhancing expression of the iHSP70 transgene in Purkinje cells or increasing the ratio of chaperone to mutant protein expression in favor of the former.

The third important outcome of this study is proof of the principle that both *Drosophila* and cell culture provide reliable models for high-throughput screening assays, and that pathways discovered in these models to affect polyglutamine-induced neurodegeneration are likely to carry over into mammalian systems. Such screens might uncover a plethora of candidate targets whose biological significance is yet to be deciphered, but from a therapeutic standpoint this issue might be moot if beneficial effects can be brought to the bedside.

MATERIALS AND METHODS

Generation and maintenance of transgenic mice

Transgenic mice expressing rat iHSP70 were generated and characterized as described previously (13,14). Three homozygous HSP70$^{(tg/tg)}$ male mice, strain CB6, were mated with 1–2 female B05 heterozygous mice (6), producing mixed CB6 and FVB genetic backgrounds. First or second generation B05$^{(tg/-)}$/HSP70$^{(tg/-)}$ mice were mated with either HSP70$^{(tg/-)}$ or HSP70$^{(tg/tg)}$ mice to produce all combinations and numbers for pathology and Rotarod analysis.

Immunohistochemistry, immunofluorescence and immunoblotting

Immunohistochemical and immunofluorescence staining were performed as described previously (7), using monoclonal anti-iHSP70 (StressGen, SPA-810) and monoclonal anti-calbindin (Sigma, CL300). We performed western blot analysis as described previously (7) with 100 µg/lane dounce-homogenized total cerebellar lysates [2% SDS, 100 mM Tris pH 6.8, 25 mM DTT, protease inhibitors (Boehringer Manheim)]. Nitrocellulose blots were probed with anti-iHSP70 (1:1000) and anti-actin (1:500) (Sigma, AC-40).

To determine whether chaperone over-expression affects solubility or extractability of ataxin-1, the cerebella of 6-week-old mice of each genotype were cut into two sagittal sections along the midline so as to allow two distinct extraction procedures; half the cerebellum was minced by a razor blade, then sonicated in 700 µl of 5× Laemmli sample buffer containing 3% 2-mercaptoethanol, and 8 M urea with protease inhibitors; the other half was homogenized in 0.25 M Tris pH 7.5, containing 0.2 mM sodium vanadate and 50 mM sodium fluoride drawn through an 18 gauge needle to ensure complete homogenization, and briefly spun at 2500 r.p.m. on the microcentrifuge (600 *g*). Protein determinations of the supernatant of these samples were performed using the Bradford reagent to confirm equivalent levels of each protein, and 100 µg of protein from each sample was dissolved in 5× Laemmli buffer to be loaded on a single lane of a 15-well BioRad minigel apparatus using standard conditions for running and staining.

In situ hybridization

Following a previously described method (25), 12 µm sections were cut from fixed and wax-embedded wild-type and HSP70$^{(-/-)}$ cerebellum. Sections were rehydrated, treated with proteinaseK, acetylated and dehydrated. S^{35}-labeled probes were generated with the T7/SP6 *in vitro* transcription kit (Boehringer-Mannheim). Sections were incubated with probe overnight at 55°C, washed at 62°C in 1× SSC and formamide, and RNAse A treated. The slides were dehydrated, dipped in emulsion and developed, then viewed by indirect microscopy.

Rotating rod analysis

Rotarod analysis was performed on naïve animals at 9.5 and 12.5 weeks. Test and control animals matched for age, sex and weight were tested on the Jones and Roberts accelerating Rotarod apparatus (Stoelting, IL, Ugo Bassili). The instrument accelerates from 4 to 40 r.p.m. over a period of 4 min and 30 s. Time was recorded when an animal fell off or made two consecutive revolutions, holding onto the rod. A trial was allowed to proceed for 10 min (600 s). The procedure was repeated, with four trials a day, for four consecutive days. Weights were recorded on the last day of the trial. Statistical analysis of variance and student's *t*-test were performed with Microsoft Excel (98) or InStat (2.03) and the histograms were generated in DeltaGraph (4.0).

ACKNOWLEDGEMENTS

The authors thank Dr N. Bermingham for performing the *in situ* work and Dr J. Botas, Dr R. Siefers, Dr T. Melcher and V. Brandt for constructive criticism. This work is supported by grants from the NINDS (NS27699) to H.Y.Z. and by the Neuropathology Core of the Baylor Mental Retardation Research Center. H.Y.Z. is a Howard Hughes Medical Institute Investigator.

REFERENCES

1. Zoghbi, H.Y., Pollack, M.S., Lyons, L.A., Ferell, R.E., Daiger, S.P. and Beaudet, A.L. (1988) Spinocerebellar ataxia: variable age of onset and linkage to human leukocyte antigen in a large kindred. *Ann. Neurol.*, **23**, 580–584.
2. Orr, H., Chung, M.-y., Banfi, S., Kwiatkowski, T.J.,Jr, Servadio, A., Beaudet, A.L., McCall, A.E., Duvick, L.A., Ranum, L.P.W. and Zoghbi, H.Y. (1993) Expansion of an unstable trinucleotide (CAG) repeat in spinocerebellar ataxia type 1. *Nat. Genet.*, **4**, 221–226.
3. Cummings, C.J. and Zoghbi, H.Y. (2000) Fourteen and counting: unraveling trinucleotide repeat diseases. *Hum. Mol. Genet.*, **9**, 909–916.
4. Kaytor, M.D. and Warren, S.T. (1999) Aberrant protein deposition and neurological disease. *J. Biol. Chem.*, **274**, 37507–37510.
5. Cummings, C.J., Mancini, M.A., Antalffy, B., DeFranco, D.B., Orr, H.T. and Zoghbi, H.Y. (1998) Chaperone suppression of aggregation and altered subcellular proteasome localization imply protein misfolding in SCA1. *Nat. Genet.*, **19**, 148–154.
6. Burright, E.N., Clark, H.B., Servadio, A., Matilla, T., Feddersen, R.M., Yunis, W.S., Duvick, L.A., Zoghbi, H.Y. and Orr, H.T. (1995) SCA1 transgenic mice: a model for neurodegeneration caused by an expanded CAG trinucleotide repeat. *Cell*, **82**, 937–948.
7. Cummings, C.J., Reinstein, E., Sun, Y., Antalffy, B., Jiang, Y.-h., Ciechanover, A., Orr, H.T., Beaudet, A.L. and Zoghbi, H.Y. (1999) Mutation of the E6-AP ubiquitin ligase reduces nuclear inclusion frequency while accelerating polyglutamine-induced pathology in SCA1 mice. *Neuron*, **24**, 879–892.
8. Fernandez-Funez, P., Nino-Rosales, M.L., de Gouyon, B., She, W.C., Luchak, J.M., Martinez, P., Turiegano, E., Benito, J., Capovilla, M., Skinner, P.J. *et al.* (2000) Identification of genes that modify ataxin-1-induced neurodegeneration. *Nature*, **408**, 101–106.
9. Warrick, J.M., Chan, H.Y., Gray-Board, G.L., Chai, Y., Paulson, H.L. and Bonini, N.M. (1999) Suppression of polyglutamine-mediated neurodegeneration in *Drosophila* by the molecular chaperone HSP70. *Nat. Genet.*, **23**, 425–428.
10. Kazemi-Esfarjani, P. and Benzer, S. (2000) Genetic suppression of polyglutamine toxicity in *Drosophila*. *Science*, **287**, 1837–1840.
11. Chan, H.Y., Warrick, J.M., Gray-Board, G.L., Paulson, H.L. and Bonini, N.M. (2000) Mechanisms of chaperone suppression of polyglutamine disease: selectivity, synergy and modulation of protein solubility in *Drosophila*. *Hum. Mol. Genet.*, **9**, 2811–2820.
12. Clark, H.B., Burright, E.N., Yunis, W.S., Larson, S., Wilcox, C., Hartman, B., Matilla, A., Zoghbi, H.Y. and Orr, H.T. (1997) Purkinje cell expression of a mutant allele of *SCA1* in transgenic mice leads to disparate effects on motor behaviors, followed by a progressive cerebellar dysfunction and histological alterations. *J. Neurosci.*, **17**, 7385–7395.
13. Marber, M.S., Mestril, R., Chi, S.H., Sayen, M.R., Yellon, D.M. and Dillmann, W.H. (1995) Overexpression of the rat inducible 70-kD heat stress protein in a transgenic mouse increases the resistance of the heart to ischemic injury. *J. Clin. Invest.*, **95**, 1446–1456.
14. Rajdev, S., Hara, K., Kokubo, Y., Mestril, R., Dillmann, W., Weinstein, P.R. and Sharp, F.R. (2000) Mice overexpressing rat heat shock protein 70 are protected against cerebral infarction. *Ann. Neurol.*, **47**, 782–791.
15. Skinner, P.J., Koshy, B., Cummings, C., Klement, I.A., Helin, K., Servadio, A., Zoghbi, H.Y. and Orr, H.T. (1997) Ataxin-1 with extra glutamines induces alterations in nuclear matrix-associated structures. *Nature*, **389**, 971–974.
16. Muchowski, P.J., Schaffar, G., Sittler, A., Wanker, E.E., Hayer-Hartl, M.K. and Hartl, F.U. (2000) Hsp70 and hsp40 chaperones can inhibit self-assembly of polyglutamine proteins into amyloid-like fibrils. *Proc. Natl Acad. Sci. USA*, **97**, 7841–7846.
17. Krobitsch, S. and Lindquist, S. (2000) Aggregation of huntingtin in yeast varies with the length of the polyglutamine expansion and the expression of chaperone proteins. *Proc. Natl Acad. Sci. USA*, **97**, 1589–1594.
18. Li, C.Y., Lee, J.S., Ko, Y.G., Kim, J.I. and Seo, J.S. (2000) Heat shock protein 70 inhibits apoptosis downstream of cytochrome c release and upstream of caspase-3 activation. *J. Biol. Chem.*, **275**, 25665–25671.
19. Jana, N.R., Zemskov, E.A., Wang, G. and Nukina, N. (2001) Altered proteasomal function due to the expression of polyglutamine-expanded truncated N-terminal huntingtin induces apoptosis by caspase activation through mitochondrial cytochrome c release. *Hum. Mol. Genet.*, **10**, 1049–1059.
20. Gabai, V.L., Meriin, A.B., Yaglom, J.A., Volloch, V.Z. and Sherman, M.Y. (1998) Role of Hsp70 in regulation of stress-kinase JNK: implications in apoptosis and aging. *FEBS Lett.*, **438**, 1–4.
21. Mosser, D.D., Caron, A.W., Bourget, L., Meriin, A.B., Sherman, M.Y., Morimoto, R.I. and Massie, B. (2000) The chaperone function of hsp70 is

required for protection against stress-induced apoptosis. *Mol. Cell. Biol.*, 20, 7146–7159.
22. Liu, Y.F., Dorow, D. and Marshall, J. (2000) Activation of MLK2-mediated signaling cascades by polyglutamine-expanded huntingtin. *J. Biol. Chem.*, 275, 19035–19040.
23. Liu, Y.F. (1998) Expression of polyglutamine-expanded Huntingtin activates the SEK1-JNK pathway and induces apoptosis in a hippocampal neuronal cell line. *J. Biol. Chem.*, 273, 28873–28877.
24. Lin, X., Antalffy, B., Kang, D., Orr, T. and Zoghbi, H.Y. (2000) Polyglutamine expansion in ataxin-1 downregulates specific neuronal genes before pathogenic changes in spinocerebellar ataxia type 1. *Nat. Neurosci.*, 3, 157–163.
25. Albrecht, U., Eichele, G., Helms, J. and Lu, H.-C. (1997) Visualization of gene expression patterns by *in situ* hybridization. In Daston, G.P. (ed.), *Molecular and Cellular Methods in Developmental Toxicology*. CRC Press, Boca Raton, FL, 49–78.

EXHIBIT E

The Journal of Neuroscience, March 15, 2003 · 23(6):2203–2211 · 2203

Heat Shock Protein 70 Chaperone Overexpression Ameliorates Phenotypes of the Spinal and Bulbar Muscular Atrophy Transgenic Mouse Model by Reducing Nuclear-Localized Mutant Androgen Receptor Protein

Hiroaki Adachi,[1] Masahisa Katsuno,[1] Makoto Minamiyama,[1] Chen Sang,[1] Gerassimos Pagoulatos,[2] Charalampos Angelidis,[2] Moriaki Kusakabe,[3] Atsushi Yoshiki,[4] Yasushi Kobayashi,[1] Manabu Doyu,[1] and Gen Sobue[1]

[1]Department of Neurology, Nagoya University Graduate School of Medicine, 65 Tsurumai-cho Showa-ku, Nagoya 466-8550, Japan, [2]Department of General Biology, University of Ioannina, School of Medicine, Ioannina GR-45110, Greece, [3]ANB Tsukuba Institute, ALOKA Company, Ltd., 1103 Fukaya, Kasumigaura, Niihari, Ibaraki 300-0134, Japan, and [4]Experimental Animal Division, Department of Biological Systems, BioResource Center, The Institute of Physical and Chemical Research (RIKEN) Tsukuba Institute 3-1-1 Koyadai, Tsukuba, Ibaraki 305-0074, Japan

Spinal and bulbar muscular atrophy (SBMA) is an inherited motor neuron disease caused by the expansion of the polyglutamine (polyQ) tract within the androgen receptor (AR). The nuclear inclusions consisting of the mutant AR protein are characteristic and combine with many components of ubiquitin–proteasome and molecular chaperone pathways, raising the possibility that misfolding and altered degradation of mutant AR may be involved in the pathogenesis. We have reported that the overexpression of heat shock protein (HSP) chaperones reduces mutant AR aggregation and cell death in a neuronal cell model (Kobayashi et al., 2000). To determine whether increasing the expression level of chaperone improves the phenotype in a mouse model, we cross-bred SBMA transgenic mice with mice overexpressing the inducible form of human HSP70. We demonstrated that high expression of HSP70 markedly ameliorated the motor function of the SBMA model mice. In double-transgenic mice, the nuclear-localized mutant AR protein, particularly that of the large complex form, was significantly reduced. Monomeric mutant AR was also reduced in amount by HSP70 overexpression, suggesting the enhanced degradation of mutant AR. These findings suggest that HSP70 overexpression ameliorates SBMA phenotypes in mice by reducing nuclear-localized mutant AR, probably caused by enhanced mutant AR degradation. Our study may provide the basis for the development of an HSP70-related therapy for SBMA and other polyQ diseases.

Key words: **HSP70; chaperone; polyglutamine; SBMA; transgenic mice; protein degradation**

Introduction

Polyglutamine (polyQ) diseases are inherited neurodegenerative disorders caused by the expansion of a trinucleotide CAG repeat in the causative genes (Zoghbi and Orr, 2000). To date, nine polyQ diseases have been identified (Ross, 2002). Spinal and bulbar muscular atrophy (SBMA) is a polyQ disease, characterized by proximal muscle atrophy, weakness, contraction fasciculations, and bulbar involvement (Kennedy et al., 1968; Sobue et al., 1989; Takahashi, 2001). In SBMA, a polymorphic CAG repeat with 14–32 CAGs expands to 40–62 CAGs in the first exon of the androgen receptor (*AR*) gene (Tanaka et al., 1996) and has somatic mosaicism (Tanaka et al., 1999). There is an inverse correlation between the CAG repeat size and the age at onset or the disease severity in SBMA (Doyu et al., 1992; Igarashi et al., 1992; La Spada et al., 1992). In SBMA, nuclear inclusions (NIs) containing mutant AR have been observed in the brainstem motor nuclei, spinal motor neurons, and some visceral organs (Li et al., 1998a,b). Such neuronal inclusions are common pathological features in polyQ diseases and are also colocalized with many components of ubiquitin–proteasome and molecular chaperones (Chai et al., 1999; Huynh et al., 2000; Adachi et al., 2001; Zander et al., 2001; Schmidt et al., 2002), raising the possibility that misfolding and altered degradation of the mutant protein may be involved in the pathogenesis of SBMA as well as other polyQ diseases (Stenoien et al., 1999; Waelter et al., 2001). Furthermore, these chaperones and proteasomes would facilitate refolding or proteolysis of the mutant protein and may play a role in protecting neuronal cells against the toxic properties of the expanded polyQ (Cummings et al., 1998; Kobayashi et al., 2000). We have shown recently that overexpression of heat shock proteins (HSPs) decreases the aggregate formation of truncated AR with the expanded polyQ and markedly prevents cell death in the neuronal cell model of SBMA (Kobayashi et al., 2000; Kobayashi and Sobue, 2001). HSP70 overexpression has been reported to enhance the solubility and degradation of mutant AR (Bailey et al., 2002). HSPs have also been shown to suppress aggregate formation and cellular toxicity in a wide range of polyQ disease models (Cummings et al., 1998; Warrick et al., 1999; Carmichael et al., 2000). Recently, overexpression of the inducible form of rat

Received Nov. 5, 2002; revised Dec. 31, 2002; accepted Dec. 31, 2002.

This work was supported by a Center of Excellence grant from the Ministry of Education, Culture, Sports, Science, and Technology of Japan and by grants from the Ministry of Health, Labor, and Welfare of Japan. We thank Sugiko Yokoi for her technical assistance.

Correspondence should be addressed to Dr. Gen Sobue, Department of Neurology, Nagoya University Graduate School of Medicine, 65 Tsurumai-cho Showa-ku, Nagoya, 466-8550, Japan. E-mail: sobueg@med.nagoya-u.ac.jp.

 0270-6474/03/232203-09$15.00/0

HSP70 ameliorated neurologic deficits and the neuronal degeneration of spinocerebellar ataxia type 1 (SCA1) transgenic mice, whereas the NIs consisting of mutant ataxin-1 were not reduced (Cummings et al., 2001).

In the present study, we report that overexpression of the inducible form of human HSP70 markedly ameliorated clinical and pathological phenotypes, and that this amelioration was correlated with the reduction of nuclear-localized mutant AR protein complexes in the mouse model of SBMA (Katsuno et al., 2002). Furthermore, the amount of monomeric mutant AR was also significantly reduced in the double-transgenic mice, suggesting that the degradation of mutant AR may have been accelerated by the overexpression of HSP70.

Materials and Methods

Assessment of motor ability. All animal experiments were performed in accordance with the National Institutes of Health *Guide for the Care and Use of Laboratory Animals* and were approved by the Nagoya University Animal Experiment Committee. Motor ability was assessed using an Economex Rotarod (Columbus Instruments, Columbus, OH) on a weekly basis as described previously (Adachi et al., 2001). The period for which a mouse could remain on a rotating axle (diameter, 3.6 cm; speed of rotation, 16 rpm) without falling was measured. Three trials were performed, and the longest duration on the rod was recorded for every mouse. The timer was stopped if the mouse fell from the rod or after an arbitrary limit of 180 sec. Cage activity was measured weekly while each mouse was in a transparent acrylic cage (16 × 30 × 14 cm, width × depth × height) within a soundproofed box as described previously (Katsuno et al., 2002). Spontaneous motor activity was measured by means of an animal behavior system (Neuroscience Inc., Tokyo, Japan), which monitored and counted all spontaneous movements, both vertical and horizontal, including locomotion, rearing, head movements, etc. All counts were automatically totaled and recorded in 24 hr.

Immunohistochemistry. We perfused 20 ml of a 4% paraformaldehyde fixative in 0.1 M phosphate buffer, pH 7.4, through the left cardiac ventricle of mice deeply anesthetized with ketamine–xylazine, postfixed tissues in 10% phosphate-buffered formalin, and processed tissues for paraffin embedding. Then we deparaffinized 4-μm-thick tissue sections, dehydrated with alcohol, and treated for antigen retrieval (Katsuno et al., 2002). For the HSP70 immunohistochemical study, the paraffin sections were pretreated with trypsin (Dako, Glostrup, Denmark) for 20 min at 37°C. The tissue sections were blocked with normal animal serum (1:20) and incubated with mouse anti-expanded polyQ (1:10,000) (1C2; Chemicon, Temecula, CA) and goat polyclonal antibody to HSP70 (1:500) (K-20; Santa Cruz Biotechnology, Santa Cruz, CA). Then the sections were incubated with biotinylated anti-species-specific IgG (Vector Laboratories, Burlingame, CA). Immune complexes were visualized using streptavidin–horseradish peroxidase (Dako) and 3,3′-diaminobenzidine (Dojindo, Kumamoto, Japan) substrate. Sections were counterstained with methyl green.

For double-labeling immunohistochemistry, sections were preincubated with normal horse serum diluted in 0.02 M PBS buffer, pH 7.4, containing bovine serum albumin. The sections were then incubated with goat anti-HSP70 antibody (1:500) (K-20; Santa Cruz) at 4°C overnight, washed with 0.02 M PBS buffer, incubated with biotinylated horse anti-goat IgG, stained with streptavidin–alkaline phosphatase, and visualized with fast red. 1C2 antibody (1:10,000; Chemicon) was subsequently applied to sections at 4°C overnight. After being washed, the sections were incubated with horseradish peroxidase-labeled donkey anti-mouse Ig $F(ab')_2$ (Amersham Biosciences, Buckinghamshire, UK), which had been demonstrated to cross-react with neither goat nor horse sera, and visualized with 3,3′-diaminobenzidine. For double-immunofluorescence staining of the spinal cord, sections were blocked with 5% normal horse serum and then sequentially incubated with K-20 antibody (1:500; Santa Cruz Biotechnology) and 1C2 antibody (1:10,000; Chemicon) at 4°C overnight. After incubation with biotinylated horse anti-goat IgG (Vector Laboratories) for 8 hr at 4°C, the sections were incubated with Alexa-488-conjugated streptavidin (1:400; Molecular Probes, Leiden, The Netherlands) and Alexa-568-conjugated goat anti-mouse IgG (1:1300; Molecular Probes), which had been demonstrated to cross-react with neither goat nor horse sera, for 8 hr at 4°C. The sections were then examined and photographed under a confocal laser scanning microscope (MRC 1024; Bio-Rad, Hercules, CA).

As for the immunohistochemistry of SBMA patients, nine patients with clinicopathologically and genetically confirmed SBMA (age, 51–84 years; mean, 64.3) and three non-neurological controls (age, 51–76 years; mean, 64.0) served as the subjects of the present study. Paraffin-embedded sections of the spinal cord and brain were obtained and examined in the same way as for the transgenic mice.

Quantification of 1C2-positive cells in the spinal cord and muscle. For the assessment of 1C2-positive cells, 4-μm-thick coronal sections of the thoracic spinal cord and gastrocnemius muscle stained by 1C2 antibody (1:10,000; Chemicon) were prepared, and the number of 1C2-positive cells for one mouse was counted using a light microscope with a computer-assisted image analyzer (Luzex FS; Nikon, Tokyo, Japan). For the assessment of 1C2-positive cells in the ventral horn of the spinal cord, 50 consecutive transverse sections of the thoracic spinal cord were prepared, and the 1C2-positive cells present within the ventral horn on every fifth section were counted as described previously (Terao et al., 1996; Adachi et al., 2001). Populations of 1C2-positive cells were expressed as the number per square millimeter. For the assessment of 1C2-positive cells in the muscle, 1C2-positive cells were calculated from counts of >500 fibers in randomly selected areas and were expressed as the number per 100 muscle fibers.

Western blots. We exsanguinated mice under ketamine–xylazine anesthesia and snap-froze their tissues with powdered CO_2 in acetone. Frozen tissue (0.1 gm wet weight) was homogenized in 1000 μl of lysis buffer (50 mM Tris-HCl, pH 8.0, 150 mM NaCl, 1% NP-40, 0.5% deoxycholate, and 0.1% SDS with 1 mM PMSF and aprotinin at 6 μg/ml). Homogenates were spun at 2500 × *g* for 15 min at 4°C. The protein concentration of the supernatant was determined using detergent-compatible protein assay (Bio-Rad). Each lane on a 5–20% SDS-PAGE gel was loaded with protein (200 μg for the spinal cord and 80 μg for the muscle from the supernatant fraction), which was transferred to Hybond-P membranes (Amersham Biosciences) using 25 mM Tris, 192 mM glycine, 0.1% SDS, and 10% methanol as transfer buffer. Kaleidoscope prestained standards were used as size markers (Bio-Rad). Proteins were then transferred to Hybond-P membranes, which were subsequently blocked in 5% milk in TBS containing 0.05% Tween 20 and incubated with appropriate primary antibodies using standard techniques. Primary antibodies were used at the following concentrations: rabbit anti-AR antibody (1:1000 N-20; Santa Cruz Biotechnology); mouse anti-HSP70/heat shock cognate 70 (HSC70) antibody (1:5000, W-27; Santa Cruz Biotechnology). We performed second antibody probing and detection using the ECL+plus kit (Amersham Biosciences). The HRP-conjugated secondary antibodies used were anti-rabbit Ig $F(ab')_2$ and anti-mouse Ig $F(ab')_2$ (1:5000; Amersham Biosciences). Nuclear and cytoplasmic fractions were extracted with a NE-PER Nuclear and Cytoplasmic Extraction Reagents Kit according to the protocol of the manufacturer (Pierce, Rockford, IL). Each lane on a 5–20% SDS-PAGE gel was loaded with 200 μg of protein for the spinal cord and 80 μg for the muscle from each fraction. Immunoprecipitation was performed using 1 mg of the total protein lysate, 10 μl of protein G–Sepharose (Amersham Biosciences), and 5 μl of anti-AR antibody (N-20; Santa Cruz Biotechnology). Protein was eluted from beads by boiling for 3 min in 10 μl of elution buffer (50 mM Tris-HCl, pH 6.8, 2% SDS, 60 μl/ml 2-mercaptoethanol, and 10% glycerol). The elutes were loaded on SDS–polyacrylamide gels. Blots were sequentially probed with goat anti-HSP70 antibody (K-20; Santa Cruz Biotechnology).

The signal intensity was analyzed using the NIH Image program (version 1.62). Relative signal intensity was computed as the signal intensity of each sample divided by that of the AR-97Q/HSP70$^{(-/-)}$ mice.

Filter-trap assay. Filtration of proteins through a 0.2 μm cellulose acetate membrane (Sartorius AG, Goettingen, Germany) was performed using a slot-blot apparatus (Bio-Rad). The membranes were washed

three times with TBS buffer and supported by three pieces of filter paper (Bio-Rad). We also put 0.45 μm nitrocellulose membrane (Bio-Rad) under the cellulose acetate membrane to capture the monomeric AR protein passing through this membrane. Samples of protein (200 μg) for the spinal cord and for the muscle (80 μg) were prepared in a final volume of 200 μl in lysis buffer, loaded, and gently vacuumed. Membranes were washed three times with TBS containing 0.05% Tween 20. Slot-blots were probed as described for Western blots.

Statistical analysis. We analyzed data using the unpaired *t* test and log-rank test from Statview software version 5 (Hulinks, Tokyo, Japan).

Results

Nondeleterious effects of HSP70 overexpression and generation of double-transgenic mice

Because HSP70s have a wide variety of functions, we examined whether the overexpression of HSP70 under the control of the human β-actin promoter has deleterious effects on phenotypes in mice (Plumier et al., 1995). Motor function in the mice with HSP70 overexpression was not affected; a Rotarod task until 40 weeks revealed no impairment in either hemizygous or homozygous transgenic mice overexpressing HSP70 (data not shown). Histological examination at 40 weeks of age did not show any detectable effect on the neuronal cell morphology and population and on the muscular structure in the overexpression of human HSP70 alone (data not shown). These studies indicated that the overexpression of human HSP70 alone does not impair neuronal development and motor function.

To determine whether the overexpression of human HSP70 could ameliorate the disease phenotype of the SBMA transgenic mouse model, we crossed the mice expressing full-length human AR with 97-polyQ tract (AR-97Q mice, 4–6 line) (Katsuno et al., 2002) with mice that overexpress human HSP70 under the control of the human β-actin promoter (Plumier et al., 1995). The SBMA model (AR-97Q mice) shows small body size, short lifespan, progressive muscle atrophy and weakness, and reduced cage activity (Katsuno et al., 2002). Because the phenotypes of these SBMA transgenic mice are markedly pronounced in male transgenic mice similarly to SBMA patients (Katsuno et al., 2002), we used male transgenic mice in this study. We generated the AR-97Q/HSP70$^{(tg/tg)}$ mice as homozygotes and the AR-97Q/HSP70$^{(tg/-)}$ mice as hemizygotes, as well as the AR-97Q/HSP70$^{(-/-)}$ mice as a control transgenic mouse line. The SBMA transgene expression was at the hemizygous level in all AR-97Q/HSP70 double-transgenics.

Human HSP70 overexpression ameliorates motor phenotypes of SBMA transgenic mice

To determine whether HSP70 overexpression has an ameliorative effect on the motor phenotypes, we performed the Rotarod task and the measurement of locomotor cage activity by infrared sensor system with the double-transgenic mice (Fig. 1*A*,*B*). The AR-97Q/HSP70$^{(-/-)}$ mice showed motor impairment on the Rotarod task as early as 9 weeks after birth; by 12 weeks and 25 weeks of age they began to show significant impairment compared with AR-97Q/HSP70$^{(tg/-)}$ mice ($p < 0.05$) and AR-97QHSP70$^{(tg/tg)}$ mice ($p < 0.001$), respectively. (Fig. 1*A*). Although both the AR-97Q/HSP70$^{(tg/tg)}$ and AR-97Q/HSP70$^{(tg/-)}$ mice performed better than the AR-97Q/HSP70$^{(-/-)}$ mice, the AR-97Q/HSP70$^{(tg/tg)}$ mice were on the rod longer than the AR-97Q/HSP70$^{(tg/-)}$ mice during the trial. The locomotor cage activity of the AR-97Q/HSP70$^{(-/-)}$ mice was also significantly decreased at 21 weeks in comparison with the other two double-transgenics ($p < 0.05$) (Fig. 1*B*). No lines were distinguishable in terms of body weight at birth. The AR-97Q/HSP70$^{(-/-)}$ mice lost weight significantly earlier than the AR-97Q/HSP70$^{(tg/tg)}$ mice ($p < 0.01$) (Fig. 1*C*). The survival rate was significantly more prolonged in the AR-97Q/HSP70$^{(tg/-)}$ and AR-97Q/HSP70$^{(tg/tg)}$ mice than in the AR-97Q/HSP70$^{(-/-)}$ mice ($p < 0.01$ and $p < 0.005$, respectively) (Fig. 1*D*). The affected AR-97Q/HSP70$^{(-/-)}$ mice exhibited motor weakness, with dragging of the legs or short steps, whereas the AR-97Q/HSP70$^{(tg/tg)}$ mice showed almost normal ambulation and the AR-97Q/HSP70$^{(tg/-)}$ mice only

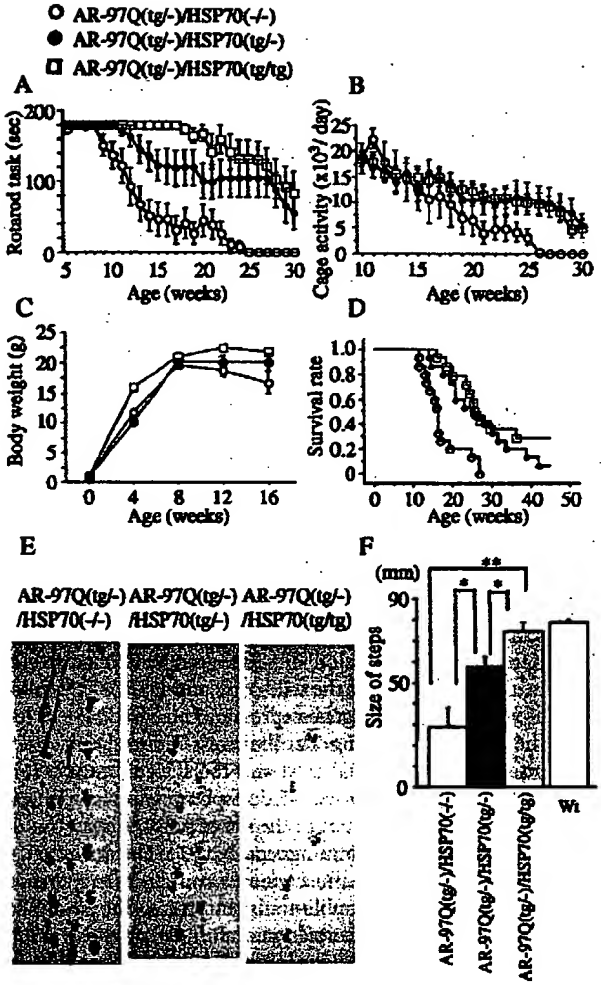

Figure 1. Effects of human HSP70 overexpression on the symptomatic phenotypes of male AR-97Q mice. Rotarod task (*A*; $n = 10$), cage activity (*B*; $n = 10$), body weight (*C*; $n = 12$), and survival rate (*D*; $n = 14$) of the AR-97Q/HSP70$^{(-/-)}$, AR-97Q/HSP70$^{(tg/-)}$, and AR-97Q/HSP70$^{(tg/tg)}$ mice. All parameters were significantly different among AR-97Q/HSP70$^{(-/-)}$ mice, AR-97Q/HSP70$^{(tg/tg)}$, and AR-97Q/HSP70$^{(tg/-)}$ mice ($p < 0.001$, $p < 0.05$, $p < 0.05$, and $p < 0.005$, respectively). AR-97Q mice overexpressing human HSP70 lasted longer on the Rotarod and showed higher cage activity than AR-97Q/HSP70$^{(-/-)}$ mice. The AR-97Q/HSP70$^{(-/-)}$ mice lost weight earlier than the other two double-transgenics. Survival was prolonged in AR-97Q/HSP70$^{(tg/-)}$ and AR-97Q/HSP70$^{(tg/tg)}$ mice compared with AR-97Q/HSP70$^{(-/-)}$ mice. *E*, Footprints of representative 16-week-old AR-97Q/HSP70$^{(-/-)}$, AR-97Q/HSP70$^{(tg/-)}$, and AR-97Q/HSP70$^{(tg/tg)}$ mice. Front paws are indicated in *red* and hindpaws in *blue*. AR-97Q/HSP70$^{(-/-)}$ mice exhibit motor weakness, with dragging of the legs; AR-97Q/HSP70$^{(tg/tg)}$ mice walk almost normally; and AR-97Q/HSP70$^{(tg/-)}$ mice walk with somewhat short steps. *F*, The size of steps was measured in 16-week-old AR-97Q/HSP70$^{(-/-)}$, AR-97Q/HSP70$^{(tg/-)}$, and AR-97Q/HSP70$^{(tg/tg)}$ mice ($n = 4$), respectively. Each column shows an average of steps of the hindpaw. AR-97Q/HSP70$^{(tg/-)}$ and AR-97Q/HSP70$^{(tg/tg)}$ mice walked with significantly longer steps than AR-97Q/HSP70$^{(-/-)}$ mice. *$p < 0.05$; **$p < 0.01$. Error bars indicate SD. *Wt*, Wild type.

somewhat short steps (Fig. 1*E*). The AR-97Q/HSP70$^{(tg/-)}$ and AR-97Q/HSP70$^{(tg/tg)}$ mice showed significantly longer steps than the AR-97Q/HSP70$^{(-/-)}$ mice (Fig. 1*F*). Although both the AR-97Q/HSP70$^{(tg/tg)}$ and AR-97Q/HSP70$^{(tg/-)}$ mice showed ameliorated phenotypic expressions, the AR-97Q/HSP70$^{(tg/tg)}$ mice were better than the AR-97Q/HSP70$^{(tg/-)}$ mice in most of the parameters, suggesting that the improved motor phenotype depended on the HSP70 expression level rather than on the genetic background.

Expression levels of HSP70 in double-transgenic mice

We examined whether the AR-97Q/HSP70 double-transgenic mice express increased levels of the HSP70 protein in the spinal cord and skeletal muscle. Immunohistochemical studies of double-transgenic mice stained with the specific antibody for HSP70 confirmed that spinal neurons and muscular cells expressed the HSP70 (Fig. 2*A–C*). The HSP70 was diffusely distributed to the nuclei and occasionally formed various-sized NIs (Fig. 2*A–C*). Glial cells also showed diffuse nuclear staining and NIs of HSP70 protein (data not shown). Western blot analysis revealed that the HSP70 expression level was fivefold greater in the AR-97Q/HSP70$^{(tg/-)}$ mice and 10-fold greater in the AR-97Q/HSP70$^{(tg/tg)}$ mice than endogenous HSP70 in the AR-97Q/HSP70$^{(-/-)}$ mice in the spinal cord and muscle (Fig. 2*D*). The AR-97Q transgene expression did not alter HSP70 expression levels in the spinal cord of the wild-type and HSP70$^{(tg/tg)}$ mice, whereas the AR-97Q transgene expression increased HSP70 levels in the muscle, suggesting that the stress-induced response is different between the spinal cord and the skeletal muscle (Fig. 2*D*). Absence of the stress-induced response was also demonstrated in the nervous system of the other polyQ disease model mice (Jana et al., 2000; Cummings et al., 2001). The nuclear fraction of the spinal cord and muscle surely contained an increased amount of HSP70 in the double-transgenic mice. The amount of HSP70 in the nuclear fraction was most abundant in the AR-97Q/HSP70$^{(tg/tg)}$ mice (Fig. 2*E*). The increased HSP70 was coimmunoprecipitated with mutant AR, suggesting that HSP70 directly binds to the mutant AR protein (Fig. 2*F*).

Colocalization of HSP70 with mutant AR in the nuclei

We evaluated the colocalization of HSP70 and mutant AR in the AR-97Q/HSP70 double-transgenic mice. We performed double-labeling immunohistochemistry and immunofluorescence double-staining with two primary antibodies: goat anti-HSP70 and mouse anti-expanded polyQ (1C2). These double-immunostaining studies revealed that HSP70 (Fig. 3*A,C*) and mutant AR (Fig. 3*B,D*) present diffusely in the nuclei and colocalize each other (Fig. 3*B,E*) in the spinal anterior horn neurons of the AR-97Q/HSP70$^{(tg/tg)}$ mice. We also determined that such diffuse staining of HSP70 in the nuclei was also present in the spinal neurons of SBMA patients (Fig. 3*F,J*). Immunofluorescence double-staining with anti-HSP70 and anti-expanded polyQ antibodies revealed that the endogenous HSP70 (Fig. 3*G,K*) and mutant AR (Fig. 3*H,L*) were colocalized on the NI (Fig. 3*I*) and diffusely in the nuclei (Fig. 3*M*) in the spinal cord neurons of SBMA patients, suggesting that the endogenous HSP70 preferentially coexists with mutant AR and exerts its function in the nuclei of SBMA patients as well.

Overexpression of HSP70 decreases the nuclear-localized mutant AR

An immunohistochemical study for mutant AR using 1C2 antibody showed a marked reduction in diffuse nuclear staining and NIs in the AR-97Q/HSP70$^{(tg/-)}$ or the AR-97Q/HSP70$^{(tg/tg)}$ mice compared with the AR-97Q/HSP70$^{(-/-)}$ mice in the spinal motor neurons (Fig. 4*A–C*) and muscles (Fig. 4*D–F*). The AR-97Q/HSP70$^{(-/-)}$ mice showed intense and frequent 1C2 staining in the nuclei (Fig. 4*A,D*), whereas the 1C2 staining was infrequent

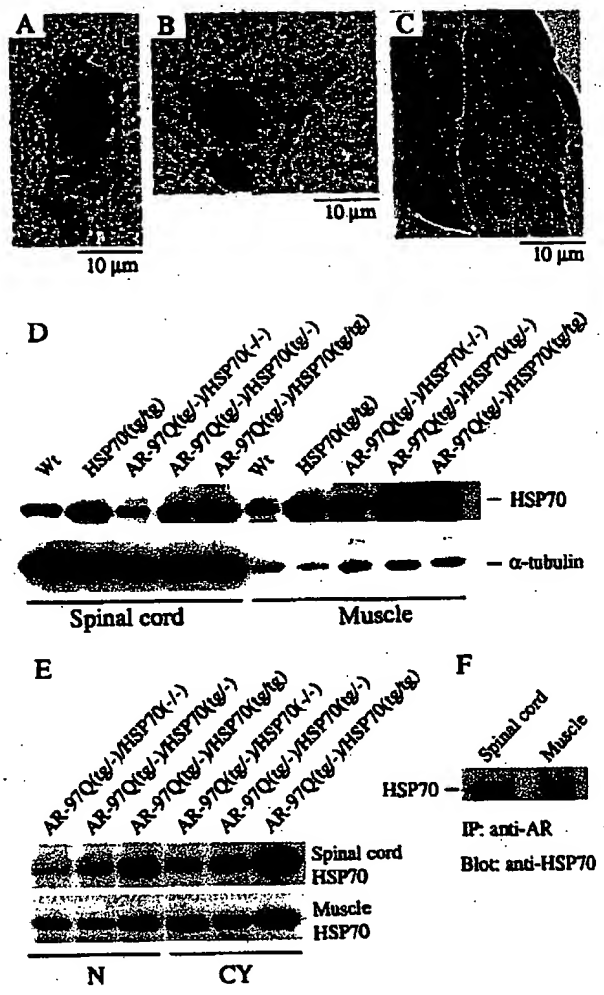

Figure 2. Increased HSP70 expression in double-transgenic mice. *A–C*, Immunohistochemical study from the 16-week-old AR-97Q/HSP70$^{(tg/-)}$ mice in the spinal anterior horn and skeletal muscle stained with the antibody specific for the HSP70. The immunoreactivity of HSP70 was localized to the nuclei with intense and diffuse staining, and small NIs were present in the anterior horn cell (*A*). A large nuclear inclusion was also present in the anterior horn cell (*B*). Skeletal muscle showed diffuse nuclear staining and NIs (*C*). *D, E*, Western blot analysis of total spinal cord and muscle protein lysate immunolabeled with an antibody against HSP70. AR-97Q/HSP70$^{(tg/-)}$ and AR-97Q/HSP70$^{(tg/tg)}$ mice express higher levels of HSP70 than wild-type (*Wt*) and AR-97Q/HSP70$^{(-/-)}$ mice (*D*). The HSP70 expression level is fivefold higher in AR-97Q/HSP70$^{(tg/-)}$ mice and 10-fold higher in the AR-97Q/HSP70$^{(tg/tg)}$ mice than endogenous HSP70 in AR-97Q/HSP70$^{(-/-)}$ mice in the spinal cord and muscle, respectively (*D*). The AR-97Q transgene expression did not alter HSP70 levels in the spinal cord, whereas the AR-97Q transgene expression gained the respective HSP70 levels in the muscle (*D, E*). Therefore, the AR-97Q transgene expression in the double-transgenics alters HSP70 levels in the muscle but not in the spinal cord. *E*, Western blots of nuclear and cytoplasmic extracts immunolabeled with an antibody against HSP70. HSP70 localized in the nucleus (*N*) as well as in the cytoplasm (*CY*) in the spinal cord and muscle of all lines examined. AR-97Q/HSP70$^{(tg/tg)}$ mice expressed the largest amount of HSP70 in both extracts. *F*, Immunoprecipitation (*IP*) Western blots for HSP70. Soluble fractions were collected from the spinal cord and muscle, and equal protein concentrations were immunoprecipitated with an antibody to the N-terminal portion of AR and immunoblotted for HSP70. Coimmunoprecipitation of the HSP70 chaperone and the polyQ-expanded mutant AR was detected.

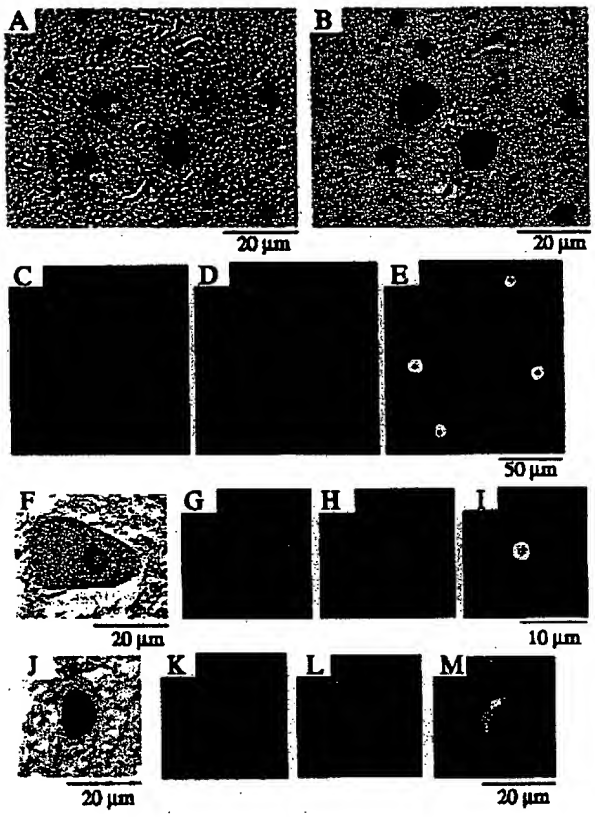

Figure 3. Colocalization of the nuclear-localized HSP70 chaperone with mutant AR. Immunohistochemical analysis for the antibody specific to the HSP70 as well as to the expanded polyQ stretch (immunostained with a monoclonal antibody, 1C2) in the spinal cords of 16-week-old AR-97Q/HSP70$^{(tg/tg)}$ mice (*A–E*) and SBMA patients (*F–M*). Double-labeling immunohistochemistry revealed diffuse nuclear staining for goat anti-HSP70 (*A*) and expanded polyQ (*B*), suggesting that HSP70 and mutant AR are colocalized in the spinal motor neurons of AR-97Q/HSP70$^{(tg/tg)}$ mice. Immunofluorescence double-staining with antibodies against HSP70 and the expanded polyQ also revealed that HSP70 and mutant AR are colocalized as shown in HSP70 (*C*, *green*), expanded-polyQ (*D*, *red*), and an overlay of the two signals (*E*, *yellow*). Diffuse staining of neuronal nuclei for HSP70 is also observed in the spinal neurons (*F*, *J*) of SBMA patients. Immunofluorescence double-staining with anti-HSP70 (*green*) and anti-expanded polyQ (*red*) antibodies revealed that the HSP70 (*G*) and mutant AR (*H*) are colocalized on the NI (shown in *yellow* in *I*) in the spinal anterior horn cell. The diffuse nuclear colocalization of HSP70 (*K*) and mutant AR (*H*) was also observed in the SBMA posterior horn cell (*M*). This cell also has an NI (*L*, *M*).

in the AR-97Q/HSP70$^{(tg/-)}$ mice (Fig. 4*B*,*E*) and much less frequent in the AR-97Q/HSP70$^{(tg/tg)}$ mice (Fig. 4*C*,*F*). Quantitative assessment of diffuse nuclear staining for 1C2 in the spinal motor neurons (Fig. 4*G*) and muscles (Fig. 4*H*) revealed significantly more positive cells in the AR-97Q/HSP70$^{(-/-)}$ mice than in the AR-97Q/HSP70$^{(tg/-)}$ and AR-97Q/HSP70$^{(tg/tg)}$ mice. However, the 1C2-positive cell populations were not statistically different in the AR-97Q/HSP70$^{(tg/-)}$ and the AR-97Q/HSP70$^{(tg/tg)}$ mice. The neuronal cell population in the spinal ventral horn in the AR-97Q/HSP70$^{(-/-)}$, AR-97Q/HSP70$^{(tg/-)}$, and AR-97Q/HSP70$^{(tg/tg)}$ mice was not significantly decreased compared with that in the wild-type mice (data not shown).

Overexpression of HSP70 decreases the high-molecular-weight mutant AR protein and monomeric mutant AR protein

Western blot analysis showed that the high-molecular-weight form of mutant AR protein complexes was retained in the stacking gel as well as a band of monomeric mutant AR monomer in the spinal cord and muscle of the transgenic mice (Fig. 5). The mutant AR within the stacking gel was diminished in the AR-97Q/HSP70$^{(tg/-)}$ and AR-97Q/HSP70$^{(tg/tg)}$ mice compared with the AR-97Q/HSP70$^{(-/-)}$ mice (Fig. 5*A*,*B*). In addition, the AR-97Q/HSP70$^{(-/-)}$ mice had more monomeric mutant AR protein than the AR-97Q/HSP70$^{(tg/-)}$ or AR-97Q/HSP70$^{(tg/tg)}$ mice (Fig. 5*A*,*B*). The mutant AR protein within the stacking gel was found primarily in the nuclear fraction (Fig. 5*C*). The mutant AR within the stacking gel and monomeric form of the nuclear fraction in the spinal cord and muscle were also decreased in the AR-97Q/HSP70$^{(tg/-)}$ and AR-97Q/HSP70$^{(tg/tg)}$ mice (Fig. 5*C*). These observations suggested that the overexpression of HSP70 markedly decreases not only the high-molecular-weight mutant AR protein present primarily in the nuclear fraction but also the monomeric mutant AR protein.

We next performed a filter-trap assay for the quantitative analysis of the large molecular aggregated and soluble monomeric form of the mutant AR protein (Wanker et al., 1999). Only the larger-sized mutant AR protein was retained on the cellulose acetate membrane (pore diameter, 0.2 μm), whereas the nitrocellulose membrane captured proteins of all sizes (Fig. 6*A*). We also put the nitrocellulose membrane under the cellulose acetate membrane to capture the soluble monomeric AR protein passing through this membrane (Fig. 6*B*). Values were normalized to endogenous α-tubulin using the nitrocellulose membrane. Using this approach, we analyzed the ability of the HSP70 to decrease the large aggregated or soluble monomeric mutant AR protein. Overexpression of HSP70 resulted in a significant decrease in large aggregated as well as soluble monomeric mutant AR protein in a dose-dependent manner (Fig. 6*A–C*). The endogenous AR protein was not retained on the cellulose acetate membrane in wild-type mice (data not shown). These results indicate that the HSP70 decreases not only the mutant AR protein complexes in the large aggregated form but also the soluble monomeric mutant AR as observed on Western blot analysis. These observations also suggested that overexpression of HSP70 enhanced the function of the ubiquitin–proteasome pathway and subsequently accelerated the degradation of monomeric mutant AR protein.

Discussion

We generated a transgenic mouse model carrying a full-length AR containing 97 CAGs (Katsuno et al., 2002). This model showed progressive muscular atrophy and weakness as well as diffuse nuclear staining and NIs consisting of the mutant AR. These phenotypes were very pronounced in male transgenic mice, similar to those in SBMA (Katsuno et al., 2002). Here we demonstrate that the overexpression of human HSP70 exerts dose-dependent therapeutic effects on motor dysfunction in this mouse model. Mutant AR and HSP70 colocalized diffusely to the nuclei and to the NIs in the neurons and muscles of the AR-97Q/HSP70 double-transgenic mice. The overexpression of HSP70 served to decrease the nuclear-localized mutant AR protein complexes in large aggregated form in the double-transgenic mice. Monomeric mutant AR was also significantly reduced by HSP70 overexpression, suggesting that it could accelerate the turnover of mutant AR.

In our SBMA transgenic mouse model, nuclear translocation of mutant AR, which is dependent on the testosterone level, has been demonstrated to be essential for mutant AR-induced neurotoxicity (Katsuno et al., 2002). Reduction of the testosterone level by castration diminished nuclear-localized mutant AR and markedly prevented phenotypic expression in the male trans-

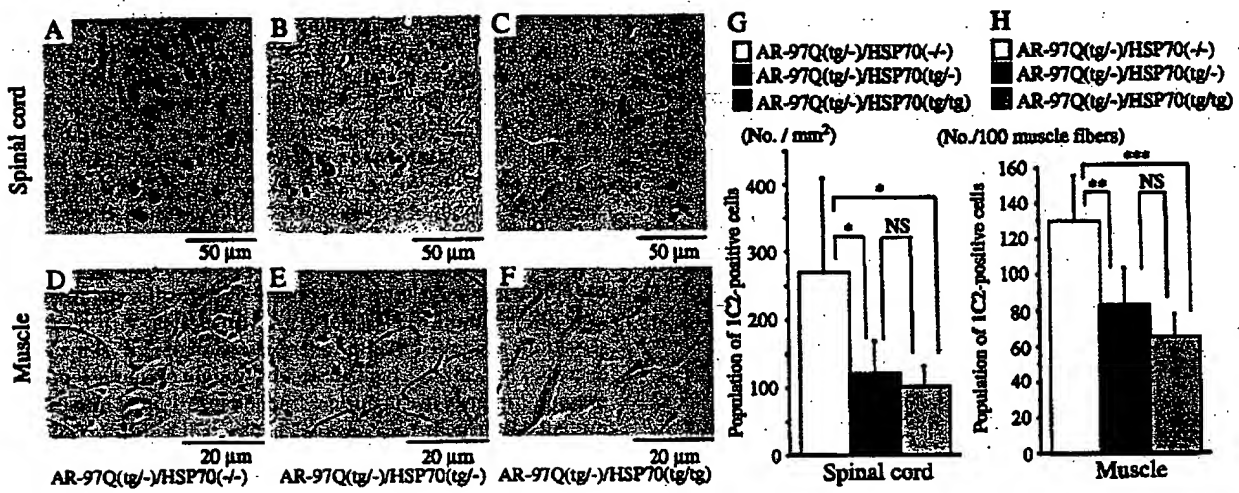

Figure 4. HSP70 decreases nuclear-localized mutant AR in double-transgenic mice. Immunohistochemical study of the spinal anterior horn (*A–C*) and muscle (*D–F*) of AR-97Q/HSP70 $^{(-/-)}$ and AR-97Q/HSP70 double-transgenic mice stained with a monoclonal antibody (1C2) against abnormally expanded polyQ (16 weeks old). AR-97Q/HSP70 $^{(-/-)}$ mice have intense and frequent staining for 1C2 in the nucleus (*A*, *D*). AR-97Q/HSP70 $^{(tg/-)}$ (*B*, *E*), and AR-97Q/HSP70 $^{(tg/tg)}$ (*C*, *F*) mice exhibit low levels of 1C2 staining in the nucleus. *G*, *H*, Quantitative assessment of diffuse nuclear staining for 1C2 in the spinal ventral horn (*G*) and muscle (*H*). Positively stained nuclei were estimated by counting in the thoracic spinal ventral horn and muscle using six transgenic mice (16 weeks of age). There are significantly more 1C2-positive cells in AR-97Q/HSP70 $^{(-/-)}$ mice than in AR-97Q/HSP70 $^{(tg/-)}$ mice or AR-97Q/HSP70 $^{(tg/tg)}$ mice in both tissues. Results are expressed as means ± SD for six mice. The differences in 1C2-positive cell populations are not statistically significant between AR-97Q/HSP70 $^{(tg/-)}$ and AR-97Q/HSP70 $^{(tg/tg)}$ mice. $^{*}p < 0.05$; $^{**}p < 0.01$; $^{***}p < 0.001$.

genic mice, whereas testosterone administration enhanced the nuclear localization of mutant AR and caused significant motor dysfunction in the female transgenic mice (Katsuno et al., 2002). In particular, the large aggregated complexes of the mutant AR protein detected in the stacking gel or slowly migrating species in the Western blot analysis in the nuclear fraction were well correlated with the phenotypic expression in this mouse model (Katsuno et al., 2002). This suggested that oligomeric or polymeric mutant AR large complex molecules positively associated with other molecules would exert the toxicity rather than monomeric mutant AR (Katsuno et al., 2002).

In the present study, we demonstrated that the amount of nuclear-localized mutant AR protein, particularly that of the large complex form present in the stacking gel or trapped by the cellulose acetate membrane, was significantly reduced in the AR-97/HSP70 double-transgenic mice. Thus, the overexpression of HSP70 is suggested to exert its amelioration of the phenotypic expression by diminishing the amount of nuclear-localized mutant AR protein. However, in the previously reported SCA1 transgenic mouse model, NIs of the mutant protein were not apparently decreased in the double-transgenic mice with rat HSP70 overexpression, although the neurological deficit and neuronal degeneration were ameliorated (Cummings et al., 2001). Because the gain of amelioration for phenotypic expression in the model mice of Cummings et al. (2001) was mild even in the double-transgenics with HSP70 homozygotes, the change in the frequency of the NIs would not have been significant enough to detect. In our mouse model, NIs were present only in the small subpopulation of neurons and muscles, particularly in the early phase of phenotypic expression, whereas the 1C2-positive nuclei were abundant (Katsuno et al., 2002). In addition, 1C2-positive neurons are more extensive than those of NI-bearing neurons in the tissues of the autopsied samples from patients with polyQ diseases, and the distribution of 1C2-positive neurons is well correlated with the neurological symptoms (Yamada et al., 2001). These observations suggest that 1C2 staining is a more sensitive histological marker for the detection of the nuclear localization of the mutant protein with an expanded polyQ stretch compared with NIs detected by antibodies for the responsible protein.

The interesting observation in our study was the diminution of monomeric mutant AR in the double-transgenic mice with overexpression of HSP70. Recently, HSP70 overexpression in the cell culture model has revealed enhanced solubility of mutant AR with an expanded polyQ and degradation through the ubiquitin–proteasome system (Bailey et al., 2002). Overexpression of chaperones generally enhances the function of the ubiquitin–proteasome pathway and subsequently accelerates protein degradation (Bukau and Horwich, 1998). The ubiquitin–proteasome pathway, particularly its activity, is known to be related to chaperone expression levels (Bukau and Horwich, 1998). The molecular mechanism for this relationship remains unsolved, but recently CHIP (C terminal of HSC70-interacting protein), U-box-type E3 ubiquitin ligase, has been shown to interact with HSP90 or HSP70 (Connel et al., 2001) and ubiquitylate unfolded proteins trapped by molecular chaperones and degrades them, thus acting as a "quality control E3" (Murata et al., 2001). Furthermore, there is a cofactor of HSC70/HSP70, Bcl-2 associated athanogene 1, which possesses a ubiquitin-like domain and promotes binding of HSC70/HSP70 to the proteolytic complex (Lüders et al., 2000). Although such coupling factors between the HSP70 chaperone system and the protein degradation machinery for mutant AR are unknown at present, if the similar E3 for mutant AR is present, it could ubiquitylate and degrade mutant AR as a result of interacting with HSP70. In this scenario, the overexpression of HSP70 may accelerate E3-dependent capture of mutant AR and its degradation through the proteasome pathway. A remarkable reduction of the monomeric mutant AR in the double-transgenics with HSP70 overexpression can be the reflection of the accelerated degradation of mutant AR through the HSP70-mediated E3–proteasome system. Interaction between mutant AR and HSP70 detected by coimmunoprecipitation and Western blot analysis in the double-transgenic mice would support this view. The overexpression of HSP70 could enhance the degradation of the mo-

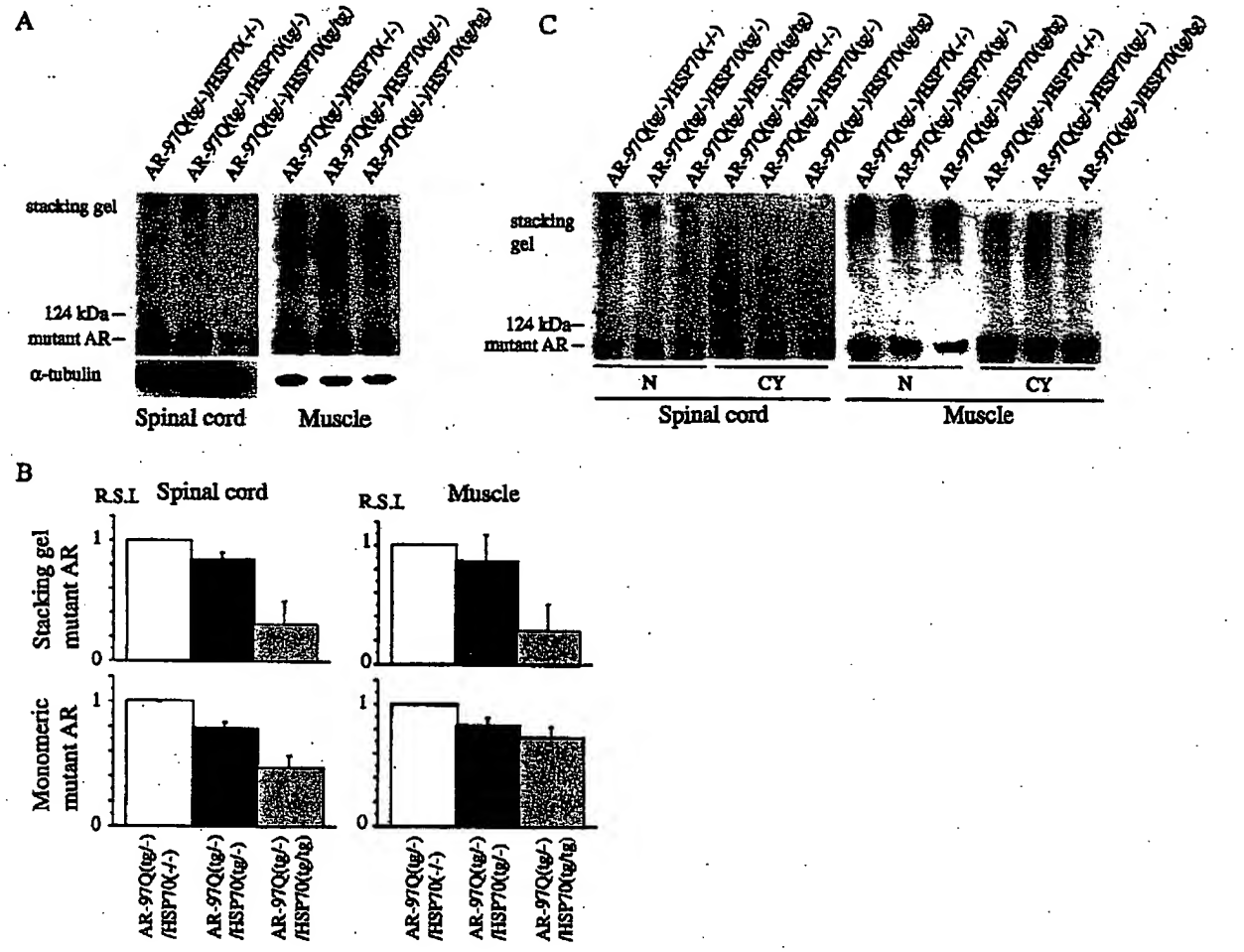

Figure 5. HSP70 decreases nuclear-localized mutant AR protein complexes as well as monomeric mutant AR. *A*, *B*, Western blot analysis of total tissue homogenates from the spinal cord and muscle of AR-97Q/HSP70$^{(-/-)}$, AR-97Q/HSP70$^{(tg/-)}$, and AR-97Q/HSP70$^{(tg/tg)}$ mice (16 weeks of age) immunolabeled by an antibody against AR (N-20). The mutant AR appearing within the stacking gel and monomeric mutant AR were diminished in AR-97Q/HSP70$^{(tg/-)}$ and AR-97Q/HSP70$^{(tg/tg)}$ mice compared with AR-97Q/HSP70$^{(-/-)}$ mice (*A*, *B*). Values of mutant AR were normalized to endogenous α-tubulin and expressed as the ratio to those of AR-97Q/HSP70$^{(-/-)}$ mice (*B*). Values are expressed as means ± SD for three mice. *C*, Western blot analysis of nuclear (*N*) and cytoplasmic (*CY*) fractions from the spinal cord and muscle of AR-97Q/HSP70$^{(-/-)}$, AR-97Q/HSP70$^{(tg/-)}$, and AR-97Q/HSP70$^{(tg/tg)}$ mice (16 weeks of age) immunolabeled by N-20. Mutant AR protein within the stacking gel was found primarily in the nuclear fraction. The mutant AR within the stacking gel of the nuclear fraction also significantly decreased in the spinal cord and muscle of AR-97Q/HSP70$^{(tg/tg)}$ mice. *R.S.I.*, Relative signal intensity.

nomeric mutant AR, presumably through the HSP70-interacting quality control E3 activation, and subsequently it could reduce the amount of nuclear-localized mutant AR, resulting in the amelioration of phenotypic expression induced by mutant AR. To substantiate this, however, one needs to identify the HSP70-interacting E3 ligase, which recognizes mutant AR as a substrate.

Another possibility is that overexpressed HSP70 directly renaturates the misfolded mutant AR and normalizes the interaction of mutant AR with proteins that are essential to maintain the cell function (Hendricks and Hartl, 1993). The overexpression of HSP70 and HSP40 or HSC70 and *Drosophila* human DNAJ homolog-1 (dHdj-1) changed the distribution and morphologic pattern of NI formation of mutant huntingtin and ataxin-1 (Cummings et al., 1998; Fernandez-Funez et al., 2000; Muchowski et al., 2000). The overexpression of dHdj-1 and HSP70 increased the proportion of the monomeric mutant protein with an expanded polyQ, suggesting that chaperones modulate the biochemical properties of mutant polyQ-bearing protein (Chan et al., 2000). It has been proposed that the disease proteins with an expanded polyQ participate in inappropriate protein–protein interactions that lead to cell dysfunction and eventual cell death (Sherman and Goldberg, 2001). Molecular chaperones can be involved in the conformational modification by stabilizing the unfolded mutant proteins and can facilitate or inhibit the interaction with self or other proteins (Opal and Zoghbi, 2002). To date, a number of proteins that interact with polyQ-bearing disease protein have been cloned, including huntingtin-associated protein (Li et al., 1995), huntingtin-interacting protein (Kalchman et al., 1997), glyceraldehyde-3-phosphate dehydrogenase (Burke et al., 1996), leucine-rich acidic nuclear protein (Matilla et al., 1997), polyglutamine tract-binding protein-1 (Waragai et al., 1999), 130 kDa human TATA-binding protein-associated factor subunit of the human transcription factor TFIID (Shimohata et al., 2000), and cAMP response element-binding protein (CREB) binding protein (CBP) (Nucifora et al., 2001; Zander et al., 2001). CBP has been demonstrated to interact with mutant AR, colocalize in the NIs, and reduce the mutant AR-induced cell toxicity by CBP overexpression in the cell culture model by modifying CBP-dependent transcriptional activity (McCampbell et al., 2000). HSP70 may reduce the toxicity of

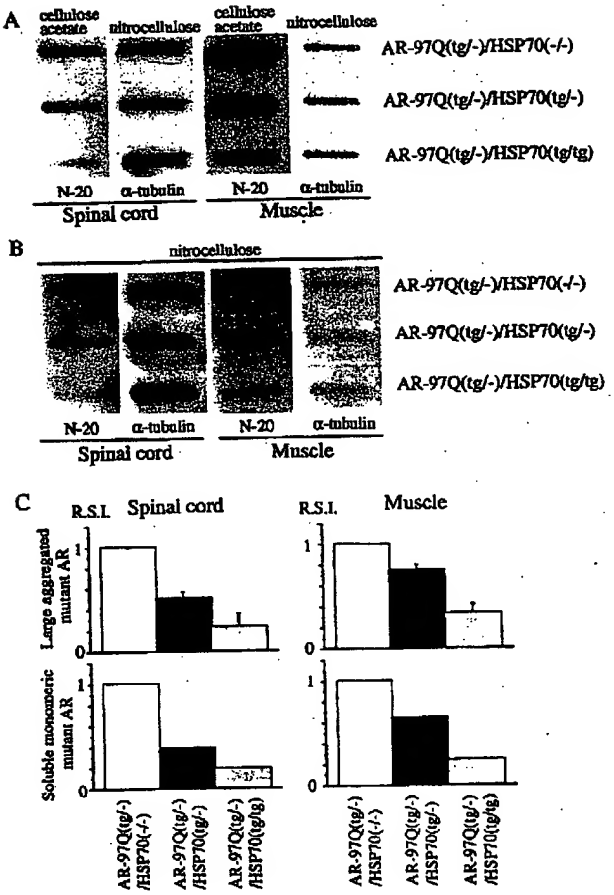

Figure 6. HSP70 decreases large aggregated mutant AR protein and soluble monomeric mutant AR protein. *A–C*, Filter-trap assay of total tissue homogenates from the spinal cord and muscle of AR-97Q/HSP70$^{(-/-)}$, AR-97Q/HSP70$^{(tg/-)}$, and AR-97Q/HSP70$^{(tg/tg)}$ mice (16 weeks of age) immunolabeled by an antibody against AR (N-20). Large aggregated mutant AR complexes were trapped by the cellulose acetate membrane (*A*), and soluble monomeric mutant AR passing through the cellulose acetate membrane was trapped by the nitrocellulose membrane beneath the cellulose acetate membrane (*B*). Endogenous α-tubulin using the nitrocellulose membrane was also shown (*A*, *B*). The normalized value of large aggregated mutant AR and soluble monomeric mutant AR against endogenous α-tubulin is shown in *C*. Relative values against those of AR-97Q/HSP70$^{(-/-)}$ mice were expressed as means ± SD for three mice or a mean of two mice (*C*). The trapped AR protein was reduced in the spinal cord and muscle of AR-97Q/HSP70$^{(tg/-)}$ and AR-97Q/HSP70$^{(tg/tg)}$ mice in both membranes (*A*, *B*). This reduction was most evident in AR-97Q/HSP70$^{(tg/tg)}$ mice (*A–C*), suggesting that the overexpression of HSP70 resulted in a significant, dose-dependent decrease in large aggregated and soluble monomeric mutant AR protein. *R.S.I.*, Relative signal intensity.

mutant AR proteins through the inhibition or acceleration of the interaction with these proteins. However, interacting protein involvement in association with mutant AR still needs to be investigated.

The other possible avenue by which HSP70 acts to improve polyQ-induced toxicity is the anti-apoptotic activities of HSP70. HSP70 suppresses apoptosis by inhibiting the *c*-Jun N-terminal kinase (Gabai et al., 1998) or by inhibiting cytochrome *c* release and caspase-3 activation (Li et al., 2000; Jana et al., 2001). Furthermore, HSP40 and mammalian relative of DNAJ chaperones can inhibit caspase-3 and caspase-9 activation mediated by mutant huntingtin, independent of huntingtin aggregation (Zhou et al., 2001; Chuang et al., 2002). However, the involvement of anti-apoptotic activities of HSPs in protection against mutant AR toxicity through reducing the nuclear-localized mutant AR remains to be elucidated.

In summary, the overexpression of HSP70 significantly ameliorates the phenotypes of SBMA transgenic mice by reducing the amount of nuclear-localized mutant AR protein, particularly that of the large complex form. The amount of monomeric mutant AR was also reduced by HSP70 overexpression, suggesting enhanced degradation of mutant AR. A recent study revealed that the ansamycin antibiotic Geldanamycin induced a heat shock response and inhibited aggregation of mutant huntingtin in COS-1 cells (Sittler et al., 2001). Thus, HSP70 overexpression would provide a potential therapeutic avenue for SBMA and other polyQ diseases.

References

Adachi H, Kume A, Li M, Nakagomi Y, Niwa H, Do J, Sang C, Kobayashi Y, Doyu M, Sobue G (2001) Transgenic mice with an expanded CAG repeat controlled by the human AR promoter show polyglutamine nuclear inclusions and neuronal dysfunction without neuronal cell death. Hum Mol Genet 10:1039–1048.

Bailey CK, Andriola IF, Kampinga HH, Merry DE (2002) Molecular chaperones enhance the degradation of expanded polyglutamine repeat androgen receptor in a cellular model of spinal and bulbar muscular atrophy. Hum Mol Genet 11:515–523.

Bukau KT, Horwich AL (1998) The Hsp70 and Hsp60 chaperone machines. Cell 92:351–366.

Burke JR, Enghild JJ, Martin ME, Jou YS, Myers RM, Roses AD, Vance JM, Strittmatter WJ (1996) Huntingtin and DRPLA proteins selectively interact with the enzyme GAPDH. Nat Med 2:347–350.

Carmichael J, Chatellier J, Woolfson A, Milstein C, Fersht AR, Rubinsztein DC (2000) Bacterial and yeast chaperones reduce both aggregate formation and cell death in mammalian cell models of Huntington's disease. Proc Natl Acad Sci USA 97:9701–9705.

Chai Y, Koppenhafer SL, Bonini NM, Paulson HL (1999) Analysis of the role of heat shock protein (Hsp) molecular chaperones in polyglutamine disease. J Neurosci 19:10338–10347.

Chan HYE, Warrick JM, Gray-Board GL, Paulson HL, Bonini NM (2000) Mechanisms of chaperone suppression of polyglutamine disease: selectivity, synergy and modulation of protein solubility in *Drosophila*. Hum Mol Genet 9:2811–2820.

Chuang JZ, Zhou H, Zhu M, Li SH, Li XJ, Sung CH (2002) Characterization of a brain-enriched chaperone, MRJ, that inhibits Huntingtin aggregation and toxicity independently. J Biol Chem 277:19831–19838.

Connel P, Ballinger CA, Jiang J, Wu Y, Thompson LJ, Höfeld J, Patterson C (2001) The co-chaperone CHIP regulates protein triage decisions mediated by heat shock proteins. Nat Cell Biol 3:93–96.

Cummings CJ, Mancini MA, Antalffy B, DeFranco DB, Orr HT, Zoghbi HY (1998) Chaperone suppression of aggregation and altered subcellular proteasome localization imply protein misfolding in SCA1. Nat Genet 19:148–154.

Cummings CJ, Sun Y, Opal P, Antalffy B, Mestril R, Orr HT, Dillmann WH, Zoghbi HY (2001) Overexpression of inducible HSP70 chaperone suppresses neuropathology and improves motor function in SCA1 mice. Hum Mol Genet 10:1511–1518.

Doyu M, Sobue G, Mukai E, Kachi T, Yasuda T, Mitsuma T, Takahashi A (1992) Severity of X-linked recessive bulbospinal neuronopathy correlates with size of the tandem CAG repeat in androgen receptor gene. Ann Neurol 23:707–710.

Fernandez-Funez P, Nino-Rosales ML, de Gouyon B, She WC, Luchak JM, Martinez P, Turiegano E, Benito J, Capovilla M, Skinner PJ, McCall A, Canal I, Orr HT, Zoghbi HY, Botas J (2000) Identification of genes that modify ataxin-1-induced neurodegeneration. Nature 408:101–106.

Gabai VL, Meriin AB, Yaglom JA, Volloch VZ, Sherman MY (1998) Role of Hsp70 in regulation of stress-kinase JNK: implications in apoptosis and aging. FEBS Lett 438:1–4.

Hendricks JP, Hartl FU (1993) Molecular chaperone functions of heat-shock proteins. Annu Rev Biochem 62:349–384.

Huynh DP, Figueroa K, Hoang N, Pulst SM (2000) Nuclear localization or inclusion body formation of ataxin-2 are not necessary for SCA2 pathogenesis in mouse or human. Nat Genet 26:44–50.

Igarashi S, Tanno Y, Onodera O, Yamazaki M, Sato S, Ishikawa A, Miyatani N, Nagashima M, Ishikawa Y, Sahashi K, Ibi T, Miyatake T, Tsuji S (1992)

Strong correlation between the number of CAG repeats in androgen receptor genes and the clinical onset of features of spinal and bulbar muscular atrophy. Neurology 42:2300–2302.

Jana NR, Tanaka M, Wang GH, Nukina N (2000) Polyglutamine length-dependent interaction of Hsp40 and Hsp70 family chaperones with truncated N-terminal huntingtin: their role in suppression of aggregation and cellular toxicity. Hum Mol Genet 9:2009–2018.

Jana NR, Zemskov EA, Wang GH, Nukina N (2001) Altered proteasomal function due to the expression of polyglutamine-expanded truncated N-terminal huntingtin induces apoptosis by caspase activation through mitochondrial cytochrome c release. Hum Mol Genet 10:1049–1059.

Kalchman MA, Koide HB, McCutcheon K, Graham RK, Nichol K, Nishiyama K, Kazemi-Esfarjani P, Lynn FC, Wellington C, Metzler M, Goldberg YP, Kanazawa I, Gietz RD, Hayden MR (1997) HIP1, a human homologue of *S. cerevisiae* Sla2p, interacts with membrane-associated huntingtin in the brain. Nat Genet 16:44–53.

Katsuno M, Adachi H, Kume A, Li M, Nakagomi Y, Niwa H, Sang C, Kobayashi Y, Doyu M, Sobue G (2002) Testosterone reduction prevents phenotypic expression in a transgenic mouse model of spinal and bulbar muscular atrophy. Neuron 35:843–854.

Kennedy WR, Alter M, Sung JH (1968) Progressive proximal spinal and bulbar muscular atrophy of late onset: a sex-linked recessive trait. Neurology 18:671–680.

Kobayashi Y, Sobue G (2001) Protective effect of chaperones on polyglutamine diseases. Brain Res Bull 56:165–168.

Kobayashi Y, Kume A, Li M, Doyu M, Hata M, Ohtsuka K, Sobue G (2000) Chaperones Hsp70 and Hsp40 suppress aggregate formation and apoptosis in cultured neuronal cells expressing truncated androgen receptor protein with expanded polyglutamine tract. J Biol Chem 275:8772–8778.

La Spada AR, Roling DB, Harding AE, Warner CL, Spiegel R, Hausmanowa-Petrusewicz I, Yee WC, Fischbeck KH (1992) Meiotic stability and genotype-phenotype correlation of the trinucleotide repeat in X-linked spinal and bulbar muscular atrophy. Nat Genet 2:301–304.

Li CY, Lee JS, Ko YG, Kim JI, Seo JS (2000) Heat shock protein 70 inhibits apoptosis downstream of cytochrome c release and upstream of caspase-3 activation. J Biol Chem 275:25665–25671.

Li M, Miwa S, Kobayashi Y, Merry DE, Tanaka F, Doyu M, Hashizume Y, Fischbeck KH, Sobue G (1998a) Nuclear inclusions of the androgen receptor protein in spinal and bulbar muscular atrophy. Ann Neurol 44:249–254.

Li M, Nakagomi Y, Kobayashi Y, Merry DE, Tanaka F, Doyu M, Mitsuma T, Fischbeck KH, Sobue G (1998b) Nonneural nuclear inclusions of androgen receptor protein in spinal and bulbar muscular atrophy. Am J Pathol 153:695–701.

Li XJ, Li SH, Sharp AH, Nucifora Jr FC, Schilling G, Lanahan A, Worley P, Snyder SH, Ross CA (1995) A huntingtin-associated protein enriched in brain with implications for pathology. Nature 378:398–402.

Lüders J, Demand J, Höhfeld J (2000) The ubiquitin-related BAG-1 provides a link between the molecular chaperones Hsc70/Hsp70 and the proteasome. J Biol Chem 275:4613–4617.

Matilla A, Koshy BT, Cummings CJ, Isobe T, Orr HT, Zoghbi HY (1997) The cerebellar leucine-rich acidic nuclear protein interacts with ataxin-1. Nature 389:974–978.

McCampbell A, Taylor JP, Taye AA, Robitschek J, Li M, Walcott J, Merry D, Chai Y, Paulson H, Sobue G, Fischbeck KH (2000) CREB-binding protein sequestration by expanded polyglutamine. Hum Mol Genet 9:2197–2202.

Muchowski PJ, Schaffar G, Sittler A, Wanker EE, Hayer-Hartl MK, Hartl FU (2000) Hsp70 and hsp40 chaperones can inhibit self-assembly of polyglutamine proteins into amyloid-like fibrils. Proc Natl Acad Sci USA 97:7841–7846.

Murata S, Minami Y, Minami M, Chiba T, Tanaka K (2001) CHIP is a chaperone-dependent E3 ligase that ubiquitylates unfolded protein. EMBO Rep 2:1133–1138.

Nucifora Jr FC, Sasaki M, Peters MF, Huang H, Cooper JK, Yamada M, Takahashi H, Tsuji S, Troncoso J, Dawson VL, Dawson TM, Ross CA (2001) Interference by huntingtin and atrophin-1 with cbp-mediated transcription leading to cellular toxicity. Science 291:2423–2428.

Opal P, Zoghbi HY (2002) The role of chaperones in polyglutamine disease. Trends Mol Med 8:232–236.

Plumier JC, Ross BM, Currie RW, Angelidis CE, Kazlaris H, Kollias G, Pagoulatos GN (1995) Transgenic mice expressing the human heat shock protein 70 have improved post-ischemic myocardial recovery. J Clin Invest 95:1854–1860.

Ross CA (2002) Polyglutamine pathogenesis: emergence of unifying mechanisms for Huntington's disease and related disorders. Neuron 35:819–822.

Schmidt T, Lindenberg KS, Krebs A, Schols L, Laccone F, Herms J, Rechsteiner M, Riess O, Landwehrmeyer GB (2002) Protein surveillance machinery in brains with spinocerebellar ataxia type 3: redistribution and differential recruitment of 26S proteasome subunits and chaperones to neuronal intranuclear inclusions. Ann Neurol 51:302–310.

Sherman MY, Goldberg AL (2001) Cellular defenses against unfolded proteins: a cell biologist thinks about neurodegenerative diseases. Neuron 29:15–32.

Shimohata T, Nakajima T, Yamada M, Uchida C, Onodera O, Naruse S, Kimura T, Koide R, Nozaki K, Sano Y, Ishiguro H, Sakoe K, Ooshima T, Sato A, Ikeuchi T, Oyake M, Sato T, Aoyagi Y, Hozumi I, Nagatsu T, et al. (2000) Expanded polyglutamine stretches interact with TAFII130,interfering with CREB-dependent transcription. Nat Genet 26:29–36.

Sittler A, Lurz R, Lueder G, Priller J, Hayer-Hartl MK, Hartl FU, Lehrach H, Wanker EE (2001) Geldanamycin activates a heat shock response and inhibits huntingtin aggregation in a cell culture model of Huntington's disease. Hum Mol Genet 10:1307–1315.

Sobue G, Hashizume Y, Mukai E, Hirayama M, Mitsuma T, Takahashi A (1989) X-linked recessive bulbospinal neuronopathy: a clinicopathological study. Brain 112:209–232.

Stenoien DL, Cummings CJ, Adams HP, Mancini MG, Patel K, DeMartino GN, Marcelli M, Weigel NL, Mancini MA (1999) Polyglutamine-expanded androgen receptors form aggregates that sequester heat shock proteins,proteasome components and SRC-1,and are suppressed by the HDJ-2 chaperone. Hum Mol Genet 8:731–741.

Takahashi A (2001) Hiroshi Kawahara (1858–1918). J Neurol 248:241–242.

Tanaka F, Doyu M, Ito Y, Matsumoto M, Mitsuma T, Abe K, Aoki M, Itoyama Y, Fischbeck KH, Sobue G (1996) Founder effect in spinal and bulbar muscular atrophy (SBMA). Hum Mol Genet 5:1253–1257.

Tanaka F, Reeves MF, Ito Y, Matsumoto M, Li M, Miwa S, Inukai A, Yamamoto M, Doyu M, Yoshida M, Hashizume Y, Terao S, Mitsuma T, Sobue G (1999) Tissue-specific somatic mosaicism in spinal and bulbar muscular atrophy (SBMA) is dependent on CAG repeat length and androgen receptor gene expression level. Am J Hum Genet 65:966–973.

Terao S, Sobue G, Hashizume Y, Li M, Inagaki T, Mitsuma T (1996) Age-related changes in human spinal ventral horn cells with special reference to the loss of small neurons in the intermediate zone: a quantitative analysis. Acta Neuropathol (Berl) 92:109–114.

Waelter S, Boeddrich A, Lurz R, Scherzinger E, Lueder G, Lehrach H, Wanker EE (2001) Accumulation of mutant huntingtin fragments in aggresome-like inclusion bodies as a result of insufficient protein degradation. Mol Biol Cell 12:1393–1407.

Wanker EE, Scherzinger E, Heiser V, Sittler A, Eickhoff H, Lehrach H (1999) Membrane filter assay for detection of amyloid-like polyglutamine-containing protein aggregates. Methods Enzymol 309:375–386.

Waragai M, Lammers C, Takeuchi S, Imafuku I, Udagawa Y, Kanazawa I, Kawabata M, Mouradian MM, Okazawa H (1999) PQBP-1,a novel polyglutamine tract-binding protein,inhibits transcription activation by Brn-2 and affects cell survival. Hum Mol Genet 8:977–987.

Warrick JM, Chan HY, Gray-Board GL, Chai Y, Paulson HL, Bonini NM (1999) Suppression of polyglutamine-mediated neurodegeneration in *Drosophila* by the molecular chaperone HSP70. Nat Genet 23:425–428.

Yamada M, Wood JD, Shimohata T, Hayashi S, Tsuji S, Ross CA, Takahashi H (2001) Widespread occurrence of intranuclear atrophin-1 accumulation in the central nervous system neurons of patients with dentatorubral-pallidoluysian atrophy. Ann Neurol 49:14–23.

Zander C, Takahashi J, Hachimi KHE, Fujigasaki H, Albanese V, Lebre AS, Stevanin G, Duyckaerts C, Brice A (2001) Similarities between spinocerebellar ataxia type 7 (SCA7) cell models and human brain: proteins recruited in inclusions and activation of caspase-3. Hum Mol Genet 10:2569–2579.

Zhou H, Li SH, Li XJ (2001) Chaperone suppression of cellular toxicity of huntingtin is independent of polyglutamine aggregation. J Biol Chem 276:48417–48424.

Zoghbi HY, Orr HT (2000) Glutamine repeats and neurodegeneration. Annu Rev Neurosci 23:217–247.

Colloquium

Chaperoning brain degeneration

Nancy M. Bonini*

Department of Biology, University of Pennsylvania, Howard Hughes Medical Institute, Philadelphia, PA 19104-6018

***Drosophila* has emerged as a premiere model system for the study of human neurodegenerative disease. Genes associated with neurodegeneration can be expressed in flies, causing phenotypes remarkably similar to those of the counterpart human diseases. Because human neurodegenerative diseases, including Huntington's and Parkinson's diseases, are disorders for which few cures or treatments are available, *Drosophila* brings to bear powerful genetics to the problem of these diseases. The molecular chaperones were the first modifiers defined that interfere in the progression of such disease phenotypes in *Drosophila*. Hsp70 is a potent suppressor of both polyglutamine disease and Parkinson's disease in *Drosophila*. These studies provide the promise of treatments for human neurodegeneration through the up-regulation of stress and chaperone pathways.**

Huntington's and Parkinson's diseases are late-onset, progressive human neurodegenerative diseases associated with selective neuronal loss and abnormal protein accumulations. Huntington's disease is one of a class of human diseases known as the polyglutamine repeat diseases (see ref. 1 for review). This class also includes dentatorubropallidoluysian atrophy (DRPLA), spinobulbar muscular atrophy (SBMA) and spinocerebellar ataxias type 1, 2, 3 (also known as Machado–Joseph disease, MJD), 6, 7, and 17. The polyglutamine diseases are characterized by the expansion of a run of the amino acid glutamine within the ORF of the respective proteins. The expanded polyglutamine domain confers dominant toxicity on the respective disease proteins, leading to neuronal dysfunction and degeneration. These diseases are also associated with abnormal protein accumulations containing the disease protein, typically in the form of nuclear inclusions. These inclusions immunostain for ubiquitin, suggesting that they contain misfolded or abnormally folded protein, potentially targeted for proteasomal degradation.

Dominant Parkinson's disease is characterized by selective loss of dopaminergic neurons in the substantia nigra pars compacta. Abnormal protein accumulations, known as Lewy bodies, typify the disease. Lewy bodies are cytoplasmic aggregates composed primarily of the protein α-synuclein (2); they contain ubiquitinated protein, suggesting that the accumulating protein has been targeted for degradation. Causal association of abnormal α-synuclein function with Parkinson's disease was found when two mutations in α-synuclein, A30P and A53T, were described in rare familial forms (3, 4).

Drosophila is a powerful genetic model system, which has been well studied as a developmental system. Many genes are conserved between humans and flies, including entire gene pathways (5). *Drosophila* has a complex nervous system and displays complex behaviors, including learning and memory. Many genes known to be involved in pathways of behavior, including learning and memory, circadian behavior, and phototaxis, were first described in *Drosophila* mutants (6–8). Given these striking homologies between *Drosophila* and humans, we reasoned that the power of *Drosophila* genetics could be brought to bear on the problem of human neurodegenerative disease.

Whereas mutations have been known for many years that lead to loss of integrity of the fly brain (8, 9), we reasoned that another way to generate such models of specific interest for their application to human neurodegeneration would be to express in the fly the pathogenic human disease gene. With the phenotype in the fly resembling that of the human disease in fundamental properties, this would indicate at least some aspects of the disease process are also conserved between flies and humans. This conservation therefore would allow fly genetics to be applied to define mechanisms of disease progression and modifiers that interfere with the disease process, thus opening up the realm of *Drosophila* neurogenetics toward the cure and treatment of these devastating human disorders. Here I present a review of previous findings on *Drosophila* models of neurodegeneration, with some additional new findings.

Materials and Methods

Details of the methods used in the studies summarized here are described in previously published research reports (see refs. 10–13). The Hsp70 dominant-negative transgene encoding Hsp70.K71E was generated by mutagenesis of the Hsp70 transgene described (12).

A *Drosophila* Model for Human Neurodegenerative Disease

To establish the fly as a model system for human neurodegeneration, we decided to express in the fly the normal form and a mutant disease form of the gene encoding spinocerebellar ataxia type 3, or MJD. We used a truncated form of the disease protein in these studies, as this protein had been shown to have effects when expressed in transgenic mice (14). To do this, we subcloned cDNAs encoding a protein with a polyglutamine repeat within the normal range, MJDtrQ27, and a protein with a polyglutamine repeat within the pathogenic range, MJDtrQ78, into fly transformation vectors. The two-component GAL4-UAS system was used for transgene expression (15). Transgenic flies were obtained, and expression was directed to neural tissues. Typically, expression is directed to the eye with gmr-GAL4 or to the entire nervous system with elav-GAL4.

Expression of the control protein MJDtrQ27 has no discernable phenotype—flies are born with eyes indistinguishable from normal. Expression of the disease form of the protein, MJDtrQ78, however, has profound effects. Flies are born with eyes mildly to strongly degenerate when the gmr-GAL4 eye driver is used, with loss of red pigmentation, loss of internal eye integrity, and severe degeneration of the photoreceptor neurons (Fig. 1 *A–D*) (13). The strength of the phenotype depends on expression level of the transgene encoding the pathogenic protein—weak expression induces mild degeneration, whereas strong expression is associated with severe degeneration.

This paper results from the Arthur M. Sackler Colloquium of the National Academy of Sciences, "Self-Perpetuating Structural States in Biology, Disease, and Genetics," held March 22–24, 2002, at the National Academy of Sciences in Washington, DC.

Abbreviations: MJD, Machado–Joseph disease; DM, dorsomedial.

*E-mail: nbonini@sas.upenn.edu.

Fig. 1. Polyglutamine degeneration and suppression by the molecular chaperone Hsp70. (*Upper*) External eyes. (*Lower*) Horizontal sections through the eye to reveal the internal eye structure. (*A* and *B*) Normal fly with just the driver gmr-GAL4. (*C* and *D*) Fly expressing the pathogenic polyglutamine protein MJDtr-Q78 has severe eye degeneration, with loss of external and internal eye structure. (*E* and *F*) Flies co-expressing the toxic polyglutamine protein MJDtr-Q78 with Hsp70 have dramatically restored external and internal eye structure. Fly genotypes are *w; +/gmr-GAL4* (*A* and *B*), *w; gmr-GAL4 UAS-Hsp70/UAS-MJDtr-Q78(S)* (*C* and *D*), and *w; gmr-GAL4/UAS-MJDtr-Q78(S)* (*E* and *F*).

The phenotype was also progressive over time. Although the flies are born with various degrees of degeneration depending upon the specific transgenic insertion, degeneration becomes progressively more severe over the lifetime of the adult fly. This degeneration is seen as progressive loss of pigmentation, enhanced deterioration of internal eye integrity, and early death of the animal, associated with tremors and shaking movement.

Examination of the tissue for protein expression revealed that the pathogenic polyglutamine protein forms abnormal inclusions within the cell nuclei. Such abnormal inclusions are characteristic of the human polyglutamine diseases, where they are described as nuclear inclusions or cytoplasmic inclusions, depending upon their particular subcellular localization (16–18). In our MJD model, the inclusions are nuclear. Whereas these inclusions form early in the fly cells, degeneration of the cells does not occur for many days. The inclusions form in all cells in which the pathogenic protein is expressed, even in cells that do not degenerate and are insensitive to the pathogenic actions of the disease protein. This observation suggests that whereas the inclusions may be part of the disease process or indicative of the abnormal folding of the pathogenic protein, the mere presence of an inclusion is not sufficient for cellular degeneration. Nevertheless, such abnormal protein accumulations are characteristic of the human diseases, providing another point of similarity between the fly model and the human disorders.

These features of the fly model—late onset and progressive neurodegeneration accompanied by the formation of abnormal protein accumulations—are fundamental features of human polyglutamine disease. This fact indicates that *Drosophila* can display mechanisms of human polyglutamine degeneration. These findings indicate that *Drosophila* genetics can be applied toward defining mechanisms, cures, and treatments for such human neurodegeneration.

The Molecular Chaperone Hsp70 Is a Potent Suppressor of Polyglutamine Pathogenicity

Given that polyglutamine disease is associated with an abnormal protein conformation, the molecular chaperones may play a role in disease progression. In flies, the major stress-induced chaperone is Hsp70. Therefore, we asked whether Hsp70 might be involved in the disease process. We found that the nuclear inclusions immunostained, from initial stages of their formation, with antibodies that detect the Hsp70 proteins (12). This finding suggested the possibility that the cells were mounting a stress response against the pathogenic protein. Therefore, we asked whether it would make a difference to supply the cells with additional Hsp70 activity. To do this, we made transgenic flies that overexpress human Hsp70, which is highly conserved with fly Hsp70, but can be detected with species-specific antibodies.

Co-expression of Hsp70 dramatically suppresses the degeneration normally associated with the pathogenic polyglutamine protein MJDtr-Q78 (Fig. 1). The external eye structure is fully restored to normal, and internal eye structure is strongly restored. Moreover, not only is initial degeneration arrested but also progressive degeneration is prevented. We verified that there were no differences in transgene expression and that, rather, the added Hsp70 is protecting or compensating for the toxicity of the pathogenic disease protein.

To address whether the enzymatic ATPase activity of Hsp70 is important for the suppression, we examined transgenic flies that express a form of the constitutively expressed Hsp70, Hsc4, with a point mutation in the ATPase domain that acts *in vivo* in a dominant-negative manner (19). Co-expression of this protein with the disease protein not only fails to suppress, but actually enhances, degeneration. This finding suggests that toxicity to the polyglutamine protein is sensitive to the levels of the Hsp70 family of molecular chaperones, with added Hsp70 preventing degeneration, whereas interference with endogenous chaperone activity promotes degeneration.

We also investigated the role of the Hsp70 co-chaperone Hsp40 in protein pathogenicity, by creating transgenic flies that overexpress the fly counterpart of the human Hdj1 class of molecular chaperone, dHdj1. These flies, like those expressing Hsp70, also show strong suppression of polyglutamine toxicity (ref. 11, also ref. 20). The Hsp40 proteins show specificity in that dHdj1 is effective, whereas dHdj2 is poor at protecting against polyglutamine toxicity (11). This difference is consistent with idea that different Hsp40 class chaperones have distinct substrate specificities [see review by Hartl and colleagues in this issue (21) for more extensive discussion of Hsp70/Hsp40 functional interactions]. There appears to be selectivity for the polyglutamine protein, such that dHdj1 is more effective.

We also examined potential interactions between Hsp70 and dHdj-1. As dHdj-1 is presumably a co-chaperone for Hsp70, we anticipated that we might detect a synergy between the two proteins in suppression of pathogenicity. Indeed, although either Hsp70 or dHdj1 on its own is a strong suppressor, when they are co-expressed suppression of polyglutamine degeneration is even stronger (Fig. 2). These findings emphasize the importance of providing a sufficient complement of chaperones for suppression. In our disease model, it appears that there are sufficient levels of Hsp70 and Hsp40 alone to allow initial suppression. The late-onset nature of the degeneration may signify that the chaperone system eventually becomes overwhelmed. However, cells with a generally poor basal stress or chaperone system may require more than just Hsp70 or Hsp40 alone for significant suppression, instead requiring a complement of chaperones to effect protection.

It is of interest that the potent suppression of the adult eye degenerative phenotype by Hsp70 and dHdj1 occurs in the absence of an effect on the morphology of the aggregates formed by the pathogenic protein, as visualized by immunocytochemistry. Nuclear inclusions are formed in the fly upon chaperone suppression, and they are present in the same number and the same size as in the absence of additional chaperones. The nuclear inclusions appear the same, except that the exogenous Hsp70 and dHdj1 are now also found in the inclusions, suggesting an interaction with the pathogenic protein.

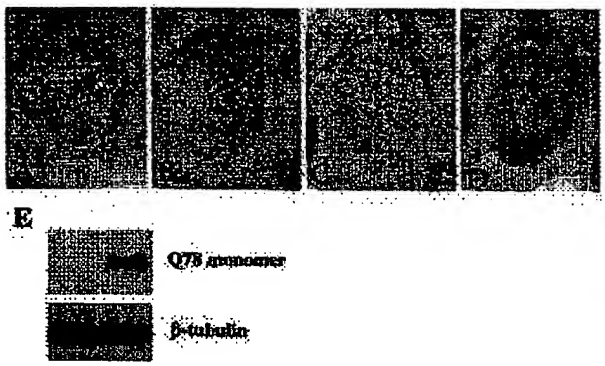

Fig. 2. Hsp70 and Hsp40 synergize in suppression of polyglutamine toxicity. Two copies of the polyglutamine protein are expressed in *A–D*, which makes the phenotype severe enough that synergy may readily be seen. (*A*) The polyglutamine protein MJDtr-Q78 causes severe degeneration. (*B* and *C*) Expression of either Hsp70 (*B*) or dHdj1 (*C*) alone has partial ability to rescue eye structure. (*D*) Expression of Hsp70 with dHdj1 results in full restoration of eye structure to normal (compare with Fig. 1*A*). Fly genotypes are *w; gmr-GAL4 UAS-MJDtrQ78/UAS-MJDtr-Q78* (*A*), *w; gmr-GAL4 UAS-MJDtr-Q78/UAS-MJDtrQ78 UAS-Hsp70* (*B*), *w; gmr-GAL4 UAS-MJDtrQ78/UAS-MJDtr-Q78 UAS-Hsp40* (*C*), and *w; gmr-GAL4 UAS-MJDtr-Q78 UAS-Hsp70/UAS-MJDtr-Q78 UAS-Hsp40*. (*E*) Chaperones increase the SDS-solubility of the pathogenic polyglutamine protein. Shown is a Western immunoblot of monomeric polyglutamine protein extracted from the heads of flies expressing the disease protein alone (left lane), or with Hsp70 (right lane). As shown in the left lane, normally most of the polyglutamine protein is SDS-insoluble, remaining within the stacking gel and poorly transferring in a Western immunoblot (see ref. 11), such that little or no protein is present as a monomer. However, in the presence of chaperones (right lane), there is a significant amount of protein now SDS-soluble that runs as a monomer. Lower gel is β-tubulin control showing equal loading. Heads are from flies of genotype *w; gmr-GAL4 UAS-MJDtrQ78/+* (left lane) and *w; gmr-GAL4 UAS-MJDtr-Q78/UAS-Hsp70* (right lane).

To address this question in another manner, we performed Western immunoblot analysis on the flies and examined the solubility properties of the pathogenic protein. By this assay, the pathogenic protein remains largely insoluble in SDS-resistant complexes that fail to enter the protein gel, remaining within the stacking gel, and transferring poorly in immunoblot analysis. However, in flies that are co-expressing the chaperones, a large amount of the pathogenic protein is now SDS-soluble and detected as a monomeric protein by Western immunoblot (Fig. 2*E*) (11).

The degree of SDS-solubility strikingly correlates with pathogenicity of the protein—dHdj2, which suppresses poorly, shows little or no change in monomer, despite high levels of coexpressed chaperone. These data suggest that the properties of the pathogenic protein have changed in the presence of the chaperones. Potentially, the protein is being maintained in a more native or normal conformation, with toxic interactions being abated, seen as a change in SDS-solubility.

Chaperone Suppression of α-Synuclein Toxicity in a *Drosophila* Model for Parkinson's Disease

The demonstration that *Drosophila* can be used to model a human neurodegenerative disease by directed expression of the respective human disease protein opened the possibility of modeling human neurodegenerative diseases other than polyglutamine diseases in the fly. Indeed, directed expression of α-synuclein, a component of Lewy bodies and mutated in familial forms of Parkinson's disease, causes adult-onset degeneration of dopaminergic neurons in *Drosophila*, thereby providing a model for Parkinson's disease (Fig. 3) (10, 22). We have

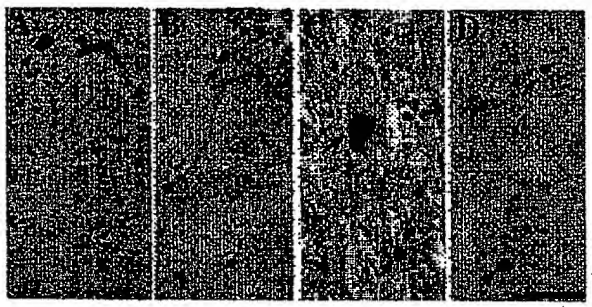

Fig. 3. α-Synuclein Lewy-body-like aggregates in flies and in Parkinson's disease patient tissue. (*A* and *B*) Brain sections through a 20-day-old fly expressing wild-type α-synuclein show Lewy-body-like aggregates in the cortex (arrow) and neuropil (arrowheads) that immunolabel for α-synuclein (*A*) and the fly stress-induced Hsp70 (*B*). (*C* and *D*) Tissue from the substantia nigra of a patient with Parkinson's disease showing Lewy bodies and Lewy pathology that immunolabel for α-synuclein (*C*) and Hsp70 (*D*). The commonalities between fly and human suggest that chaperone activity may modulate human Parkinson's disease (see ref. 10). (Bar = 3 μm.)

also determined whether we could apply the principles learned from chaperone suppression of polyglutamine pathogenicity to the problem of protein toxicity of α-synuclein in *Drosophila*.

When α-synuclein expression is directed to dopaminergic neurons in the *Drosophila* brain, select clusters of neurons show adult-onset progressive loss of cells. To define this cell loss, we prepared serial brain sections and immunostained for tyrosine hydroxylase expression, which selectively detects the dopaminergic neurons. We then counted the number of dopaminergic neurons present in the dorsomedial (DM) and dorsolateral (DL-1) clusters in the adult fly over time. We found a consistent 50% loss of dopaminergic neurons in the DM cluster, and a variable 0–50% loss of cells within the DL-1 cluster (10). Normal cell numbers were present at eclosion of the adult fly from the pupal case, with the cells degenerating over 20 days of adult life. We did not see further loss of cells, indicating that by 20 days all of the cells sensitive to α-synuclein toxicity had degenerated. Moreover, we did not detect a difference in the toxicity of normal α-synuclein, or the two mutant forms A30P and A53T.

In flies, normal α-synuclein and the mutant forms form abnormal Lewy-body-like and Lewy-neurite-like accumulations in the brain over time (Fig. 3). The Lewy-body-like aggregates appear as smaller, more loosely formed accumulations at 1 day, and become progressively larger by 20 days. As with human Lewy bodies, the fly Lewy-body-like aggregates immunolabel with antibodies to ubiquitin, indicating they may reflect accumulation of misfolded protein targeted for degradation by the proteasome. Most Parkinson's disease is sporadic and associated with accumulation of normal α-synuclein in Lewy bodies (2), consistent with the toxicity and Lewy-body-like formation by normal α-synuclein, in a manner similar to the mutant forms, in *Drosophila*.

We then asked whether co-expression of Hsp70 had an effect on α-synuclein toxicity. We co-expressed human Hsp70 with α-synuclein and counted the number of dopaminergic neurons in the DM clusters, where we detect a consistent loss of neurons upon α-synuclein expression alone.

Hsp70 had a dramatic effect to maintain dopaminergic neural numbers and prevent the degeneration of dopaminergic neurons (10). Whereas normally upon α-synuclein expression, 50% of neurons in the DM cluster were lost over 20 days in the adult, now all neurons were maintained over the 20-day period. This was the case upon expression of the wild-type α-synuclein, as well as the mutant forms A30P and A53T. We examined whether this

protection was accompanied by a change in formation of the Lewy-body-like aggregates; however, as with polyglutamine degeneration, we detected no change. This result indicates that Hsp70 fully protects against α-synuclein toxicity, despite the continued presence of aggregates. The aggregates immunolabel for the exogenous Hsp70, however, indicating a potential direct interaction of the chaperone with α-synuclein. We then asked whether there was a change in distribution of endogenous chaperones, and indeed we found that the aggregates immunolabel for the stress-induced form of fly Hsp70 (Fig. 3). This finding indicates that there might be an involvement of endogenous chaperones, and potentially a stress response, in α-synuclein toxicity.

Endogenous Chaperone Activity Plays a Role in α-Synuclein Toxicity in *Drosophila* and Potentially also in Parkinson's Disease

To ask whether endogenous chaperone levels may normally help protect against α-synuclein toxicity, the dominant-negative form of Hsc4 was co-expressed with the disease protein. This form of Hsc4 will interfere with endogenous activity of the Hsp70 family of chaperones, in effect lowering endogenous chaperone activity (19). In this situation, we noted an acceleration of α-synuclein toxicity. Whereas normally upon expression of α-synuclein, flies are born with the full complement of dopaminergic neurons in the DM clusters, in the presence of Hsc4.K71S, flies are born with a 50% loss of dopaminergic neurons. This cell loss did not progress further over time in the adult; rather, Hsc4.K71S accelerated the toxicity of α-synuclein to those cells sensitive to α-synuclein. However, we also noted that Hsc4.K71S has some toxicity to dopaminergic neurons when expressed in the absence of α-synuclein. The fact that α-synuclein and Hsc4.K71S are acting similarly with regard to dopaminergic neural loss indicates that the toxicity in both cases may share common mechanisms.

To extend our findings back to the human disease condition, we asked whether Parkinson's disease was associated with a change in chaperone function. To do this, we immunostained patient tissue with antibodies to Hsp70 and its co-chaperone Hsp40. Indeed, Lewy bodies and Lewy neurites in disease brain immunolabel for the chaperones (Fig. 3). The significance of this finding is best evaluated in the context of the fly study: in *Drosophila* the abnormal inclusions of α-synuclein immunolabel for Hsp70 and up-regulation of Hsp70 activity by directed transgenic expression mitigates the toxicity. This finding suggests that it may be of value in Parkinson's disease to up-regulate chaperone function.

Discussion

Our initial and other subsequent studies have established *Drosophila* as a model genetic system to bring to bear in the arsenal of approaches toward the combat of human neurodegenerative disease (10, 12, 13, 20, 22–26). The striking homology of a large number of fly genes with human genes—indeed of entire gene pathways—indicates that fundamental properties of degeneration modeled in flies may be conserved in humans. Whereas the demonstration of the fly as an outstanding *in vivo* model for human neurodegeneration is significant, of great importance is the use of those models to reveal disease mechanisms and pioneer ways to interfere in the disease process.

The implication that chaperones may be of interest in such neurodegenerative diseases finds its roots in an even simpler model system than *Drosophila*—the yeast *Saccharomyces cerevisiae*. Indeed, protein conformational changes relevant to human prion disease are found in yeast in the study of endogenous yeast prions such as Sup35 (27), where Hsp104 was described as a regulator of the prion state (28). The *Drosophila* studies establish that chaperone modulation can be applied to the nervous system *in vivo* in the context of neurodegeneration.

In *Drosophila*, the chaperones are found to be potent modulators both of polyglutamine toxicity and of α-synuclein toxicity in models for human polyglutamine disease and Parkinson's disease. Not only does added chaperone activity prevent disease, but interfering with endogenous chaperone activity accelerates pathogenesis. This finding indicates that chaperone activity is central to the disease process, being modulated upon both up-regulation and interference. Moreover, these studies in *Drosophila* for polyglutamine toxicity have been found to translate to mammalian models for polyglutamine toxicity. Up-regulation of Hsp70 in transgenic mice expressing the Ataxin-1 pathogenic polyglutamine disease protein leads to protection against behavioral and cellular pathology (29).

How are the chaperones modulating protein toxicity? *In vivo* in flies, chaperones modulate the solubility properties of the polyglutamine protein concomitant with a modulation in the toxicity. However, no morphological change in the aggregates is detected. This is the case for both polyglutamine and α-synuclein toxicity. Studies of polyglutamine aggregation and protein solubility in yeast remarkably parallel the fly findings, where chaperones modulate solubility but aggregates are still present (30). One possibility is that the chaperones are modulating the structure of the protein, and this is not visible in the large aggregates. Prefibrils or protofibrils may be the toxic entity (see refs. 31 and 32)—smaller clumps and misconformations of the disease protein that precede or are independent of large, visible aggregates. Chaperones may be modulating these abnormal and toxic conformations, thereby preventing neurodegeneration. This conceivably can happen in the absence of an effect on large, visible aggregates, which are a different form of the disease protein, perhaps even inert or protective.

Another possibility is that chaperones, by interacting with the disease protein, prevent abnormal interactions with other proteins in the cell that are causal in toxicity. However, clearly, just anything that physically interacts with the disease protein appears not to have an effect to suppress, as demonstrated by the dHdj2 studies for polyglutamine disease. Whereas dHdj-2 is in association with the polyglutamine protein in the aggregates, as it co-localizes by immunocytochemistry, it fails to suppress toxicity (11).

Another possibility is that of chaperone depletion. Because of an abnormal or misfolded conformation, pathogenic disease proteins may cause cellular depletion of chaperone activity. Chaperones are required for the proper folding and function of many cellular proteins with diverse roles. Therefore, slow depletion of chaperones from the cellular milieu could lead to the failure of many cellular processes.

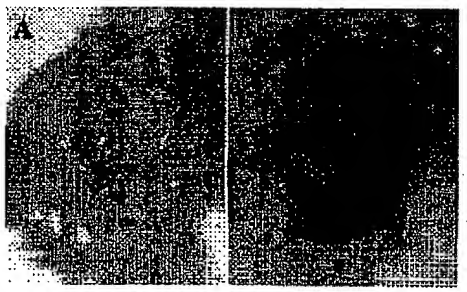

Fig. 4. Interfering with endogenous chaperone activity causes a severely degenerate eye phenotype. (*A*) Expression of a dominant-negative form of Hsp70 causes loss of pigmentation and deterioration of eye structure, similar to the expression of the polyglutamine protein in flies (see Fig. 1*C*). The genotype of the fly was *w; gmr-GAL4 UAS-Hsp70.K71E*. (*B*) Normal fly eye for comparison.

The role of chaperone depletion is intriguing because of the ability of chaperones to phenocopy aspects of disease protein expression. In the α-synuclein studies, expression of Hsc4.K71S on its own caused some loss of dopaminergic neurons, indicating that dopaminergic neurons are sensitive to compromised chaperone activity [also supported by other studies of α-synuclein and Parkinson's disease-associated proteins (33, 34)]. In the studies of the Hsc4.K71S transgene in flies, Elefant and Palter (19) noted that in some situations the protein was toxic, inducing a misfolded protein response accompanied by a degeneration reminiscent of neurodegenerative disease. We have also found that expressing Hsp70.K71E in the eye causes an external eye phenotype strikingly similar to the polyglutamine disease phenotype (Fig. 4). These studies suggest that compromising chaperone levels alone is phenotypically similar to the pathogenic actions of polyglutamine and α-synuclein proteins, indicating that chaperone interference is a major contributing factor to neurodegeneration. Cell specificity differs between polyglutamine and α-synuclein toxicity, with pathogenic polyglutamine protein appearing to be much more generally toxic in *Drosophila* than α-synuclein. However, this observation could be explained by cellular differences in the chaperone response to the specific protein in different tissues.

With the ever-accelerating development of fly models for various human neurodegenerative diseases, and tremendous interest in such models for both standard genetic and pharmacological approaches, *Drosophila* may reveal new cures and treatments of relevance to human neurodegeneration, including polyglutamine and Parkinson's diseases.

I thank Mark Fortini and Anthony Cashmore for comments. I receive funding support from the David and Lucile Packard Foundation and the National Institutes of Health, and I am an Assistant Investigator of the Howard Hughes Medical Institute.

1. Zoghbi, H. Y. & Orr, H. T. (2000) *Annu. Rev. Neurosci.* **23**, 217–247.
2. Spillantini, M. G., Schmidt, M. L., Lee, V. M., Trojanowski, J. Q., Jakes, R. & Goedert, M. (1997) *Nature (London)* **388**, 839–840.
3. Kruger, R., Kuhn, W., Muller, T., Woitalla, D., Graeber, M., Kosel, S., Przuntek, H., Epplen, J. T., Schols, L. & Riess, O. (1998) *Nat. Genet.* **18**, 106–108.
4. Polymeropoulos, M. H., Lavedan, C., Leroy, E., Ide, S. E., Dehejia, A., Dutra, A., Pike, B., Root, H., Rubenstein, J., Boyer, R., *et al.* (1997) *Science* **276**, 2045–2047.
5. Adams, M. D., Celniker, S. E., Holt, R. A., Evans, C. A., Gocayne, J. D., Amanatides, P. G., Scherer, S. E., Li, P. W., Hoskins, R. A., Galle, R. F., *et al.* (2000) *Science* **287**, 2185–2195.
6. Benzer, S. (1967) *Proc. Natl. Acad. Sci. USA* **58**, 1112–1119.
7. Dudai, Y., Jan, Y. N., Byers, D., Quinn, W. G. & Benzer, S. (1976) *Proc. Natl. Acad. Sci. USA* **73**, 1684–1688.
8. Benzer, S. (1971) *J. Am. Med. Assoc.* **218**, 1015–1022.
9. Heisenberg, M. & Bohl, K. (1979) *Z. Naturforsch.* **34**, 143–147.
10. Aulnick, P. K., Chan, H. Y., Trojanowski, J. Q., Lee, V. M. & Bonini, N. M. (2002) *Science* **295**, 865–868.
11. Chan, H. Y., Warrick, J. M., Gray-Board, G. L., Paulson, H. L. & Bonini, N. M. (2000) *Hum. Mol. Genet.* **9**, 2811–2820.
12. Warrick, J. M., Chan, H. Y., Gray-Board, G. L., Chai, Y., Paulson, H. L. & Bonini, N. M. (1999) *Nat. Genet.* **23**, 425–428.
13. Warrick, J. M., Paulson, H. L., Gray-Board, G. L., Bui, Q. T., Fischbeck, K. H., Pittman, R. N. & Bonini, N. M. (1998) *Cell* **93**, 939–949.
14. Kawaguchi, Y., Okamoto, T., Taniwaki, M., Aizawa, M., Inoue, M., Katayama, H., Nakamura, S., Nishimura, M., Akiguchi, I., Kimura, J., *et al.* (1994) *Nat. Genet.* **8**, 221–228.
15. Brand, A. H. & Perrimon, N. (1993) *Development (Cambridge, U.K.)* **118**, 401–415.
16. Davies, S. W., Turmaine, M., Cozens, B. A., DiFiglia, M., Sharp, A. H., Ross, C. A., Scherzinger, E., Wanker, E. E., Mangiarini, L. & Bates, G. P. (1997) *Cell* **90**, 537–548.
17. DiFiglia, M., Sapp, E., Chase, K. O., Davies, S. W., Bates, G. P., Vonsattel, J. P. & Aronin, N. (1997) *Science* **277**, 1990–1993.
18. Paulson, H. L., Perez, M. K., Trottier, Y., Trojanowski, J. Q., Subramony, S. H., Das, S. S., Vig, P., Mandel, J.-L., Fischbeck, K. H. & Pittman, R. N. (1997) *Neuron* **19**, 333–344.
19. Elefant, F. & Palter, K. (1999) *Mol. Biol. Cell* **10**, 2101–2117.
20. Kazemi-Esfarjani, P. & Benzer, S. (2000) *Science* **287**, 1837–1840.
21. Sakahira, H., Breuer, P., Hayer-Hartl, M. K. & Hartl, F. U. (2002) *Proc. Natl. Acad. Sci. USA* **99**, Suppl. 4, 16412–16418.
22. Feany, M. B. & Bender, W. W. (2000) *Nature (London)* **404**, 394–398.
23. Fernandez-Funez, P., Nino-Rosales, M. L., de Gouyon, B., She, W.-C., Luchak, J. M., Martinez, P., Turiegano, E., Benito, J., Capovilla, M., Skinner, P. J., *et al.* (2000) *Nature (London)* **408**, 101–106.
24. Jackson, G., Salecker, I., Dong, X., Yao, X., Arnheim, N., Faber, P., MacDonald, M. & Zipursky, S. (1998) *Neuron* **21**, 633–642.
25. Marsh, J. L., Walker, H., Theisen, H., Zhu, Y., Fielder, T., Purcell, J. & Thompson, L. M. (2000) *Hum. Mol. Genet.* **9**, 13–25.
26. Wittmann, C. W., Wszolek, M. F., Shulman, J. M., Salvaterra, P. M., Lewis, J., Hutton, M. & Feany, M. B. (2001) *Science* **293**, 711–714.
27. Serio, T. R. & Lindquist, S. L. (2000) *Trends Cell Biol.* **10**, 98–105.
28. Chernoff, Y. O., Lindquist, S. L., Ono, B., Inge-Vechtomov, S. G. & Liebman, S. W. (1995) *Science* **268**, 880–884.
29. Cummings, C. J., Sun, Y., Opal, P., Antalffy, B., Mestril, R., Orr, H. T., Dillmann, W. H. & Zoghbi, H. Y. (2001) *Hum. Mol. Genet.* **10**, 1511–1518.
30. Muchowski, P. J., Schaffar, G., Sittler, A., Wanker, E. E., Hayer-Hartl, M. K. & Hartl, F. U. (2000) *Proc. Natl. Acad. Sci. USA* **97**, 7841–7846.
31. Bucciantini, M., Giannoni, E., Chiti, F., Baroni, F., Formigli, L., Zurdo, J., Taddei, N., Ramponi, G., Dobson, C. & Stefani, M. (2002) *Nature (London)* **416**, 507–511.
32. Walsh, D., Klyubin, I., Fadeeva, J., Cullen, W., Anwyl, R., Wolfe, M., Rowan, M. & Selkoe, D. (2002) *Nature (London)* **416**, 535–539.
33. Imai, Y., Soda, M., Inoue, H., Hattori, N., Mizuno, Y. & Takahashi, R. (2001) *Cell* **105**, 891–902.
34. Shimura, H., Schlossmacher, M. G., Hattori, N., Frosch, M. P., Trockenbacher, A., Schneider, R., Mizuno, Y., Kosik, K. S. & Selkoe, D. J. (2001) *Science* **293**, 263–269.

letter

Suppression of polyglutamine-mediated neurodegeneration in *Drosophila* by the molecular chaperone HSP70

John M. Warrick[1], H.Y. Edwin Chan[1], Gladys L. Gray-Board[1], Yaohui Chai[2], Henry L. Paulson[2] & Nancy M. Bonini[1]

At least eight inherited human neurodegenerative diseases are caused by expansion of a polyglutamine domain within the respective proteins[1,2]. This confers dominant toxicity on the proteins, leading to dysfunction and loss of neurons. Expanded polyglutamine proteins form aggregates, including nuclear inclusions (NI), within neurons, possibly due to misfolding of the proteins[3–5]. NI are ubiquitinated and sequester molecular chaperone proteins and proteasome components[6–8], suggesting that disease pathogenesis includes activation of cellular stress pathways to help refold, disaggregate or degrade the mutant disease proteins. Overexpression of specific chaperone proteins reduces polyglutamine aggregation in transfected cells[7–9], but whether this alters toxicity is unknown. Using a *Drosophila melanogaster* model of polyglutamine disease[10], we show that directed expression of the molecular chaperone HSP70 suppresses polyglutamine-induced neurodegeneration *in vivo*. Suppression by HSP70 occurred without a visible effect on NI formation, indicating that polyglutamine toxicity can be dissociated from formation of large aggregates. Our studies indicate that HSP70 or related molecular chaperones may provide a means of treating these and other neurodegenerative diseases associated with abnormal protein conformation and toxicity.

Machado-Joseph disease (MJD), also known as spinocerebellar ataxia type 3, is the most common dominantly inherited progressive ataxia caused by polyglutamine expansion[11–13]. Expression of a truncated form of the human MJD protein with an expanded polyglutamine domain causes progressive neural degeneration in mouse transgenic models[14] and in *Drosophila*[10]. In polyglutamine diseases, including MJD, abnormal protein aggregation is observed, typically as NI (refs 3–5). In *Drosophila*, mutant MJD protein also forms NI (ref. 10). We addressed the ability of chaperone proteins to modulate polyglutamine disease *in vivo* by first determining whether the major stress-induced molecular chaperone in the fly, HSP70, associated with mutant polyglutamine protein in our *Drosophila* model of polyglutamine disease.

We expressed protein using the GAL4/UAS system[15]. When expanded polyglutamine protein (MJDtr-Q78) is directed to the fly eye with the glass multiple reporter (GMR) element, expression begins at the morphogenetic furrow, the first major differentiation event of fly eye development[16]. MJDtr-Q78 protein is cytoplasmic upon initial expression in cells near the furrow, but the protein undergoes aggregation to form prominent NI as differentiation proceeds toward the posterior of the eye field[10]. The control protein, with a normal polyglutamine repeat (MJDtr-Q27), remains cytoplasmic and does not form aggregates. Co-labelling for HSP70 in controls indicated a low level of cytoplasmic staining that was unchanged from that in normal eye discs (Fig. 1*a–c*). In contrast, eye fields of larvae expressing the mutant protein, MJDtr-Q78, showed HSP70 staining localized to the NI (Fig. 1*d,e*). Under stress conditions, HSP70 is thought to prevent aggregation or assist in the refolding of misfolded protein[17]. Our data indicate that mutant polyglutamine protein is recognized as abnormal by the cells, as evidenced by localization of HSP70 to the NI.

These studies implicated HSP70 in the response *in vivo* to mutant polyglutamine protein. We next addressed whether overexpression of HSP70 alters toxicity of the disease protein. We made transgenic flies bearing the human gene encoding HSP70 UAS-HSPA1L (ref. 18). Human HSPA1L (encoded by *HSPA1L*) is highly homologous to fly HSP70 (74% identical, 85% similar at the protein level); we anticipated that HSPA1L would function *in vivo* in *Drosophila*.

When we co-expressed HSPA1L with MJDtr-Q78, HSPA1L suppressed polyglutamine-induced degeneration (Fig. 2). Normally, MJDtr-Q78 causes severe degeneration, resulting in loss

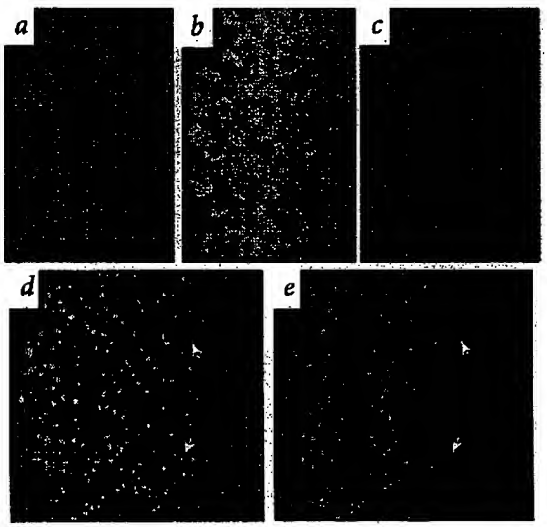

Fig. 1 *Drosophila* HSP70 localizes to nuclear inclusions. Confocal images are shown of the eye portion of eye-antennal imaginal discs from third instar larvae, stained with antibodies to detect *Drosophila* HSP70 (*a,c,e*) and polyglutamine protein (*b,d*). Eye development progresses from posterior to anterior across the eye field of the disc, such that the disc presents a temporal sequence of development with older cells toward the posterior tip (left). *a*, Wild-type eye disc showing fly HSP70 expression. A low level of cytoplasmic expression was seen. *b,c*, Eye disc from a larva expressing the control polyglutamine protein MJDtr-Q27, stained for expression of the polyglutamine protein (*b*) and HSP70 (*c*). No change in HSP70 expression was observed. Larvae were of genotype *w*; GMR-GAL4/UAS-MJDtr-Q27. *d,e*, Eye disc from a larva expressing the expanded polyglutamine protein MJDtr-Q78, immunostained for polyglutamine protein (*d*) and HSP70 (*e*). The expanded polyglutamine protein forms NI; HSP70 is localized to the NI. In the younger part of the eye field toward the furrow, newly formed NI were occasionally observed that did not label for HSP70 (arrows), whereas in more mature cells toward the posterior of the disc, all NI labelled for HSP70. Larvae were of genotype *w*; GMR-GAL4/UAS-MJDtr-Q78(5).

[1]*Department of Biology, University of Pennsylvania, Philadelphia, Pennsylvania, USA.* [2]*Department of Neurology, University of Iowa College of Medicine, Iowa City, Iowa, USA. Correspondence should be addressed to N.M.B. (e-mail: nbonini@sas.upenn.edu).*

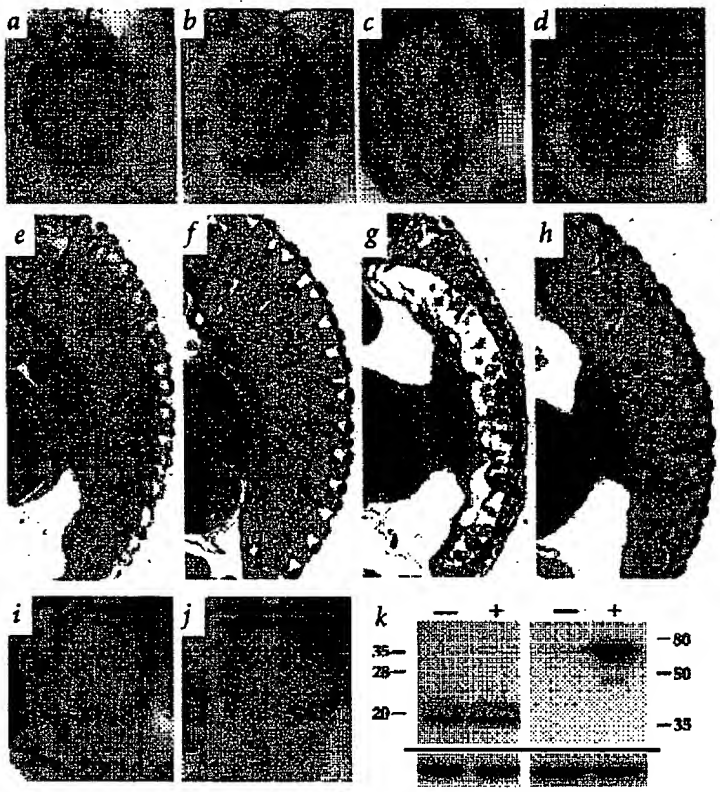

Fig. 2 HSP70 suppresses polyglutamine-induced neurodegeneration *in vivo*. Eyes (*a–d*) and retinal sections (*e,f*) of flies expressing expanded polyglutamine protein and human HSPA1L are shown. *a,e*, Control fly expressing only the promoter transgene, GMR-GAL4. The eye is normal. Flies were genotype *w*; GMR-GAL4/+. *b,f*, Flies expressing *HSPA1L*. Eye structure appears grossly normal. More detailed analysis revealed abnormalities in nuclear position and photoreceptor rhabdomere morphology when HSPA1L is expressed by GMR-GAL4. Flies were genotype *w*; GMR-GAL4/UAS-HSPA1L. *c,g*, Flies expressing the expanded polyglutamine protein MJDtr-Q78. These flies have degenerate eyes that lack pigment and show severe loss of retinal structure. Flies were genotype *w*; GMR-GAL4/UAS-MJDtr-Q78. *d,h*, Flies expressing both MJDtr-Q78 and HSPA1L. Co-expression of HSPA1L ameliorates the degenerative effects of MJDtr-Q78. The eye appears normal externally. Internally, eye structure is largely restored, although photoreceptor rhabdomere specializations are not made. Flies were genotype *w*; GMR-GAL4 UAS-MJDtr-Q78(S)/UAS-HSPA1L. Control experiments showed lack of suppression of the MJDtr-Q78 degeneration by other transgenes (*i,j*) and lack of an effect of HSPA1L on the GAL4/UAS expression system by immunoblot analysis. Flies co-expressing both MJDtr-Q78 and a human cytoskeletal protein Tau (*i*) or a developmental protein Eya (*j*) showed no modification of the degeneration phenotype (*c*), demonstrating that co-expression of two transgenes by a single GAL4 promoter line has no effect on phenotype. An additional transgene tested was the cellular regulator *yan*. We also tested whether co-expression of the UAS-MJDtr-Q78 transgene would ameliorate the late-lethal phenotype of directed killer gene activity *rpr* and *hid*; in neither case was the lethal phenotype modified (data not shown), indicating co-expression of two transgenes by a single GAL4 promoter does not alter expression levels. Flies were genotype *w*; GMR-GAL4 UAS-MJDtr-Q78(S)/UAS-htau or UAS-eya. *k*, Western immunoblot analysis of protein levels in flies expressing the control protein MJDtr-Q27 alone (– lanes) or with HSPA1L (+ lanes). Left, MJDtr-Q27 protein, detected with an antibody against the HA tag. The expression levels are similar in both samples. Right, the exogenously expressed human HSPA1L protein. HSPA1L is present only in the '+' sample. Bottom, loading controls showing similar levels of β-tubulin detected per lane. Flies were genotype *w*; GMR-GAL4/UAS-MJDtr-Q27 (– lanes) and *w*; GMR-GAL4 UAS-HSPA1L/UAS-MJDtr-Q27 (+ lanes).

of the retina. With co-expressed HSPA1L, however, external eye pigmentation was completely rescued (Fig. 2*c,d*). Sectioning of the brain revealed that retinal structure was partially restored (Fig. 2*g,h*). The disease phenotype was suppressed to a greater extent in flies expressing moderate or weak levels of expanded polyglutamine protein, as more of the eye structure was restored, including specializations.

We addressed specificity of HSPA1L suppression with a number of control studies. First, co-expression of any additional transgene with MJDtr-Q78 did not have an effect on the phenotype, indicating that suppression of degeneration is not due to co-expression of two transgenes, rather than one, by a *GAL4* promoter (Fig. 2*i,j*). Second, co-expression of HSPA1L did not modify the disrupted eye phenotype caused by expression of other proteins with the GAL4/UAS system, including the cytoskeletal protein MAP2C and the developmental protein Eyeless (data not shown). Additional studies indicated that HSPA1L does not function as a survival factor in known *Drosophila* apoptotic pathways because there was no modification of killer gene activity. Third, we detected no difference in MJDtr-Q78 expression levels by immunocytochemistry in the presence or absence of co-expressed HSPA1L (Fig. 4). Quantitative expression analysis of the control protein MJDtr-Q27 (which does not form aggregates, allowing accurate western-blot analysis) also revealed no change in transgene expression despite co-expression of HSPA1L (Fig. 2*k*). These studies indicate that suppression of degeneration by HSPA1L is due to suppression of polyglutamine protein toxicity, and not a nonspecific effect of HSPA1L on the GAL4/UAS system.

To address whether HSPA1L modulated polyglutamine-induced toxicity broadly within the nervous system, we targeted expression of MJDtr-Q78 to all neurons with an ELAV promoter line[19]. This normally resulted in complete lethality or early adult death (Table 1). But with HSPA1L co-expression, toxicity was diminished such that adult viability was partially restored

Table 1 • HSP70 diminishes polyglutamine protein toxicity in the nervous system

	MJDtr-Q78 expression	
	Strong	Moderate
Elav alone	0% survival	males begin to die at 4 d; 50% death at 6 d (range 4–9 d)
Elav+HSPA1L	2% male survival 30% female survival	males begin to die 9 d; 50% death at 15 d (range 9–20 d)

Elav, ELAV-GAL4; HSPA1L, UAS-HSPA1L. MJDtr-Q78 flies bear insertions UAS-MJDtr-Q78(S) for strong expression and UAS-MJDtr-Q78(M) for moderate expression. Expression levels have been quantified by immunocytochemistry, and correlate with the phenotype[10].

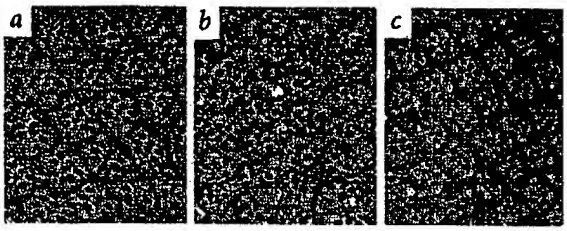

Fig. 3 HSP70 slows progressive degeneration of the nervous system. Tangential sections of the eyes of four-day-old flies bearing the ELAV-GAL4 promoter line, which targets expression to all neurons. *a*, Control fly, bearing only the transgene for the promoter element ELAV-GAL4. The eye shows the normal, highly regular pattern of photoreceptor cell rhabdomeres surrounded by the pigment lattice. Fly was genotype *w* ELAV-GAL4. *b*, Fly expressing expanded polyglutamine protein. The eye shows progressive degeneration, seen as disruption of the highly regular rhabdomere pattern. Flies at one day have a less disrupted photoreceptor pattern[10], compared with four-day-old flies shown here, indicating that the degeneration is progressive. Fly was genotype *w* ELAV-GAL4; UAS-MJDtr-Q78(M). *c*, Fly co-expressing expanded polyglutamine protein and HSPA1L. The eye shows little degeneration, retaining the highly regular ommatidial lattice, compared with expression of the expanded polyglutamine protein alone in (*b*). Fly was genotype *w* ELAV-GAL4; UAS-MJDtr-Q78(M)/UAS-HSPA1L.

(Table 1). Moreover, adult flies expressing moderate levels of MJDtr-Q78 usually live less than 2 weeks, with 50% dying by 6 days, but with co-expressed HSPA1L these flies lived approximately twice as long (Table 1, column 2). Sectioning of the eyes to examine neural structure revealed that HSPA1L not only extended lifespan, but also slowed progressive degeneration (Fig. 3). These data indicate that HSPA1L overexpression ameliorates toxicity of expanded polyglutamine protein when expressed selectively within the eye or broadly within the nervous system.

A characteristic of expanded polyglutamine proteins is that they form NI, although the relationship of aggregates to disease is uncertain[20,21]. We thus addressed whether HSPA1L suppression of protein toxicity was accompanied by a change in aggregate formation. To do this, we immunostained eye discs of larvae expressing MJDtr-Q78 alone, or MJDtr-Q78 and HSPA1L. Normally, NI are prominent in developing cells of larvae expressing MJDtr-Q78 (Fig. 4*a*). With co-expressed HSPA1L, NI remained prominent with no differences in onset, size or number (Fig. 4*a*,*b*). Most of the ectopic HSPA1L was cytoplasmic, but a fraction was recruited to the NI (Fig. 4*b*–*e*), similar to endogenous fly HSP70 (Fig. 1). The exogenous chaperone co-localization of MJDtr-Q78 protein *in vivo* is consistent with the possibility that HSPA1L diminishes toxicity, at least in part, by direct interaction with the disease protein. These data support previous findings indicating that NI formation *per se* may not be causally linked to disease[20,21]. In the suppressed situation, however, recruitment of exogenous HSPA1L to the NI may neutralize or diminish possible deleterious effects of aggregates.

The ATPase activity of HSP70 is essential to its functions in modulating protein folding and aggregation[17]. We addressed whether HSP70 normally has a role in mitigating polyglutamine disease using a fly line bearing a mutant form of the major constitutively expressed fly *hsp70*, *hsc4*, with an amino acid substitution in the ATP-binding domain[22] (UAS-HSC4.K71S). This transgene produces a protein that interferes in a dominant-negative manner with normal HSC4 chaperone activity *in vitro* and *in vivo*[22]. Expression of HSC4.K71S had no effect itself when expressed by GMR-GAL4, but it did potentiate polyglutamine-mediated degeneration (Fig. 5). These data suggest that endogenous activity of HSP70 molecular chaperones normally serves to mitigate deleterious effects of the mutant protein in the transgenic fly model. Potentially, such endogenous chaperone activity protects cells from continued exposure to abnormal polyglutamine protein, contributing to the late-onset nature of the phenotype.

We have shown that a molecular chaperone modulates neurotoxicity *in vivo* in a *Drosophila* model of human polyglutamine disease. Our data demonstrate normal association of HSP70 with mutant disease protein, suppression of disease pathology by overexpressing HSPA1L and enhancement of disease pathology by a dominant-negative form of a constitutive *Drosophila* HSP70, HSC4. The potential for molecular chaperones to modulate disease pathology has been suggested by their ability to modify protein aggregation[7–9,23,24]. We have demonstrated that added expression of a molecular chaperone *in vivo* suppresses neurodegenerative disease, but suppression occurs in the absence of an observable effect on protein aggregation. Thus, ridding the cell of NI does not appear to be the mechanism by which HSP70 mitigates protein toxicity. Our co-localization studies suggest a direct interaction of HSP70 with polyglutamine protein *in vivo*, although HSP70 may exert its effects through modulation of other cellular pathways, and the response may include other molecular chaperones, such as HSP40. Given the similarity of polyglutamine-disease features between flies and humans[10,25], our findings suggest that modulation of chaperone activity may be of therapeutic benefit. Because many different human neurodegenerative diseases appear due to toxic protein structures[26–29], these findings may be applicable to other human neurodegenerative disorders as well.

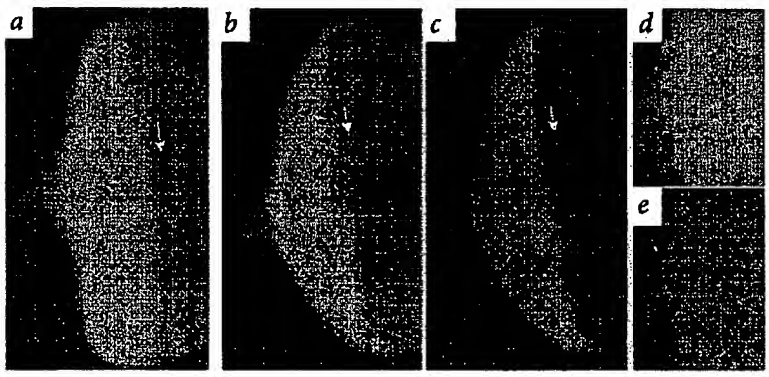

Fig. 4 NI formation in flies expressing polyglutamine protein and HSPA1L. Immunofluorescent images of eye imaginal discs. Polyglutamine protein was detected with antibody to HA (*a*,*b*,*d*); HSPA1L detected with antibody to human HSP70 (*c*,*e*). The onset of transgene expression begins at the furrow (*a*–*c*, white arrow), older cells to the left. *a*, NI formation in developing eye cells of flies expressing MJDtr-Q78. At the onset of transgene expression at the furrow (arrow), the protein is cytoplasmic. With time, the protein forms prominent NI. Larva was genotype *w*; GMR-GAL4/UAS-MJDtr-Q78(S). *b*–*e*, Eye disc of larvae co-expressing polyglutamine protein and HSPA1L, double-labelled for polyglutamine protein (*b*,*d*) and HSPA1L (*c*,*e*). NI are still prominent (*c*,*d*). Some HSPA1L localized to NI, but much of the cellular HSPA1L protein remains diffusely cytoplasmic (*c*,*e*). Larvae were genotype *w*; GMR-GAL4 UAS-MJDtr-Q78(S)/UAS-HSPA1L. *d*,*e*, Twofold higher magnification views of (*b*) and (*c*), respectively. Arrow highlights NI co-labelled for polyglutamine protein and HSPA1L.

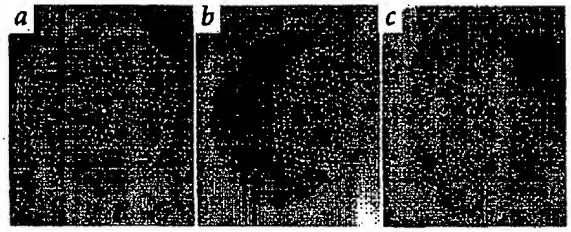

Fig. 5 A dominant-negative form of a constitutively expressed cytoplasmic fly HSP70 enhances polyglutamine disease. *a*, Fly expressing the constitutive form of HSP70, HSC4, with a dominant-negative mutation in the ATPase domain that inhibits ATPase activity[22]. No effect on the eye is observed. Flies were genotype *w*; GMR-GAL4/UAS-HSC4.K71S. *b*, Fly with weak expression of MJDtr-Q78. On mild expression of the expanded polyglutamine protein, external eye structure is normally only modestly disrupted. Flies were genotype *w*; GMR-GAL4 UAS-MJDtr-Q78(W)/+. *c*, Flies co-expressing polyglutamine protein weakly and mutant HSC4 show enhanced eye degeneration (*c*). Co-expression of MJDtr-Q78 strongly with Hsc4.K71S was fully lethal (data not shown). Flies were genotype w; GMR-GAL4 UAS-MJDtr-Q78(W)/UAS-Hsc4.K71S.

Methods

Drosophila genetics. Fly culture and crosses were performed at 25 °C following standard protocols. Fly lines bearing UAS-MJDtr-Q27 and UAS-MJDtr-Q78 transgenes have been described[10]. Transgenic flies expressing human *HSPA1L* were made by subcloning the cDNA (ref. 18) into the pUAST transformation vector[15]. We generated transgenic lines following standard procedures[30]. We obtained fly lines bearing GMR-GAL4, ELAV-GAL4 (line C155), UAS-htau and UAS-Map2c from *Drosophila* stock centres. Fly lines bearing UAS-yan (EP598) were a gift from G. Rubin. Fly lines bearing UAS-eyeless were a gift from W. Gehring. Fly lines bearing UAS-HSC4.K71S were a gift from K. Palter. Lines expressing cell-death genes *hid* and *rpr* were gifts from H. Steller, K. White and J. Abrams. In *Drosophila*, HSPA1L expression had a minor effect on nuclear position within the retina, resulting in a broadened distribution of nuclei. This appears to be an effect on the accessory cells of the eye that also express GMR and not the neurons because eye morphology was normal when HSPA1L expression was directed selectively to neurons with ELAV-GAL4. Crosses (Table 1) were performed by mating females homozygous for ELAV-GAL4 to males bearing the UAS-MJDtr-Q78 insertion and UAS-HSPA1L as required in *trans* to balancer chromosomes. Moderate expression of MJDtr-Q78 did not have an effect on the number of adult flies that emerge compared with control crosses. At least 300 flies were scored per cross, except for strong expression of MJDtr-Q78 by ELAV-GAL4 alone, which is lethal. ELAV-GAL4 is on the X chromosome, thus expression of ELAV-GAL4 in males is twice the level of that in females due to dosage compensation.

Microscopy, immunohistochemistry and immunoblot analysis. Eye discs were dissected and stained with antibodies as described[10]. We detected haemagglutinin (HA)-tagged polyglutamine protein with a rabbit polyclonal antibody to haemagglutinin (Y-11, 1:200, Santa Cruz). *Drosophila* HSP70 protein was detected with a monoclonal antibody to the fly protein (MAB-007, 1:200, Affinity BioReagents). We detected HSPA1L with an antibody specific to the human protein (SPA812, 1:200, StressGen). Secondary antibodies were conjugated to fluorescein (1:500) or Texas Red (1:50, Jackson ImmunoResearch). Confocal microscopy was performed on a Leica model TCS SP ultraviolet and visible confocal imaging spectrophotometer microscope. For light microscopic sections, adult heads (0–1 day old) were fixed in paraformaldehyde and embedded in epon for horizontal sections (1 µm), then stained with toluidine blue and methylene blue as described[10].

Immunoblot analysis. We solubilized 30 fly heads of the appropriate genotypes in Laemmli buffer (150 µl). Samples (20 µl per lane) were separated by standard polyacrylamide techniques (12% acrylamide gels), immunoblotted and detected as described[5], except that ECL reagent was from Amersham. Blots were re-probed after stripping according to manufacturer's suggestions by incubating at 55 °C for 30 min. We used anti-HA (12CA5, 1:3,000; Boehringer), anti-H-HSP70 (1:10,000) and anti-β-tubulin (E7, 1:1000; Developmental Studies Hybridoma Bank) antibodies. Secondary antibodies were goat anti-mouse and goat anti-rabbit coupled to HRP (1:4,000, Boehringer).

Acknowledgements

We thank A. Cashmore and L. Lillien for critical reading of the manuscript. This research was funded in part by grants from the R.J. Carver Charitable Trust, faculty start-up funding from the University of Iowa Howard Hughes Medical Institute Resources Program (H.L.P.), the Wills Foundation (J.M.W.), the Wellcome Trust (H.Y.E.C.), the HDSA Coalition for the Cure, Hereditary Disease Foundation, Alzheimer's Foundation and the David and Lucile Packard Foundation (N.M.B.).

Received 10 August; accepted 1 November 1999.

1. Paulson, H. Protein fate in neurodegenerative proteinopathies: polyglutamine diseases join the (mis)fold. *Am. J. Hum. Genet.* **64**, 339–345 (1999).
2. Perutz, M. Glutamine repeats and neurodegenerative diseases: molecular aspects. *Trends Biochem. Sci.* **24**, 58–63 (1999).
3. Davies, S.W. *et al.* Formation of neuronal intranuclear inclusions underlies the neurological dysfunction in mice transgenic for the HD mutation. *Cell* **90**, 537–548 (1997).
4. DiFiglia, M. *et al.* Aggregation of huntingtin in neuronal intranuclear inclusions and dystrophic neurites in brain. *Science* **277**, 1990–1993 (1997).
5. Paulson, H.L. *et al.* Intranuclear inclusions of expanded polyglutamine protein in spinocerebellar ataxia type 3. *Neuron* **19**, 333–344 (1997).
6. Chai, Y., Koppenhafer, S., Shoesmith, S., Perez, M. & Paulson, H. Evidence for proteasome involvement in polyglutamine disease: localization to nuclear inclusions in SCA3/MJD and suppression of polyglutamine aggregation *in vitro*. *Hum. Mol. Genet.* **8**, 673–682 (1998).
7. Cummings, C.J. *et al.* Chaperone suppression of aggregation and altered subcellular proteasome localization imply protein misfolding in SCA1. *Nature Genet.* **19**, 148–154 (1998).
8. Stenoien, D. *et al.* Polyglutamine-expanded androgen receptors form aggregates that sequester heat shock proteins, proteasome components and SRC-1, and are suppressed by the HDJ-2 chaperone. *Hum. Mol. Genet.* **8**, 731–741 (1999).
9. Chai, Y., Koppenhafer, S., Bonini, N. & Paulson, H. Analysis of the role of heat shock protein (Hsp) chaperones in polyglutamine disease. *J. Neurosci.* (in press).
10. Warrick, J.M. *et al.* Expanded polyglutamine protein forms nuclear inclusions and causes neural degeneration in Drosophila. *Cell* **93**, 939–949 (1998).
11. Ranum, L. *et al.* Spinocerebellar ataxia type 1 and Machado-Joseph disease: incidence of CAG expansions among adult-onset ataxia patients from 311 families with dominant, recessive, or sporadic ataxia. *Am. J. Hum. Genet.* **57**, 603–603 (1995).
12. Schols, L. *et al.* Trinucleotide expansion within the MJD1 gene presents clinically as spinocerebellar ataxia and occurs most frequently in German SCA patients. *Hum. Mol. Genet.* **4**, 1001–1005 (1995).
13. Durr, A. *et al.* Spinocerebellar ataxia 3 and Machado-Joseph disease: clinical, molecular and neuropathologic features. *Ann. Neurol.* **39**, 490–491 (1996).
14. Ikeda, H. *et al.* Expanded polyglutamine in the Machado-Joseph disease protein induces cell death *in vitro* and *in vivo*. *Nature Genet.* **13**, 196–202 (1996).
15. Brand, A.H. & Perrimon, N. Targeted gene expression as a means of altering cell fates and generating dominant phenotypes. *Development* **118**, 401–415 (1993).
16. Wolff, T. & Ready, D.F. In *The Development of Drosophila melanogaster* (eds Bate, M. & Martinez-Arias, A.) 1277–1325 (Cold Spring Harbor Laboratory Press, Cold Spring Harbor, New York, 1993).
17. Hartl, F. Molecular chaperones in cellular protein folding. *Nature* **381**, 571–580 (1996).
18. Hunt, C. & Morimoto, R. Conserved features of eukaryotic hsp70 genes revealed by comparison with the nucleotide sequence of human hsp70. *Proc. Natl Acad. Sci. USA* **82**, 6455–6459 (1985).
19. Lin, D.M. & Goodman, C.S. Ectopic and increased expression of fasciclin II alters motoneuron growth cone guidance. *Neuron* **13**, 507–523 (1994).
20. Klement, I. *et al.* Ataxin-1 nuclear localization and aggregation: role in polyglutamine-mediated disease in SCA1 transgenic mice. *Cell* **95**, 41–53 (1998).
21. Saudou, F., Finkbeiner, S., Devys, D. & Greenberg, M. Huntingtin acts in the nucleus to induce apoptosis but death does not correlate with the formation of intranuclear inclusions. *Cell* **95**, 55–66 (1998).
22. Elefant, F. & Palter, K. Tissue-specific expression of dominant negative mutant *Drosophila HSC70* causes developmental defects and lethality. *Mol. Biol. Cell* **10**, 2101–2117 (1999).
23. DebBurman, S., Raymond, G., Caughey, B. & Lindquist, S. Chaperone-supervised conversion of prion protein to its protease-resistant form. *Proc. Natl Acad. Sci. USA* **94**, 13938–13943 (1997).
24. Glover, J. & Lindquist, S. Hsp104, Hsp70, and Hsp40: a novel chaperone system that rescues previously aggregated proteins. *Cell* **94**, 73–82 (1998).
25. Jackson, G. *et al.* Polyglutamine-expanded human huntingtin transgenes induce degeneration of *Drosophila* photoreceptor neurons. *Neuron* **21**, 633–642 (1998).
26. Landsbury, P. Jr Structural neurobiology: are seeds at the root of neuronal degeneration? *Neuron* **19**, 1151–1154 (1997).
27. Prusiner, S. Prion diseases and the BSE crisis. *Science* **278**, 245–251 (1997).
28. Selkoe, D. Alzheimer's disease: genotypes, phenotypes, and treatments. *Science* **275**, 630–631 (1997).
29. Polymeropoulos, M. *et al.* Mutation in the α-synuclein gene identified in families with Parkinson's disease. *Science* **276**, 2045–2047 (1997).
30. Rubin, G.M. & Spradling, A.C. Genetic transformation of *Drosophila* with transposable element vectors. *Science* **218**, 348–353 (1982).

Bacterial and yeast chaperones reduce both aggregate formation and cell death in mammalian cell models of Huntington's disease

Jenny Carmichael*, Jean Chatellier†‡, Adrian Woolfson§, César Milstein§, Alan R. Fersht†, and David C. Rubinsztein*¶

*Department of Medical Genetics, Wellcome Trust Centre for Molecular Mechanisms in Disease, Cambridge Institute for Medical Research, Wellcome/Medical Research Council Building, Addenbrooke's Hospital, Hills Road, Cambridge, CB2 2XY, United Kingdom; †Centre for Protein Engineering and Cambridge University Chemical Laboratory, Medical Research Council Centre, Hills Road, Cambridge CB2 2QH, United Kingdom; and §Medical Research Council Laboratory of Molecular Biology, Hills Road, Cambridge CB2 2QH, United Kingdom

Contributed by Alan R. Fersht, June 19, 2000

Huntington's disease (HD) is an autosomal dominant neurodegenerative condition caused by expansions of more than 35 uninterrupted CAG repeats in exon 1 of the huntingtin gene. The CAG repeats in HD and the other seven known diseases caused by CAG codon expansions are translated into long polyglutamine tracts that confer a deleterious gain of function on the mutant proteins. Intraneuronal inclusions comprising aggregates of the relevant mutant proteins are found in the brains of patients with HD and related diseases. It is crucial to determine whether the formation of inclusions is directly pathogenic, because a number of studies have suggested that aggregates may be epiphenomena or even protective. Here, we show that fragments of the bacterial chaperone GroEL and the full-length yeast heat shock protein Hsp104 reduce both aggregate formation and cell death in mammalian cell models of HD, consistent with a causal link between aggregation and pathology.

Huntington's disease (HD) is an autosomal dominant neurodegenerative condition associated with abnormal movements, cognitive deterioration, and psychiatric symptoms. The causative mutation is a (CAG)n trinucleotide-repeat expansion of more than 35 repeats, which is translated into an abnormally long polyglutamine tract in the huntingtin protein (reviewed in refs. 1 and 2).

HD is a member of a family of neurodegenerative diseases caused by CAG/polyglutamine expansions, which include spinobulbar muscular atrophy (SBMA), spinocerebellar ataxias (SCA) types 1, 2, 3, 6, and 7, and dentatorubral–pallidoluysian atrophy (DRPLA). All diseases are dominantly inherited (except for SBMA, which is X-linked). In all cases, age at onset correlates inversely with repeat number (reviewed in ref. 2). The polyglutamine expansion mutation causes disease by conferring a novel deleterious function on the mutant protein, and the severity correlates with increasing CAG repeat number and expression levels in transgenic mice (3) and in cell culture models (4).

Although each of these diseases is associated with specific regions of neurodegeneration (which, in some cases, overlap), they probably are caused by similar pathological processes. A hallmark of many of these diseases, including HD (5), SBMA (6), DRPLA (7), and SCA types 1 (8), 2 (9), 3 (10), 6 (11), and 7 (12), is the development of intracellular protein aggregates (inclusions) in the vulnerable neurons. A pathological role for inclusions is suggested by the correlation of the number of inclusions in the cortex of HD patients with CAG repeat number, which reflects disease severity (13). Inclusion formation precedes neurological dysfunction in some HD transgenic mice (14) and is associated with predisposition to cell death in cell culture models of HD (15–17), DRPLA (18), SBMA (19), SCA3 (10), and SCA6 (11).

The hypothesis that inclusions have a direct pathogenic role in these diseases has been challenged by experiments reporting a dissociation between cell death and inclusion formation in primary cell cultures; inhibition of ubiquitination was associated with decreased aggregate formation but more cell death (20). These findings were not straightforward, because inhibition of ubiquitination also increased apoptosis in cells expressing wild-type (wt) huntingtin constructs and others have suggested that these data still may be compatible with a pathogenic role for huntingtin polymerization (21). Klement and colleagues (22, 23) suggested that inclusions may not be pathogenic, because deletion of the self-association domain from a *SCA1* transgene with expanded repeats prevented the inclusion formation seen in mice expressing full-length mutant *SCA1* transgenes, but both mouse models developed a SCA-like phenotype. Perutz (21) argued that this conclusion was unwarranted, because deletion of these 122 residues would turn the protein into a random coil. Thus, the experiment shows that Purkinje cell expression of denatured, truncated ataxin-1 gives rise to ataxia. One cannot argue that this effect was related to the polyglutamine expansion, because no data were presented for mice expressing wt polyglutamine lengths in ataxin-1 with deletion of the self-association domain. Recently, Cummings *et al.* (24) showed that loss of function of the E6-AP ubiquitin ligase reduced the formation of nuclear inclusions but accelerated polyglutamine-induced pathology in SCA1 mice. Although these data suggest that large, visible inclusions may not be required for cell death, the authors considered other possibilities that are compatible with a pathological role for inclusions. The loss of E6-AP activity may not have had a direct effect on the ubiquitination and clearance of ataxin-1 (24) but may have increased the half-lives of many other cellular proteins, which, at abnormally high steady-state levels, may have enhanced the cellular sensitivity to the SCA1 mutation (or aggregates).

Polyglutamine (polyQ) diseases have been studied extensively by using exon 1 fragments of huntingtin, because large fragments of the HD, SCA3, and DRPLA gene products do not induce inclusion formation or cell death in cell culture models (10, 15,

Abbreviations: HD, Huntington's disease; SBMA, spinobulbar muscular atrophy; SCA, spinocerebellar ataxias; DRPLA, dentatorubral–pallidoluysian atrophy; EGFP, enhanced green fluorescent protein; Hsp, heat shock protein; wt, wild type.

‡Present address: Avidis SA, Biopôle Clermont-Limagne, 63360 Saint Beauzire, France.

¶To whom reprint requests should be addressed. E-mail: dcr1000@cus.cam.ac.uk.

The publication costs of this article were defrayed in part by page charge payment. This article must therefore be hereby marked "*advertisement*" in accordance with 18 U.S.C. §1734 solely to indicate this fact.

Article published online before print: *Proc. Natl. Acad. Sci. USA*, 10.1073/pnas.170280697. Article and publication date are at www.pnas.org/cgi/doi/10.1073/pnas.170280697

16, 19). A small N-terminal polyQ-containing part(s) of huntingtin is found in inclusions *in vivo* (5), but the exact nature and role of this fragment(s) is unclear. Although exon 1 models may not be specific for HD, they are powerful tools for studying inclusion formation in relation to cell death/dysfunction in cultured cells and transgenic mice. We have used cell models of HD comprising an exon 1 fragment with varying CAG repeat lengths tagged at the N terminus with enhanced green fluorescent protein (EGFP) (4, 17). This model, like other published cell models (15, 16, 19), shows many of the features observed *in vivo*: constructs with repeat lengths in the normal size range (23 glutamines) do not aggregate, but constructs with 43 or more glutamines do aggregate and enhance cell death, and these phenotypes correlate with the duration and levels of transgene expression (4, 17). The deleterious effects of polyglutamine mutations have been observed in both neuronal (e.g., PC12) and nonneuronal (e.g., COS-7) cell lines, consistent with the notion that although neuronal cell death and neurological symptoms are the cardinal features of these diseases, the mutations also can affect nonneuronal cells in humans and in mouse models (25–28).

In this study we show that fragments of the bacterial chaperone GroEL and the full-length yeast heat shock protein (Hsp) Hsp104 reduce both aggregate formation and cell death in mammalian cell models of HD, consistent with a direct, causal link between aggregation and cell dysfunction/death. In addition, we show that a monomer comprising GroEL residues 191–345 (29) and an artificial heptamer formed by seven copies of a GroEL minichaperone (residues 191–376) have chaperone activity in mammalian cells. Thus, we resolve another important debate (30, 31) by providing direct evidence that the large, central cavity of GroEL is not essential for its aggregate-reducing activity *in vivo*. Aggregate formation and cell death also were reduced by the K620T mutant of Hsp104, which impairs its oligomerization *in vitro* (32). Thus, efficient oligomerization may not be an essential requirement for all Hsp104 functions, in a fashion analogous to the GroEL 191–345 monomer.

Materials and Methods

Plasmid Construction. MC_7 was constructed by inserting a minichaperone GroEL into GroES in the pRSETA vector (33). The DNA sequence encoding a part of the mobile loop of GroES (residues 16–33) was removed by PCR, as described (34), using the oligonucleotides 5′-TCC GGC TCT GCA GCG G-3′ and 5′-TCC AGA GCC AGT TTC AAC TTC TTT ACG C-3′, creating a unique *Bam*HI site (bold characters) and the vector pRSETA-GroESΔloop. The *groEL* minichaperone gene [corresponding to the apical domain of GroEL, residues 191–376 (29)] was amplified by PCR by using primers containing a *Bam*HI site (underlined) 5′-TTC GGA TCC GAA GGT ATG CAG TTC GAC C-3′ and 5′-GTT GGA TCC AAC GCC GCC TGC CAG TTT C-3′ and cloned into the unique *Bam*HI site of pRSETA-GroESΔloop vector, thus inserting the minichaperone GroEL(191–376) in-frame into the GroESΔloop sequence.

We PCR-amplified the genes encoding MC_7, GroEL wt (full-length *groEL*), Hsp104 wt, and Hsp104 K620T from bacterial expression vectors (pRSETA for the MC_7 and GroEL constructs and pGal for the Hsp104 constructs) and cloned them into the mammalian expression vector pCDNA 3.1/His B (Invitrogen). To allow cloning into the corresponding sites in the pCDNA vector, the primers for the GroEL constructs had *Bsu*36I and *Eco*RI restriction sites (for GroEL wt and MC_7) incorporated in them and the primers for the Hsp104 constructs had *Bam*HI and *Not*I restriction sites incorporated in them. The primers were as follows: GroEL wt *Bsu*36I, 5′-ACGTCCTAAGGATATGGCAGCTAAAGACGTAAAATTC-3′; GroEL wt *Eco*RI, 5′-ACGTGGATTCTTACATCATGCCGCCCATGCCACC-3′; MC_7 *Bsu*36I, 5′-ACGTCCTAAGGATATGAATATTCGTCCATTGCATGAT-3′; MC_7 *Eco*RI, 5′-ACGTGAATTCTTACGCTTCAACAATTGCCAGAAT-3′; Hsp104 *Bam*HI, 5′-ACGTGGATCCAATGAACGACCAAACGCAATTTAC-3′; Hsp104 *Not*I, 5′-ACGTGCGGCCGCTTAATCTAGGTCATCATCAATTTCC-3′.

ApGroEL (corresponding to the apical domain of GroEL residues 191–345) was released from pRSETA (29) with *Eco*RI and *Bam*HI (New England Biolabs) and subcloned into the respective restriction sites in the pCDNA 3.1/His B. All constructs were validated by sequencing.

The HD exon 1 constructs in pEGFP-C1 constructs have been described (4, 17).

Cell Culture and Transfection Experiments. COS-7 and PC12 cells were cultured, transfected, and fixed as described (4, 17). We used a 3:1 or 5:1 molar ratio of pCDNA 3.1/His B constructs to HD exon 1 construct DNA to ensure that all cells expressing HD exon 1 constructs also expressed the appropriate pCDNA 3.1/His B construct. In all such experiments, we used a total of 2 μg of DNA per 3.5-cm dish and kept the amount of the HD exon 1 construct constant in test and control conditions. We analyzed between 300 and 600 EGFP-expressing cells per slide (blinded) in multiple, randomly chosen visual fields. The proportion of HD exon 1-expressing cells with one or more intracellular inclusions was used as a measure of inclusion formation, following Cummings *et al.* (35). Odds ratios and *P* values were determined by unconditional logistical regression analysis, using the general log-linear analysis option of SPSS 9 software (SPSS, Chicago).

For Western blotting, cell lysates were electrophoresed on 15% denaturing gels, and an anti-His_6 mouse mAb (CLONTECH) diluted 1:2,500 was used as the primary antibody. Blots were probed with horseradish peroxidase-labeled anti-mouse antibody (Amersham Pharmacia) and bands were detected with the ECL (enhanced chemiluminescent) detection reagent (Amersham Pharmacia).

Results

Bacterial and Yeast Chaperones Reduce Polyglutamine Aggregation. In this study we have tested the effects of five molecular chaperone constructs on inclusion formation and cell death in cell models of HD. These included wt yeast Hsp104 (Hsp104 wt), which reduces aggregation when overexpressed in yeast models of HD (36). No close mammalian homologues of this protein are known. Hsp104 wt was compared with the K620T mutation (Hsp104 K620T) in the second nucleotide-binding domain (32). This mutation impairs oligomerization *in vitro*, with only a partial reduction in ATPase activity (32). We examined the bacterial chaperonin GroEL (GroEL wt), a large complex comprising 14 identical, ≈57.5-kDa subunits organized in a two-ring structure. We tested whether the large, central cavity of GroEL was essential for its chaperone activity by studying a monomeric minichaperone corresponding to part of its apical polypeptide-binding domain (residues 191–345) (apGroEL) (29). We also investigated the effect of placing seven copies of a GroEL minichaperone (residues 191–376) in a ring, which we called MC_7. This mimics the organization of one of the rings of wt GroEL. MC_7 was made by inserting GroEL residues 191–376 in the place of part of the highly mobile loop (residues 16–33) of the bacterial cochaperonin GroES (J. Chatellier, Fergal Hill, and A.R.F., unpublished results). GroES forms a stable structure of seven ≈10.4-kDa subunits (37). When analyzed by both analytical size-exclusion chromatography and analytical ultracentrifugation, recombinant MC_7 formed heptamers comprising seven 30-kDa subunits, and electron microscopic studies of MC_7 revealed a diameter similar to that of GroEL wt (O. Llorca, J. Chatellier, J.-L. Carrascosa, and A.R.F., unpublished data). The yeast and bacterial chaperone constructs described above were

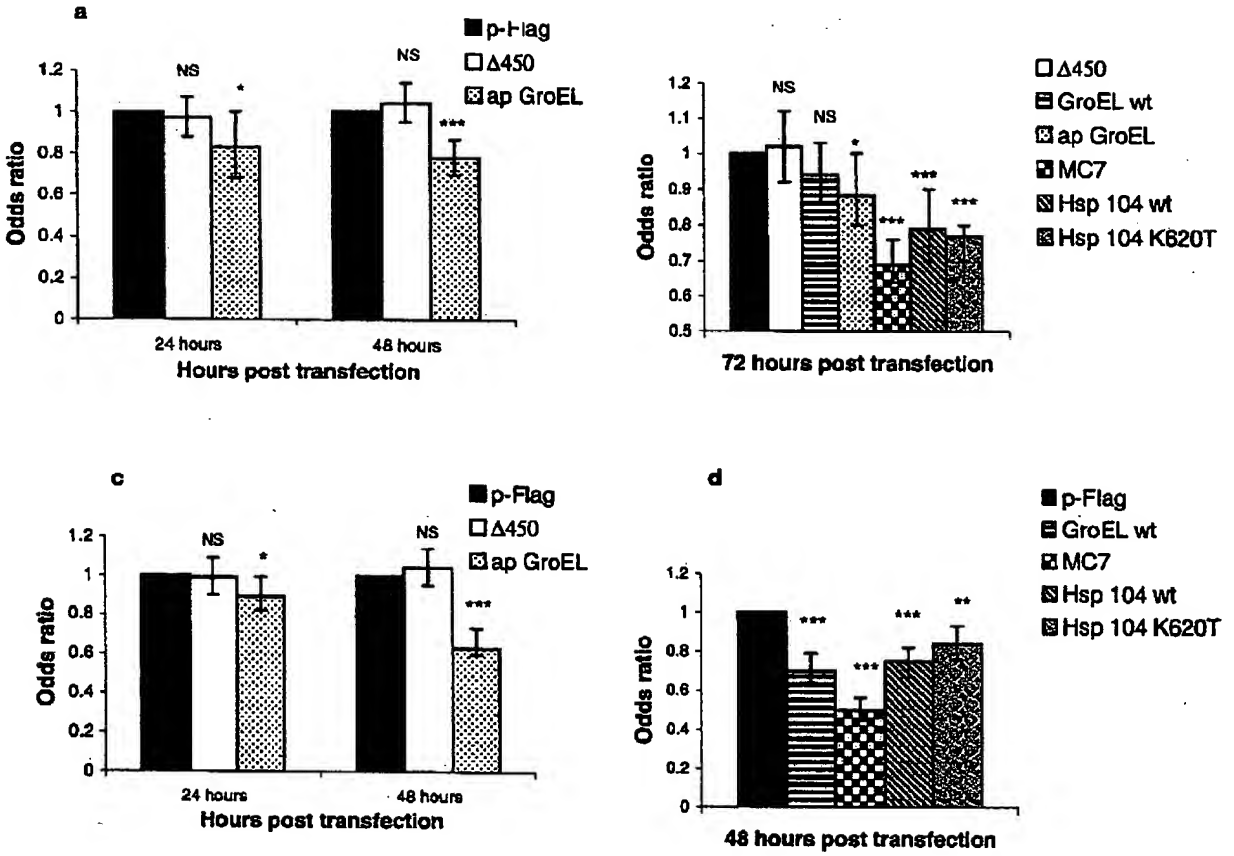

Fig. 1. Suppression of inclusion formation by apGroEL, MC_7, Hsp104 wt, and Hsp104 K620T in COS-7 (*a* and *b*) and PC12 (*c* and *d*) cells. In all experiments, the odds ratios are derived from 2–4 independent experiments, each done in triplicate, where we have compared test constructs with pFLAG. (Error bars = 95% confidence intervals for the odds ratios.) (*a*) COS-7 cells cotransfected with EGFP-HDQ74 and apGroEL and control plasmids. (*b*) COS-7 cells cotransfected with EGFP-HDQ53 and all test and control plasmids. (*c*) PC12 cells cotransfected with EGFP-HD74 and apGroEL and control plasmids. (*d*) PC12 cells cotransfected with EGFP-HD74 and all test and control plasmids (except for apGroEL, which is shown in *c*). *, $P < 0.05$; **, $P < 0.001$; ***, $P < 0.0001$; NS = $P > 0.05$.

expressed from the mammalian expression vector pcDNA 3.1/HisB; proteins of appropriate sizes from lysates of transfected cells were detected by Western blotting by using an anti-His_6 antibody (data not shown).

The functions of GroEL wt, apGroEL, MC_7, Hsp104 wt, and Hsp104 K620T were investigated by cotransfecting each of the test constructs into either COS-7 or PC12 (rat pheochromocytoma) cell lines with constructs expressing EGFP-tagged–exon 1 fragments of huntingtin with 53 or 74 glutamines (EGFP-HDQ53 and EGFP-HDQ74, respectively) (4, 17). The empty pFLAG expression vector and a J domain-deleted form of the human Hsp40 homologue, HDJ2 (called Δ450) (17, 35), were used as controls. A 3:1 or 5:1 molar ratio of chaperone (and control plasmid) to EGFP-HD exon 1 constructs was used to ensure that all EGFP-expressing cells also expressed the chaperone or control plasmid (38). Data from our experiments (each performed in triplicate on two to four occasions) are expressed as odds ratios, which are the proportions of EGFP-expressing cells with inclusions divided by proportions of EGFP-expressing cells without inclusions when cotransfected with the chaperones, divided by the same ratio, when cotransfected with the control plasmids. Odds ratios were considered to be the most appropriate summary statistic, because the percentage of cells with inclusions under specified conditions varied between experiments on different days, whereas the relative change in the proportion of cells with inclusions induced by an experimental perturbation is expected to be more consistent (17, 38).

We tested the effects of these chaperones at various time points (see Fig. 1). In general, we analyzed the EGFP-HDQ74 construct at 48 h, where 40–50% of EGFP-positive cells had inclusions and 40–45% of EGFP-positive cells had fragmented nuclei when cotransfected with pFLAG. EGFP-HDQ53 was analyzed in the greatest detail at 72 h to allow sufficient formation of inclusions (30–40% of EGFP-positive cells had inclusions and 24–33% cells had fragmented nuclei when cotransfected with pFLAG). apGroEL, MC_7, Hsp104 wt, and Hsp104 K620T significantly reduced the proportions of EGFP-positive cells with aggregates in both COS-7 and PC12 lines, compared with the control constructs (Fig. 1). The most pronounced effects were observed with MC_7, where aggregation was reduced by 50% in PC12 cells and by 30% in COS-7 cells. apGroEL consistently and significantly reduced aggregation caused by EGFP-HDQ53 and EGFP-HDQ74, and effects were

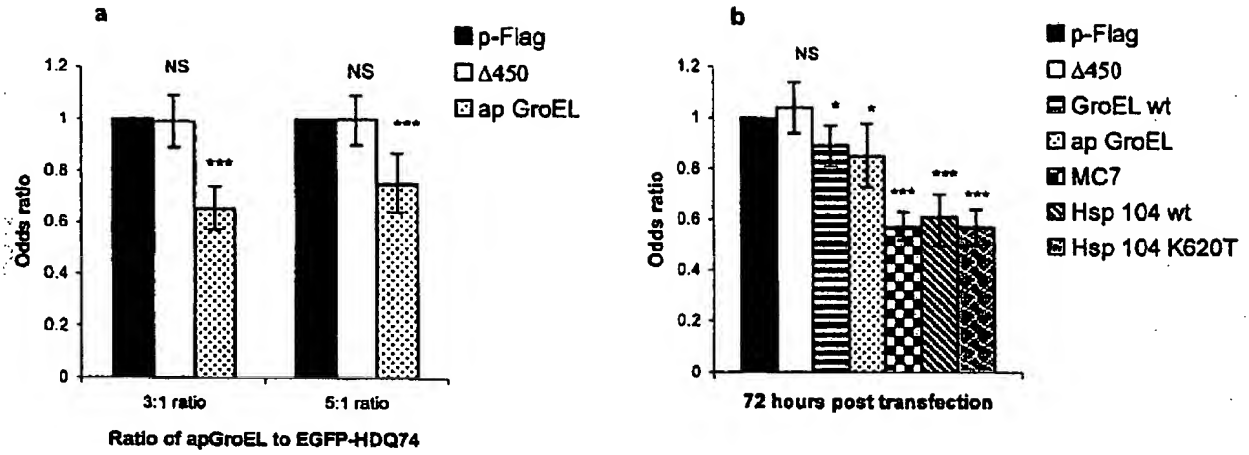

Fig. 2. Reduction of nuclear fragmentation in COS-7 cells after coexpression of EGFP-HDQ74 (*a*) and EGFP-HDQ53 (*b*) with apGroEL, MC_7, Hsp104 wt, and Hsp104 K620T. Cells were analyzed after 48 h (*a*) and 72 h (*b*). In all experiments, the odds ratios are derived from 2–4 independent experiments, each done in triplicate, where we have compared test constructs with pFLAG. (Error bars = 95% confidence intervals for the odds ratios.) *, $P < 0.05$; **, $P < 0.001$; ***, $P < 0.0001$; NS = $P > 0.05$.

seen in both cell lines. GroEL wt significantly reduced inclusions in PC12 cells, but the reduction was not significant in COS-7 cells. Δ450 showed no difference in inclusion formation compared with pFLAG (Fig. 1). We previously have tested a large number of different proteins for their ability to modify aggregation in these cell lines, and virtually all of these have no effect or they enhance aggregation (17, 38). This confirms that the effects we have reported here are specific.

Bacterial and Yeast Chaperones Reduce Cell Death. Nuclear fragmentation can be assessed accurately in polyglutamine disease models in COS-7 cells (17, 39, 40). Because PC12 cells transiently expressing EGFP-HDQ74 appear to have less obvious nuclear fragmentation, it is difficult to quantify this phenotype objectively in this cell line. We scored the proportion of EGFP-positive cells with fragmented nuclei in COS-7 cells to determine whether a reduction in inclusion formation was associated with a reduction in cell death (Fig. 2). GroEL wt, apGroEL, MC_7, and both Hsp104 wt and Hsp104 K620T reduced the proportion of EGFP-positive cells with fragmented vs. normal nuclei compared with the control plasmids. Δ450 did not modify cell death when compared with pFLAG (Fig. 2).

We performed immunocytochemical analyses in COS-7 cells coexpressing GroEL wt, apGroEL, MC_7, or Hsp104 and EGFP-huntingtin mutant exon 1 fragments, because previous studies have shown that some heat shock proteins colocalize with polyglutamine inclusions (17, 35, 41). The chaperones used here did not colocalize with these polyglutamine inclusions (data not shown).

Discussion

Our data strengthen the case for a pathological role for aggregates in polyglutamine diseases, because our panel of bacterial and yeast chaperones reduced both aggregate formation and cell death in cell culture models of HD. We previously have reported that EGFP-HDQ74-expressing COS-7 cells with inclusions showed significantly more nuclear fragmentation at 24, 48, and 72 h posttransfection compared with either EGFP-HDQ23-expressing cells or EGFP-HDQ74-expressing cells without inclusions, which had similar death rates (17). The same association between inclusion formation and cell death was observed when we generated intracellular aggregates with EGFP fused to 19–35 alanines and compared these cells with those expressing native EGFP or EGFP fused to 7 alanines, which did not aggregate (39). Previous studies have shown that the Hsp40 homologue HDJ-1 (41) and the polyglutamine-binding peptide QBP1 (40) reduce both inclusion formation and cell death in tissue culture models. It is possible that HDJ-1 modifies cell death processes via pathways independent of its effects on aggregation formation, because it is a cochaperone of Hsp70, which may be able to directly modulate cell death pathways (42). Nagai *et al.* (40) suggested that QBP1 may exert its effect on cell death by inhibiting interactions of polyglutamine proteins with other molecules and that its aggregate-reducing effect consequently may be an epiphenomenon. These caveats to the link between aggregation and death are extremely unlikely with the panel of chaperones that we tested, because these bacterial and yeast proteins are unlikely to impact directly on mammalian death pathways (independent of aggregation) and apGroEL, MC_7 (J. Chatellier, Fergal Hill, and A.R.F., unpublished results), and Hsp104 all have chaperone activity *in vitro* (29, 32).

It is notable that bacterial and yeast chaperones can function in mammalian cells, and the data from apGroEL and MC_7 inform the important debate relating to whether the large, central cavity of GroEL is essential for all aspects of its activity (30, 31). GroEL wt did not appear to be as efficient as the apGroEL and MC_7 minichaperones, presumably because its activity *in vitro* and *in vivo* is GroES-dependent (29), in contrast to the minichaperones. This report of minichaperones directly reducing aggregation in mammalian cells suggests that the large, central cavity of GroEL is not essential for all of its activities and that the apical fragment can act independently of the microenvironment fostered by the complex structure of native multimeric GroEL, as demonstrated previously in *Escherichia coli* and bacteriophage λ (33). Our findings that Hsp104 can act in mammalian cells complement the observations that this protein reduces polyglutamine aggregation and cell death in a *Caenorhabditis elegans* model that were published while we were writing this paper (43). Aggregate formation and cell death also were reduced by the K620T mutant of Hsp104, which impairs its oligomerization *in vitro* (32). Although transient oligomerization may occur *in vivo*, Hsp104 may not require efficient oligomer-

ization for all of its functions, in a manner analogous to the GroEL(191–345) monomer.

Although our results support a pathological role for inclusions, they are not necessarily incompatible with previous data (20, 22–24), because it is possible that mutant forms of these proteins also may be toxic in the absence of visible aggregation. Because these chaperones reduce cell death, they may provide the basis for therapeutic strategies not only for polyglutamine diseases, but also for more common neurodegenerative conditions associated with protein aggregation, including forms of motor neuron disease, Parkinson's disease, and Alzheimer's disease.

We thank Drs. Chris Cummings, Huda Zoghbi, and Susan Lindquist for the HDJ-2/HSDJ and Hsp104 constructs. We are grateful to Evan Reid, Rainer Duden, Andreas Wyttenbach, and Jina Swartz for helpful discussion. J. Carmichael is an Action Research Training Fellow and is grateful for a Sackler Studentship, and D.C.R. is a Glaxo Wellcome Research Fellow. J. Chatellier was a Marie Curie EU fellow. C.M. and A.W. are grateful for a grant from the National Foundation for Cancer Research (USA), and A.R.F. is grateful for a grant from the Wellcome Trust.

1. The Huntington's Disease Collaborative Research Group (1993) *Cell* **72**, 971–983.
2. Rubinsztein, D. C., Wyttenbach, A. & Rankin, J. (1999) *J. Med. Genet.* **36**, 265–270.
3. Davies, S. W., Turmaine, M., Cozens, B. A., DiFiglia, M., Sharp, A. H., Ross, C. A., Scherzinger, E., Wanker, E. E., Mangiarini, L. & Bates, G. P. (1997) *Cell* **90**, 537–548.
4. Narain, Y., Wyttenbach, A., Rankin, J., Furlong, R. A. & Rubinsztein, D. C. (1999) *J. Med. Genet.* **36**, 739–746.
5. DiFiglia, M., Sapp, E., Chase, K. O., Davies, S. W., Bates, G. P., Vonsattel, J. P. & Aronin, N. (1997) *Science* **277**, 1990–1993.
6. Li, M., Miwa, S., Kobayashi, Y., Merry, D. E., Yamamoto, M., Tanaka, F., Doyu, M., Hashizume, Y., Fischbeck, K. H. & Sobue, G. (1998) *Ann. Neurol.* **44**, 249–254.
7. Igarashi, S., Koide, R., Shimohata, T., Yamada, M., Hayashi, Y., Takano, H., Date, H., Oyake, M., Sato, T., Sato, A., *et al.* (1998) *Nat. Genet.* **18**, 111–117.
8. Skinner, P. J., Koshy, B. T., Cummings, C. J., Klement, I. A., Helin, K., Servadio, A., Zoghbi, H. Y. & Orr, H. T. (1997) *Nature (London)* **389**, 971–974.
9. Koyano, S., Uchihara, T., Fujigasaki, H., Yagishita, S. & Iwabuchi, K. (1999) *Neurosci. Lett.* **273**, 117–120.
10. Paulson, H. L., Perez, M. K., Trottier, Y., Trojanowski, J. Q., Subramony, S. H., Das, S. S., Vig, P., Mandel, J. L., Fischbeck, K. H & Pittman, R. N. (1997) *Neuron* **19**, 333–334.
11. Ishikawa, K., Fujigasaki, H., Saegusa, H., Ohwada, K., Fujita, T., Iwamoto, H., Komatsuzaki, Y., Toru, S., Toriyama, H., Watanabe, M., *et al.* (1999) *Hum. Mol. Genet.* **8**, 1185–1193.
12. Holmberg, M., Duyckaerts, C., Durr, A., Cancel, G., Gourfinkel-An, I., Damier, P., Faucheux, B., Trottier, Y., Hirsch, E. C., Agid, Y. *et al.* (1998) *Hum. Mol. Genet.* **7**, 913–918.
13. Becher, M. W., Kotzuk, J. A., Sharp, A. H., Davies, S. W., Bates, G. P., Price, D. L. & Ross, C. A. (1997) *Neurobiol. Dis.* **4**, 387–397.
14. Davies, S. W., Turmaine, M., Cozens, B. A., DiFiglia, M., Sharp, A. H., Ross, C. A., Scherzinger, E., Wanker, E. E., Mangiarini, L. & Bates, G. P. (1997) *Cell* **90**, 537–548.
15. Martindale, D., Hackam, A., Wieczorek, A., Ellerby, L., Wellington, C., McCutcheon, K., Singaraja, R., Kazemi-Esfarjani, P., Devon, R., Kim, S. U., *et al.* (1998) *Nat. Genet.* **18**, 150–154.
16. Cooper, J. K., Schilling, G., Peters, M. F., Herring, W. J., Sharp, A. H., Kaminsky, Z., Masone, J., Khan, F. A., Delanoy, M., Borchelt, D. R., *et al.* (1998) *Hum. Mol. Genet.* **7**, 783–790.
17. Wyttenbach, A., Carmichael, J., Swartz, J., Furlong, R. A., Narain, Y., Rankin, J. & Rubinsztein, D. C. (2000) *Proc. Natl. Acad. Sci. USA* **97**, 2898–2903.
18. Sato, A., Shimohata, T., Koide, R., Takano, H., Sato, T., Oyake, M., Igarashi, S., Tanaka, K., Inuzuka, T., Nawa, H., *et al.* (1999) *Hum. Mol. Genet.* **8**, 997–1006.
19. Ellerby, L. M., Hackam, A. S., Propp, S. S., Ellerby, H. M., Rabizadeh, S., Cashman, N. R., Trifiro, M. A., Pinsky, L., Wellington, C. L., Salvesen, G. S., *et al.* (1999) *J. Neurochem.* **2**, 185–195.
20. Sadou, F., Finkbeiner, S., Devys, D. & Greenberg, M. E. (1998) *Cell* **95**, 55–66.
21. Perutz, M. F. (1999) *Trends Biochem. Sci.* **24**, 58–63.
22. Klement, I. A., Skinner, P. J., Kaytor, M. D., Yi, H., Hersch, S. M., Clark, H. B., Zoghbi, H. Y. & Orr, H. T. (1998) *Cell* **95**, 41–53.
23. Orr, H. T., Skinner, P. A., Klement, C. J., Cummings, C. J. & Zoghbi, H. J. (1998) *Am. J. Hum. Genet.*, Suppl., A8.
24. Cummings, C. J., Reinstein, E., Sun, Y., Antalffy, B., Jiang, Y., Ciechanover, A., Orr, H. T., Beaudet, A. L.& Zoghbi, H. Y. (1999) *Neuron* **24**, 879–892.
25. Sawa, A., Wiegand, G. W., Cooper, J., Margolis, R. L., Sharp, A. H., Lawler, J. F., Jr., Greenamyre, J. T., Snyder, S. H. & Ross, C. A (1999) *Nat. Med.* **5**, 1194–1198.
26. Sathasivam, K., Hobbs C., Turmaine, M., Mangiarini, L., Mahal, A., Bertaux, F., Wanker, E. E., Doherty, P., Davies, S. W. & Bates, G. P. (1999) *Hum. Mol. Genet.* **8**, 813–822.
27. Arenas, J., Campos, Y., Ribacoba, R., Martin, M. A., Rubio, J. C., Ablanedo, P. & Cabello, A. (1998) *Ann Neurol.* **43**, 397–400.
28. Hurlbert, M. S., Zhou, W., Wasmeier, C., Kaddis, F. G., Hutton, J. C. & Freed, C. R. (1999) *Diabetes* **48**, 649–651.
29. Zahn, R., Buckle, A. M., Perrett, S., Johnson, C. M., Corrales, F. J., Golbik, R. & Fersht, A. R. (1996) *Proc. Natl. Acad. Sci. USA* **93**, 15024–15029.
30. Wang, J. D., Michelitsch, M. D. & Weissman, J. S. (1998) *Proc. Natl. Acad. Sci. USA* **95**, 12163–12168.
31. Weber, F., Keppel, F., Georgopoulos, C., Hayer-Hartl, M. K. & Hartl, F. U. (1998) *Nat. Struct. Biol.* **5**, 977–985.
32. Schirmer, E. C., Queitsch, C., Kowal, A. S., Parsell, D. A. & Lindquist, S. (1998) *J. Biol. Chem.* **273**, 15546–15552.
33. Chatellier, J., Hill, F., Lund, P. A. & Fersht, A. R. (1998) *Proc. Natl. Acad. Sci. USA* **95**, 9861–9866.
34. Hemsley, A., Arnheim, N., Toney, M. D., Cortopassi, G. & Galas, D. J. (1989) *Nucleic Acids Res.* **17**, 6545–6551.
35. Cummings, C. J., Mancini, M. A., Antalffy, B., DeFranco, D. B., Orr, H. T. & Zoghbi, H. Y. (1998) *Nat. Genet.* **19**, 148–154.
36. Krobitsch, S. & Lindquist, S. (2000) *Proc. Natl. Acad. Sci. USA* **97**, 1589–1594.
37. Hunt, J. F., Weaver, A. J., Landry, S. J., Gierasch, L. & Deisenhofer, J (1996) *Nature (London)* **379**, 37–45.
38. Furlong, R. A., Narain, Y., Rankin, J., Wyttenbach, A. & Rubinsztein, D. C. (2000) *Biochem. J.* **346**, 577–581.
39. Rankin, J., Wyttenbach, A. & Rubinsztein, D. C. (2000) *Biochem J.* **348**, 15–19.
40. Nagai, Y., Tucker, T., Ren, H., Kenan, D. J., Henderson, B. S., Keene. J. D., Strittmatter, W. J. & Burke, J. R. (2000) *J. Biol. Chem.* **275**, 10437–10442.
41. Chai, Y., Koppenhafer, S. L., Bonini, N. M. & Paulson, H. L. (1999) *J. Neurosci.* **19**, 10338–10347.
42. Warrick, J. M., Chan, H. Y., Gray-Board, G. L., Chai, Y., Paulson, H. L. & Bonini, N. M. (1999) *Nat. Genet.* **23**, 425–428.
43. Satyal, S. H., Schmidt, E., Kitagawa, K., Sondheimer, N., Lindquist, S., Kramer, J. M. & Morimoto R. I. (2000) *Proc. Natl. Acad. Sci. USA* **97**, 5750–5755.

Human Molecular Genetics, 2000, Vol. 9, No. 13 2009–2018

Polyglutamine length-dependent interaction of Hsp40 and Hsp70 family chaperones with truncated N-terminal huntingtin: their role in suppression of aggregation and cellular toxicity

Nihar Ranjan Jana, Motomasa Tanaka, Guang-hui Wang and Nobuyuki Nukina*

Laboratory for CAG Repeat Diseases, RIKEN Brain Science Institute, 2–1 Hirosawa, Wako-shi, Saitama 351-0198, Japan

Received 18 April 2000; Revised and Accepted 19 June 2000

Huntington's disease (HD) is an autosomal dominant neurodegenerative disorder caused by polyglutamine expansion in the disease protein, huntingtin. In HD patients and transgenic mice, the affected neurons form characteristic ubiquitin-positive nuclear inclusions (NIs). We have established ecdysone-inducible stable mouse Neuro2a cell lines that express truncated N-terminal huntingtin (tNhtt) with different polyglutamine lengths which form both cytoplasmic and nuclear aggregates in a polyglutamine length- and inducer dose-dependent manner. Here we demonstrate that newly synthesized polyglutamine-expanded truncated huntingtin interacts with members of Hsp40 and Hsp70 families of chaperones in a polyglutamine length-dependent manner. Of these interacting chaperones, only Hdj-2 and Hsc70 frequently (Hdj-2 > Hsc70) co-localize with both the aggregates in the cellular model and with the NIs in the brains of HD exon 1 transgenic mice. However, Hdj-2 and Hsc70 do not co-localize with cytoplasmic aggregates in the brains of transgenic mice despite these chaperones being primarily localized in the cytoplasmic compartment. This strongly suggests that the chaperone interaction and their redistribution to the aggregates are two completely different phenomena of the cellular unfolded protein response. This unfolded protein response is also evident from the dramatic induction of Hsp70 on expression of polyglutamine-expanded protein in the cellular model. Transient overexpression of either Hdj-1 or Hsc70 suppresses the aggregate formation; however, suppression efficiency is much higher in Hdj-1 compared with Hsc70. Overexpression of Hdj-1 and Hsc70 is also able to protect cell death caused by polyglutamine-expanded tNhtt and their combination proved to be most effective.

INTRODUCTION

Expansion of CAG triplets within the coding regions of target genes is the cause of several autosomal dominant neurodegenerative diseases including Huntington's disease (HD), several spinocerebellar ataxias (SCAs), dentatorubral pallidoluysian atrophy and X-linked spinal bulbar muscular atrophy (SBMA) (1–3). One of the common characteristic features of all the above diseases is the formation of insoluble aggregates, in particular intranuclear aggregates or nuclear inclusions (NIs) (4–6). The affected neurons in the brains of HD patients show NIs containing N-terminal huntingtin fragments (7–9), and transgenic mice expressing exon 1 of the HD gene containing >115 CAG repeats also have neuronal NIs even before they develop neurological symptoms (10). These findings led us to postulate that such NIs are toxic and responsible for the pathology of HD. In fact, several cellular models of HD also demonstrate that the nuclear aggregates of polyglutamine protein are associated with cell death (11–15). However, two recent studies have raised the possibility that this aggregation may not be the primary factor causing cell death (16,17).

The mechanism that leads the polyglutamine-expanded proteins to aggregate is unknown. One hypothesis is that the glutamine repeats are able to form a polar zipper, an unusual motif for protein–protein interaction (18,19). This polar zipper was predicted to form either between two different molecules with glutamine repeats or within one molecule, forming a hairpin loop. Aggregate formation would then be enhanced by an expanded polyglutamine tract via transglutaminase-catalyzed cross-linking (20) or by aberrant interaction with other proteins dependent on polyglutamine length (21–23). There is also the possibility that the extended polyglutamine tract may destabilize the native conformation of the protein, thereby causing the protein to misfold and aggregate. The fact that the NIs are ubiquitinated raises the possibility that the polyglutamine-expanded proteins become misfolded, with protein degrading machinery such as proteasomes being affected. Indeed recent reports suggest that NIs in SCA1 (24), SCA3 (25,26) and SBMA (27) co-localize with chaperone Hdj-2 and proteasome components. Furthermore, overexpression of the chaperone suppressed the aggregate formation in those studies.

*To whom correspondence should be addressed. Tel: +81 48 467 9702; Fax: +81 48 462 4796; Email: nukina@bmin.riken.go.jp

Correct protein folding is an essential biological process, and for correct folding in the cellular milieu, many proteins interact with molecular chaperones. The heat shock protein 70 (Hsp70) class of molecular chaperones is thought to bind early in the folding process to the extended conformation of a polypeptide chain with a preference for hydrophobic sequences, and to maintain the polypeptide in a soluble conformation (28,29). ATP binding and hydrolysis on Hsp70 are coupled to substrate binding and release by conformational changes in the chaperone that represent cooperation between the substrate binding and ATPase domains of Hsp70 (30,31). To facilitate protein folding, Hsp70 must interact with a co-chaperone protein that regulates its ATPase activity (32–34). A major class of Hsp70 co-chaperone proteins is the Hsp40 family. These chaperones also bind to a misfolded substrate and are capable of initiating refolding and of preventing aggregation without the help of Hsp70 (35). On release from the chaperone, a polypeptide may either fold to its native conformation or enter into the degradation machinery of the cells. Chaperones may also play an active role in directing misfolded or mutant proteins to proteolysis by ubiquitin–proteasome pathways (36,37).

In the present study, we hypothesized that the polyglutamine-expanded huntingtin protein is probably misfolded and that the cellular chaperone system may be affected. Therefore, we investigated the involvement of various chaperones in the pathogenesis of HD using HD exon 1 transgenic mice and an inducible stable mouse Neuro2a cell line that expresses truncated N-terminal huntingtin (tNhtt) containing different polyglutamine lengths. We demonstrate that several chaperones of the Hsp family interact with newly synthesized tNhtt in a polyglutamine length-dependent manner and that some chaperones are also co-localized with the aggregates. We further show that the transient overexpression of some of these chaperones reduces the aggregate formation as well as cellular toxicity caused by expanded polyglutamine tracts.

RESULTS

Interaction of Hsp40 and Hsp70 chaperone families with polyglutamine-expanded tNhtt

We have established stable and inducible mouse Neuro2a cell lines that express tNhtt with enhanced green fluorescent protein (EGFP) containing 16, 60 and 150 glutamine residues. These cell lines are denoted HD 16Q-23, 60Q-14 and 150Q-28 and the expressed proteins are tNhtt-16Q, -60Q and -150Q, respectively. Using this cellular model, we showed that the formation of aggregates and cell death induced by tNhtt were polyglutamine length- and inducer dose-dependent (38). In the present study, we used these cell lines to examine the interaction of various chaperones with normal and polyglutamine-expanded tNhtt. Each cell line was differentiated with N^6,2-*O*-dibutyryl-cAMP (dbcAMP) and induced with ponasterone A for 2 days and then the total cell lysate prepared for immunoprecipitation by anti-green fluorescent protein (anti-GFP). The immunoprecipitates were analyzed by SDS–PAGE and immunoblotting. The blots were first probed with either anti-huntingtin or anti-GFP to confirm the immunoprecipitation of GFP–huntingtin protein with various glutamine repeats (Fig. 1A). Both anti-GFP and anti-huntingtin detected two major bands in HD 150Q-28 cell lysate because of the instability of the longer CAG repeats which was further confirmed by PCR analysis. The blots were then sequentially probed with different chaperone antibodies. Figure 1 shows the polyglutamine length-dependent co-immunoprecipitation of Hdj-1 and Hdj-2 chaperones. Both Hdj-2 (Fig. 1B) and Hdj-1 (Fig. 1C) precipitated well with tNhtt-150Q, very poorly with tNhtt-60Q, but did not precipitate at all with tNHtt-16Q. The interaction of Hdj-1 was further confirmed by transient transfection of the HD 16Q-23, 60Q-14 and 150Q-28 cells with Hdj-1 expression plasmid, immunoprecipitation by anti-GFP antibody and detection by V5-tag antibody (Fig. 1D). Control experiments containing mouse IgG instead of anti-GFP antibody resulted in no precipitation of the chaperones. In the reverse experiments using both anti-Hdj-1 and anti-Hdj-2 antibodies, we also observed co-immunoprecipitation of tNhtt-150Q with Hdj-1 and Hdj-2 (data not shown). In another experiment, differentiated HD 150Q-28 cells were induced for different time periods (from 5 h to 3 days) and the cells collected at each time-point then processed for immunoprecipitation with anti-GFP antibody. A blot of the precipitated proteins was then probed with anti-Hdj-2 antibody. The result

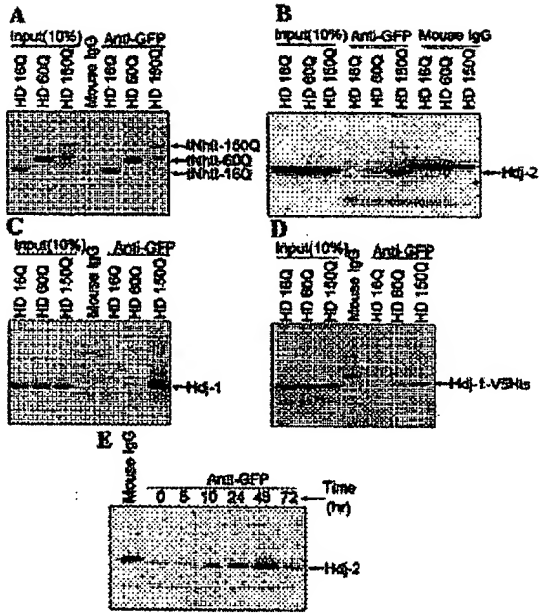

Figure 1. Polyglutamine length-dependent co-immunoprecipitation of Hdj-2 and Hdj-1 chaperones with tNhtt. HD 16Q-23, 60Q-14 and 150Q-28 cell lines were differentiated with 5 mM dbcAMP and induced with 1 μM ponasterone A for 2 days. The total cell lysate was immunoprecipitated with anti-GFP and the immunoprecipitated materials were analyzed by immunoblotting. Blots were sequentially probed with huntingtin (A), Hdj-2 (B) and Hdj-1 (C) antibody. (D) The above-mentioned cell lines were transfected with Hdj-1 expression plasmids and, 24 h after transfection, cells were treated with dbcAMP and ponasterone A for another 24 h and then total cell lysate was processed for immunoprecipitation by anti-GFP. The blot was probed with V5 antibody. (E) Differentiated HD 150Q-28 cells were induced for different time periods and the total cell lysate processed for immunoprecipitation by anti-GFP. Protein on the blot was detected with anti-Hdj-2.

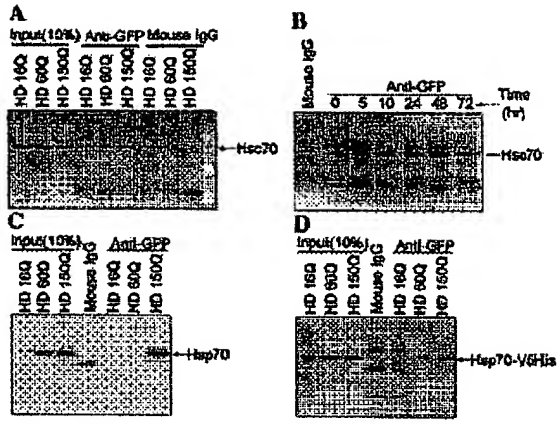

Figure 2. Co-immunoprecipitation of Hsc70 and Hsp70 chaperones with the polyglutamine-expanded tNhtt. (A, B and C) Cells were treated and processed for immunoprecipitation as described in Figure 1B, E and C, respectively. Blots were probed with either anti-Hsc70 (A and B) or anti-Hsp70 (C). (D) HD 150Q-28 cells were transfected with Hsp70 expression plasmids. Total cell lysate was processed for immunoprecipitation and protein was detected with V5 antibody.

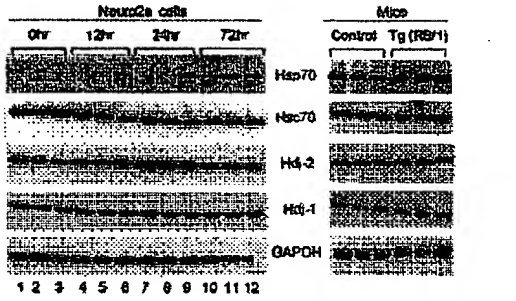

Figure 3. Effect of expanded-polyglutamine protein on expression levels of various chaperones. Differentiated HD 16Q-23, 60Q-14 and 150Q-28 cell lines were induced with 1 μM ponasterone A for different time periods and then the total cell lysate was analyzed by immunoblotting. Equal amounts of protein (20 μg) were loaded in each lane. Lanes 1, 4, 7 and 10, cell lysate expressing tNhtt-16Q; lanes 2, 5, 8 and 11, cell lysate expressing tNhtt-60Q; lanes 3, 6, 9 and 12, cell lysate expressing tNhtt-150Q. Brains from 30- to 36-week-old transgenic mice and age-matched controls were used.

shows that the immunoprecipitated Hdj-2 due to newly synthesized tNhtt-150Q was detected from 10 h onwards and increased steadily up to 2 days (Fig. 1E). The amount of immunoprecipitated Hdj-2 decreased on the third day due to a gradual increase in aggregate formation of the soluble protein.

Figure 2A and C demonstrate similar polyglutamine length-dependent co-immunoprecipitation of Hsc70 and Hsp70 chaperones with tNhtt. Reverse experiments were also carried out to confirm the results (data not shown). Interactions of Hsp70 (Fig. 2D) and Hsc70 (data not shown) were further confirmed by transfecting cells with their respective expression plasmids, immunoprecipitating with anti-GFP antibody and probing a blot with V5 antibody. Figure 2B shows the time dependency of the immunoprecipitatable Hsc70. Several other chaperones, namely Hsp27, Hsp60, Hsp90α and Hsp104, were tested in similar co-immunoprecipitation experiments, but none was immunoprecipitated by anti-GFP antibody.

Expanded polyglutamine protein elicits stress response

Surprisingly, during the immunoprecipitation experiment we observed a very high level of induction of Hsp70 in HD 60Q-14 and 150Q-28 cells. Consequently, we examined the expression levels of various other interacting chaperones in cells induced for different time periods as well as in transgenic mice (R6/1 line) with age-matched controls. In the cellular system, although Hsp70 was normally undetectable, its expression was dramatically up-regulated in a polyglutamine length-dependent manner (Fig. 3). However, the expression levels of various other chaperones, namely Hdj-1, Hdj-2 and Hsc70, did not change. No differences in the expression levels of any of the chaperones were observed between control and transgenic mice (Fig. 3). In both control and transgenic mice, Hsp70 was normally expressed at quite high levels and did not show any further increase in transgenic mice until 30–35 weeks when the mice began to display severe HD symptoms.

Co-localization of Hdj-2 and Hsc70 chaperones with the polyglutamine aggregates in the cellular model

Since the chaperones interacted with the soluble form of polyglutamine-expanded tNhtt, we next examined whether the aggregated form also contained those chaperones. Therefore, we performed immunocytochemical staining of those chaperones. In wild-type Neuro2a cells or HD 16Q-28, 60Q-14 and 150Q-28 cells, endogenous Hdj-2 and Hsc70 were primarily localized in the cytoplasmic compartment with very faint nuclear staining. However, on induction of the mutant protein in HD 60Q-14 or 150Q-28 cells these chaperones redistributed to the aggregates and showed co-localization with GFP aggregates (Fig. 4). The staining pattern of Hsc70 in the aggregates was much weaker and the frequency of the Hsc70 positively stained aggregates were also comparatively lower than Hdj-2. However, we were unable to find any Hdj-1- and Hsp70-positive aggregates in either HD 60Q-14 or 150Q-28 cells, although both interacted with the polyglutamine-expanded protein.

Redistribution of Hdj-2 and Hsc70 chaperones to the NIs in HD exon 1 transgenic mice

We next examined the subcellular localization of various chaperones in the brains of HD exon 1 transgenic mice. On immunostaining of the R6/1 transgenic mice brain sections, we found localization of Hdj-2 and Hsc70 chaperones to the NIs (Fig. 5). In control mice, these chaperones were mainly localized to the cytoplasm. A quantitative estimation of the ubiquitin-, Hdj-2- and Hsc70-positive NIs in the cerebral cortex and striatum area is shown in Figure 2B. Immunofluorescence staining was performed to visualize the respective positively stained fluorescein isothiocyanate (FITC)-labeled NIs, and nuclei were counterstained with propidium iodide. The brains of R6/1 transgenic mice at 10–12 weeks contained

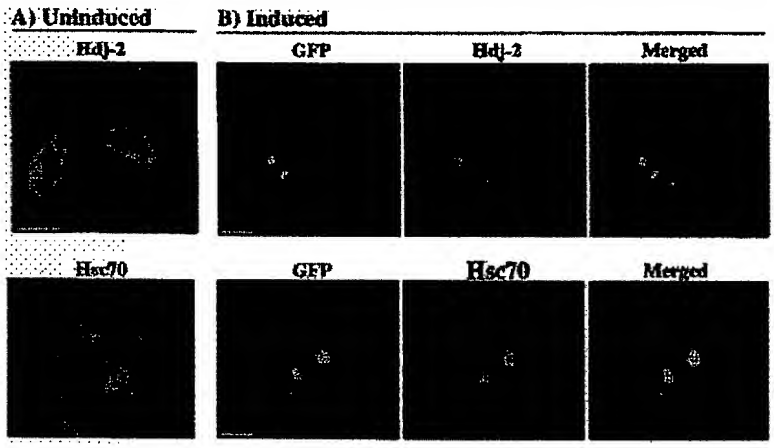

Figure 4. Localization of Hdj-2 and Hsc70 chaperones in the polyglutamine aggregates. Differentiated HD 150Q-28 cells were left untreated (A) or treated with ponasterone A (B) for 2 days and then cells were processed for immunofluorescence staining. Cy3-conjugated (red) secondary antibody was used to label either Hdj-2 or Hsc70. Merging (yellow) of the two signals (red and green) illustrates co-localization. Scale bars: (A) 20 μm; (B, top) 20 μm; (B, bottom) 10 μm.

~17% of ubiquitin-positive NIs, which increased to 72% at 30–35 weeks. However, Hdj-2- and Hsc70-positive NIs were undetectable at 10–12 weeks and detectable to 51 and 25%, respectively, at 30–35 weeks. In 10- to 12-week-old R6/2 mice, the percentage of ubiquitin-, Hdj-2- and Hsc70-positive NIs were relatively higher than in 30- to 35-week-old R6/1 mice. The frequency of Hdj-2- and Hsc70-positive NIs were much lower compared with that of ubiquitin-positive NIs, and the frequency of Hsc70-positive NIs was ~50% lower than that of Hdj-2-positive NIs in both transgenic mice. Hdj-1 and Hsp70 did not localize to the NIs in both transgenic mice. Figure 6 demonstrates immunofluorescence double labeling of the Hdj-2 chaperone and ubiquitin in transgenic mouse brain sections. Anti-ubiquitin positively stained nuclear and many cytoplasmic aggregates. However, anti-Hdj-2 antibody mostly stained the nuclear aggregates. A similar phenomenon was observed in the case of Hsc70. Several other Hsps, i.e. Hsp27, Hsp60, Hsp90α and Hsp105, did not localize to the NIs.

Suppression of polyglutamine protein aggregation by Hdj-1 and Hsc70 chaperones

Next we examined whether the interaction of the chaperone with polyglutamine-expanded tNhtt was trying to keep the polyglutamine protein in a soluble form or whether it was enhancing the process of aggregation. We addressed this problem by overexpressing those chaperones into the HD 150Q-28 cells. Overexpression of Hdj-1 efficiently prevented aggregate formation in HD 150Q-28 cells (Fig. 7A). Hsc70 overexpression (Fig. 7B) also had a significant effect on aggregate suppression; however, Hsp70 (Fig. 7C) had no effect. Co-expression of either Hsc70 or Hsp70 with Hdj-1 did not improve the suppressive effect that was observed with over-expression of Hdj-1 alone. The J-domain deleted form of Hdj-1 or ATPase domain deletion mutant of Hsc70 also had a significant effect on suppression of aggregate formation (Fig. 7A and B). However, overexpression of only the J-domain of Hdj-1 or only the ATPase domain of Hsc70 had no effect. The J-domain deletion mutant of Hdj-1 or ATPase domain deletion mutant of Hsc70 both retain their capacity to bind with the polyglutamine-expanded tNhtt as evidenced from immuno-precipitation (data not shown). A similar suppressive effect of Hdj-1 and Hsc70 on polyglutamine protein aggregation was also observed in HD 60Q-14 cell lines. We further confirmed our result by transiently transfecting those chaperones along with pIND-tNhtt-EGFP-150Q at different ratios into Neuro2a cells stably expressing VgRXR (the functional ecdysone receptor). Twenty-four hours after transfection, cells were induced with ponasterone A (1 μM) and, at 48 h post-transfection, cells were fixed and processed for immuno-fluorescence staining of Hdj-1 and Hsc70 by V5 antibody. As shown in Figure 8, either Hdj-1 or Hsc70 along with poly-glutamine-expanded huntingtin efficiently prevent aggregate formation and counting of the aggregates (Fig. 8D) in the transfected cells revealed a dramatic extent of aggregate suppression.

Hdj-1 and Hsc70 chaperones protect against cell death caused by expanded polyglutamine protein

The ability of the Hdj-1 and Hsc70 chaperones to suppress aggregate formation prompted us to investigate the change in cellular toxicity caused by polyglutamine-expanded tNhtt. We used HD 150Q-28 cells for this investigation. On induction with 1 μM ponasterone A, the differentiated HD 150Q-28 cells showed ~22–36% death on the third and fourth days. Over-expression of Hdj-1 significantly protected against this cell death. Hsc70 also showed a small suppressive effect on cellular toxicity but this was not statistically significant. Co-expression of Hsc70 with Hdj-1 improved the protective effect further in comparison with Hdj-1 alone (Fig. 9A). The expression levels of Hdj-1, Hsc70 and tNhtt-150Q are shown in Figure 9B.

DISCUSSION

Protein aggregation is the most common characteristic feature among the polyglutamine diseases. The mechanism that causes

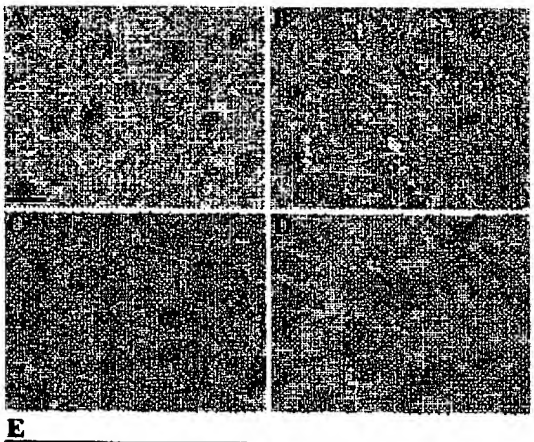

E

Ubiquitin and chaperones	Positively stained NI (%)		
	R6/1 (10-12 weeks)	R6/1 (30-35 weeks)	R6/2 (10-12 weeks)
Ubiquitin	17 ± 6	72 ± 12	86 ±15
Hdj-2	NII	51 ± 8	65 ± 7
Hsc70	NII	25 ± 8	34 ± 6

Figure 5. Co-localization of Hdj-2 and Hsc70 chaperones to the NIs in the brains of HD exon 1 transgenic mice. Brain sections from control and transgenic 30- to 36-week-old mice of were used for immunohistochemical staining. (A) Control mouse brain stained with anti-Hdj-2 antibody. (B) Transgenic mouse (R6/1) brain stained with anti-Hdj-2 antibody. (C) Control mouse brain stained with anti-Hsc70 antibody. (D) Transgenic mouse (R6/1) brain stained with anti-Hsc70 antibody. Scale bars, 50 μm. (E) Quantification of ubiquitin-, Hdj-2- and Hsc70-positive NIs in the R6/1 and R6/2 lines of HD exon 1 transgenic mice. Positively stained NIs were estimated by counting ~500 propidium iodide-stained nuclei in different parts of the cerebral cortex and striatum using three transgenic mice of each age group. Values are means ± SD.

polyglutamine-expanded proteins to aggregate is not fully understood. Here, we demonstrate that several chaperones of the Hsp family interact with polyglutamine-expanded protein in a glutamine repeat length-dependent manner. This suggests that polyglutamine-expanded proteins are misfolded and become prone to aggregation and that the misfolding propensity is directly proportional to the length of the glutamine repeats. Among several chaperones tested, the members of the Hsp40 (Hdj-1 and Hdj-2) and Hsp70 (both constitutive and inducible form) families bind to the polyglutamine-expanded proteins.

Of these four interacting chaperones, Hdj-2 and Hsc70 were frequently co-localized with the aggregates in both the cellular and HD exon 1 transgenic mouse model, indicating that their interaction might be involved in enhancing the process of aggregation. The hypothesis was further supported by the fact that the yeast chaperone Hsp104 has been shown to be necessary for the conversion of prions from soluble to insoluble form through the stabilization of certain folding intermediates. This phenomenon was lost when Hsp104 was overexpressed or removed from the system (39,40). However, in both our cellular and transgenic mouse models, the staining pattern of Hsc70 in the aggregates was very weak and the frequency of positively stained aggregates was also quite low compared with that of Hdj-2. Furthermore, immunofluorescence double labeling between Hdj-2 and ubiquitin in the transgenic mouse brain section revealed that the Hdj-2 associated with only nuclear and not cytoplasmic aggregates. This indicates that Hdj-2 and Hsc70 are most likely not involved in the aggregation process, since these chaperones are mostly cytoplasmic, and if their interaction helps polyglutamine proteins to aggregate we would expect at least some cytoplasmic aggregates to be positively stained for these chaperones.

One possible explanation as to why the chaperones bind to the nuclear aggregates follows. The polyglutamine-expanded proteins escape from the cytoplasmic chaperone barrier, gradually accumulate and form aggregates inside the nucleus. When the aggregates are sufficiently large, a stress response is induced. As a result, the chaperone targets the nuclear aggregates but eventually the attempt is unsuccessful. Alternatively, the chaperones might help the expanded polyglutamine protein to enter the nucleus, where the chaperone-bound polyglutamine protein complex associates with the neighboring molecules and forms aggregates. The nuclear environment possibly favors the aggregation process because the nucleus is less efficient than the cytoplasm in refolding or degrading misfolded proteins (16,41,42). From our observations, it is conceivable that the chaperone interaction with the soluble form of polyglutamine-expanded proteins and their

Figure 6. Immunofluorescence double labeling of ubiquitin and Hdj-2 in the NI. Brain sections from 30- to 36-week-old transgenic mice (R6/1) was used. Brain section was incubated with anti-Hdj-2 (anti-mouse) and anti-ubiquitin (anti-rabbit) antibodies and then labeled with anti-rabbit FITC-conjugated and anti-mouse Cy3-conjugated antibodies. (A) Hdj-2 (red). (B) Ubiquitin (green). (C) Overlay of the two signals (yellow). Scale bar, 50 μm.

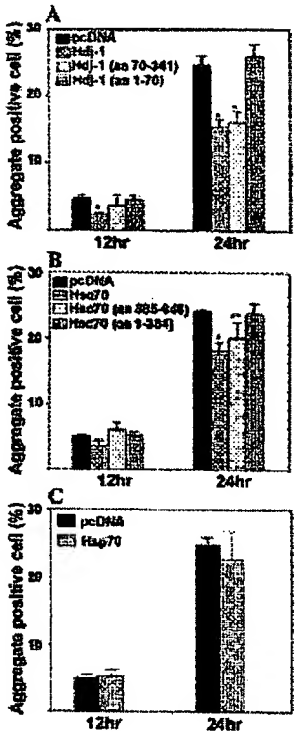

Figure 7. Effect of overexpression of various chaperones on polyglutamine protein aggregation. HD 150Q-28 cells were transfected with empty pcDNA or Hdj-1, Hsc70 or Hsp70 expression vector. After 24 h, cells were re-plated in the chamber slides and, after another 24 h, cells were differentiated (5 mM dbcAMP) and induced (100 nM ponasterone A) simultaneously. Aggregate formation was monitored at 12 and 24 h post-induction. (A) Effect of overexpression of full-length or various deletion mutants of Hdj-1. (B) Effect of overexpression of full-length and various deletion mutants of Hsc70. (C) Effect of overexpression of Hsp70. Values are means ± SEM; $n = 4$. $^*P < 0.001$; $^*P < 0.01$, compared with respective empty pcDNA-transfected experiment with respect to time.

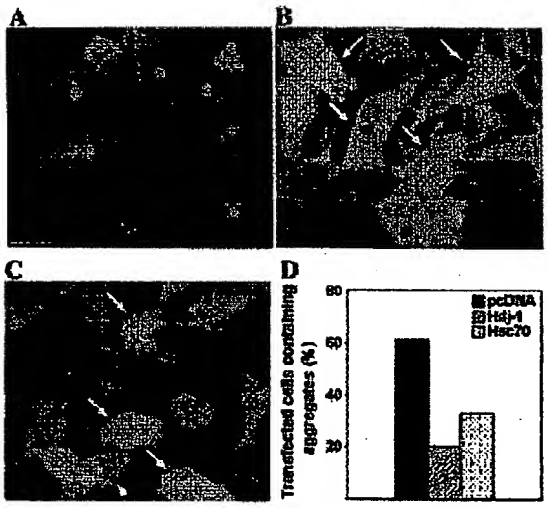

Figure 8. Immunofluorescence demonstration of the prevention of polyglutamine protein aggregation in cells overexpressing either Hdj-1 or Hsc70 chaperones. Neuro2a cells stably expressing VgRXR were transfected with either Hdj-1 or Hsc70 (2 μg each) along with pIND-tNhtt-EGFP-150Q (0.5 μg) and, 24 h after transfection, cells were induced with 1 μM ponasterone A. Twenty-four hours post-induction, cells were processed for immunofluorescence staining of Hdj-1 and Hsc70. Cy3-conjugated secondary antibody was used to label the Hdj-1 and Hsc70. (A) Cells transfected with pIND-tNhtt-EGFP-150Q and an empty pcDNA vector. (B) Cells transfected with Hdj-1 and pIND-tNhtt-EGFP-150Q. Arrows indicate cells expressing both Hdj-1 and tNhtt-150Q. (C) Cells transfected with Hsc70 and pIND-tNhtt-EGFP-150Q. Arrows indicate cells expressing both Hsc70 and tNhtt-150Q. The arrowhead indicates the cell containing aggregates. (D) Quantification of the number of aggregates in the cells that overexpressed Hdj-1 and Hsc70 chaperones. Scale bar, 20 μm.

recruitment to the polyglutamine aggregates are two completely different phenomena of the cellular unfolded protein response.

The co-localization of Hdj-2 chaperone to the NIs has been demonstrated in SCA1 (24), SCA3 (26) and SBMA (27) and in all the disease models examined overexpression of Hdj-2 chaperone suppresses aggregate formation. Co-localization of Hdj-1 and Hsp70 with the NIs and suppression of aggregate formation by Hdj-1 has also been demonstrated in SCA3 (26). In the cellular model of HD used in the present study, we found suppression of aggregate formation by Hdj-1 and Hsc70. This strongly suggests that the common target of Hsp40 and Hsp70 family members are any polyglutamine-expanded protein and that Hsp40 and Hsp70 are effective in the suppression of polyglutamine-mediated protein aggregation. However, the suppression efficiency differs among the members of these two families of chaperones. Our results suggest that Hsp40 family members are much more effective in aggregation suppression compared with members of the Hsp70 family. Whether these differences also exist among the members of the same family has yet to be determined.

The Hsp40 family chaperones are known to be co-chaperones for the Hsp70 family and modulate the cellular protein folding by binding to misfolded polypeptides via the C-terminal domain and regulating the ATPase activity of the Hsp70 family members through the N-terminal J-domain (33,34). However, there are reports that the members of the Hsp40 family are also capable of refolding the misfolded substrates and preventing aggregation without the help of Hsp70 family members (35,43). The fact that the J-domain deletion mutant of Hdj-1 still suppresses the aggregate formation strongly suggests that the Hsp40 family chaperones can work alone and also possibly in cooperation with the Hsp70 family to suppress aggregation. How those chaperones are involved in the folding process of unfolded polyglutamine-expanded protein is not clear. Possibly, at higher concentrations, the chaperone-bound folding intermediate efficiently prevents the intra- and intermolecular polar zipper formation and keeps the polyglutamine protein in a soluble form while enhancing their degradation by ubiquitin–proteasome pathways at the same time. The Hsp40 and Hsp70 families of chaperones have been shown to play a critical role in the rapid

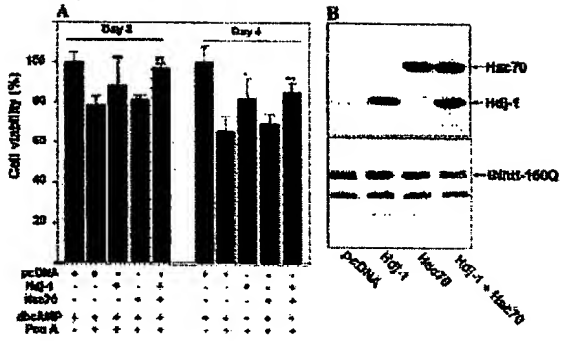

Figure 9. Reduction of polyglutamine-mediated cellular toxicity on overexpression of Hdj-1 and Hsc70 chaperones. HD 150Q-28 cells were transfected with empty vector (pcDNA) or plasmids encoding Hdj-1 or Hsc70. After 24 h, cells were re-plated to the 96-well plates, differentiated (5 mM dbcAMP) and induced (1 μM ponasterone A) simultaneously. Cell viability was measured by MTT assay and monitored at the third and fourth days of induction. Values are the means ± SEM; $n = 12$. $^*P < 0.01$; $^{**}P < 0.001$, compared with pcDNA-transfected and ponasterone A-treated experiment. (B) Expression levels of various transfected chaperones and tNhtt-150Q detected at 48 h post-transfection. Twenty-four hours after transfection, cells were differentiated and induced as indicated above. Chaperones on the blot were detected by ECL with 30 s exposure and tNhtt-150Q was detected with 1 min exposure.

degradation of misfolded proteins by the ubiquitin–proteasome pathway (36,37).

Another interesting observation in the present study was the polyglutamine length-dependent induction of Hsp70 in the cellular model, despite being unable to detect any major changes in Hsp70 levels in the HD exon 1 transgenic mice (R6/1) until 30–35 weeks, when they showed severe HD symptoms. The induction of Hsp70 has also been reported in the cellular model of SCA3 but not in their transgenic model (26). Many stressful conditions induce Hsp70, which increases the cell's tolerance to stress. Induction of Hsp70 by polyglutamine-expanded protein suggests that the cell is under stress and trying to compensate. However, the factors generating this stress are currently unknown. One possibility is that the utilization and redistribution of chaperones as well as proteasomes (unpublished data) to the aggregates creates a deficit in their normal active cellular pool, which in turn increases the accumulation of misfolded proteins and ultimately creates stress. Our hypothesis is supported by the observation that inhibition of proteasome function leads to the induction of various chaperones (44). Moreover, the cellular deficit of chaperones and proteasomes might ultimately result in disease progression by disturbing vital cellular function.

In the present study, we found that overexpression of the Hsp40 family chaperones significantly reduces the cellular toxicity created by polyglutamine-expanded tNhtt. This protective effect was further improved by overexpressing Hsp40 with Hsc70. Recently, overexpression of the Hsp40 chaperone has also been reported to suppress the cell death due to mutant SCA3 protein (26). Moreover, an *in vivo* study in a *Drosophila* SCA3 disease model demonstrated that overexpression of Hsp70 suppresses polyglutamine-induced neurodegeneration and delays the progression of the disease without a visible effect on NI formation (45). In the cellular model of SCA3, Hsp70 overexpression does not have a suppressive effect on aggregate formation (26). In the cellular model for HD, we were unable to detect any significant suppression of aggregate formation or cellular toxicity on Hsp70 overexpression. One possible explanation is that in cellular models, endogenous Hsp70 is highly induced by polyglutamine-expanded protein and therefore further overexpression does not make a further difference. However, the specificity of Hsp70 protection against polyglutamine protein-mediated cell death remains to be explained, since Hsp70 itself is anti-apoptotic and can rescue the cell from stress-induced apoptosis (46,47).

The challenge is to determine whether the Hsp40 and Hsp70 family chaperones really suppress the aggregation and protect the neurodegeneration in the *in vivo* HD transgenic mouse model. If so, and if there are no adverse effects of overexpression, then these chaperones may prove to be effective therapeutic molecules by which to slow the progression of HD and also other polyglutamine diseases.

MATERIALS AND METHODS

Mice

Heterozygous HD exon 1 transgenic male mice of R6/1 (115 CAG repeats) and R6/2 (145 CAG repeats) lines were obtained from the Jackson Laboratory (Bar Harbor, ME) (Jackson codes: B6CBA-TgN [Hdexon1]61 and B6CBA-TgN[Hdexon1]62) and maintained by crossing carrier males with CBA females. The genotyping and CAG repeat sizing was carried out using a PCR assay and Genescan, respectively, as described previously (48). Mice (transgenic and their age-matched controls) were sacrificed using ether anesthesia, and their brains carefully removed and collected in Tissue-Tek (Sakura Finetek, Tokyo, Japan), frozen with powdered solid CO_2 and stored at –80°C.

Antibodies

Antibodies utilized in this study were purchased from the following sources. The rabbit polyclonal anti-Hdj-1 (SPA-400) and mouse monoclonal anti-Hsp70 (SPA-810) were purchased from StressGen Biotechnologies (Victoria, British Columbia). Mouse monoclonal anti-Hdj-2 (MS-225) was from Neomarkers (Union City, CA). Goat polyclonal anti-Hsc70 (sc-1059), goat polyclonal anti-Hsp60 (sc-1052), rabbit polyclonal anti-Hsp105 (sc-1805), goat polyclonal anti-Hsp90α and goat polyclonal anti-Hsp27 (sc1798) were from Santa Cruz Biotechnology (Santa Cruz, CA). Mouse monoclonal anti-GAPDH (MAB374) was from Chemicon International (Tenecula, CA). Rabbit polyclonal anti-huntingtin (corresponding to N-terminal amino acid sequences) was raised in our laboratory. Goat anti-rabbit IgG–Cy3, goat anti-mouse IgG–Cy3 and donkey anti-goat IgG–Cy3 (Molecular Probes, Eugene, OR) were utilized as secondary antibodies in indirect immunofluorescence. Horseradish peroxidase (HRP)-conjugated anti-mouse IgG and anti-rabbit IgG (Amersham Life Science, Little Chalfont, UK) and anti-goat IgG (Santa Cruz Biotechnology) were utilized as secondary antibodies in immunoblotting.

Expression plasmids

The tNhtt expression constructs pIND-tNhtt-EGFP-16Q, pIND-tNhtt-EGFP-60Q and pIND-tNhtt-EGFP-150Q have been described previously (39). Each construct contains 1–90 amino acids of tNhtt with a different polyglutamine length fused to the N-terminus of EGFP. The Hsp70 and Hsp40 expression vectors in pcDNA3.1/GS were obtained from Invitrogen (Carlsbad, CA). The full-length Hsc70 cDNA was isolated from human brain total RNA by using RT–PCR. Primer sequences were 5′-GTGGCTTCCTTCGTTATTGG-3′ (sense) and 5′-TTAATCAACCTCTTCAATGGTGGG-3′ (antisense). Proof reading polymerase (TaKaRa, Kyoto, Japan) was used in the PCR reaction. PCR fragments were A-tailed and ligated into pGEM-T Easy Vector (Promega, Madison, WI) and confirmed by sequencing. The full-length, ATPase domain (amino acids 1–384) and the ATPase domain deletion (amino acids 385–646) mutant of Hsc70 expression vector in pcDNA6/V5-His were prepared using PCR and subcloning the product in frame into the *Kpn*I–*Xho*I site of the vector. The primer sequences were: 5′-ACGGGGTACCATGGCCAAGGGACCTGCAC-3′ (sense, for full-length and ATPase domain mutant); 5′-ACGGGGTACCATGGTGTCTGGAGACAAGTC-3′ (sense, for ATPase domain deletion mutant); 5′-ACCGCTCGAGCGGATCAACCTCTTCAATGG-3′ (antisense for full-length and ATPase domain deletion mutant); and 5′-ACCGCTCGAGGGCTGCCTGGACAGCTGCACCATAAGC-3′ (antisense for ATPase domain mutant). The J-domain mutant (amino acids 1–70) or J-domains deletion (amino acids 70–341) mutant of Hdj-1 was also constructed from full-length Hdj-1 by subcloning the PCR product into the *Bam*HI–*Xho*I site of the pcDNA6/V5-His plasmid. Primer sequences were: 5′-ACGCGGATCCACCATGGGTAAAGACTACTACCA-3′ (sense for J-domain mutant); 5′-ACCGCTCGAGTTCCTCCCCGTAGCGGTCGA-3′ (antisense for J-domain mutant); 5′-ACGCGGATCCACCATGGGCCTAAAGGGGAGTGGCC-3′ (sense for J-domain deletion mutant); and 5′-ACCGCTCGAGATATATTGGAAGAACCTGCT-3′ (antisense for J-domain deletion mutant). Underlined sequences represent the sites for restriction enzymes.

Cell culture and treatments

Mouse Neuro2a cells stably expressing tNhtt-EGFP-16Q, tNhtt-EGFP-60Q and tNhtt-EGFP-150Q were regularly maintained in Dulbecco's modified Eagle's medium (Life Technologies, Gaithersburg, MD) supplemented with 10% fetal bovine serum, 0.4 mg/ml zeocin and 0.4 mg/ml G418. Establishment of stable cell lines has been described earlier (39). Cells were differentiated by treating 5 mM dbcAMP (N^6,2′-*O*-dibutyryladenosine-3′:5′-cyclic monophosphate sodium salt (Nacalai Tesque, Kyoto, Japan) and induced with different concentrations (0.1–2 μM) of ponasterone A (Invitrogen).

Co-immunoprecipitation experiments

Cells were washed with cold phosphate-buffered saline (PBS), scraped, pelleted by centrifugation and lysed on ice for 30 min with RIPA buffer (10 mM HEPES pH 7.4, 150 mM NaCl, 10 mM EDTA, 2.5 mM EGTA, 1% Triton X-100, 0.1% SDS, 1% sodium deoxycholate, 10 mM NaF, 5 mM $Na_4P_2O_7$, 0.1 mM Na_3VO_4, 1 mM PMSF, 0.1 mg/ml Aprotinin). Cell lysate was briefly sonicated, centrifuged for 10 min at 15 000 *g* at 4°C and the supernatants (total soluble extract) were used for immunoprecipitation. Protein concentration was measured according to the method of Bradford using Bio-Rad protein assay reagent (Bio-Rad, Hercules, CA) and bovine serum albumin as a standard. For each immunoprecipitation experiment, 200 μg of protein in 0.2 ml of RIPA buffer was incubated either with 5 μl (2 μg) of anti-GFP antibody or 4 μl (2 μg) of normal mouse IgG. After 5–6 h of incubation at 4°C with rotation, 10 μl of magnetic protein G beads (Perspective Biosystems, Framingham, MA) were added and incubation was continued at 4°C overnight. The beads were pulled down with a magnet (Dynal, Oslo, Norway) and washed six times with RIPA buffer. Bound proteins were eluted from the beads with SDS (1×) sample buffer, vortexed, boiled for 5 min and analyzed by immunoblotting.

Immunoblotting

The total cell lysate, mouse brain total soluble extracts (homogenate after centrifugation at 15 000 *g* for 10 min) or the immunoprecipitated proteins were separated through SDS–polyacrylamide gel (7.5–20%) electrophoresis and transferred onto PVDF membrane (Immobilon-P; Millipore, Bedford, MA). The membranes were successively incubated in blocking buffer [5% skim milk in TBST (50 mM Tris pH 7.5, 0.15 M NaCl, 0.05% Tween)], with primary antibody in TBST, and then with secondary antibody conjugated with HRP in TBST. Detection was carried out with enhanced chemiluminescence (ECL) reagent (Amersham Life Science).

Immunofluorescence techniques

Cells grown in chamber slides were differentiated and induced together for 2 days. Cells were washed twice with PBS, fixed with 4% paraformaldehyde in PBS for 20 min, permeabilized with 0.5% Triton X-100 in PBS for 5 min, washed extensively and then blocked with 5% non-fat dried milk in TBST for 1 h. Primary antibody incubation was carried out overnight at 4°C. After several washings with TBST, cells were incubated with appropriate secondary antibody for 1 h, washed several times and mounted in antifade solution (Vectashield Mounting Media; Vector, Burlingame, CA). The primary antibodies, anti-Hdj-2 and anti-Hdj-1, were used at 1:1000 dilution and anti-Hsc70, anti-Hsp70, anti-Hsp60, anti-Hsp105 and anti-Hsp90α were used at 1:250 dilution. Secondary antibodies conjugated with Cy3 were used at 1:1000 dilution. Samples were observed using a confocal microscope (Fluoview; Olympus, Tokyo, Japan) and digital images were assembled using Adobe Photoshop. For immunofluorescence staining of various chaperones and ubiquitin in the transgenic mouse brain sections, the sections were fixed and incubated with different primary antibody in a similar manner to that described for the immunohistochemistry. The appropriate FITC- or Cy3-conjugated secondary antibody was used to visualize the expression and localization. In some experiments, nuclei were counterstained with propidium iodide.

Immunohistochemistry

The frozen brains mounted on Tissue-Tek were sectioned in freezing microtome to 20 μm thickness. Sections were fixed with 4% paraformaldehyde in PBS for 20 min, washed several

times, blocked with 5% non-fat dried milk for 1 h and then incubated overnight with primary antibody. Staining was carried out using ABC Elite kit (Vector). Briefly, after primary antibody incubation, sections were washed and incubated for 1 h at room temperature with the appropriate biotinylated secondary antibody, washed, incubated with ABC reagent, washed, exposed for several minutes to DAB substrate, washed, dehydrated, cleared and mounted. Dilutions of the different primary antibodies used were the same as described for immunofluorescence.

Transfections, quantitation of aggregate formation and cell viability

Transfection of various chaperones (2 μg/well each) was carried out in 60 mm tissue cultured plates using Lipofectamine 2000 (Life Technologies) according to the manufacturer's instructions. Twenty-four hours after transfection, cells were collected, counted by Trypan blue and re-plated into the chamber slides (for counting aggregation) or 96-well tissue cultured plates (for cell viability assay). Forty-eight hours post-transfection, cells were treated with dbcAMP and ponasterone A. For counting aggregation, 1×10^3 cells were seeded into each well of the chamber slides and, for cell viability assay, 5×10^3 cells were seeded into each well of 96-well plates. Both aggregate formation and cell viability were monitored at different time-points. Aggregate formation was manually counted under a fluorescence microscope and the cells containing more than one aggregate were considered to have a single aggregate. Cell viability was determined using the 3-(4,5-dimethylthiazol-2-yl)-2,5-diphenyl tetrazolium bromide (MTT) assay described previously (39). Statistical analysis was performed using paired *t*-test, with $P < 0.05$ considered statistically significant.

In other experiments, we transiently transfected 0.5 μg of pIND-tNhtt-EGFP-150Q along with different concentrations of various chaperones (0.5–2 μg) into mouse Neuro2a cells stably transfected with pVgRXR which express a functional ecdysone receptor. Twenty-four hours after transfection, cells were differentiated with 5 mM dbcAMP and induced with 1 μM of ponasterone A. At 24 h post-transfection, cells were processed for immunofluorescence staining of Hdj-1 and Hsc70 using V5 antibody. The appropriate Cy3-conjugated secondary antibody was used to visualize the transfected cells. The number of aggregates was counted using ~100 transfected cells for quantitative estimation.

ACKNOWLEDGEMENT

This work was supported partly by a grant from the Ministry of Health and Welfare.

REFERENCES

1. Ross, C.A. (1995) When more is less: pathogenesis of glutamine repeats neurodegenerative diseases. *Neuron*, **15**, 493–496.
2. Paulson, H.L. and Fischbeck, K.H. (1996) Trinucleotide repeats in neurogenetic disorders. *Ann. Rev. Neurosci.*, **19**, 79–107.
3. Reddy, P.S. and Housman, D.E. (1997) The complex pathology of trinucleotide repeats. *Curr. Opin. Cell. Biol.*, **9**, 364–372.
4. Ross, C.A. (1997) Intranuclear neuronal inclusions: a common pathogenic mechanism of glutamine-repeat neurodegenerative diseases? *Neuron*, **19**, 1147–1150.
5. Kim, T.W. and Tanzi, R.E. (1998) Neuronal intranuclear inclusions in polyglutamine diseases: nuclear weapons or nuclear fallout? *Neuron*, **21**, 657–659.
6. Paulson, H.L. (1999) Protein fate in neurodegenerative proteinopathies: polyglutamine diseases join the misfold. *Am. J. Hum. Genet.*, **64**, 339–345.
7. DiFiglia, M., Sapp, E., Chase, K.O., Davies, S.W., Bates, G.P., Vonsattel, J.P. and Aronin, N. (1997) Aggregation of huntingtin in neuronal intranuclear inclusions and dystrophic neurites in brain. *Science*, **277**, 1990–1993.
8. Becher, M.W., Kotzuk, J.A., Sharp, A.H., Davies, S.W., Bates, G.P., Price, D.L. and Ross, C.A. (1998) Intranuclear neuronal inclusions in Huntington's disease and dentatorubral and pallidoluysian atrophy: correlation between the density of inclusions and IT15 CAG triplet repeat length. *Neurobiol. Dis.*, **4**, 387–397.
9. Gutekunst, C.A., Li, S.H., Yi, H., Mulroy, J.S., Kuemmerle, S., Jones, R., Rye, D., Ferrante, R.J., Hersch, S.M. and Li, X.J. (1999) Nuclear and neuropil aggregates in Huntington's disease: relationship to neuropathology. *J. Neurosci.*, **19**, 2522–2534.
10. Davies, S.W., Turmaine, M., Cozens, B.A., DiFiglia, M., Sharp, A.H., Ross, C.A., Scherzinger, E., Wanker, E.E., Mangiarini, L. and Bates, G.P. (1997) Formation of neuronal intranuclear inclusions underlines the neurological disfunction in mice transgenic for HD mutation. *Cell*, **90**, 537–548.
11. Cooper, J.K., Schilling, G., Peters, M.F., Herring, W.J., Sharp, A.H., Kaminsky, Z., Masone, J., Khan, F.A., Delanoy, M., Borchelt, D.R. *et al.* (1998) Truncated N-terminal fragments of huntingtin with expanded glutamine repeats form nuclear and cytoplasmic aggregates in cell culture. *Hum. Mol. Genet.*, **7**, 783–790.
12. Martindale, D., Hackam, A., Wieczorek, A., Ellerby, L., Wellington, C., McCutcheon, K., Singaraja, R., Kazemi-Esfarjani, P., Devon, R., Kim, S.U. *et al.* (1998) Length of huntingtin and its polyglutamine tract influences localization and frequency of intranuclear aggregates. *Nature Genet.*, **18**, 150–154.
13. Hackam, A.S., Singaraja, R., Zhang, T., Gan, L. and Hayden, M.R. (1999) *In vitro* evidence for both the nucleus and cytoplasm as subcellular sites of pathogenesis in Huntington's disease. *Hum. Mol. Genet.*, **8**, 25–33.
14. Moulder, K.L., Onodera, O., Burke, J.R., Strittmatter, W.J. and Johnson Jr, E.M. (1999) Generation of neuronal intranuclear inclusions by polyglutamine-GFP: analysis of inclusion clearance and toxicity as a function of polyglutamine length. *J. Neurosci.*, **19**, 705–715.
15. Li, S.-H., Cheng, A.L., Li, H. and Li, X.-J. (1999) Cellular defects and altered gene expression in PC12 cells stably expressing mutant huntingtin. *J. Neurosci.*, **19**, 5159–5172.
16. Klement, I.A., Skinner, P.J., Kaytor, M.D., Yi, H., Hersch, S.M., Clark, H.B., Zoghbi, H.Y. and Orr, H.T. (1998) Ataxin-1 nuclear localization and aggregation: role in polyglutamine-induced disease in *SCA1* transgenic mice. *Cell*, **95**, 41–53.
17. Saudou, F., Finkbeiner, S., Devys, D. and Greenberg, M.E. (1998) Huntingtin acts in the nucleus to induce apoptosis but death does not correlate with the formation of intranuclear inclusions. *Cell*, **95**, 55–66.
18. Perutz, M.F., Johnson, T., Suzuki, M. and Finch, J.T. (1994) Glutamine repeats as polar zippers: their possible role in inherited neurodegenerative diseases. *Proc. Natl Acad. Sci USA*, **91**, 5355–5358.
19. Stott, K., Blackburn, J.M., Butler, P.J.G. and Perutz, M. (1995) Incorporation of glutamine repeats makes protein oligomerize: implications for neurodegenerative diseases. *Proc. Natl Acad. Sci. USA*, **92**, 6509–6513.
20. Kahlem, P., Terre, C., Green, H. and Djian, P. (1996) Peptides containing glutamine repeats as substrates for transglutaminase-catalyzed cross-linking: relevance to diseases of the nervous system. *Proc. Natl Acad. Sci. USA*, **93**,14580–14585.
21. Sittler, A., Walter, S., Wedemeyer, N., Hasenbank, R., Scherzinger, E., Eickhoff, H., Bates, G.P., Lehrach, H. and Wanker, E.E. (1998) SH3GL3 associates with the huntingtin exon-1 protein and promotes the formation of polygln-containing protein aggregates. *Mol. Cell.*, **2**, 427–436.
22. Li, X.-J., Li, S.-H., Sharp, A.H., Nucifora, F.C., Schilling, G., Lanahan, A., Worley, P., Snyder, S.H. and Ross, C.A (1995) A huntingtin associated protein enriched in brain with implications for pathology. *Nature*, **378**, 398–402.
23. Faber, P.W., Barnes, G.T., Srinidhi, J., Chen, J., Gusella, J.F. and MacDonald, M.E. (1998) Huntingtin interacts with a family of WW domain proteins. *Hum. Mol. Genet.*, **7**, 1463–1474.
24. Cummings, C.J., Mancini, M.A., Antalffy, B., DeFranco, D.B., Orr, H.T. and Zoghbi, H.Y. (1998) Chaperone suppression of aggregation and

altered subcellular proteasome localization imply protein misfolding in *SCA1*. *Nature Genet.*, **19**, 148–154.
25. Chai, Y., Koppenhafer, S.L., Shoesmith, S.J., Perez, M.K. and Paulson, H.L. (1999) Evidence for proteasome involvement in polyglutamine disease: localization to nuclear inclusions in SCA3/MJD and supression of polyglutamine aggregation *in vitro*. *Hum. Mol. Genet.*, **8**, 673–682.
26. Chai, Y., Koppenhafer, S.L., Bonini, N.M. and Paulson, H.L. (1999) Analysis of the role of heat shock protein (hsp) molecular chaperones in polyglutamine disease. *J. Neurosci.*, **19**, 10338–10347.
27. Stenoien, D.L., Cummings, C.J., Adams, H.P., Mancini, M.G., Patel, K., DeMartino, G.N., Marcelli, M., Weigel, N.L. and Mancini M.A. (1999) Polyglutamine-expanded androgen receptors form aggregates that sequester heat shock proteins, proteasome components and SRC-1, and are suppressed by the HDJ-2 chaperone. *Hum. Mol. Genet.*, **8**, 731–741.
28. Landry, S.J., Jordan, R., McMacken, R. and Gierasch, L.M. (1992) Different conformations for the same polypeptide bound to chaperones DnaK and GroEL. *Nature*, **355**, 455–457.
29. Blond-Elguindi, S., Cwirla, S.E., Dower, W.J., Lipshutz, R.J., Sprang, S.R., Sambrook, J.F. and Gething, M.J. (1993) Affinity panning of a library of peptides displayed on bacteriophages reveals the binding specificity of BiP. *Cell*, **75**, 717–728.
30. Kamath-Loeb, A.S., Lu, C.Z., Suh, W.C., Lonetto, M.A. and Gross, C.A. (1995) Analysis of three DnaK mutant proteins suggests that progression through the ATPase cycle requires conformational changes. *J. Biol. Chem.*, **270**, 30051–30059.
31. Pang, K.L., Hilgenberg, L., Wang, N.M. and Chirico, W.J. (1996) Conformations of the nucleotide and polypeptide binding domains of a cytosolic Hsp70 molecular chaperone are coupled. *J. Biol. Chem.*, **271**, 21559–21565.
32. Cyr, D.M. (1997) The Hsp40 (DnaJ related) family of proteins. In Gething, M.J. (ed.), *Guidebook to Molecular Chaperones and Protein Folding Factors*. Oxford University Press, Oxford, UK, pp. 89–95.
33. Hartl, F.U. (1996) Molecular chaperones in cellular protein folding. *Nature*, **381**, 571–580.
34. Hendricks, J.P. and Hartl, F.U. (1993) Molecular chaperone functions of heat shock proteins. *Annu. Rev. Biochem.*, **62**, 349–384.
35. Lu, Z. and Cyr, D.M. (1998) The conserved carboxyl terminus and zinc finger-like domain of the co-chaperone Ydj1 assist Hsp70 in protein folding. *J. Biol. Chem.*, **273**, 5970–5978.
36. Lee, D.H., Sherman, M.Y. and Goldberg, A.L. (1996) Involvement of molecular chaperone Ydj1 in the ubiquitin-dependent degradation of short-lived and abnormal proteins in *Saccharomyces cerevisiae*. *Mol. Cell. Biol.*, **16**, 4773–4781.
37. Bercovich, B., Stancovsky, I., Mayer, A., Blumenfeld, N., Laszlo, A., Schwartz, A.L. and Ciechanover, A. (1997) Ubiquitin-dependent degradation of certain protein substrates *in vitro* requires the molecular chaperone Hsc70. *J. Biol. Chem.*, **272**, 9002–9010.
38. Wang, G.H., Mitsui, K., Kotliarova, S., Yamashita, A., Nagao, Y., Tokuhiro, S., Iwatsubo, T., Kanazawa, I. and Nukina, N. (1999) Caspase activation during apoptotic cell death induced by expanded polyglutamine in N2a cells. *Neuroreport*, **10**, 2435–2438.
39. Chernoff, Y.O., Lindquist, S.L., Ono, B., Inge-Vechtomov, S.G. and Liebman, S.W. (1995) Role of the chaperone protein Hsp104 in propagation of the yeast prion-like factor [psi+]. *Science*, **268**, 880–884.
40. DebBurman, S.K., Raymond, G.J., Caughey, B. and Lindsquit, S.L. (1997) Chaperone-supervised conversion of prion protein to its protease-resistant form. *Proc. Natl Acad. Sci.*, **94**, 13938–13943.
41. Perez, M.K., Paulson, H.L., Pendse, S.J., Saionz, S.J., Bonini, N.M. and Pittman, R.N. (1998). Recruitment and the role of nuclear localization in polyglutamine-mediated aggregation. *J. Cell Biol.*, **143**, 1457–1470.
42. Michels, A.A., Kanon, B., Konings, A.W.T., Ohtsuka, K., Bensaude, O. and Kampinga, H.H. (1997) Hsp70 and Hsp40 chaperone activities in the cytoplasm and the nucleus of mammalian cells. *J. Biol. Chem.*, **272**, 33283–33289.
43. Meacham, G.C., Lu, Z., King, S., Sorscher, E., Tousson, A. and Cyr, D.M. (1999) The Hdj-2/Hsc70 chaperone pair facilitates early step in CFTR biogenesis. *EMBO J.*, **18**, 1492–1505.
44. Bush, K.T., Goldberg, A.L. and Nigam, S.K. (1997) Proteasome inhibition leads to a heat-shock response, induction of endoplasmic reticulum chaperones and thermotolerance. *J. Biol. Chem.*, **272**, 9086–9092.
45. Warrick, J.M., Chan, H.Y.E., Gray-Board, G.L., Chai, Y., Paulson, H.L. and Bonini, N.M. (1999) Suppression of polyglutamine-mediated neurodegeneration in *Drosophila* by the molecular chaperone Hsp70. *Nature Genet.*, **23**, 425–428.
46. Jaattela, M., Wissing, D., Kokholm, K., Kallunki, T. and Egeblad, M. (1998) Hsp70 exerts its anti-apoptotic function downstream of caspase-3-like proteases. *EMBO J.*, **17**, 6124–6134.
47. Mosser, D.D., Caron, A.W., Bourget, L., Denis-Larose, C. and Massie, B. (1997) Role of the human heat shock protein hsp70 in protection against stress-induced apoptosis. *Mol. Cell. Biol.*, **17**, 5317–5327.
48. Mangiarini, L., Sathasivam, K., Seller, M., Cozens, B., Harper, A., Hetherington, C., Lawton, M., Trottier, Y., Lehrach, H., Davies, S.W. and Bates, G.P. (1996) Exon-1 of the HD gene with an expanded CAG repeat is sufficient to cause a progressive neurological phenotype in transgenic mice. *Cell*, **87**, 493–506.

EXHIBIT J

THE JOURNAL OF BIOLOGICAL CHEMISTRY
Vol. 275, No. 12, Issue of March 24, pp. 8772–8778, 2000

Printed in U.S.A.

Chaperones Hsp70 and Hsp40 Suppress Aggregate Formation and Apoptosis in Cultured Neuronal Cells Expressing Truncated Androgen Receptor Protein with Expanded Polyglutamine Tract*

(Received for publication, November 15, 1999)

Yasushi Kobayashi‡, Akito Kume‡, Mei Li‡, Manabu Doyu‡, Mami Hata§, Kenzo Ohtsuka§, and Gen Sobue‡¶

From the ‡Department of Neurology, Nagoya University School of Medicine, 65 Tsurumai-cho, Showa-ku, Nagoya 466-8550, Japan and the §Laboratory of Experimental Radiology, Aichi Cancer Center Research Institute, Chikusa-ku, Nagoya 464-8681, Japan

Spinal and bulbar muscular atrophy (SBMA) is one of a group of human inherited neurodegenerative diseases caused by polyglutamine expansion. We have previously demonstrated that the SBMA gene product, the androgen receptor protein, is toxic and aggregates when truncated. Heat shock proteins function as molecular chaperones, which recognize and renaturate misfolded protein (aggregate). We thus assessed the effect of a variety of chaperones in a cultured neuronal cell model of SBMA. Overexpression of chaperones reduces aggregate formation and suppresses apoptosis in a cultured neuronal cell model of SBMA to differing degrees depending on the chaperones and their combinations. Combination of Hsp70 and Hsp40 was the most effective among the chaperones in reducing aggregate formation and providing cellular protection, reflecting that Hsp70 and Hsp40 act together in chaperoning mutant and disabled proteins. Although Hdj2/Hsdj chaperone has been previously reported to suppress expanded polyglutamine tract-formed aggregate, Hsdj/Hdj2 showed little effect in our system. These findings indicate that chaperones may be one of the key factors in the developing of CAG repeat disease and suggested that increasing expression level or enhancing the function of chaperones will provide an avenue for the treatment of CAG repeat disease.

Spinal and bulbar muscular atrophy (SBMA)[1] is an X-linked neurodegenerative disease caused by the expansion of a CAG repeat in the first exon of the androgen receptor (AR) gene (1). In SBMA patients, a normally polymorphic CAG repeat (10–36 CAGs) expands to 38–66 CAGs. The number of CAGs is inversely correlated with the age of onset of the disease (2–4). To date, seven other CAG repeat diseases have been identified, including Huntington's disease (5), dentatorubralpallidoluysian atrophy (6, 7), and five spinocerebellar ataxias: 1, 2, 3, 6, and 7) (8–14). These disorders likely share a common pathogenesis involving the gain of a toxic function associated with the expanded polyglutamine tract.

Processing of the polyglutamine-containing disease protein by proteases (*e.g.* caspase family) may liberate truncated fragments with the polyglutamine tract (15–18). Truncated proteins with the expanded polyglutamine tracts cause neurodegeneration in transgenic mice as well as *Drosophila* and cause cell death in transfected cells (19–24). In addition to cellular toxicity, truncated proteins with the expanded polyglutamine tracts have been shown to form aggregates, likely through hydrogen bonding or transglutaminase activity (25–27). Studies of CAG repeat disease patients and transgenic mice have revealed that nuclear inclusions formed by the disease protein are a common pathological feature of these diseases (23, 28–31, 33, 34). In SBMA, nuclear inclusions containing AR protein have been mainly observed in the regions of SBMA central nervous system susceptible to degeneration, including the brain stem motor nuclei and spinal motor neurons (33, 34). The finding that nuclear inclusions are ubiquitinated raises the possibility that alterations in the major intracellular system for degrading proteins, the ubiquitin-proteasome pathway, may be involved in the pathogenesis of CAG repeat diseases. The proteasome is a large multicatalytic protease complex that is critical for many cellular processes including cell cycle control, differentiation, antigen presentation, and cell survival (35). Perturbations in proteasome function are associated with altered expression levels of stress response or heat shock proteins (36). These proteins function as molecular chaperones, which recognize and renaturate misfolded proteins under normal and stressed conditions. In addition, chaperones may maintain proteins in an appropriate conformation (37). Recently, overexpression of Hdj-2/Hsdj has been reported to decrease aggregate formation by expanded polyglutamine tract (38, 39). It has been postulated that the Hsp70 and the Hsp40 chaperone family members act together to promote cellular protein folding and renaturate misfolded protein (40–42). We hypothesized that the ability of Hsp70 and Hsp40 chaperones to facilitate refolding or proteolysis of mutant protein may be a key factor for neuronal cells to defend themselves against the toxic properties of expanded polyglutamine tract. The studies reported here demonstrate that overexpression of chaperones, especially a combination of Hsp70 and Hsp40, reduces aggregate formation and apoptosis in cultured neuronal cells expressing truncated androgen receptor protein with an expanded polyglutamine tract.

* This work was supported by grants from the Ministry of Health and Welfare of Japan, by a Center of Excellence grant from the Ministry of Education, Sciences, Sports and Culture of Japan, and by a grant from the Naitou foundation. The costs of publication of this article were defrayed in part by the payment of page charges. This article must therefore be hereby marked "*advertisement*" in accordance with 18 U.S.C. Section 1734 solely to indicate this fact.

¶ To whom correspondence should be addressed: Dept. of Neurology, Nagoya University School of Medicine, 65 Tsurumai-cho, Showa-ku, Nagoya 466-8550, Japan. Tel.: 81-52-744-2385; Fax: 81-52-744-2384; E-mail: sobueg@med.nagoya-u.ac.jp.

[1] The abbreviations used are: SBMA, spinal and bulbar muscular atrophy; AR, androgen receptor; Ab, antibody; R.S.I., relative signal intensity; TUNEL, terminal deoxytransferase-mediated dUTP nick end labeling.

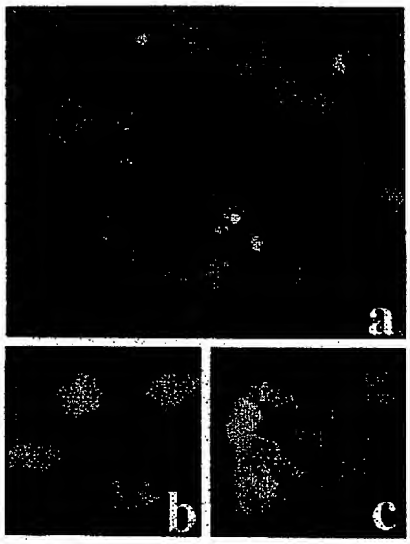

FIG. 1. **Subcellular localization of expanded and truncated AR in Neuro2a cells.** Transient expression of expanded and truncated AR (0.4 μg of DNA/well) in Neuro2a cell (20,000 cells/well) was accomplished by transfection with Effectene (Qiagen) in a 4-chamber slide. Overlay of the two images taken by laser confocal microscopy at 48 h after transfection. *a* and *c*, cells transfected with expanded and truncated AR-GFP (tAR97-GFP) contain tAR97-GFP aggregates. Some aggregates localized to nuclear (*yellow*), and others localized to cytoplasm (*green*). *b*, cells transfected with truncated AR-GFP (tAR24-GFP) show GFP signal localized to cytoplasm (*green*) (counter-stained with propidium iodide).

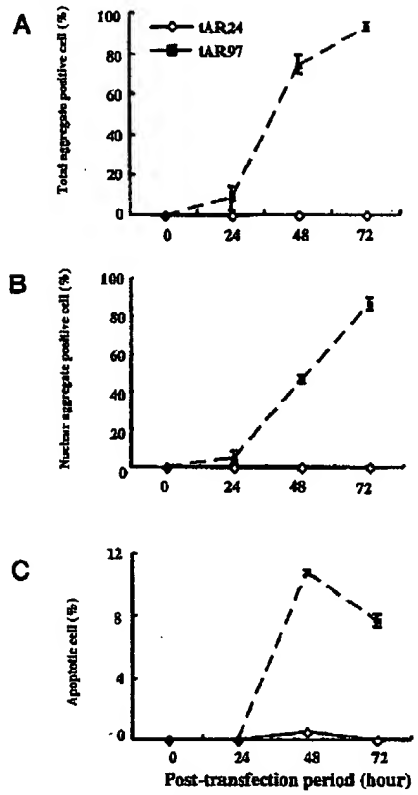

FIG. 2. **Frequency of cells with aggregate, nuclear aggregate, or apoptosis in transfecting Neuro2a cells with tAR-GFP constructs.** *A*, total aggregate-positive cells that contain aggregates cytoplasm and/or nucleus. *B*, nuclear aggregate-positive cells that contain nuclear aggregate with/without cytoplasmic aggregates. *C*, apoptotic cells that are TUNEL-positive. Values are the means ± S.E.

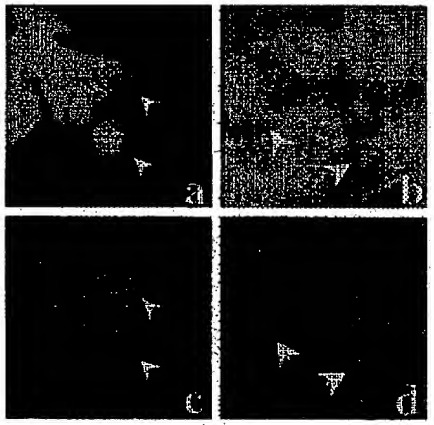

FIG. 3. **Nuclear aggregate containing cells are preferentially positive in TUNEL assay.** TUNEL assay was performed at 48 h after transfection of tAR97-GFP construct. *a* and *c*, *arrowheads* indicate nuclear aggregate containing cells (*a*), which were also positive in TUNEL assay (*c*). *b* and *d*, *arrows* point to cytoplasmic aggregate containing cells (*b*), which were negative in TUNEL assay (*d*) (counter-stained with Hoechst33258).

EXPERIMENTAL PROCEDURES

Plasmid Constructs

Truncated AR—Human AR cDNAs containing 24 or 97 CAG repeats (18) were subcloned into pcDNA3.1 (Invitrogen, Carlsbad, CA). After the constructs were digested with *Afl*II and blunt-ended, the polymerase chain reaction-amplified coding sequence of GFP (0.8 kilobase) was inserted into the digested constructs to create truncated AR constructs (24 CAG repeats, 215 N-terminal amino acids; 97 CAG repeats, 442 N-terminal amino acids of AR).

Chaperones—Construction of pCMV-Hsp70 was described as previously (41). For the construction of pRC-Hsp40, a 1.5-kilobase *Eco*RI fragment containing the entire coding region of human Hsp40 (43) was excised from the cDNA clone and subcloned in pRC/CMV (Invitrogen). For the construction of pRC-Hsdj, the polymerase chain reaction-amplified coding sequence of Hsdj (1.1 kilobase) (44) was subcloned in pRC/CMV. All the constructs used here were confirmed by DNA sequence analysis.

Antibodies

Anti-Hsp70 Ab (rabbit polyclonal IgG) (45) and anti-Hsp40 Ab (rabbit polyclonal IgG) (46) were previously described. To raise an antibody against human Hsdj (anti-Hsdj Ab), a 50 N-terminal amino acid-deleted Hsdj recombinant protein was used for immunization in rabbit and affinity-purified.[2] Anti-hemagglutinin Ab (Santa Cruz Biotechnology, Santa Cruz, CA), anti-rabbit IgG conjugated with Cy-3 (Amersham Pharmacia Biotech), and anti-rabbit IgG conjugated with horseradish peroxidase (Amersham Pharmacia Biotech) were employed.

Immunofluorescence

Transient expression of truncated AR and/or chaperones in Neuro2a cell line (mouse neuroblastoma cell) was accomplished by transfection with Effectene (Qiagen) in a four-chamber slide (Nalge Nunc International, Naperville, IL) coated with rat tail collagen (Roche Diagnostics GmbH, Mannheim, Germany) in Dulbecco's modified Eagle's medium (Life Technologies, Inc.) supplemented with 10% fetal calf serum. After overnight incubation with transfection reagents, transfected cells were cultured in differentiation medium (Dulbecco's modified Eagle's medium supplemented with 2% fetal calf serum and 20 μM retinoic acid). At each time point (0, 24, 48, and 72 h) after transfection, cells were fixed with methanol for 5 min at room temperature, followed by counter staining with propidium iodide (Molecular Probes, Eugene, OR) and mounted in Gelvatol.

[2] K. Ohtsuka and M. Hata, manuscript in preparation.

Hsp70, Hsp40 or Hsdj were detected with anti-Hsp70 Ab (1:100), anti-Hsp40 Ab (1:100), or anti-Hsdj Ab (1:10), respectively, incubated at 4 °C for overnight, and subsequently stained with anti-rabbit IgG conjugated with Cy-3. Counter stain was done with Hoechst33258 (Molecular Probes) or TOTO-3 (Molecular Probes).

Quantitative Analysis of TUNEL Assay and Truncated AR Aggregate Formation

The cells were assayed for the presence of fragmented DNA by TUNEL assay using a DeadEnd™ Apoptosis Detection Kit (Promega, Madison, WI) according to the manufacturer's protocol with minor modification. Briefly, cells were fixed with 4% paraformaldehyde at each time point (0, 24, 48, and 72 h) after transfection. Fixed cells were incubated with terminal deoxynucleotidyl transferase to be incorporated with biotinylated deoxynucleotides, subsequently stained with Streptavidin-Texas Red conjugate (Life Technologies, Inc.) and Hoechst33258. A laser confocal scan microscope (MRC1024, Bio-Rad) and a conventional fluorescent microscope were used for quantitative analysis. Duplicate slides were graded blindly in two independent trials. Each slide had over 200 transfected cells. Cells were categorized by localization of aggregates: total aggregate-positive, which are cells containing aggregates in cytoplasm and/or nucleus, and nuclear aggregate-positive, which are cells containing aggregates in nucleus. The frequency was calculated as the number of indicated signal-positive cells divided by that of GFP-positive cells.

Western Blots

48 h after transfection, cells were lysed in RIPA buffer (50 mM Tris, 150 mM NaCl, 1% Nonidet P-40, 0.1% sodium dodecyl sulfate, 10 μg/ml aprotinin). Insoluble debris was pelleted, and the protein concentration of the supernatant was determined using a DC protein assay (Bio-Rad). A 20-μg sample was electrophoresed on a standard sodium dodecyl sulfate-polyacrylamide gel and transferred to Hybond-P (Amersham Pharmacia Biotech). Blots were probed with the indicated antibodies using standard techniques and developed with enhanced chemiluminescence reagents (Amersham Pharmacia Biotech). The signal intensity was quantified by densitometry. Relative signal intensity (R.S.I.) was computed as the signal intensity of indicated lanes divided by that of nontransfected cells.

Proliferation Assay

Neuro2a cells (500,000 cells/60-mm culture dish) were cotransfected with truncated ARs (tAR24 or tAR97) and chaperones as described above. Cells were plated at a density of 5,000/well in 96-well dish just after transfection. Transfected cells were cultured in 100 μl/well of differentiation medium. 20 μl/well of CellTiter 96® Aqueous One Solution (Promega) was added at each time point (0, 24, 48, and 72 h) after transfection. After 4 h of incubation at 37 °C, the absorbance at 490 nm was recorded using an enzyme-linked immunosorbent assay plate reader. The background absorbance of medium alone was subtracted from these data. The proliferation index was calculated as the mean absorbance of cells at the indicated time point divided by the mean absorbance of cells just after transfection.

In Vitro Aggregation Assay

GST-tAR65-HA was purified as described previously (24). Construction of His-tagged human Hsp40 was as described (40) and expressed in *Escherichia coli* strain BL21. Cells were grown at 37 °C to around 0.8 at A_{600} and induced for 2 h with 1 mM isopropyl-β-D-thiogalactopyanoside. His-Hsp40 was purified with TALON kit (CLONTECH, Palo Alto, CA) according to a manufacture's protocol. A bacterial expression plasmid, pTE-Hsc70, which contains human heat shock cognate 70 (Hsc70) cDNA, was a kind gift of Dr. N. Imamoto (Osaka University, Osaka, Japan). Hsc-70 was purified as described previously (47).

5 pmol of GST-tAR65-HA was incubated with 100 pM of recombinant Hsc70 and/or Hsp40 in reaction buffer (100 mM Tris-HCl, pH 7.5, 100 mM NaCl, 10 mM dithiothreitol, 5 mM ATP, and 5 mM $MgCl_2$). The mixture was incubated at 37 °C for 30 min, terminated with equal amount of 2× SDS Laemmli loading buffer and subjected to Western blot as described above. The signal intensity was quantified by densi-

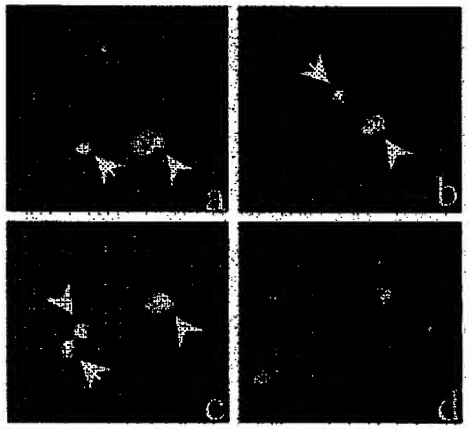

FIG. 4. **Colocalization of endogenous chaperones with polyglutamine-formed aggregates.** Overlay of the three images taken by laser confocal microscopy at 48 h after transfection. *Arrows* point to nuclear aggregates, and *arrowheads* indicate cytoplasmic aggregates. Hsp70 (*a*), Hsp40 (*b*), and Hsdj/Hdj2 (*c*) colocalized to nuclear aggregates (*white*) and cytoplasmic aggregates (*yellow*), respectively. In addition, endogenous chaperones (*red*) preferentially existed in cytoplasm. *d*, control sample stained with second antibody alone did not show any nonspecific signals (counter-stained with TOTO-3).

FIG. 5. **Suppression of polyglutamine-formed aggregation in cells overexpressing chaperones.** Transient expression of expanded and truncated AR (0.2 μg of DNA/well) and chaperones or empty vector (0.2 μg of DNA/well) in Neuro2a cell (20,000 cells/well) was accomplished by transfection with Effectene (Qiagen) in a four-chamber slide. Overlay of the two images taken by laser confocal microscopy at 48 h after transfection. Cells were cotransfected with tAR97-GFP and empty vector (*a*), cotransfected with tAR97-GFP and Hsp70 (*b*), cotransfected with tAR97-GFP and Hsp40 (*c*), cotransfected with tAR97-GFP and Hsdj/Hdj2 (*d*), cotransfected with tAR97-GFP and Hsp70/Hsp40 (*e*), or cotransfected with tAR97-GFP and Hsp70/Hsdj (*f*). Cells cotransfected with tAR97-GFP and Hsp70/Hsp40 or Hsp70 demonstrated diffuse distribution pattern of tAR97-GFP rather than aggregated pattern (counter-stained with propidium iodide).

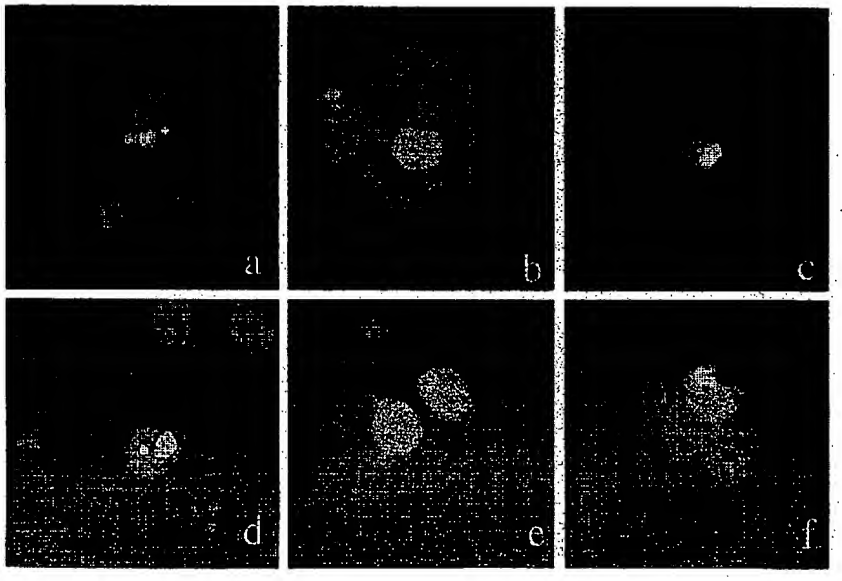

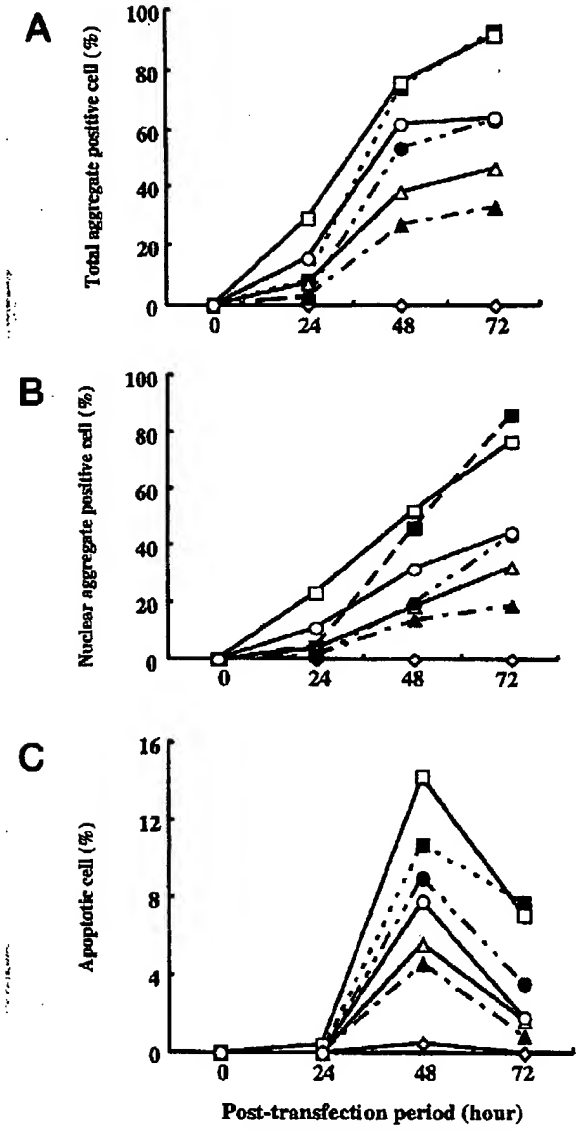

FIG. 6. **Frequency of cells with aggregate, nuclear aggregate, or apoptosis in cotransfecting Neuro2a cells with tAR-GFP and chaperones.** *A*, total aggregate-positive cells that contain aggregates cytoplasm and/or nucleus. *B*, nuclear aggregate-positive cells that contain nuclear aggregate with/without cytoplasmic aggregates. *C*, TUNEL-positive cells. ♦, tAR24; ■, tAR97; △, +Hsp70; ●, +Hsp40; □, +HSD/J; ▲, +Hsp70/40; ○, +Hsp70/HSDJ.

tometry. Aggregate index was computed as the signal intensity of aggregate band divided by that of monomer band.

Statistical Analysis

Results were analyzed using analysis of variance and Student's *t* test if appropriate from Statview software version 5.

RESULTS

A Neuronal Cultured Cell Model of SBMA—We first examined whether truncated and expanded AR (tAR97) forms aggregate and is toxic to Neuro2a cell line. Transient expression of tAR97 induced aggregate formation in cytoplasm and/or nucleus and cellular toxicity in Neuro2a cell line (Figs. 1 and 2). 72 h after transfection, over 90% of transfected cells (92.8 ± 1.1%) had aggregates. As for the localization of aggregate, the longer the cells transfected with tAR97 were cultured, the larger the proportion of nuclear aggregate-positive cells was. 72 h after transfection, more than 80% of transfected cells (86.4 ± 1.6%) had nuclear aggregates (Fig. 2*B*). Moreover, most of the apoptotic cells had nuclear aggregates, whereas cells containing cytoplasmic aggregate alone had few apoptotic cells (Fig. 3). In contrast, the cells transfected with tAR24 had few aggregates and few apoptotic cells (Figs. 1 and 2). The neuronal cultured cell model has shown nuclear aggregates, which are pathological hallmark of CAG repeat disease, and an apoptosis, which might be mediated by cellular toxicity of expanded polyglutamine tract. These results indicate that this neuronal cultured cell model could be utilized as a cell model of SBMA. We thus employed this cell model for further studies.

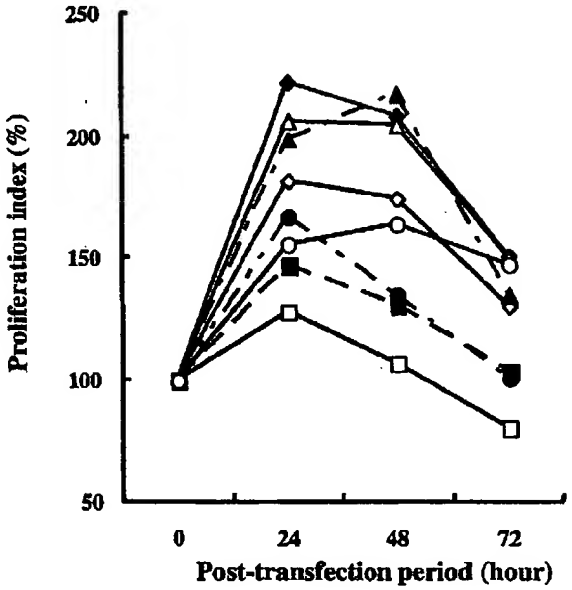

FIG. 7. **Proliferation assay of cotransfecting Neuro2a cells with tAR-GFP and chaperones.** ♦, control; ◇, tAR24; ■, tAR97; △, +Hsp70; □, +Hsdj; ●, +Hsp40; ▲, +Hsp70/40; ○, +Hsp70/Hsdj.

Endogenous Chaperones Are Colocalized with Expanded and Truncated AR-formed Aggregates—We next assessed whether chaperones are colocalized with tAR97-formed aggregates in our neuronal cell model of SBMA. Endogenous chaperones in tAR97-transfected and nontransfected Neuro2a cells were discernible predominantly in cytoplasm with limited nuclear staining. Laser confocal microscopic analysis has demonstrated that the endogenous chaperones Hsp70, Hsp40, and Hsdj are up-regulated in the cells containing aggregates and clearly colocalized with aggregates irrespective of the localization of aggregate (Fig. 4). These data had suggested that the cells transfected with tAR97 induce the expression levels of chaperones to protect themselves against a cellular toxicity of expanded polyglutamine tract. However, the amount of induced endogenous chaperones might be insufficient to protect themselves, because the suppression of protein aggregation by chaperone requires a relatively large molar excess of chaperones (48).

Overexpression of Chaperones Reduces Aggregate Formation and Apoptosis Induced by Expanded and Truncated AR—To determine whether a sufficient amount of chaperones could be effective to protect cells against a cellular toxicity of expanded polyglutamine tract, we had overexpressed chaperones in cotransfection with tAR97 in the cell model of SBMA. Overex-

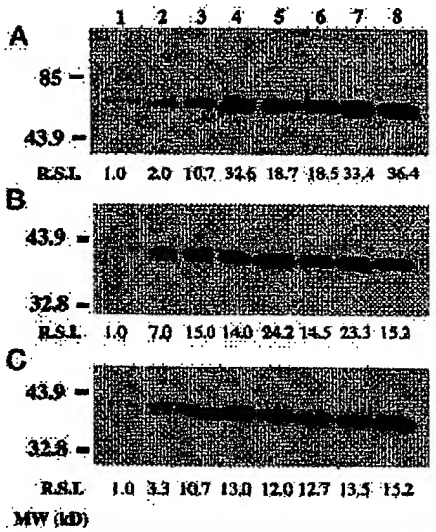

FIG. 8. **Expression levels of chaperones in the cotransfected experiments.** Western blotting analysis revealed the expression level of Hsp70 (*A*), Hsp40 (*B*), and Hsdj/Hdj2 (*C*). *Lane 1*, nontransfected Neuro2a cells; *lane 2*, cells transfected with tAR24-GFP construct; *lane 3*, cells transfected with tAR97-GFP construct; *lane 4*, cells cotransfected with tAR24-GFP and Hsp70; *lane 5*, cells cotransfected with tAR97-GFP and Hsp40; *lane 6*, cells cotransfected with tAR97-GFP and Hsdj/Hdj2; *lane 7*, cells cotransfected with tAR97-GFP and Hsp70/Hsp40; *lane 8*, cells cotransfected with tAR97-GFP and Hsp70/Hsdj. R.S.I. was computed as the signal intensity of indicated lanes divided by that of nontransfected cells.

pression of both Hsp70 and Hsp40 or Hsp70 alone significantly reduces both aggregate formation and cell death, whereas overexpression of Hsdj/Hdj2 alone shows little effect. Especially, Hsp70 and Hsp40 in combination displayed the strongest effects in both the reduction of aggregate formation and the suppression of apoptosis (Figs. 5 and 6 and Table I). In addition, overexpression of both Hsp70 and Hsdj/Hdj2 or Hsp40 alone was less effective to reduce aggregate formation and cell death than overexpression of both Hsp70 and Hsp40 or Hsp70 alone. Furthermore, there was a parallel correlation between the reduction of aggregate formation and the suppression of apoptosis in these cotransfected experiments.

We further examined whether chaperones reduce a tAR97-induced cellular toxicity. Proliferation assay revealed that cells cotransfected with both Hsp70 and Hsp40 or with Hsp70 alone were more proliferative than the cells cotransfected with other chaperones ($p < 0.05$ at 48 h after transfection by analysis of variance; Fig. 7). In addition, chaperones and their combinations showed neither cellular toxicity nor proliferative effect when transfected with chaperones alone in this proliferative assay (data not shown).

Expression Levels of Chaperones in the Cotransfected Experiments—We next examined expression levels of chaperones in the cotransfected experiment. Although nontransfected Neuro2a cells expressed a small quantity of Hsp70, Hsp40, and Hsdj/Hdj2 (*lanes 1* in Fig. 8, *A*, *B*, and *C*, respectively), cells transfected with tAR24 had a large quantity of chaperones (Hsp70 (2.0 R.S.I.), Hsp40 (7.0 R.S.I.), and Hsdj/Hdj2 (3.3 R.S.I.); *lanes 2* in Fig. 8, *A*, *B*, and *C*, respectively). Moreover, cells transfected with tAR97 expressed a larger quantity of chaperones (Hsp70 (10.7 R.S.I.), Hsp40 (15.0 R.S.I.), and Hsdj/Hdj2 (10.7 R.S.I.); *lanes 3* in Fig. 8, *A*, *B*, and *C*, respectively). Cells cotransfected with expanded and tAR97 and Hsp70 and/or Hsp40 have shown a much larger quantity of Hsp70 or Hsp40 (Hsp70, *lanes 4* (32.6 R.S.I.), *7* (33.4 R.S.I.), and *8* (36.4

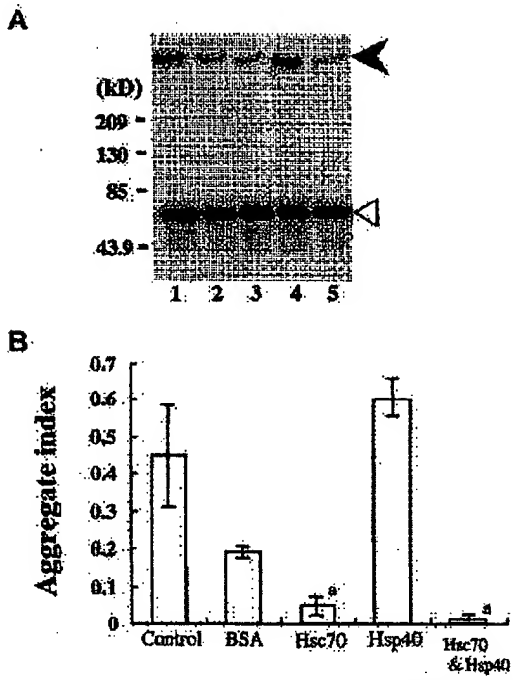

FIG. 9. ***In vitro* aggregation assay.** Purified GST-tAR65-HA protein was incubated with indicated chaperones (20-fold molar excess), followed by Western blotting analysis. *A*, example of blot. *Lane 1*, incubation with no additive; *lane 2*, with bovine serum albumin; *lane 3*, with Hsc70; *lane 4*, with Hsp40; *lane 5*, with Hsp70/Hsp40. *Closed arrowhead* points to aggregates of GST-tAR65-HA, and *open triangle* indicates monomers. *B*, aggregate index. Values are the means ± S.E. *a*, $p < 0.01$ *versus* control and bovine serum albumin by Student's *t* test.

R.S.I.) in Fig. 8*A*; Hsp40, *lanes 5* (24.2 R.S.I.) and *7* (23.3 R.S.I.) in Fig. 8*B*); however, cells cotransfected with Hsdj/Hdj2 have demonstrated relatively low overexpression of Hsdj/Hdj2 compared with others (Hsdj/Hdj2, *lanes 6* (12.7 R.S.I.) and *8* (15.2 R.S.I.) in Fig. 8*C*).

Chaperones Decrease in Vitro Aggregation of Expanded Polyglutamine Tract—We previously reported that expanded polyglutamine tract forms aggregates *in vitro* in a polyglutamine length-dependent manner (24). We next assessed the ability of Hsc70 and Hsp40 to reduce *in vitro* aggregation of expanded and truncated AR (tAR65) using our *in vitro* aggregation system. As expected, 20-fold molar excess of Hsc70 and Hsp40 or Hsc70 alone effectively suppressed *in vitro* aggregation of tAR65 (Hsc70/Hsp40 *versus* bovine serum albumin, $p < 0.01$; Hsc70 *versus* bovine serum albumin, $p < 0.01$ by Student's *t* test) (Fig. 9). However, Hsp40 alone has little ability to suppress aggregation.

DISCUSSION

The present study first demonstrated that overexpression of chaperones, especially combination of Hsp70 and Hsp40, reduce cytotoxicity and aggregate formation induced by expanded polyglutamine tract in our cultured neuronal cell model of SBMA. These findings suggest that the chaperones may be one of the key factors in the development of CAG repeat disease.

We previously reported that a truncated and expanded AR forms aggregate and is toxic to Cos-7 and MN-1 cells (24). In addition, we observed nuclear inclusions in SBMA (33, 34). In other CAG repeat diseases, truncated and expanded polyglutamine fragments of disease proteins have been also shown to form aggregates and have toxicity in transfected cells, transgenic mice, and flies (19–24). However, the role of aggregates

TABLE I

Frequency of cells with aggregate, nuclear aggregate, or apoptosis in cotransfecting Neuro2a cells with tAR-GFP and chaperones

Values are the means ± S.E.

Construct	Post-transfection period		
	24 h[a]	48 h[a]	72 h[a]
Aggregate-positive cell			
tAR24+emp vector	0.0 ± 0.0	0.0 ± 0.0	0.0 ± 0.0
tAR97+emp vector	8.4 ± 3.0	74.5 ± 2.4	92.8 ± 1.1
tAR97+Hsp70	7.3 ± 2.8	38.7 ± 3.9[c]	46.9 ± 0.8[c]
tAR97+Hsp40	2.5 ± 0.0	53.6 ± 2.1[c]	63.8 ± 2.5[c]
tAR97+Hsdj	29.4 ± 2.7[b]	76.2 ± 1.9	91.5 ± 1.4
tAR97+Hsp70/40	3.2 ± 0.5	26.9 ± 2.8[c]	33.3 ± 7.9[c]
tAR97+Hsp70/Hsdj	16.9 ± 1.3	61.9 ± 2.5[b]	64.4 ± 13.7
Nuclear aggregate positive cell			
tAR24+emp vector	0.0 ± 0.0	0.0 ± 0.0	0.0 ± 0.0
tAR97+emp vector	4.6 ± 1.8	46.3 ± 1.0	86.4 ± 1.6
tAR97+Hsp70	3.6 ± 1.4	18.3 ± 1.5[c]	32.4 ± 2.9[c]
tAR97+Hsp40	0.7 ± 0.1	19.8 ± 2.5[c]	43.9 ± 3.6[c]
tAR97+Hsdj	23.4 ± 3.7[c]	52.1 ± 0.8[c]	76.6 ± 1.8[c]
tAR97+Hsp70/40	1.6 ± 0.0	13.8 ± 0.4[c]	19.0 ± 3.8[c]
tAR97+Hsp70/Hsdj	10.8 ± 2.1	31.7 ± 8.7[c]	44.4 ± 9.6[c]
Apoptotic cell			
tAR24+emp vector	0.0 ± 0.0	0.5 ± 0.8	0.0 ± 0.0
tAR97+emp vector	0.0 ± 0.0	10.8 ± 0.1	7.7 ± 0.2
tAR97+Hsp70	0.0 ± 0.0	5.6 ± 0.2[c]	1.7 ± 0.7[c]
tAR97+Hsp40	0.0 ± 0.0	9.0 ± 0.4[c]	3.6 ± 2.1
tAR97+Hsdj	0.4 ± 0.2	14.3 ± 2.1	7.1 ± 0.4
tAR97+Hsp70/40	0.0 ± 0.0	4.6 ± 1.1[c]	0.9 ± 0.5[c]
tAR97+Hsp70/Hsdj	0.0 ± 0.0	7.8 ± 1.2[b]	1.8 ± 0.1[c]

[a] $p < 0.05$ by analysis of variance.

[b] $p < 0.05$ *versus* cells transfected with tAR97 and empty vector at the same time point.

[c] $p > 0.01$ *versus* cells transfected with tAR97 and empty vector at the same time point.

in the pathogenesis of CAG repeat diseases is controversial (23, 49). The relationship between aggregate formation, particularly in the nucleus, and induction of apoptosis still remains to be resolved. Our results reveal that combination Hsp70 and Hsp40 or Hsp70 alone has a favorable effect in a cellular protection as well as suppression of aggregate formation and that combination of Hsp70 and Hsp40, especially, has the strongest effect among them. Our results were in accordance with the reports that the chaperone function of Hsp70 is critically dependent on the cooperation with Hsp40 (40, 41, 42). The chaperone activity of Hsp70 family is regulated by Hsp70 ATPase activity (52), and Hsp40 stimulates the Hsp70 ATPase by increasing the rate of ATP hydrolysis (40). In other conformational diseases, the study about mutant copper/zinc superoxide dismutase (SOD-1)-associated amyotrophic lateral sclerosis also displayed that increasing the level of Hsp70 reduced formation of mutant SOD-containing aggregates in cultured primary motor neurons expressing mutant SOD-1 and prolonged their survival (51). It is therefore reasonable to consider that disease gene product-formed aggregates are directly associated with the induction of neurodegenaration in CAG repeat disease and other conformation diseases. We thus reasoned that overexpression of both Hsp70 and Hsp40 chaperones reduce cytotoxicity induced by aggregate formation with disease gene product in CAG repeat disease and other conformation diseases.

The question is the molecular mechanism for the reduction of cytotoxicity through inhibition of expanded and truncated AR-formed aggregate by overexpression of chaperones. Although it has been proposed that expanded polyglutamine tract-formed aggregates participate in inappropriate protein-protein interactions that lead to cell death, the nature of such interactions and the mechanism by which cell death is induced remain unclear. Molecular chaperones could be involved in the actual formation of expanded polyglutamine tract-formed aggregates by stabilizing the unfolded protein in an intermediate conformation that has the propensity to interact with self or other proteins. To date, several proteins interacting with polyglutamine tract-containing disease gene product have been cloned, including huntingtin-associated protein (53), huntingtin-interacting protein (54), glyceraldahyde-3-phosphate dehydrogenase (55), leucine-rich acidic nuclear protein (56), and PQBP-1 (polyglutamine tract-binding protein-1) (57). These interacting proteins are candidate players in the pathogenesis of CAG repeat disease. Chaperones might reduce cytotoxicity of expanded and truncated AR through inhibiting the interaction of expanded polyglutamine-formed aggregate with these proteins.

Another possibility is that overexpression of chaperones is enhancing the function of the ubiquitin-proteasome pathway for mutant protein degradation because the function of the ubiquitin-proteasome pathway is related with the expression level of chaperones (36). Nuclear aggregates are ubiquitinated and are colocalized with chaperones and proteasome, implicating the ubiquitin-proteasome degradation pathway in the pathogenesis of CAG repeat disease (33, 34, 38, 58). The report that the inhibition of proteasome function accelerates aggregate formation by polyglutamine tract also implies the ubiquitin-proteasome degradation pathway plays a direct role in modulating aggregation in CAG repeat disease (58). In Alzheimer's disease, one of the conformational disease, amyloid β-protein, which is a major component of senile plaque, could interfere with ubiquitin-dependent protein degradation pathway by inhibiting the 26 S proteasome. Consequently, it may lead to neuronal damage observed in Alzheimer's disease (59). Similarly, expanded polyglutamine tract would interfere with ubiquitindependent protein degradation pathway and lead to neuronal damage in CAG repeat disease. Thus overexpression of chaperones would enhance the function of proteasome, leading to protecting cells expressing truncated and expanded AR against a cellular toxicity of expanded polyglutamine tract.

Recently, there are reports that overexpression of Hsdj/Hdj2 in HeLa cells decreases the frequency of mutant ataxin-1 and mutant AR aggregation (38, 39); however, overexpression of Hsdj/Hdj2 has little effect of reducing aggregate formation and providing cellular proliferation in our result. These differences of results may arise from the difference in cell lineage, the different origin of Hsdj/Hdj2, or the expression level of Hsdj/Hdj2 in transfected cells. Previous studies used a non-neural cell line (HeLa cell), whereas we used a neural cell line (Neuro2a). The difference in cell lineages could influence the relations of chaperones, aggregation, and cell death. Although Hsdj we employed in this study is 99% identical to Hsdj2 employed in other reports at the level of amino acid sequence (32, 44), the relationship between Hsdj and Hdj2 remains to be studied. Alternatively, ineffectiveness of Hsdj/Hdj2 in our study might be explained by relatively low overexpression of the protein in comparison with Hsp70 and/or Hsp40, as shown in Western blotting analysis.

In contrast to our results, two groups have provided evidence against a critical role of intranuclear aggregates in neuronal cell death (49, 60). The results opposite to ours could arise from the difference of cell type/animal (primary neuron/animal *versus* cell line) or interventions (neurotrophic factors/suppression of ubiquitin-conjugating enzyme/inhibition of ataxin-1 self-association *versus* overexpression of chaperones). However, we cannot rule out the possibility that our observation, a parallel correlation between the reduction of aggregate formation and suppression of apoptosis in our system, might occur coincidentally. Thus, Hsps could reduce aggregate formation as a molecular chaperone and independently suppress apoptosis in our cell system through a different molecular mechanism. Al-

though Hsp70 was reported to have an anti-apoptotic effect, the mechanism of such effect remains veiled (50). Therefore, discussion of this possibility needs to await future studies.

Finally, the findings described in this report highlight that chaperones play a role in the developing of CAG repeat disease. These results suggested that increasing expression level or enhancing the function of chaperones provides an avenue for the treatment of CAG repeat disease. Further studies of cellular and animal models are required to determine the precise mechanism of neurodegeneration of CAG repeat disease mediated by expanded polyglutamine tract as well as therapeutic approach.

Acknowledgments—We thank Dr. Kenneth H. Fischbeck, Dr. Diane E. Merry, and Dr. Paul Taylor for the critical review of the manuscript. We are also grateful to Sugiko Yokoi, Michiyo Matsumoto, and Jun Du for technical assistance.

REFERENCES

1. La Spada, A. R., Wilson, E. M., Lubahn, D. B., Harding, A. R., and Fischbeck, K. H. (1991) *Nature* **352**, 77–79
2. Doyu, M., Sobue, G., Mukai, E., Kachi, T., Yasuda, T., Mitsuma, T., and Takahashi, A. (1992) *Ann. Neurol.* **32**, 707–710
3. Igarashi, S., Tanno, Y., Onodera, O., Yamazaki, M., Sato, S., Ishikawa, A., Miyatani, N., Nagashima, M., Ishikawa, Y., Sahashi, K., Ibi, T., Miyatake, T., and Tsuji, S. (1992) *Neurology* **42**, 2300–2302
4. La Spada, A. R., Roling, D. B., Harding, A. E., Warner, C. L., Spiegel, R., Hausmanowa-Petrusewicz, I., Yee, W. C., and Fischbeck, K. H. (1992) *Nat. Genet.* **2**, 301–304
5. The Huntington's Disease Collaborative Research Group (1993) *Cell* **72**, 971–983
6. Koide, R., Ikeuchi, T., Onodera, O., Tanaka, H., Igarashi, S., Endo, K., Takahashi, H., Kondo, R., Ishikawa, A., Hayashi, T., Saito, M., Tomoda, A., Miike, T., Naito, H., Ikuta, F., and Tsuji, S. (1994) *Nat. Genet.* **6**, 9–13
7. Nagafuchi, S., Yanagisawa, H., Sato, K., Shirayama, T., Ohsaki, E., Bundo, M., Takeda, T., Tadokoro, K., Kondo, I., Murayama, N., Tanaka, Y., Kikushima, H., Umino, K., Kurosawa, H., Furukawa, T., Nihei, K., Inoue, T., Sano, A., Komura, O., Takahashi, M., Yoshizawa, T., Kanazawa, I., and Yamada, M.(1994) *Nat. Genet.* **6**, 14–18
8. Kawaguchi, Y., Okamoto, T., Taniwaki, M., Aisawa, M., Inoue, M., Katayama, S., Kawakami, H., Nakamura, S., Nisimura, M., Akiguchi, I., Kimura, J., Narumiya, S., and Kakizuka, A. (1994) *Nat. Genet.* **8**, 221–227
9. Orr, H. T., Chung, M.-Y., Banfi, S., Kwiatkowski, J. T. J., Servadio, A., Beaudet, A. L., McCall, A. E., Duvick, L. A., Ranum, L. P. W., and Zoghbi, H. Y. (1993) *Nat. Genet.* **4**, 221–226
10. Pulst, S. M., Nechiporuk, A., Nechiporuk, T., Gispert, S., Chen, X. N., Cendes, I. L., Pearlman, S., Starkman, S., Diaz, G. O., Lunkes, A., DeJong, P., Rouleau, G. A., Auburger, G., Korenberg, J. R., Figueroa, C., and Sahba, S. (1996) *Nat. Genet.* **14**, 269–276
11. Sanpei, K., Takano, H., Igarashi, S., Sato, T., Oyake, M., Sasaki, H., Wakisaka, A., Tashiro, K., Ishida, Y., Ikeuchi, T., Koide, R., Saito, M., Sato, A., Tanaka, T., Hanyu, S., Takiyama, Y., Nishizawa, M., Shimizu, N., Nomura, Y., Segawa, M., Iwabuchi, K., Eguchi, I., Tanaka, H., Takahashi, H., and Tsuji, S. (1996) *Nat. Genet.* **14**, 277–284
12. Imbert, G., Saudou, F., Yvert, G., Devys, D., Trottier, Y., Garnier, J. M., Weber, C., Mandel, J. L., Cancel, G., Abbas, N., Dürr, A., Didierjean, O., Stevanin, G., Agid, Y., and Brice, A. (1996) *Nat. Genet.* **14**, 285–291
13. Zhuchenko, O., Bailey, J., Bonnen, P., Ashizawa, T., Stockton, D. W., Amos, C., Dobyns, W. B., Subramony, S. H., Zoghbi, H. Y., and Lee, C. C. (1997) *Nat. Genet.* **15**, 62–69
14. David, G., Abbas, N., Stevanin, G., Durr, A., Yvert, G., Cancel, G., Weber, C., Imbert, G., Saudou, F., Antoniou, E., Drabkin, H., Gemmill, R., Giunti, P., Benomar, A., Wood, N., Ruberg, M., Agid, Y., Mandel, J. L., and Brice, A. (1997) *Nat. Genet.* **17**, 65–70
15. Goldberg, Y. P., Nicholson, D. W., Rasper, D. M., Kalchman, M. A., Koide, H. B., Graham, R. K., Bromm, M., Kazemi-Esfarjani, P., Thornberry, N. A., Vaillancourt, J. P., and Hayden, M. R. (1996) *Nat. Genet.* **13**, 442–449
16. Miyashita, T., Okamura-Oho, Y., Mito, Y., Nagafuchi, S., and Yamada, M. (1997) *J. Biol. Chem.* **272**, 29238–29242
17. Wellington, C. L., Ellerby, L. M., Hackam, A. S., Margolis, R. L., Trifiro, M. A., Singaraja, R., McCutcheon, K., Salvesen, G. S., Propp, S. S., Bromm, M., Rowland, K. J., Zhang, T., Rasper, D., Roy, S., Thornberry, N., Pinsky, L., Kakizuka, A., Ross, C. A., Nicholson, D. W., Bredesen, D. E., and Hayden, M. R. (1998) *J. Biol. Chem.* **273**, 9158–9167
18. Kobayashi, Y., Miwa, S., Merry D. E., Kume, A., Li, M., Doyu, M., and Sobue, G. (1998) *Biochem. Biophys. Res. Commun.* **252**, 145–150
19. Davies, S. W., Turmaine, M., Cozens, B. A., DiFiglia, M., Sharp, A. H., Ross, C. A., Scherzinger, E., Wanker, E. E., Mangiarini, L., and Bates, G. P. (1997) *Cell* **90**, 537–548
20. Ikeda, H., Yamaguchi, M., Sugai, S., Ase, Y., Narumiya, S., and Kakizuka, A. (1996) *Nat. Genet.* **13**, 196–202
21. Warrick, J. M., Paulson, H. L., Gray-Board, G. L., Bui, Q. T., Fischbeck, K. H., Pittman, R. N., and Bonini, N. M. (1998) *Cell* **93**, 939–949
22. Martindale, D., Hackam, A., Wieczorek, A., Ellerby, L., Wellington, C., McCutcheon, K., Singaraja, R., Kazemi-Esfarjani, P., Devon, R., Kim, S. U., Bredesen, D. E., Tufaro, F., and Hayden, M. R. (1998) *Nat. Genet.* **18**, 150–154
23. Igarashi, S., Koike, R., Shimohata, T., Yamada, M., Hayashi, Y., Takano, H., Date, H., Oyake, M., Sato, T., Sato, A., Egawa, S., Ikeuchi, T., Tanaka, H., Nakano, R., Tanaka, K., Hozumi, I., Inuzuka, T., Takahashi, H., and Tuji, S. (1998) *Nat. Genet.* **18**, 111–117
24. Merry, D. E., Kobayashi, Y., Bailey, C. K., Taye, A. A., and Fischbeck, K. H. (1998) *Hum. Mol. Genet.* **7**, 693–701
25. Perutz, M. F., Johnson, T., Suzuki, M., and Finch, J. T. (1994) *Proc. Natl. Acad. Sci. U. S. A.* **91**, 5355–5358
26. Stott, K., Blackburn J. M., Butler, P. J. G., and Perutz, M. (1995) *Proc. Natl. Acad. Sci. U. S. A.* **92**, 6509–6513
27. Kahlem, P., Terre, C., Green, H., and Djian, P. (1996) *Proc. Natl. Acad. Sci. U. S. A.* **93**, 14580–14585
28. DiFiglia, M., Snapp, E., Chase, K. O., Davies, S. W., Bates, G. P., Vonsattel, J. P., and Aronin, N. (1997) *Science* **227**, 1990–1993
29. Paulson, H. L., Das, S. S., Crino, P. B., Perez, M. K., Patel, S. C., Gotsdiner, D., Fischbeck, K. H., and Pittman, R. N.(1997) *Ann. Neurol.* **41**, 453–462
30. Paulson, H. L., Perez, D. M. K., Trottier, Y., Trojanowski, J. Q., Subramony, S. H., Das, S. S., Vig, P., Mandel, J.-L., Fischbeck, K. H., and Pittman, R. N. (1997) *Neuron* **19**, 333–344
31. Matilla, A., Koshy, B. T., Cummings, C. J., Isobe, T., Orr, H. T., and Zoghbi, H. Y. (1997) *Nature* **389**, 974–978
32. Chellaiah, A., Davis, A. Mohanakumar, T. (1998) *Biochim. Biophys. Acta* **1174**, 111–113
33. Li., M., Miwa, S., Kobayashi, Y., Merry, D., Tanaka, F., Doyu, M., Hashizume, Y., Fischbeck, K. H., and Sobue, G. (1998) *Ann. Neurol.* **44**, 249–254
34. Li, M., Nakagomi, Y., Kobayashi, Y., Merry, D. E., Tanaka, F., Doyu, M., Mitsuma, T., Fischbeck, K. H., and Sobue, G. (1998) *Am. J. Pathol.* **153**, 695–701
35. Ciechanover, A. (1997) *Cell* **91**, 249–254
36. Bukau, K. T., and Horwich, A. L. (1998) *Cell* **92**, 351–366
37. Hendricks, J. P., and Hartl, F. U. (1993) *Annu. Rev. Biochem.* **62**, 349–384
38. Cummings, C. J., Mancini, M. A., Antalffy, B., DeFranco, D. B., Orr, H. T., and Zoghbi, H. Y. (1998) *Nat. Genet.* **19**, 148–154
39. Stenoien, D. L., Cummings, C. J., Adams, H. P., Mancini, M. G., Patel, K., DeMartino, G. N., Marcelli, M., Weigel, N. L., and Mancini, M. (1999) *Hum. Mol. Genet.* **8**, 731–741
40. Minami, Y., Höhfeld, J., Ohtsuka, K., and Hart, F. (1996) *J. Biol. Chem.* **271**, 19617–19624
41. Michels, A. A., Kanon, B., Konings, A. W. T., Ohtsuka, K., Bensaude, O., and Kampinga, H. H. (1997) *J. Biol. Chem.* **272**, 33283–33289
42. Frydman, J., Nimmesgern, E., Ohtsuka, K., and Hartl, F.-U. (1994) *Nature* **370**, 111–117
43. Ohtsuka, K. (1993) *Biochem. Biophys. Res. Commun.* **197**, 235–240
44. Oh, S., Iwabori, A., and Kato, S. (1993) *Biochim. Biophys. Acta* **1174**, 114–118
45. Ohtsuka, K., Tanabe, K., Nakamura, H., and Sato, C. (1986) *Radiat. Res.* **108**, 34–42
46. Hattori, H., Liu, Y.-C., Tohnai, I., Ueda, M., Kaneda, T., Kobayashi, T., Tanabe, K., and Ohtsuka, K. (1992) *Cell Struct. Funct.* **17**, 77–86
47. Imamoto, N., Matsoka Y., Kurihara T., Kohno K., Miyagi M., Sakiyama, F., Okada, Y., Tsunasawa, S., and Yoneda, Y. (1992) *J. Cell Biol.* **119**, 1047–1061
48. Lu, Z., and Cyr, D. M. (1998) *J. Biol. Chem.* **273**, 5970–5978
49. Saudou, F., Finkbeiner, S., Devys, D., and Greenberg, M. E. (1998) *Cell* **95**, 55–66
50. Jäättelä, M., Wissing, D., Kokholm, K., Kallunki, T., and Egeblad, M. (1998) EMBO J. **17**, 6124–6134
51. Bruening, W., Roy, J., Giasson, B., Figlewicz, D. A., Mushynski, W. E., and Durham, H. D. (1999) *J. Neurochem.* **72**, 693–699
52. McCarty, J. S., Buchberger, A., Reinstein, J., and Bukau, B. (1995) *J. Mol. Biol.* **249**, 126–137
53. Li, X. J., Li, S. H., Sharp, A. H., Nucifora, F. C. Jr., Schilling, G., Lanahan, A., Worley, P., Snyder, S. H., and Ross, C. A. (1995) *Nature* **378**, 398–402
54. Kalchman, M. A., Koide, H. B., McCutcheon, K., Graham, R. K., Nichol, K., Nishiyama, K., Kazemi-Esfarjani, P., Lynn, F. C., Wellington, C., Metzler, M., Goldberg, Y. P., Kanazawa, I., Gietz, R. D., and Hayden, M. R. (1997) *Nat. Genet.* **16**, 44–53
55. Burke, J. R., Enghild, J. J., Martin, M. E., Jou, Y. S., Myers, R. M., Roses, A. D., Vance, J. M., and Strittmatter, W. J. (1996) *Nat. Med.* **2**, 347–350
56. Matilla, A., Koshy, B. T., Cummings, C. J., Isobe, T., Orr, H. T., and Zoghbi, H. Y. (1997) *Nature* **389**, 974–978
57. Waragai, M., Lammers, C., Takeuchi, S., Imafuku, I., Udagawa, Y., Kanazawa, I., Kawabata, M., Mouradian, M. M., and Okazawa, H. (1999) *Hum. Mol. Genet.* **8**, 977–987
58. Chai, Y., Koppenhafer, S. L., Shoesmith, S. J., Perez, M. K., and Paulson, H. L. (1999) *Hum. Mol. Genet.* **8**, 673–682
59. Gregori, L., Fuchs, C., Figueiredo-Pereira, M. E., Nostrand, W. E. V., and Goldgaber, D. (1995) *J. Biol. Chem.* **270**, 19702–19708
60. Klement, I. A., Skinner, P. J., Kaytor, M. D., Yi, H., Hersch, S. M., Clark, H. B., Zoghbi, H. Y., and Orr, H. T. (1998) *Cell* **95**, 41–53

EXHIBIT K

THE JOURNAL OF BIOLOGICAL CHEMISTRY
Vol. 278, No. 27, Issue of July 4, pp. 25143–25150, 2003
Printed in U.S.A.

Hsp105α Suppresses the Aggregation of Truncated Androgen Receptor with Expanded CAG Repeats and Cell Toxicity*

Received for publication, March 24, 2003, and in revised form, April 21, 2003
Published, JBC Papers in Press, April 24, 2003, DOI 10.1074/jbc.M302975200

Keiichi Ishihara‡, Nobuyuki Yamagishi‡, Youhei Saito‡, Hiroaki Adachi§, Yasushi Kobayashi§, Gen Sobue§, Kenzo Ohtsuka¶, and Takumi Hatayama‡‖

From the ‡Department of Biochemistry, Kyoto Pharmaceutical University, 5 Nakauchi-cho, Misasagi, Yamashina-ku, Kyoto 607-8414, the §Department of Neurology, Nagoya University Graduate School of Medicine, 65 Tsurumai-cho Showa-ku, Nagoya 466-8550, and the ¶Department of Environmental Biology, College of Bioscience and Biotechnology, Chubu University, Matsumoto-cho 1200, Kasugai 487-8501, Japan

Spinal and bulbar muscular atrophy (SBMA) is a neurodegenerative disorder caused by the expansion of a polyglutamine tract in the androgen receptor (AR). The N-terminal fragment of AR containing the expanded polyglutamine tract aggregates in cytoplasm and/or in nucleus and induces cell death. Some chaperones such as Hsp40 and Hsp70 have been identified as important regulators of polyglutamine aggregation and/or cell death in neuronal cells. Recently, Hsp105α, expressed at especially high levels in mammalian brain, has been shown to suppress apoptosis in neuronal cells and prevent the aggregation of protein caused by heat shock *in vitro*. However, its role in polyglutamine-mediated cell death and toxicity has not been studied. In the present study, we examined the effects of Hsp105α on the aggregation and cell toxicity caused by expansion of the polyglutamine tract using a cellular model of SBMA. The transient expression of truncated ARs (tARs) containing an expanded polyglutamine tract caused aggregates to form in COS-7 and SK-N-SH cells and concomitantly apoptosis in the cells with the nuclear aggregates. When Hsp105α was overexpressed with tAR97 in the cells, Hsp105α was colocalized to aggregates of tAR97, and the aggregation and cell toxicity caused by expansion of the polyglutamine tract were markedly reduced. Both β-sheet and α-helix domains, but not the ATPase domain, of Hsp105α were necessary to suppress the formation of aggregates *in vivo* and *in vitro*. Furthermore, Hsp105α was found to localize in nuclear inclusions formed by ARs containing an expanded polyglutamine tract in tissues of patients and transgenic mice with SBMA. These findings suggest that overexpression of Hsp105α suppresses cell death caused by expansion of the polyglutamine tract without chaperone activity, and the enhanced expression of the essential domains of Hsp105α in brain may provide an effective therapeutic approach for CAG repeat diseases.

Spinal and bulbar muscular atrophy (SBMA)[1] is an X-linked motor neuropathy characterized by proximal muscle atrophy, weakness, contraction fasciculation, and bulbar involvement (1, 2). In SBMA patients, a normally polymorphic CAG repeat (10–36 CAGs) in exon 1 of the androgen receptor (AR) gene expands to 40–62 CAGs (3), and nuclear inclusions containing mutant and truncated ARs with an expanded polyglutamine tract are characteristically found in the residual motor neurons in the brain stem and spinal cord (4) as well as in the skin, testis, and other visceral organs (5). In addition to SBMA, expansions of CAG repeats encoding polyglutamine tracts in unrelated proteins are responsible for at least another eight different neurodegenerative diseases including Huntington's disease (6), dentatorubral pallidoluysian atrophy (7, 8), Machado-Joseph disease (9), and several types of spinocerebellar ataxia (10–15). All of these disorders show a late onset of neurological symptoms with progressive neuronal dysfunction and eventual neuronal loss, although the susceptible regions in the nervous system differ among the various disorders. The appearance of intranuclear aggregates/inclusions in neurons is associated with these neurodegenerative diseases. The intranuclear inclusions contain the insoluble protein aggregates of abnormal proteins or their fragments, heat shock proteins, and components of the ubiquitin-dependent proteasome degradation pathway (16, 17). Although the nature of the toxic insult of a polyglutamine mutation and its cell-biological consequences in each disease are unclear, it is possible that the polyglutamine expansion interferes with basic cellular processes such as transcription, protein degradation, and survival/death signaling (17). However, the exact role of these protein aggregates in polyglutamine pathology is still controversial because large polyglutamine aggregates may provide an advantage over small oligomers by exposing less potentially dangerous protein surfaces (18). The cellular components involved in protein folding and degradation are also associated with intracellular inclusions in other neurodegenerative diseases not caused by polyglutamine expansion, including Alzheimer's, Parkinson's, and the prion diseases (19), which suggests that common mechanistic principles may underlie these misfolding diseases in general.

A considerable effort has been made to find molecules that suppress polyglutamine aggregation and cell death/toxicity for therapeutic purposes (20–22). In general, the misfolding and aggregation of proteins are prevented by molecular chaperones (23, 24). Some molecular chaperones such as heat shock protein (Hsp) 70 and Hsp40 have recently been identified as important regulators of polyglutamine aggregation and/or cell death in *in*

* This work was supported in part by a grant-in-aid for scientific research from the Ministry of Education, Science, Culture, and Sports of Japan (to T. H.). The costs of publication of this article were defrayed in part by the payment of page charges. This article must therefore be hereby marked "*advertisement*" in accordance with 18 U.S.C. Section 1734 solely to indicate this fact.

‖ To whom correspondence should be addressed. Fax: 81-75-595-4758; E-mail: hatayama@mb.kyoto-phu.ac.jp.

[1] The abbreviations used are: SBMA, spinal and bulbar muscular atrophy; AR, androgen receptor; BSA, bovine serum albumin; GFP, green fluorescent protein; HA, hemagglutinin; PBS, phosphate-buffered saline; tAR, truncated androgen receptor; TUNEL, terminal nucleotidyl transferase-mediated UTP nick end labeling.

TABLE I
Primers used for construction of expression plasmids for Hsp105α deletion mutants

Expression in mammallan cell
- Hsp105N1 (a.a. 1–892)
  - Sense: 5′-CGGAGAAAGAATTGCACACTG-3′
  - Antisense: 5′-TCTAGAGGGCCCTTCGAACAA-3′
- Hsp105N2 (a.a. 1–511)
  - Sense: 5′-GGGGTACCCAGCCATGTCGGTGGTT-3′
  - Antisense: 5′-TCTAGAGGGCCCTTCGAACAA-3′
- Hsp105N3 (a.a. 1–606)
  - Sense: 5′-TAACTGCCATACCAAGTTGGC-3′
  - Antisense: 5′-TCTAGAGGGCCCTTCGAACAA-3′
- Hsp105C1 (a.a. 605–858)
  - Sense: 5′-GGGGATCCACCATGCTCGAGGCAGACATGGAATGT-3′
  - Antisense: 5′-GCTCTAGACCTAGTCCAGGTCCATGTTGAC-3′
- Hsp105C2 (a.a. 511–858)
  - Sense: 5′-GGGGATCCACCATGCTCGAGGCAGACATGGAATGT-3′
  - Antisense: 5′-GCTCTAGACCTAGTCCAGGTCCATGTTGAC-3′
- Hsp105C3 (a.a. 386–858)
  - Sense: 5′-GGGGATCCACCATGCCGGCATTTAAAGTTAGAGAG-3′
  - Antisense: 5′-GCTCTAGACCTAGTCCAGGTCCATGTTGAC-3′
- Hsp105Δβ (a.a. 1–392 + a.a. 551–858)
  - Sense: 5′-CTCGAGGCAGACATGGAATGTCCA-3′
  - Antisense: 5′-AGAAAGAATTGCACACTGCAGTGCAC-3′
- Hsp105ΔβL (a.a. 1–392 + a.a. 605–858)
  - Sense: 5′-GGGAGAGACCTTCTTAACATGTATATTG-3′
  - Antisense: 5′-AGAAAGAATTGCACACTGCAGTGCAC-3′
- Hsp105ΔL (a.a. 1–511 + a.a. 605–858)
  - Sense: 5′-GGGAGAGACCTTCTTAACATGTATATTG-3′
  - Antisense: 5′-AGAGGAGCCATCCTCTTCCTCGGT-3′

Expression in bacterial cell
- Hsp105Δβ
  - Sense: 5′-CTCGAGGCAGACATGGAATGTCCA-3′
  - Antisense: 5′-AGAAAGAATTGCACACTGCAGTGCAC-3′
- Hsp105ΔβL
  - Sense: 5′-GGGAGAGACCTTCTTAACATGTATATTG-3′
  - Antisense: 5′-AGAAAGAATTGCACACTGCAGTGCAC-3′
- Hsp105ΔL
  - Sense: 5′-GGGAGAGACCTTCTTAACATGTATATTG-3′
  - Antisense: 5′-AGAGGAGCCATCCTCTTCCTCGGT-3′

vitro assays (25), in cultured mammalian cells (26–31), in a *Drosophila* model (32) and in transgenic mice (33, 34). Hsp27 was also identified as a suppressor of polyglutamine-mediated cell death using a cellular model of Huntington's disease (35). However, because Hsp70/40 and Hsp27 suppressed polyglutamine-mediated death without suppressing polyglutamine aggregation in some experimental systems (35, 36), elucidation of the ways in which Hsps protect cells against polyglutamine mutations might be of relevance for other neurodegenerative conditions in which pathology is associated with protein deposition in neuronal cells.

Hsp105α is highly conserved in organisms from yeast to human (37–42) and is expressed in various tissues of mammals, but especially at high levels in brain (43). Recently, Hsp105α was demonstrated to have antiapoptotic properties for neuronal survival (44). Furthermore, Hsp105α prevents the aggregation of thermal denatured protein *in vitro* (45). However, its role in polyglutamine-mediated cell death/toxicity has not been studied. In the present study, we examined the role of Hsp105α in the context of polyglutamine aggregation and cell death using a cellular model of SBMA and demonstrate that Hsp105α without chaperone activity protects cells against polyglutamine-mediated cell death by reducing polyglutamine-protein aggregation. These findings suggest an important role for Hsp105α in preventing neurodegenerative diseases associated with polyglutamine expansions.

EXPERIMENTAL PROCEDURES

Plasmids—We used constructs expressing the N-terminal fragment of the AR fused to green fluorescence protein (GFP) containing 24, 65, or 97 CAG repeats (tAR24, tAR65, and tAR97, respectively) as a cellular model of SBMA (29), human Hsp70 (pCMV-Hsp70) (46), and Hsp40 (pRC-Hsp40) (29) in mammalian cells. The constructs expressing Hsp105α (pcDNA105α) and Myc-epitope/His-tagged Hsp105α (pcDNA105α-mycHis) in mammalian cells were generated by ligating a full-length mouse Hsp105α cDNA (38) into pcDNA3.1 (Invitrogen) at *Bam*HI and *Eco*RI sites and pcDNA3.1(+)-mycHis vector (Invitrogen) at *Xba*I and *Kpn*I sites, respectively. The constructs expressing Hsp105N1–N3, Δβ, ΔL, and ΔβL in mammalian cells were generated by self-ligation of DNA made by PCR using pcDNA105α-mycHis (Hsp105N1–N3) or pcDNA105α (Hsp105Δβ, ΔL, ΔβL, and C1–C3) as template DNA and a specific set of primers (Table I).

We used a construct expressing GST- and HA-tagged tAR65 (GST-tAR65-HA) in bacterial cells (47). The constructs expressing HSP105α deletion mutants in bacterial cells were generated by ligating insert DNA made by PCR using pTrcHis105-1 (45) as a template DNA and a specific set of primers (Table I) into pTrcHisA vector (Invitrogen) at the *Kpn*I site.

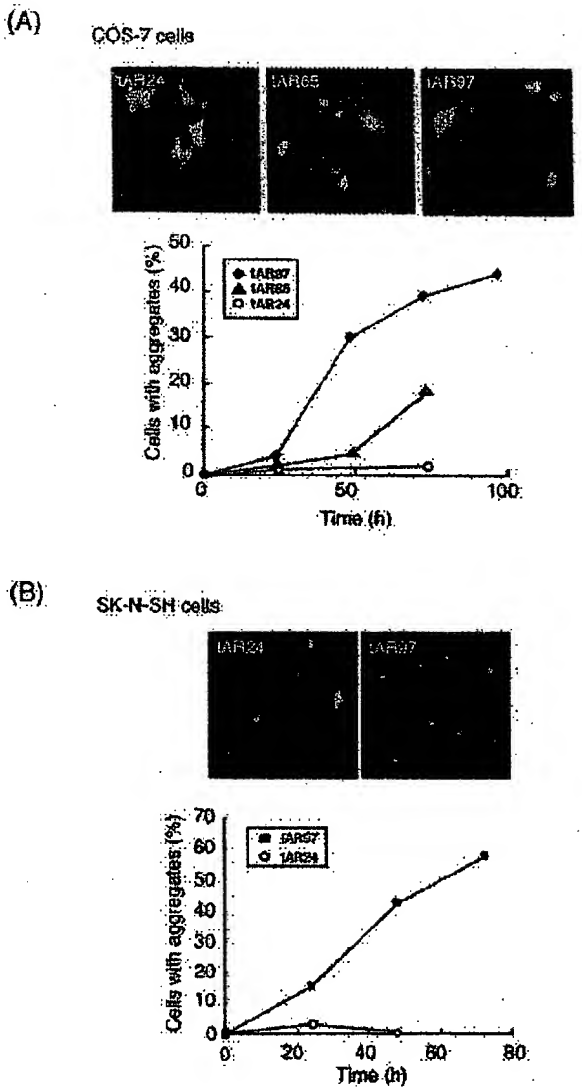

FIG. 1. **Truncated AR containing an expanded polyglutamine tract is accumulated as aggregates in COS-7 and SK-N-SH cells.** Expression plasmids for N-terminal fragments of AR containing various lengths of polyglutamine tract (tAR24, tAR65, and tAR97, 0.5 μg each) were transiently introduced into COS-7 (*A*) or SK-N-SH cells (*B*), and the cells were incubated further for 72 h. Each *upper panel* shows typical images of fluorescence of GFP which is fused to the C terminus of truncated AR, and each *lower graph* represents the rates of cells with aggregates *versus* GFP-positive cells at various times after transfection. Values represent the mean of duplicate experiments.

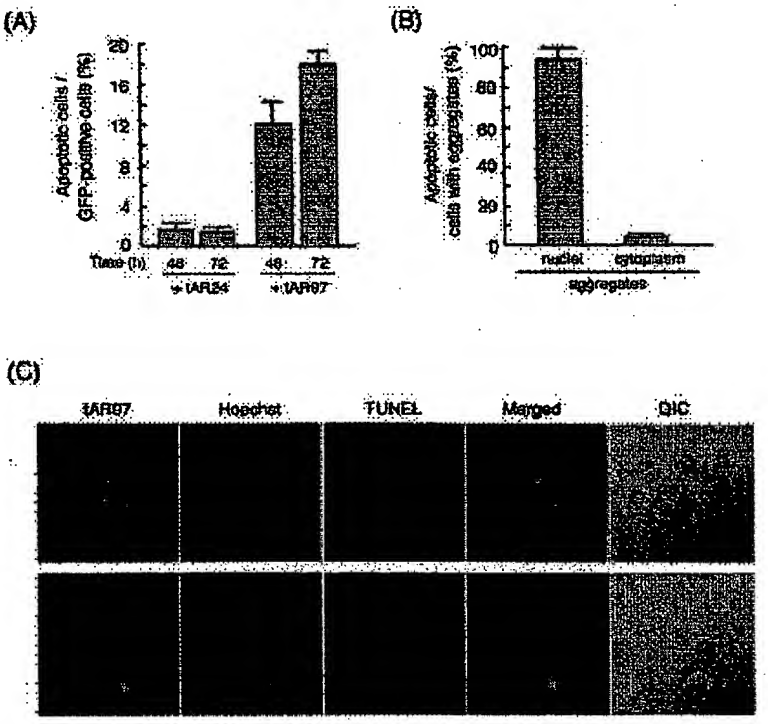

FIG. 2. **Apoptosis occurs in cells with intranuclear aggregates.** *A*, COS-7 cells were transfected with the expression plasmid for tAR24 (+ *tAR24*) or tAR97 (+ *tAR97*) and incubated further for 48 or 72 h. Then cells were fixed and stained with Hoechst 33342. Rates of cells with condensed chromatin *versus* GFP-positive cells are presented. *B*, COS-7 cells were transfected with the expression plasmid for tAR97 and incubated further for 72 h. Rates of apoptotic cells *versus* cells with aggregates in nuclei and/or cytoplasms are presented. Values in *A* and *B* represent the mean ± S.D. of three independent experiments. *C*, fragmentation of DNA in nuclei was evaluated by TUNEL methods 72 h after the transfection of tAR97. *DIC* represents a difference interference contrast image of cells.

Cell Culture and Transfection—African green monkey kidney cells (COS-7) and human neuroblastoma cells (SK-N-SH) were supplied from Riken cell bank. COS-7 cells were maintained in Dulbecco's modified Eagle's medium (Nissui Pharmaceutical) supplemented with 10% fetal bovine serum. SK-N-SH cells were maintained in α-minimal essential medium (Invitrogen) with 10% fetal bovine serum. For transfection of plasmid DNA, cells were grown on coverslips to 70–80% confluence and washed twice with Opti-MEM (Invitrogen). Then plasmid DNA was transfected into cells with DMRIE-C reagent (Invitrogen) for 14–18 h, according to the manufacturer's instructions.

Indirect Immunofluorescence—COS-7 cells grown on coverslips were washed with phosphate-buffered saline without Ca^{2+} and Mg^{2+} (PBS(−)) and fixed with 4% paraformaldehyde for 30 min at room temperature. These cells were washed with PBS(−) and incubated with blocking solution containing 3% bovine serum albumin (BSA) in PBS(−) at room temperature for 1 h. Then rabbit anti-human Hsp105 (48) or mouse anti-Hsp70 monoclonal antibody (Sigma) at a 1:300 dilution was added to the coverslips and incubated in a moist chamber at 37 °C for 1 h. After a wash with PBS(−), rhodamine-conjugated goat anti-rabbit or mouse IgG antibody (Molecular Probes) at a 1:50 dilution was added to the coverslips, and they were incubated further at 37 °C for 1 h. After another wash with PBS(−), cells were observed using a confocal laser scanning microscope (Zeiss).

Analysis of Aggregation in Vivo—COS-7 cells transfected with expression plasmid for tAR24, tAR65, or tAR97 were washed with PBS(−) and fixed with 4% paraformaldehyde for 30 min at room temperature. Cells on coverslips were washed with PBS(−) and stained with 10 μM Hoechst 33342 for 15 min at room temperature. The cells were washed with PBS(−) and then examined using a confocal laser scanning microscope. The number of transfected cells with visible aggregates and the number of transfected cells without aggregates were counted independently in randomly chosen microscopic fields in different areas of a coverslip. Approximately 300–600 transfected cells were analyzed for data in each experiment.

Detection of the Apoptotic Cells—The apoptotic cells were identified by their nuclear morphology and the terminal nucleotidyl transferase-mediated UTP nick end labeling (TUNEL) method (29). Nuclear morphology was examined by staining with Hoechst 33342. The TUNEL method was performed using a DeadEnd™ apoptosis detection kit (Promega) according to the manufacturer's instructions. Briefly, cells were fixed with 4% paraformaldehyde at 72 h after transfection. Fixed cells were incubated with biotinylated deoxynucleotides, then stained with streptavidin-rhodamine conjugate (Molecular Probes) and Hoechst 33342. Cells were then observed by confocal laser scan microscopy.

Western Blotting Analysis—Cells were lysed with a solution containing 0.1% SDS at 72 h after transfection. The cellular proteins (15 μg) were separated by 7.5% SDS-PAGE and blotted onto a nitrocellulose membrane. The membrane was incubated with rabbit anti-human Hsp105 (37) or mouse anti-Hsp70 (Sigma) antibody, then incubated with horseradish peroxidase-conjugated anti-rabbit IgG (Santa Cruz) for Hsp105 or anti-mouse IgG (Santa Cruz) for Hsp70 at a 1:2,000 dilution. These proteins were detected using the enhanced chemiluminescence (ECL) detection system (Amersham Biosciences).

Protein Purification—GST-tAR65-HA was expressed in BL21 bacterial cells on addition of 1 mM isopropyl-β-D-thiogalactopyranoside. Cells were collected and resuspended in ice-cold TEGM buffer (10 mM Tris-HCl, pH 7.4, 1 mM EDTA, 10% glycerol, and 10 mM sodium molybdate). Cells were then sonicated for 1 min and centrifuged for 30 min at 10,000 × *g*. To purify GST-tagged proteins, the supernatants were mixed with glutathione-Sepharose 4B (Amersham Biosciences) and incubated at 4 °C for 1 h. The Sepharose beads were then washed with PBS(−) and eluted with 10 mM reduced glutathione. Wild-type Hsp105α and its mutants were purified as His-tagged proteins by successive Ni^{2+}-agarose (Invitrogen) and Mono Q anion exchange column (Amersham Biosciences) chromatographies, as described previously (45).

Detection of Aggregates of Truncated AR in Vitro—GST-tAR65-HA (1 μM) was incubated with Hsp105α, its mutants, or BSA in 20 μl of buffer A (25 mM Tris-HCl, pH 7.5, 150 mM NaCl, 1 mM dithiothreitol, and 1 mM phenylmethylsulfonyl fluoride) at 30 °C for 12 h in the presence of 2 mM ADP. The reaction was stopped by the addition of 20 μl of a solution containing 2% SDS and 100 mM dithiothreitol, and the mixtures were heated at 98 °C for 5 min. After the addition of 200 μl of a 1% SDS solution, the mixture was filtered through a 0.2-μm cellulose acetate membrane (Advantec). Aggregates on the membrane were incubated with anti-HA tag antibody (1:500, Santa Cruz) then with peroxidase-conjugated anti-mouse IgG antibody (1:2000) and detected with an ECL detection system (Santa Cruz).

Immunohistochemistry—We perfused 20 ml of a 4% paraformaldehyde fixative in 0.1 M phosphate buffer, pH 7.4, through the left cardiac ventricle of SBMA transgenic mice (49) deeply anesthetized with ketamine-xylazine, postfixed tissues overnight in 10% phosphate-buffered formalin, and processed tissues for paraffin embedding. Then, 4-μm thick tissue sections were deparaffinized, dehydrated with alcohol, and

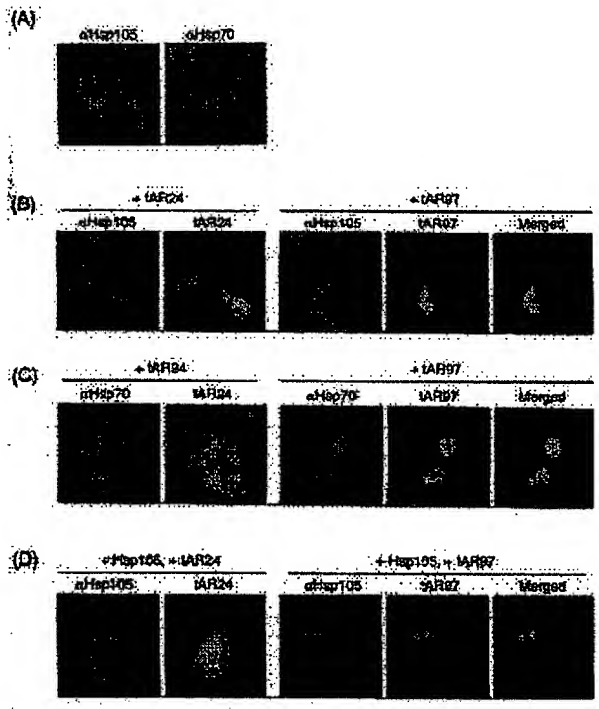

FIG. 3. **Localization of Hsp105α and Hsc70/Hsp70 in COS-7 cells with tAR97 aggregates.** *A*, control COS-7 cells were fixed, and endogenous Hsp105α (*red*) or Hsp70 (*red*) was detected by indirect immunofluorescence using anti-Hsp105 or anti-Hsp70 antibody, respectively. Nuclear morphology (*blue*) was detected by staining with Hoechst 33342. *B* and *C*, COS-7 cells were transfected with the expression plasmid for tAR24 (+ *tAR24*) or tAR97 (+ *tAR97*) and incubated further for 72 h. tAR24 or tAR97 (*green*) was detected by the green fluorescence of GFP, and endogenous Hsp105α (*red*) (*B*) and Hsp70 (*red*) (*C*) were detected by indirect immunofluorescence. Nuclear morphology (*blue*) was observed by staining with Hoechst 33342. *D*, COS-7 cells were cotransfected with expression plasmids for Hsp105α and tAR24 (+ *Hsp105*, + *tAR24*) or Hsp105α and tAR97 (+ *Hsp105*, + *tAR97*) and incubated further for 72 h. Nuclear morphology (*blue*) stained with Hoechst 33342 and tAR97 (*green*) and Hsp105α (*red*) by indirect immunofluorescence was observed.

treated in formic acid for 5 min at room temperature and with trypsin (Dako) for 20 min at 37 °C. The tissue sections were blocked with normal goat serum (1:20) and incubated with rabbit anti-mouse Hsp105 antibody (1:100). The sections were incubated with biotinylated goat anti-rabbit IgG (Vector Laboratories), and immune complexes were visualized using streptavidin-horseradish peroxidase (Dako) and 3,3'-diaminobenzidine (Dojindo) substrate and counterstained with methyl green. For the immunohistochemistry of tissues of SBMA patients, paraffin-embedded sections of the spinal cord and scrotal skin from nine patients with clinicopathologically and genetically confirmed SBMA (age 51–84 years, mean 64.3 years) were examined using rabbit anti-human Hsp105 antibody (1:100).

RESULTS

Aggregation of Truncated AR with an Expanded Polyglutamine Tract and Induction Apoptosis in COS-7 and SK-N-SH Cells—Truncated ARs containing 24, 65, or 97 polyglutamine repeats (tAR24, tAR65, or tAR97, respectively) were transiently expressed in non-neuronal (COS-7) and neuronal cells (SK-N-SH) (Fig. 1). Because these tAR constructs were connected with GFP at the C terminus, the cellular localization of these chimerical peptides was detected by fluorescence microscopy. tAR65 or tAR97, but not tAR24, aggregated in cytoplasm and/or nucleus in non-neuronal COS-7 cells as well as neuronal SK-N-SH cells, as shown previously in the neuronal Neuro2a cell line (29). Proportions of cells with aggregates increased depending on the incubation time after transfection and polyglutamine repeat length. Approximately 45 and 60% of GFP-positive cells had aggregates in the COS-7 and SK-N-SH cell lines, respectively, at 72 h after transfection of the expression plasmid for tAR97. Among the cells with aggregates of tAR97, intranuclear aggregates were detected in 40 and 8% of transfected COS-7 and SK-N-SH cells, respectively (data not shown).

Under these conditions, apoptotic cells with condensed chromatin were observed in 12 and 18% of all COS-7 cells expressing GFP at 48 and 72 h after transfection of the expression plasmid for tAR97, respectively (Fig. 2*A*). In contrast, cells expressing tAR24 showed little apoptotic morphology after the transfection (Fig. 2*A*). Most apoptotic cells had aggregates of tAR97 in the nucleus, whereas cells containing cytoplasmic aggregates exhibited few apoptotic features (Fig. 2*B*). Furthermore, when the presence of fragmented DNA was assessed by the TUNEL method, the cells with intranuclear aggregates, but not cells with cytoplasmic aggregates, were found to be positive (Fig. 2*C*). These findings suggested that the intranuclear aggregates induced apoptosis in COS-7 cells. Similar results were obtained with SK-N-SH cells (data not shown). Thus, although both non-neuronal and neuronal cells could be utilized as a cell model of SBMA, we used the COS-7 model for further study because the cells expressed the transfected plasmids markedly well.

Colocalization of Hsp105α and Hsp70 with Aggregates of Truncated AR—We next examined the cellular distribution of Hsp105α and Hsp70 in COS-7 cells by indirect immunofluorescence using anti-human Hsp105 and anti-Hsp70 antibodies. Under nonstressed conditions, endogenous Hsp105α and Hsc70/Hsp70 were localized mainly in the cytoplasm of cells (Fig. 3*A*). When tAR24 was transiently expressed in COS-7 cells, both endogenous Hsp105α and Hsp70 were also detected in the cytoplasm of the cells (Fig. 3, *B* and *C*). In contrast, when tAR97 was transiently expressed in COS-7 cells, endogenous Hsp70 was colocalized to the aggregates of tAR97, whereas endogenous Hsp105α was not. However, when overexpressed with tAR97 in cells, Hsp105α was colocalized to the aggregates of tAR97 (Fig. 3*D*), whereas Hsp105α was localized to the cytoplasm of cells in which tAR97 was not expressed. Thus, the increased amounts of Hsp105α in cells seemed necessary for the interaction with and binding to the tAR containing an expanded polyglutamine tract.

Overexpression of Hsp105α Reduced Aggregation of tAR97—Hsp105α prevents the aggregation of denatured protein *in vitro* (45) and suppresses apoptotic cell death induced by various forms of stress in neuronal PC12 cells (44). Because the overexpressed Hsp105α colocalized to intracellular aggregates of tAR97 (Fig. 3), we next examined the effects of Hsp105α on the aggregation of tAR containing an expanded polyglutamine tract. When expression plasmids for Hsp105α and tAR97 were cotransfected into COS-7 cells, the proportion of cells with tAR97 aggregates was reduced to ~50% of that transfected without Hsp105α (Fig. 4, *A* and *B*). Overexpression of Hsp70 or Hsp40 also suppressed the formation of aggregates similarly to Hsp105α, and Hsp70 and Hsp40 in combination suppressed the formation strongly. However, the suppression of aggregation by Hsp70 and Hsp40 was not enhanced by the coexpression of Hsp105α.

When cellular toxicity was analyzed by examining the nuclear morphology of cells stained with Hoechst 33342, numbers of apoptotic cells with condensed chromatin were found to be markedly reduced by coexpression of Hsp105α with tAR97 (Fig. 4*C*). Overexpression of Hsp70 and/or Hsp40 also suppressed apoptotic cell death caused by expression of tAR97. Furthermore, when various amounts of Hsp105α were coexpressed

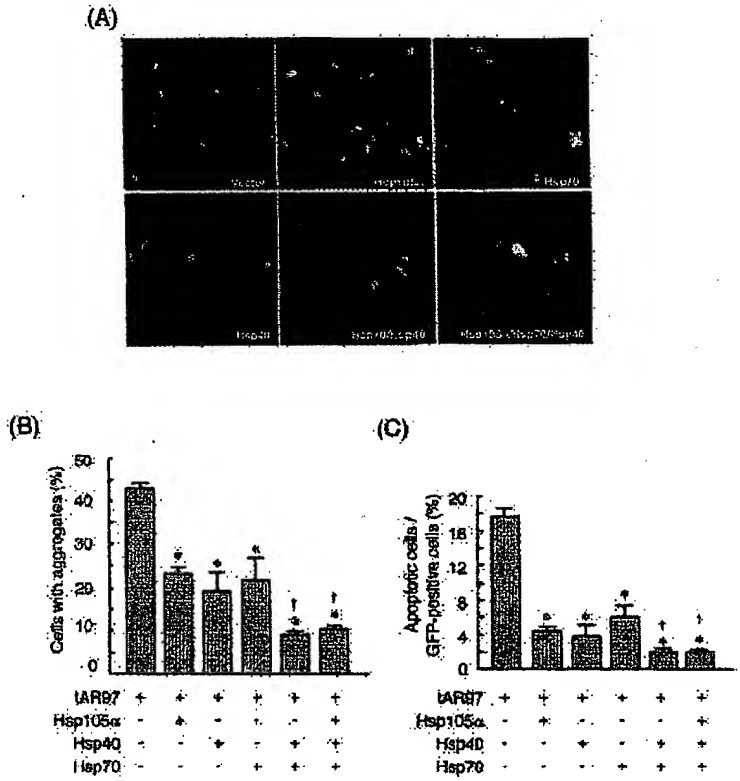

FIG. 4. **Effects of Hsp105α on aggregation of tAR97.** *A*, COS-7 cells were cotransfected with expression plasmids for tAR97 (0.5 μg) and pcDNA3.1 vector, Hsp105, Hsp70, and/or Hsp40 (1 μg each) and incubated further for 72 h. Typical images of fluorescence of GFP are shown. *B*, rates of cells with aggregates *versus* GFP-positive cells are shown. *C*, rates of apoptotic cells with condensed chromatin *versus* GFP-positive cells are shown. Values in *B* and *C* represent the mean ± S.D. of three independent experiments. Statistical significance was determined using Student's *t* test; *, $p < 0.01$ *versus* control with vector. †, $p < 0.01$ *versus* cells overexpressing Hsp70 or Hsp40 alone.

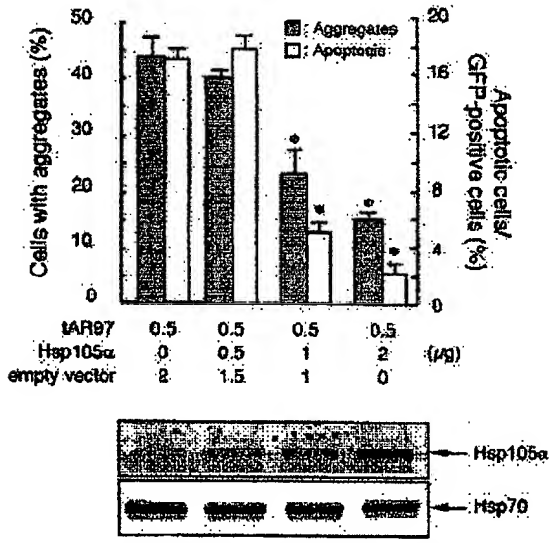

FIG. 5. **Hsp105α suppresses aggregation of tAR97 and cellular toxicity in a dose-dependent manner.** The expression plasmids for empty vector, Hsp105α, and/or tAR97 were introduced into COS-7 cells, and the cells were incubated further for 72 h. GFP fluorescence was observed using a confocal laser scan microscope. Rates of cells with aggregates or apoptotic cells/GFP-positive cells are shown as *closed* or *opened bars*, respectively. Values represent the mean ± S.D. of three independent experiments. Statistical significance was determined using Student's *t* test; *, $p < 0.01$ *versus* control with vector. *Lower panels* show Western blots of Hsp105α and Hsp70 in the cells.

with tAR97, the aggregation of tAR97 and apoptosis were both suppressed depending on cellular levels of Hsp105α (Fig. 5). Under these conditions, cellular levels of endogenous Hsp70 were not changed by overexpression of Hsp105α (Fig. 5, *lower panel*). These findings strongly suggested that when overexpressed, Hsp105α suppressed effectively not only the formation of aggregates but also the expanded polyglutamine-mediated cellular toxicity.

Identification the Domain of Hsp105α Required for Suppression of tAR97 Aggregation—Hsp105α is composed of N-terminal ATP binding, central β-sheet, loop and C-terminal α-helix domains, similar to the Hsp70 family proteins. To determine the domain of Hsp105α essential to suppress the aggregation caused by expansion of the polyglutamine tract, we constructed expression plasmids for various deletion mutants of Hsp105α, as shown in Fig. 6*A*. When coexpressed with tAR97 in COS-7 cells, the Hsp105α mutant C3 or ΔL significantly suppressed the aggregation of tAR97 as did wild-type Hsp105α (Fig. 6*B*). However, other deletion mutants failed to suppress the aggregation of tAR97. Because the C3 and ΔL mutants contain both β-sheet and α-helix domains, these domains seemed to be essential to suppress the aggregation caused by expansion of the polyglutamine tract.

Hsp105α Inhibits Aggregation of GST-tAR65 in Vitro—To examine further whether Hsp105α can directly suppress aggregation of the expanded polyglutamine tract, we analyzed the effects of Hsp105α on the aggregation of tAR65 *in vitro* (Fig. 7). GST-tAR65-HA was incubated with or without Hsp105α or its mutant, and insoluble aggregates that formed during the incubation were collected on cellulose acetate membranes. Hsp105α suppressed the aggregation of tAR65 in a dose-dependent manner (Fig. 7*A*). Furthermore, the aggregation was suppressed by wild-type Hsp105α and the mutants C3 and ΔL but not by other deletion mutants (Fig. 7*B*). Thus, it was suggested that Hsp105α itself suppressed the aggregation of truncated AR containing an expanded polyglutamine without other cellular components and that both the β-sheet and

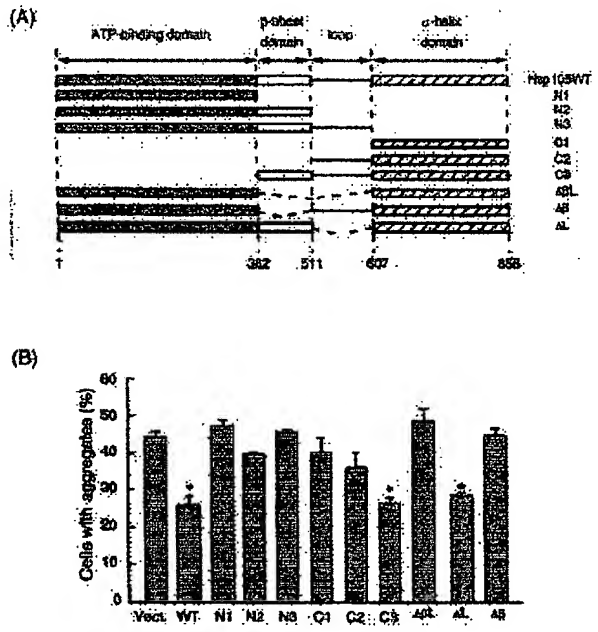

FIG. 6. **Domain of Hsp105α required for suppression of aggregation of tAR97.** *A*, schematic diagram of deletion mutants of Hsp105α. *B*, COS-7 cells were cotransfected with expression plasmid for tAR97 and deletion mutant of Hsp105α and incubated further for 72 h. GFP fluorescence was observed using a confocal laser scan microscope. Rates of cells with aggregates *versus* GFP-positive cells are shown. Values represent the mean ± S.D. of three independent experiments. Statistical significance was determined using Student's *t* test; *, $p < 0.01$ *versus* control with vector.

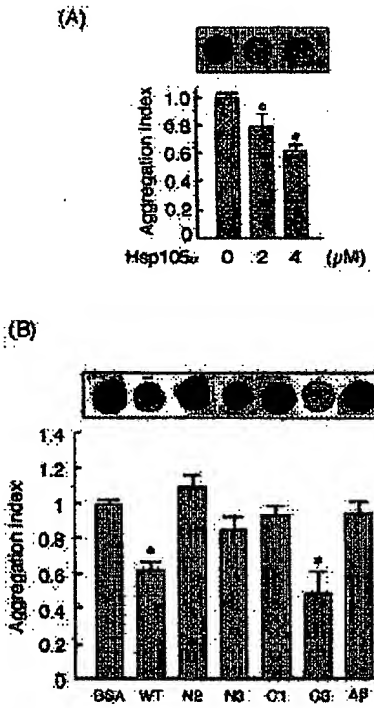

FIG. 7. **Hsp105α inhibits the aggregation of tAR65 *in vitro*.** *A*, 1 μM GST-tAR65-HA was incubated with 2 or 4 μM Hsp105α or 4 μM BSA at 25 °C for 16 h. *B*, 1 μM GST-tAR65-HA was incubated with Hsp105α, various deletion mutants of Hsp105α, or BSA (4 μM each) at 25 °C for 16 h. Then, aggregates were trapped on cellulose acetate membranes and detected by immunoblotting using anti-HA antibody. Densities of spots were quantified, and relative rates of tAR65 retained on membranes are shown as an aggregation index. Values represent the mean ± S.D. of three independent experiments. Statistical significance was determined using Student's *t* test; *, $p < 0.01$ *versus* control with BSA.

α-helix domains of Hsp105α seemed necessary for the suppression *in vitro* as well as *in vivo*.

Immunohistochemistry of Hsp105α in Nuclear Inclusions in the Tissues of SBMA Patients and Transgenic Mice—Nuclear inclusions containing mutant and truncated AR with an expanded polyglutamine have been shown to occur in residual motor neurons in the brain stem and spinal cord (4) and also in the skin, testis, and some other visceral organs of SBMA patients (5). We next examined whether Hsp105α localizes in the nuclear inclusions in these tissues of SBMA patients. As shown in Fig. 8, *A* and *B*, Hsp105α staining was observed in nuclear inclusions in neurons of the spinal anterior horn and scrotal skin epidermal cells. Furthermore, when male transgenic mice carrying a full-length AR with an expanded polyglutamine (97 repeats) tract and showing neuropathologic changes equivalent to human SBMA (49) were examined immunohistochemically, Hsp105α was also detected in nuclear inclusions in neurons of the spinal anterior horn and muscle cells (Fig. 8, *C* and *D*). However, although Hsp105α was commonly observed in nuclear inclusions in scrotal skin epidermal cells of SBMA patients and in muscle cells of the transgenic mice, only a few Hsp105-immunoreactive nuclear inclusions were observed in neurons of the spinal anterior horn of either patients or mice.

DISCUSSION

Hsp105α is a stress protein expressed at an especially high level in mammalian brain (43) and has an antiapoptotic effect in neuronal cells (44). Hsp105α prevents the aggregation of denatured proteins caused by heat shock *in vitro* but has not been shown to have chaperone activity (45). Here, we showed that Hsp105α suppressed not only the formation of intracellular aggregates but also apoptosis caused by an expansion of the polyglutamine tract in a cellular model of SBMA. Hsp105α is composed of N-terminal ATP binding, central β-sheet, loop, and C-terminal α-helix domains, similar to the Hsp70 family proteins. For the suppression of aggregation of truncated AR containing an expanded polyglutamine tract, β-sheet and α-helix domains of Hsp105α were essential *in vivo* and *in vitro*. Hsp70 binds unfolded proteins at the β-sheet domain and prevents aggregation of denatured proteins (50), and the α-helix domain is essential for stable binding to the substrate protein (50). Recently, we found that the β-sheet domain of Hsp105α could bind to denatured proteins.[2] Because Hsp105α mutants with β-sheet but not α-helix domains did not prevent the aggregation of truncated AR containing an expanded polyglutamine tract *in vivo* and *in vitro*, the α-helix domain may be necessary for stabilization of the Hsp105α-substrate complexes as is Hsp70.

Hsp70 and Hsp40 have recently been identified as important regulators of polyglutamine aggregation and/or cell death in cellular models of polyglutamine disease (29). Hsp70 promotes protein folding by an ATP-dependent process involving polypeptide segments enriched in hydrophobic residues (50, 51) and cooperates in this function with members of the Hsp40 family (52). The binding of Hsp70 to substrate proteins may prevent protein aggregation directly by shielding the interactive surfaces of nonnative polypeptides. Suppression of polyglutamine-induced neurotoxicity by expression of Hsp40 alone

[2] N. Yamagishi, K. Ishihara, and T. Hatayama, unpublished data.

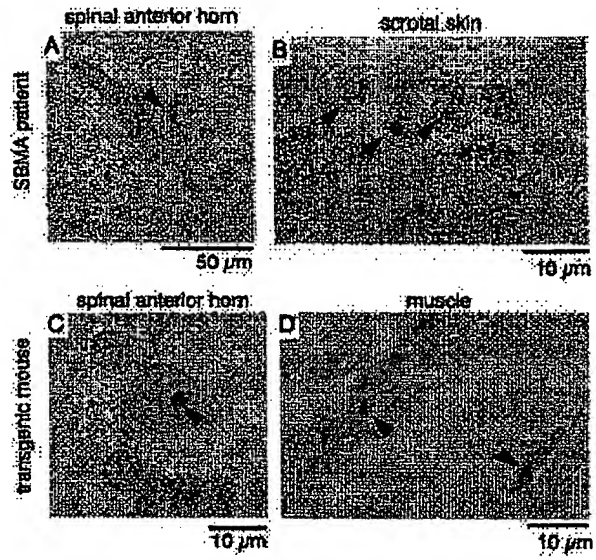

FIG. 8. **Immunohistochemistry of Hsp105α in nuclear inclusions in the tissues of patients and transgenic mice with SBMA.** Tissue sections of spinal anterior horn (*A*) and scrotal skin (*B*) from SBMA patients or spinal anterior horn (*C*) and muscle (*D*) from male AR-Q97 transgenic mice were examined using anti-human Hsp105 or rabbit anti-mouse Hsp105 antibody, respectively, and counterstained with methyl green. *Arrowheads* indicate nuclear inclusions.

is most likely caused by the ability to activate the endogenous Hsp70 for suppression of the neurotoxicity. Here, we showed that overexpression of Hsp105α alone suppressed the aggregation of truncated AR containing an expanded polyglutamine tract similarly to Hsp70 or Hsp40, whereas Hsp70 and Hsp40 in combination suppressed the aggregation much more markedly. However, because the suppression of aggregation by Hsp70 and Hsp40 was not enhanced by the coexpression of Hsp105α, Hsp105α and Hsp70/Hsp40 seem to suppress the polyglutamine-induced neurotoxicity by similar mechanisms.

In polyglutamine diseases such as spinocerebellar ataxia type 3/Machado-Joseph disease, Hsp70 colocalizes in intracellular aggregates, whereas Hsp105α is not found in the aggregates (27). In the present study, Hsp105 was detected in nuclear inclusions in neurons of the spinal anterior horn and scrotal skin epidermal cells of SBMA patients and also in neurons of the spinal anterior horn and muscle cells of SBMA transgenic mice, although only a few Hsp105-immunoreactive nuclear inclusions were observed in neurons of the spinal cord of the patients and mice. On the other hand, in a cellular model of SBMA, endogenous Hsp70 but not endogenous Hsp105α localized to aggregates of tAR97, although the overexpressed Hsp105α localized to the aggregates of tAR97. Because Hsp70 exists in much larger amounts than Hsp105α in cells, Hsp70 may interact preferentially with truncated AR containing an expanded polyglutamine tract. However, when Hsp105α was overexpressed in the cells, reaching high levels, it seemed to bind and localize to truncated AR containing an expanded polyglutamine tract like Hsp70. Thus, the existence of molecular chaperones at high concentrations in cells may be essential to prevent the aggregation of truncated AR containing an expanded polyglutamine tract.

The intranuclear aggregation of truncated AR containing an expanded polyglutamine tract and apoptotic cell death coincided in the cellular model of SBMA, and both processes were suppressed by overexpression of Hsp105α. As to the mechanism by which Hsp105α suppresses the apoptosis caused by expansion of the polyglutamine tract, one possibility is that suppression of aggregation by Hsp105α mediates suppression of apoptosis. Key components of the transcription apparatus, such as cAMP response element binding protein-binding protein, p53, and $TAF_{II}130$, are sequestered in polyglutamine-containing inclusions, then the expanded polyglutamine tract causes altered gene transcription (30, 53–57). By preventing the formation of intranuclear aggregates, Hsp105α may suppress the alteration of gene transcription caused by an expanded polyglutamine tract and eventually apoptotic cell death.

Another possibility is that the abilities of Hsp105α to suppress aggregate formation and cellular toxicity caused by expansion of the polyglutamine tract are independent. Recently, molecular chaperones, such as Hsp70, Hsp40, and Hsp27, were shown to suppress an expanded polyglutamine-mediated cellular toxicity independently of suppression of aggregation (35, 36). Although the relationship between the aggregation and the induction of apoptosis remains unknown, the suppression of cellular toxicity by molecular chaperones may be caused by the ability to inhibit apoptosis. Hsp105α suppresses heat shock-induced apoptosis in neuronal cells by preventing the activation of c-Jun N-terminal kinase (44). Because c-Jun N-terminal kinase is activated by the expanded polyglutamine tract (58), Hsp105α may also suppress the cellular toxicity by its ability to inhibit apoptosis.

In conclusion, we identified Hsp105α as a novel molecule that reduces aggregation and cellular toxicity caused by an expansion of the polyglutamine tract. Molecular chaperones, such as Hsp105α, Hsp70, Hsp40, and Hsp27, seem to suppress cell toxicity caused by an expansion of the polyglutamine tract. These findings suggest that increasing the expression levels or enhancing the function of chaperones in neurons may open up a promising approach to the treatment of polyglutamine diseases, although more studies are required to determine the precise mechanism of neurodegeneration of CAG repeat diseases.

REFERENCES

1. Kennedy, W. R., Alter, M., and Sung, J. H. (1968) *Neurology* **18**, 671–680
2. Sobue G., Hashizume, Y., Mukai, E., Hirayama, M., Mitsuma, T., and Takahashi, A. (1989) *Brain* **112**, 209–232
3. La Spada, A. R., Wilson, E. M., Lubahn, D. B., Harding, A. E., and Fischbeck, K. H. (1991) *Nature* **352**, 77–79
4. Li, M., Miwa, S., Kobayashi, Y., Merry, D. E., Yamamoto, M., Tanaka, F., Doyu, M., Hashizume, Y., Fischbeck, K. H., and Sobue, G. (1998) *Ann. Neurol.* **44**, 249–254
5. Li, M., Nakagomi, Y., Kobayashi, Y., Merry, D. E., Tanaka, F., Doyu, M., Mitsuma, T., Hashizume, Y., Fischbeck, K. H., and Sobue, G. (1998) *Am. J. Pathol.* **153**, 695–701
6. The Huntington's Disease Collaborative Research Group (1993) *Cell* **72**, 971–983
7. Koide, R., Ikeuchi, T., Onodera, O., Tanaka, H., Igarashi, S., Endo, K., Takahashi, H., Kondo, R., Ishikawa, A., Hayashi, T., Saito, M., Tomoda, A., Miike, T., Naito, H., Ikuta, F., and Tsuji, S. (1994) *Nat. Genet.* **6**, 9–13
8. Nagafuchi, S., Yanagisawa, H., Sato, K., Shirayama, T., Ohsaki, E., Bundo, M., Takeda, T., Tadokoro, K., Kondo, I., Murayama, N., Tanaka, Y., Kikushima, H., Umino, K., Kurosawa, H., Furukawa, T., Nihei, K., Inoue, T., Sano, A., Kimura, O., Takahashi, M., Yoshizawa, T., Kanazawa, I., and Yamada, M. (1994) *Nat. Genet.* **6**, 14–18
9. Kawaguchi, Y., Okamoto, T., Taniwaki, M., Aizawa, M., Inoue, M., Katayama, S., Kawamaki, H., Nakamura, S., Nishimura, M., Akiguchi, I., Kimura, J., Narumiya, S., and Kakizuka, A. (1994) *Nat. Genet.* **8**, 221–228
10. Orr, H. T., Chung, M. Y., Banfi, S., Kwiatkowski, T. J., Servadio, A., Beaudet, A. L., McCall, A. E., Duvick, L. A., Ranum, L. P., and Zoghbi, H. Y. (1993) *Nat. Genet.* **4**, 221–226
11. Pulst, S. M., Nechiporuk, A., Nechiporuk, T., Gispert, S., Chen, X. N., Lopes-Cendes, I., Pearlman, S., Starkman, S., Orozco-Diaz, G., Lunkes, A., DeJong, P., Rouleau, G. A., Auburger, G., Korenberg, J. R., Figueroa, C., and Sahba, S. (1996) *Nat. Genet.* **14**, 269–276
12. Sanpei, K., Takano, H., Igarashi, S., Sato, T., Oyake, M., Sasaki, H., Wakisaka, A., Tashiro, K., Ishida, Y., Ikeuchi, T., Koide, R., Saito, M., Sato, A., Tanaka, T., Hanyu, S., Takiyama, Y., Nishizawa, M., Shimizu, N., Nomura, Y., Segawa, M., Iwabuchi, K., Eguchi, I., Tanaka, H., Takahashi, H., and Tsuji, S. (1996) *Nat. Genet.* **14**, 277–284
13. Imbert, G., Saudou, F., Yvert, G., Devys, D., Trottier, Y., Garnier, J. M., Weber, C., Mandel, J. L., Cancel, G., Abbas, N., Durr, A., Didierjean, O., Stevanin, G., Agid, Y., and Brice, A. (1996) *Nat. Genet.* **14**, 285–291

14. Zhuchenko, O., Bailey, J., Bonnen, P., Ashizawa, T., Stockton, D. W., Amos, C., Dobyns, W. B., Subramony, S. H., Zoghbi, H. Y., and Lee, C. C. (1997) *Nat. Genet.* **15**, 62–69
15. David, G., Abbas, N., Stevanin, G., Durr, A., Yvert, G., Cancel, G., Weber, C., Imbert, G., Saudou, F., Antoniou, E., Drabkin, H., Gemmill, R., Giunti, P., Benomar, A., Wood, N., Ruberg, M., Agid, Y., Mandel, J. L., and Brice, A. (1997) *Nat. Genet.* **17**, 65–70
16. Welch, W. J., and Gambetti, P. (1998) *Nature* **392**, 23–24
17. Sherman, M. Y., and Goldberg, A. L. (2001) *Neuron* **29**, 15–32
18. Johnston, J. A., Ward, C. L., and Kopito, R. R. (1998) *J. Cell Biol.* **143**, 1883–1898
19. Schulz, J. B., and Dichgans, J. (1999) *Curr. Opin. Neurol.* **12**, 433–439
20. Heiser, V., Scherzinger, E., Boeddrich, A., Nordhoff, E., Lurz, R., Schugardt, N., Lehrach, H., and Wanker, E. E. (2000) *Proc. Natl. Acad. Sci. U. S. A.* **97**, 6739–6744
21. Kazemi-Esfarjani, P., and Benzer, S. (2000) *Science* **287**, 1837–1840
22. Nagai, Y., Tucker, T., Ren, H., Kenan, D. J., Henderson, B. S., Keene, J. D., Strittmatter, W. J., and Burke, J. R. (2000) *J. Biol. Chem.* **275**, 10437–10442
23. Hendricks, J. P., and Hartl, F. U. (1998) *Annu. Rev. Biochem.* **62**, 349–384
24. Hartl, F. U. (1996) *Nature* **381**, 571–580
25. Muchowski, P. J., Schaffar, G., Sittler, A., Wanker, E. E., Hayer-Hartl, M. K., and Hartl, F. U. (2000) *Proc. Natl. Acad. Sci. U. S. A.* **97**, 7841–7846
26. Cummings, C. J., Mancini, M. A., Antalffy, B., DeFranco, D. B., Orr, H. T., and Zoghbi, H. Y. (1998) *Nat. Genet.* **19**, 148–154
27. Chai, Y., Koppenhafer, S. L., Bonini, N. M., and Paulson, H. L. (1999) *J. Neurosci.* **19**, 10338–10347
28. Jana, N. R., Tanaka, M., Wang, G., and Nukina, N. (2000) *Hum. Mol. Genet.* **9**, 2009–2018
29. Kobayashi, Y., Kume, A., Li, M., Doyu, M., Hata, M., Ohtsuka, K., and Sobue, G. (2000) *J. Biol. Chem.* **275**, 8772–8778
30. Stenoien, D. L., Cummings, C. J., Adams, H. P., Mancini, M. G., Patel, K., DeMartino, G. N., Marcelli, M., Weigel, N. L., and Mancini, M. A. (1999) *Hum. Mol. Genet.* **8**, 731–741
31. Wyttenbach, A., Carmichael, J., Swartz, J., Furlong, R. A., Narain, Y., Rankin, J., and Rubinsztein, D. C. (2000) *Proc. Natl. Acad. Sci. U. S. A.* **97**, 2898–2903
32. Warrick, J. M., Chan, H. Y., Gray-Board, G. L., Chai, Y., Paulson, H. L., and Bonini, N. M. (1999) *Nat. Genet.* **23**, 425–428
33. Cummings, C. J., Sun, Y., Opal, P., Antalffy, B., Mestril, R., Orr, H. T., Dillmann, W. H., and Zoghbi, H. Y. (2001) *Hum. Mol. Genet.* **10**, 1511–1518
34. Adachi, H., Katsuno, M., Minamiyama, M., Sang, C., Pagoulatos, G., Angelidis, C., Kusakabe, M., Yoshiki, A., Kobayashi, Y., Doyu, M., and Sobue, G. (2003) *J. Neurosci.* **23**, 2203–2211
35. Wyttenbach, A., Sauvageot, O., Carmichael, J., Diaz-Latoud, C., Arrigo, A. P., and Rubinsztein, D. C. (2002) *Hum. Mol. Genet.* **11**, 1137–1151
36. Zhou, H., Li, S. H., and Li, X. J. (2001) *J. Biol. Chem.* **276**, 48417–48424
37. Ishihara, K., Yasuda, K., and Hatayama, T. (1999) *Biochim. Biophys. Acta* **1444**, 138–142
38. Yasuda, K., Nakai, A., Hatayama, T., and Nagata, K. (1995) *J. Biol. Chem.* **270**, 29718–29723
39. Lee-Yoon, D., Easton, D., Murawski, M., Burd, R., and Subjeck, J. R. (1995) *J. Biol. Chem.* **270**, 15725–15733
40. Plesofsky-Vig, N., and Brambl, R. (1998) *J. Biol. Chem.* **273**, 11335–11341
41. Storozhenko, S., De Pauw, P., Kushnir, S., Van Montagu, M., and Inze, D. (1996) *FEBS Lett.* **390**, 113–118
42. Mukai, H., Kuno, T., Tanaka, H., Hirata, D., Miyakawa, T., and Tanaka, C. (1993) *Gene (Amst.)* **132**, 57–66
43. Wakatsuki, T., and Hatayama, T. (1998) *Biol. Pharm. Bull.* **21**, 905–910
44. Hatayama, T., Yamagishi, N., Minabe, E., and Sakai, K. (2001) *Biochem. Biophys. Res. Commun.* **288**, 528–534
45. Yamagishi, N., Nishihori, H., Iahihara, K., Ohtsuka, K., and Hatayama, T., (2000) *Biochem. Biophys. Res. Commun.* **272**, 850–855
46. Michels, A. A., Kanon, B., Konings, A. W. T., Ohtsuka, K., Bensaude, O., and Kampinga, H. H. (1997) *J. Biol. Chem.* **272**, 33283–33289
47. Merry, D. E., Kobayashi, Y., Bailey, C. K., Taye, A. A., and Fischbeck, K. H. (1998) *Hum. Mol. Genet.* **7**, 693–701
48. Honda, K., Hatayama, T., and Yukioka, M. (1989) *Biochem. Biophys. Res. Commun.* **160**, 60–66
49. Katsuno, M., Adachi, H., Kume, A., Li, M., Nakagomi, Y., Niwa, H., Sang, C., Kobayashi, Y., Doyu, M., and Sobue, G. (2002) *Neuron* **35**, 843–854
50. Rüdiger, S., Buchberger A., and Bukau, B. (1997) *Nat. Struct. Biol.* **4**, 342–349
51. Bukau, B., and Horwich, A. L. (1998) *Cell* **92**, 351–366
52. Freeman, B. C., Myers, M. P., Schumacher, R., and Morimoto, R. I. (1995) *EMBO J.* **14**, 2281–2292
53. McCampbell, A., Taylor, J. P., Taye, A. A., Robitschek, J., Li, M., Walcott, J., Merry, D., Chai, Y., Paulson, H., Sobue, G., and Fischbeck, K. H. (2000) *Hum. Mol. Genet.* **9**, 2197–2202
54. Steffan, J. S., Kazantsev, A., Spasic-Boskovic, O., Greenwald, M., Zhu, Y. Z., Gohler, H., Wanker, E. E., Bates, G. P., Housman, D. E., and Thompson, L. M. (2000) *Proc. Natl. Acad. Sci. U. S. A.* **97**, 6763–6768
55. Kazantsev, A., Preisinger, E., Dranovsky, A., Goldgaber, D., and Housman, D. (1999) *Proc. Natl. Acad. Sci. U. S. A.* **96**, 11404–11409
56. Boutell, J. M., Thomas, P., Neal, J. W., Weston, V. J., Duce, J., Harper, P. S., and Jones, A. L. (1999) *Hum. Mol. Genet.* **8**, 1647–1655
57. Shimohata, T., Nakajima, T., Yamada, M., Uchida, C., Onodera, O., Naruse, S., Kimura, T., Koide, R., Nozaki, K., Sano, Y., Ishiguro, H., Sakoe, K., Ooshima, T., Sato, A., Ikeuchi, T., Oyake, M., Sato, T., Aoyagi, Y., Hozumi, I., Nagatsu, T., Takiyama, Y., Nishizawa, M., Goto, J., Kanazawa, I., Davidson, I., Tanese, N., Takahashi, H., and Tsuji, S. (2000) *Nat. Genet.* **26**, 29–36
58. Yasuda, S., Inoue, K., Hirabayashi, M., Higashiyama, H., Yamamoto, Y., Fuyuhiro, H., Komure, O., Tanaka, F., Sobue, G., Tsuchiya, K., Hamada, K., Sasaki, H., Takeda, K., Ichiju, H., and Kakizuka, A. (1999) *Genes Cells* **4**, 743–756